UTILIZATION OF DISCRETE FRACTURE NETWORKS FOR KINEMATIC ASSESSMENT OF BENCH SCALE FAILURES IN AN OPEN PIT MINING ENVIRONMENT

by

Matthew N.T. King

B.A.Sc., The University of British Columbia, 2005

A THESIS SUBMITTED IN PARTIAL FULFILLMENT OF

THE REQUIREMENTS FOR THE DEGREE OF

MASTER OF APPLIED SCIENCE

in

THE FACULTY OF GRADUATE AND POSTDOCTORAL STUDIES

(Mining Engineering)

THE UNIVERSITY OF BRITISH COLUMBIA

(Vancouver)

August 2023

The following individuals certify that they have read, and recommend to the Faculty of Graduate and Postdoctoral Studies for acceptance, the thesis entitled:

Utilization of Discrete Fracture Networks for Kinematic Assessment of Bench Scale Failures in an Open Pit Mining Environment

Submitted by	Matthew N.T. King	in partial fulfilment of the requirements for
the degree of	Master of Applied Science	
in	Mining Engineering	

Examining Committee:

Davide Elmo, Professor, Mining Engineering, UBC

Supervisor

Scott Dunbar, Professor, Mining Engineering, UBC

Supervisory Committee Member

ABSTRACT

In hard rock open pit mining environments the stability conditions of the bench are controlled by the structural discontinuities. Kinematic analyses of rigid blocks provide a prediction of the expected breakback following mining activities. In general, the observed breakback is steeper than that predicted using conventional kinematic analysis methods, which are known to have conservative assumptions such as ubiquity and full continuity of structures. However, this cannot be relied upon in all cases (i.e., exploration projects or mining projects not yet into construction) and design optimization or steepening does not occur until backed by empirical evidence. Utilizing a discrete fracture network (DFN) method involving polyhedral kinematics an attempt is made to see if the steeper observed designs can be predicted using structure that is stochastic and discontinuous. DFNs have limitations due to data uncertainty, in particular to the continuity of structures. Sensitivity assessments of the continuity of structures within a DFN are also investigated. Results of the DFN based kinematic analyses indicate steeper expected breakback angles compared to conventional kinematic analyses, however, the DFN results are inconsistent with the observed breakback conditions. Ultimately the DFN models failed to generate sufficient blocks to represent the actual breakback conditions. Future work is required particularly with regard to determining the validity of a DFN. Simple statistical assessments of DFNs only confirm that the DFN adheres to the input parameters such as orientation, continuity, and spacing. An additional check needs to be performed to assess if the spatial locations of the generated structures matches those of the observed structures. Additionally the potential of progressive failure of key blocks at the bench scale requires further analysis to determine its contribution to breakback of benches in a mining environment.

LAY SUMMARY

When designing an open pit mine, engineers are seeking balance between slopes that are safe and can also be excavated profitably. The steeper the slope, the more ore that can be removed. The flatter the slope, the less risk of slope failure. Each slope is designed as a series of benches.
In operating mines, engineers can improve the designs with real-world information, but mining projects at the pre-construction stages are designed more conservatively to protect against a design that could fail. To identify the optimal slope for each open pit mine, engineers can apply a number of tools to assess the rock structure and predict the likelihood of failure. A relatively new tool is discrete fracture networks (DFN); applying DFN to understand potential bench scale failures in an open pit mining environment may help create more efficient and effective designs at an early stage of project development.

PREFACE

The thesis is based on original and independent work done by the author, Matthew King. The research idea was generated from practical work experience gained from a number of open pit mine designs studies ranging from exploratory pre-feasibility studies for developing projects to design optimization studies for operating and expanding mines. The research program including the methodology, data assessments and analysis, as well as documentation of this dissertation were developed by the author. The analyses are based on real-world data that was provided anonymously or from data derived from published literature. The research was supervised by Dr. Davide Elmo at the Norman B. Keevil Institute of Mining Engineering at the University of British Columbia.

TABLE OF CONTENTS

LIST OF TABLES

LIST OF FIGURES

LIST OF ABBREVIATIONS

3DEC	Three-dimensional numerical modeling code for advanced geotechnical analysis of soil, rock, ground water, structural support, and masonry developed by Itasca
CFA	Cumulative frequency assessment
DFN	Discrete fracture network
DIPDIR	Dip direction
FOS	Factor of safety
FracMan	Fractured rock system software developed by Golder Associates
ISRM	International Society of Rock Mechanics
OPS	Open Pit Simulator (SIROMODEL) software developed by CSIRO

ACKNOWLEDGEMENTS

I would like to express my sincere gratitude to the people who have supported and encouraged me throughout the duration of being a graduate student.

Thank you to Dr. Davide Elmo for supervising my work, providing guidance and helping me navigate the challenge of being a student while also growing my young family. His patience, understanding, and support has been greatly appreciated.

Thank you to Piteau Associates Engineering Ltd. for providing financial support and allowing for this Master's work to be completed while continuing my employment. In particular, thanks to my early mentors, Mark Hawely and Al Stewart, who encouraged me along the career path that led me to conduct this research.

I would also like to thank CSIRO for providing an academic license of the SIROMODEL software that allowed me to undertake this project.

To Eleanor and Edmund, keep collecting rocks

To Meghan, sorry about all the rocks

CHAPTER 1: INTRODUCTION

Rocks are as old as the earth itself yet the field of rock mechanics and rock engineering is relatively young. Archeological remains left by ancient civilizations such as the Egyptians and Romans indicate early forays into rock mechanics and rock engineering; however, rock mechanics has only been considered a field of study for approximately 75 years. According to the International Society of Rock Mechanics (ISRM), founded in 1962:

> The field of rock mechanics and rock engineering includes all studies of the physical, mechanical, hydraulic, thermal, chemical and dynamic behaviour of rocks and rock masses, and engineering works in rock masses, using appropriate knowledge of geology (ISRM Statutes).

The aspects of the field of rock mechanics of interest in this paper are both physical and mechanical. A rock mass consists of both intact rock and structural discontinuities, the gaps between intact pieces of rock. In 1971, J.P. Ashby opened his Master's dissertation with the following: "The behaviour of discontinuous rock slopes is still only partially understood." Now, despite an improved understanding of discontinuous rock slopes, models to predict slope behaviour still require calibration and adjustment to approximate actual conditions.

When developing a mine design, kinematic analyses are used to predict the theoretical as-built slope profile - the steepness of the open pit mine. Once the mine is excavated and built out, the slope profile, or breakback, is observed and recorded. Typically, the observed breakback is steeper than what was predicted during the design phase. With operating mines, it is then possible to calibrate the design to mimic what was achieved. However, it would be preferable to

be able to optimize the design before mining activities begin. If steeper designs could be provided during the early phases of development, more mining projects would be considered as economically viable, allowing more projects to progress to the next stage.

Many of the advances in the field of rock mechanics have come as the result of advances in computer technology. Before increased computing power, which allows for complex analytical problems to be solved with precision, practitioners relied on estimates of values using trigonometry tables or stability charts. More recently, advances in technologies have allowed for greater capacity of data collection and also data computation. The application to the field of rock mechanics has allowed for solutions of more complex analytical problems and consideration of probabilistic outcomes. Despite all these advances in data collection and computational abilities, uncertainties remain in our understanding of the behaviour of excavations developed in a discontinuous rock mass. However, if we changed the kinematic analysis tool used to predict the as-built slope profile, could engineers accurately predict the observed breakback? Are discrete fracture networks the right tool?

This dissertation aims to further define the problem, utilizing a discrete fracture network for the kinematic assessment of bench scale failures in an open pit mining environment, and identify some of the uncertainties and their potential influences on the solution rather than defining a solution to the problem. It is assumed that the reader represents an informed audience with an understanding of geological engineering and rock mechanics principles.

The driving influence behind this work is to develop a better understanding of the kinematic design process in the context of open pit mining. Having worked on a number of design studies for open pit mining operations around the world, a consistent observation was made pertaining to the kinematic assessment of the expected breakback angle for a single bench; in most cases the predicted bench face angle was flatter than the observed slope performance. This is not a new observation. Across the mining industry it is generally acknowledged that as-built slopes, either from blasting trials or mining activities, tend to be steeper than the kinematic design angles used to assess the slope geometry configuration established during feasibility design studies. Though this concept is generally well known, it is not well understood as to why or how this occurs. For active operating mines the difference is readily identified through a comparison of the cumulative frequency assessment (CFA) for slope performance data and kinematic assessments. The CFA distribution from analytical kinematics is generally a broader distribution while the CFA distribution of as-built slope conditions are typically much tighter, especially if pre-split blasting methods are successfully implemented as the CFA distribution will cluster at the pre-split angle. The analytics indicate an expectation for more failures to occur at angles both flatter and steeper than what is observed in the slope documentation data.

As shown by Veillette et al. (2018); a reasonable match can be achieved through a calibration process of the conventional kinematics such that the analytical CFAs provide a curve that is quite similar to the observed bench documentation to inform future excavation within that design sector. From this calibration new design criteria can be established and provided that allow for greater reliability during excavation. While the calibration of traditional kinematics appears to be

a repeatable process it is generally valid only for the specific site conditions and does not fully explain how the rock mass behaved or is expected to behave kinematically.

Ultimately, the question is: why did conventional kinematics not predict the actual slope conditions? With the right structural model, we as engineers should be able to accurately predict the resulting slope geometry. What exactly was different between the original analytics and the observed conditions? What was the difference in the population of predicted failures and the observed failures? What was it that led a kinematically viable wedge to not be observed in the actual conditions?

The answer to these questions offers the possibility of improving the slope design process such that steeper slopes could be considered at earlier stages of the design process, increasing the efficiency of design and also of active mining operations. As the demand for minerals continues to grow and ore bodies become exhausted, increasing the efficiency of the mine design process as well as the economic viability of the mine itself, is what the industry is striving for.
The introduction of discrete fracture networks to the field of rock mechanics and rock engineering holds the potential of finding an answer to these questions.

CHAPTER 2: REVIEW OF KINEMATIC THEORY AND ANALYSIS

The assessment of slope stability in rock can be simplified to two basic components:

1. Structure, requiring the assessment of failure along structural discontinuities within the rock mass; and
2. Intact rock, requiring the assessment of failure through the intact rock within the rock mass.

Site-specific geological conditions and the scale of the slope being assessed influence whether the assessment involves one or both components.

A rock mass consists of intact rock and structural discontinuities that separate the intact pieces of rock from each other. For the following discussions, intact rock is defined as medium to very strong rock (i.e. ISRM Hardness of R3 or greater) that has potentially undergone some degree of alteration but not enough to significantly affect it (i.e. ISRM Weathering of Fresh to Slightly weathered). As established over fifty years ago by Douglas Piteau:

> The study of stability of slopes in rock is basically a problem in engineering geology and assumes that the rock mass is anisotropic, heterogeneous and discontinuous in nature and that failure tends to be confined to structural discontinuities (Piteau, 1970).

The physical and mechanical properties of a rock mass are typically significantly stronger than those of the discontinuities and therefore the main focus of assessments is going to be on the discontinuities - the weakest link. As raised by Piteau, there is an additional, important factor and that is pore water pressures along the discontinuities. This pore water pressure, along with other physical site-specific conditions such as mineralogy, lithology, weathering and alteration, local

or regional stresses (e.g., high horizontal stresses due to tectonics), slope geometry (natural or manmade), as well as strength reduction over time, need to be considered in conjunction with non-physical conditions such as risk tolerance and short or long-term intended use during the analysis and design process.

To correctly assess the stability conditions of a rock slope, either through back-analysis of failed slopes or by predicting the stability conditions of a future rock slope, it is important to understand the underlying (existing or potential) failure mechanism. Once the nature of the mechanism is known, the correct calculations can be applied.

When considering a rock slope the scale of the problem being assessed is sufficiently large that it is not simply a matter of assessing intact rock conditions, but rather assessing the rock mass conditions as whole (i.e., the interaction of the intact portions of the rock and structural discontinuities). Consequently the failure modes in a rock slope have to involve structure, rock mass, or a combination of the two.

> In rock slopes, instability occurs as a result of failure along structural discontinuities, such as bedding planes, joints, geological contacts, and faults. Instability seldom occurs in homogeneous material unless the rock is weathered or soft (Martin, D. and Piteau, D.M., 1977).

With this in mind, the underlying failure mechanism in the majority of rock slopes is going to primarily involve geological structural planes.

For structurally controlled failures, where the failure is primarily along discontinuities and the effects of intact rock mass are or are assumed to be negligible, the three main modes of failure as shown in Figure 1 and described by Hoek and Bray (1981) are:

- Planar
- Wedge
- Toppling

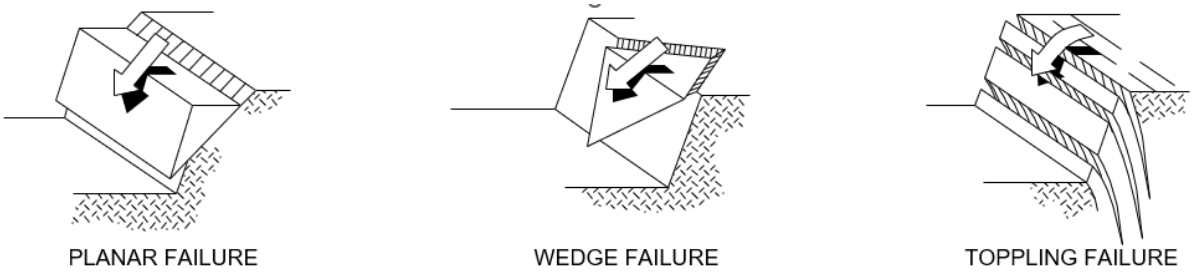

Figure 1. Typical kinematic failure modes

These are the three principal kinematic failure modes in their most basic form and should be common knowledge as part of any introduction to rock mechanics. More complex versions can be considered as follows:

- Planar – buckling in unjointed rock, three hinge buckling in jointed rock, or ploughing
- Wedge – pentahedral wedge by considering a basal joint, or polyhedral blocks that consider a rock block formed by the combination of multiple structural discontinuities
- Toppling – block toppling, flexural toppling, block flexural toppling and deep-seated flexural toppling

The more complex modes are an extrapolation of the basic failure modes and are typically applied to site-specific conditions. The discussion and review of kinematic theory presented

below will focus primarily on planar and wedge failures, which can be applied to failure of a polyhedral wedge.

2.1 Review of Kinematic Theory

The stability of a rigid block on an inclined plane is a well-known problem in Classical Mechanics, and according to Sagaseta (1986), its application was first presented by Ashby (1971) in his dissertation, "Sliding and Toppling Modes of Failure in Models and Jointed Rock Slopes" and subsequently included in many publications. Since then, research and literature on the topic has consisted of case studies, consideration of variable strengths and external loading forces, and a special case of solar rays and diurnal temperature variations that cause blocks to slide, but in general, the solution to a rigid block on an inclined plane has a known solution which has not changed significantly since first publication.

The stability of a rigid tetrahedral block (i.e., a wedge) on two inclined planes is a well-known problem in rock mechanics. Early assessments were conducted using stereographic techniques and the analytical solution was first presented by Hoek, Bray, and Boyd (1973) in their paper, "The stability of a rock slope containing a wedge resting on two intersecting discontinuities." Similar to planar failure, subsequent publications focus on case studies and consideration of strengths or other forces. The solution provided has not changed. One advancement from the original equation has been the inclusion of a basal plane in Rocscience's SWedge, which changes the tetrahedral wedge into a polyhedral wedge or block.

Planes and wedges form the basis of what one would call classic, traditional, conventional or just "simple" kinematics to describe the relatively basic assessments. Polyhedral wedges or blocks

present a new level of complexity which requires a modelling algorithm to determine the number of faces and shape of the block. It is no longer a simple manner of two structure planes intersecting a slope but rather a multi-faceted shape with concavities and convexities. Unlike plane failure or wedge failure where the "block" is always removable, with polyhedral blocks it is possible that a block cannot be removed. Early work by Warburton (1981) investigated vector analysis as a means of determining the stability of polyhedral blocks. Later Goodman and Shi (1985) presented block theory which provides a classification system for the stability of blocks. Further advancement was not made until after the early 2000s, when modelling algorithms were developed that could generate complex polyhedral blocks, largely due to increases in computational capabilities.

A general assumption for these kinematic failure modes is that the primary mode of failure involves sliding: one plane for planar failure and one or more planes for a wedge (tetrahedral or polyhedral blocks). Modes other than sliding are either ignored, e.g., rotation about an edge of the rock block and moments pertaining to rotation of the rock block, or require separate assessment, e.g., modes such as toppling.

The following sections will review and discuss the plane and wedge failure conditions and important considerations in their application for design of rock slopes with an emphasis on open pit mines. For more detail on the topic of planar and wedge failure, refer to "Rock Slope Engineering, 5th. ed" by Duncan Wyllie (2018), or any prior version of that text.

2.1.1 Plane Failure

Plane or planar failure is the simplest of stability assessments in rock mechanics because it is essentially a block on an inclined plane. The solution is a matter of determining the mass of the sliding block, the frictional resistance along the contact surface, and resolving the forces based on the geometry. While it is a relatively simple equation to solve, there are specific conditions and assumptions that need to be taken into account.

The first assumption in any calculations is that the “block” on the plane remains in contact with the discontinuity. This assumption is inherent to the failure mode because if the block were to lose contact then sliding would no longer be occurring and the mode would now be something else. Other failure modes include block toppling, block floating due excessive pore pressures, or sufficient block velocity to result in rolling or bouncing - a problem of rock fall.

In practice, widespread plane failure is generally rare in rock slopes due to the geometrical conditions required to produce such a failure. Such failure is typically associated with geological conditions that are the result of a structural environment where large planar structural discontinuities are expected to form. This mostly consists of sedimentary (bedded), as shown in Figure 2 (Wyllie, 2018), or metamorphic (foliated) areas but can also include granites if sheet joints develop. The wedge failure condition is a more general case and sometimes the plane failure condition is considered as a special case of the more general wedge failure analysis discussed later.

Figure 2. Plane failure along persistent bedding planes

Figure 3 shows a generalized example of planar failure from Hoek and Bray (1981), illustrating the conditions for which it has the potential to occur. For planar failure to occur the following conditions must exist:

i) The plane on which sliding occurs must dip perpendicular to, or nearly perpendicular to the slope face.

ii) The sliding plane must "daylight" on the slope face which means that the dip of the plane must be less than the dip of the slope face; this is referred to as "undercutting" where the slope face is steeper than a particular feature.

iii) The dip of the sliding plane must be greater than the strength of the contact surface. For dry conditions without cohesion this is the angle of friction.

iv) The upper end of the sliding surface either intersects the upper slope or terminates in a tension crack.

v) Release surfaces that provide negligible resistance to sliding must be present in the rock mass to define the lateral boundaries of the slide.

vi) Alternatively, failure can occur on a sliding plane passing through the convex "nose" of a slope.

Of these conditions, all but i) and iii) are used to identify the potential for planar failure to occur. Once the potential for planar failure has been identified whether it is critical (i.e., potential factor of safety (FOS) to be low or indicate failure) is determined by the strength conditions (friction angle); the first condition stipulates whether the failure is even going to be considered.

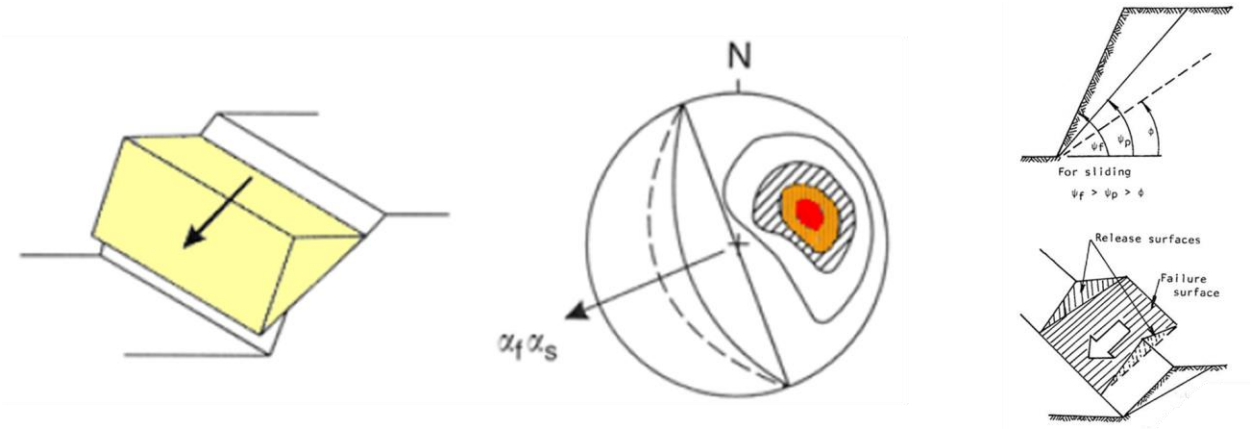

Figure 3. Idealized potential for plane failure (left); Stereonet of potential for plane failure (centre); Sliding conditions for plane failure (right)

For the first condition - perpendicularity - most literature sources indicate the plane needs to be within 20° or 30° of the slope face. As will be discussed further in the wedge analysis, planar failure can be considered as sliding that occurs along a single plane and is from a theoretical kinematic perspective unrelated to the dip direction other than the requirement to daylight (i.e., the dip direction is out of the slope and is undercut by the slope).

The second condition - daylighting or undercutting - is in practice the main condition that needs to be met because if the geometric conditions are not present then planar failure cannot occur. Conversely, in most cases, if planar structures daylight or undercut then failure is likely to occur (depending on the third condition).

With the third condition - strength conditions - if the plane is flatter than the angle of friction along the slope then the conditions will be stable because the block will not slide along the plane; however, this assumes dry conditions so the potential for movement remains (e.g., for saturated / pressurized conditions the stress conditions along the plane can result in movement) unlike the second condition where if the geometry does not exist plane failure cannot occur.

The fourth condition - upper slope continuity - is an assumption of full continuity whereby the plane either is continuous up to the upper slope or is intersected by a tension crack resulting in a modified geometry to the failure block. In geological environments where bedding or similar planar structures are expected to occur the assumption of full continuity is typically reasonable. In other settings it may only be reasonable to assume continuity for the height of a single bench excavation.

The fifth condition - negligible sliding resistance - is a necessary assumption to create the “block on a plane” structure, otherwise the sides would hold the sliding block in place and there would be an exposed or undercut plane with no movement occurring. This is often referred to as “lateral release” and the existence of these features is generally to be expected based on typical

orthogonal structural relationships in geological environments where bedding, foliation, or sheet joints exist.

The sixth condition - convex slope failure - is similar to the fifth, but defines that lateral release is not required if the geometrical configuration of the slope provides the lateral release. For example, if the sliding plane is fully continuous through a convex “nose” of a slope.

This initial generalized assessment can identify if it is physically possible for planar failure to occur, but it does not mean that planar failure will occur. Calculations are required for that to be determined. This initial assessment narrows down the size of the database that needs further assessment.

2.1.2 Stability Calculation of Planar Failure

Stability assessments of the plane failure condition can be done using stereographic projection techniques or commercially available software such as Rocscience’s RocPlane. Alternatively, the basic calculations can be completed by hand or using spreadsheet or scripted programs.

Stereographic Techniques

Stereographic techniques for stability assessments of planar failure are limited to identifying the critical modes provided the conditions are dry and cohesionless; however, the resulting answer is limited to an FOS < 1 (unstable), FOS = 1 (at equilibrium), or FOS > 1 (stable).

The process involves drawing a friction cone and the planar window lines for the desired range (i.e., 20° to 30° DIPDIR of the slope) then determining whether the planes are within the cone (stable), on the cone (at equilibrium), or outside the cone (unstable); anything outside the planar window is assumed to not be a planar failure.

Calculations

The plane equation is simply the solution of the free body diagram of a block on a plane and is commonly represented in the 2D form of an infinite slope. This representation is generally valid provided the geometrical conditions and strength conditions are appropriate. This will be discussed further in the wedge analysis section.

The common base form is a simple equation that considers the presence of a tension crack and water along the sliding plane or in the tension crack. Additional forces to consider are seismic from earthquake or blasting, surcharge loads, or reinforcement such as rock bolting. These forces would need to be added to the free body diagram and tangential components resolved to include in the equation.

During the bench design process it is generally assumed that tension cracks do not exist unless their presence is known. For the height of a single bench excavation the conditions are commonly assumed to be dry or depressurized given the limited scale of the slope. Depending on the degree of ground disturbance or blasting damage it can be assumed that without controlled blasting any cohesion is lost as a result of mining activities. These assumptions lead to a simplification of the base form of the plane equation down to a ratio of the tangent of the friction

to the tangent of the sliding plane. This is because without cohesion or water the weight of the block is cancelled out in the resisting and driving forces, leaving just the friction and the dip of the plane.

The base form of the equation can be rearranged using trigonometry identity manipulations to be presented with few terms (as shown in the Rocscience Verification Manual, 2019). However, as with all rederivation of equations care needs to be taken to ensure that there are no transcription errors in final print copies. In Read and Stacey (2009) the FOS for planar failure is presented in a rearranged form that results in a lower-than-actual FOS, leading to a more conservative design.

2.1.3 Wedge Failure

Wedge failures can occur over a much broader range of geological and geometrical conditions compared to plane failure; consequently, the study of wedge stability is an important component of rock slope engineering. The solution is much more complex because instead of a problem that simplifies to the basic block on a plane, it is the solution to a tetrahedral block. Like with plane failure, there are a number of assumptions that need to be taken into account, with the added complication of the sliding direction.

In practice, wedge failures are potentially the most common and occur in most geological conditions provided the structure exists (illustrated in Figure 4, Wyllie (2018)). As with plane failure there is a kinematic assessment to identify the potential for unstable wedges and a stability calculation to determine the factor of safety.

Figure 4. Typical wedge with sliding on both planes (left); Wedge formed by bedding and jointing, sliding on one plane (right)

As depicted in Figure 5 (Wyllie, 2018), for wedge failure to occur the following conditions, presented in a parallel fashion to the planar failure, must exist:

i) The direction of plunge of the line of intersection resulting from the formation of the wedge must be within a "wedge window" of perpendicularity to the slope face (see discussion below).

ii) The line of intersection between the two planes must "daylight" on the slope face which means the dip of the line of intersection of the two wedge forming discontinuity planes must be less than the dip of the slope face.

iii) The dip of the line of intersection must be such that the strength of the two planes are reached

iv) The upper end of the line of intersection either intersects the upper slope or terminates in a tension crack.

v) Two planes are required to form the wedge.

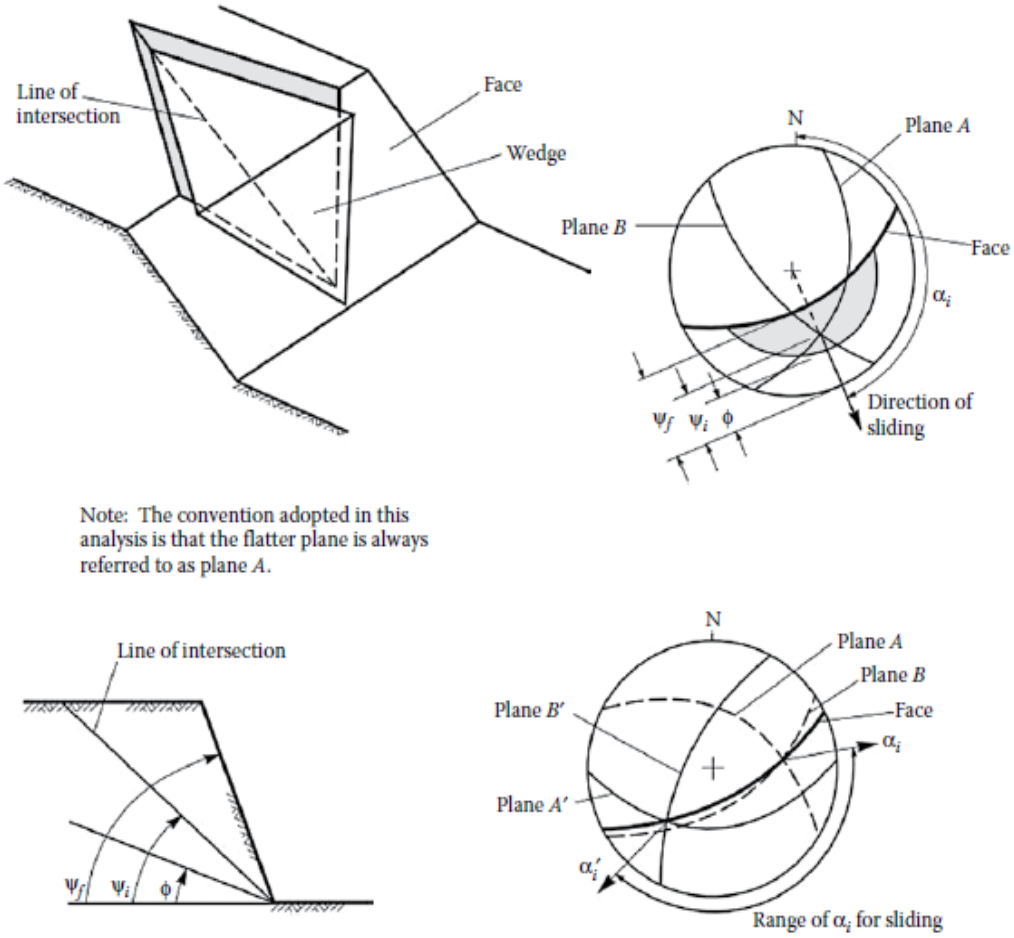

Figure 5. Conditions for wedge failure

Of these conditions, ii), iii) and v) are used to identify the potential for wedge failure to occur. Once the potential for wedge failure has been identified, whether it is critical (i.e., potential FOS to be low or indicating failure) is determined by stability calculations. Similar to plane failure, a "wedge window" can be established stipulating whether the failure is going to be considered.

Unlike the plane window which is generally agreed upon, there is not a consistently accepted "wedge window" within which the sliding direction of wedges is considered valid. With planar failure, the geometry of the sliding direction of the block on the plane is readily known as following the dip vector of the plane, since only one structure is involved and sliding is steepest due to gravity. Structures outside the plane window are excluded early in the analysis process.

With wedge failure, the line of intersection needs to be determined prior to deciding which wedges to include or exclude; consequently, all structures need to be assessed. Once the orientation of the resulting wedge has been determined, then its validity based on an obliquity check using a "wedge window" can be applied. The actual sliding direction of the wedge follows the line of intersection or one of the planes, as will be discussed later. As with plane failure, if daylighting or undercutting does not occur then there are no wedges formed to be assessed.

The third condition - the dip of the line of intersection - is more difficult to quickly assess for a wedge because of the geometry involved. With the additional plane involved in wedge failure the geometry needs to be known and the strength condition on both planes (which may or may not be the same) is required. Unlike the plane condition that is a simple "tilt test" of comparing frictional strength to the dip of the plane, for the wedge condition the line of intersection between the two planes must first be determined and then compared to the frictional strength along both planes.

The fourth condition - upper slope continuity - is again the assumption of full continuity on the structure involved in the formation of the wedge.

The fifth condition - two planes to form a wedge - differs from that of the planar assessment in that the two wedge-forming planes are specific planes. For planar assessment there is the assumption of lateral release features existing but with the wedge condition the two planes need to be identified.

Whether the wedge slides along both planes or just one plane can be determined from stereographic methods, as shown in Figure 6 from Yoon (2002), where (a) Single plane sliding: block movement is in the direction L1 along plane J1 only; (b) Double plane sliding: block movement is in the direction L12 along planes J1 and J2. (SL, great circle of slope face; J1 and J2, great circles of joint planes; LSL, true dip of slope face; L1 and L2, true dip lines of J1 and J2; L12, line of intersection between J1 and J2). A simple test: if the dip direction of either plane lies between the dip direction of the slope face and the direction of the line of intersection, then sliding occurs along one plane.

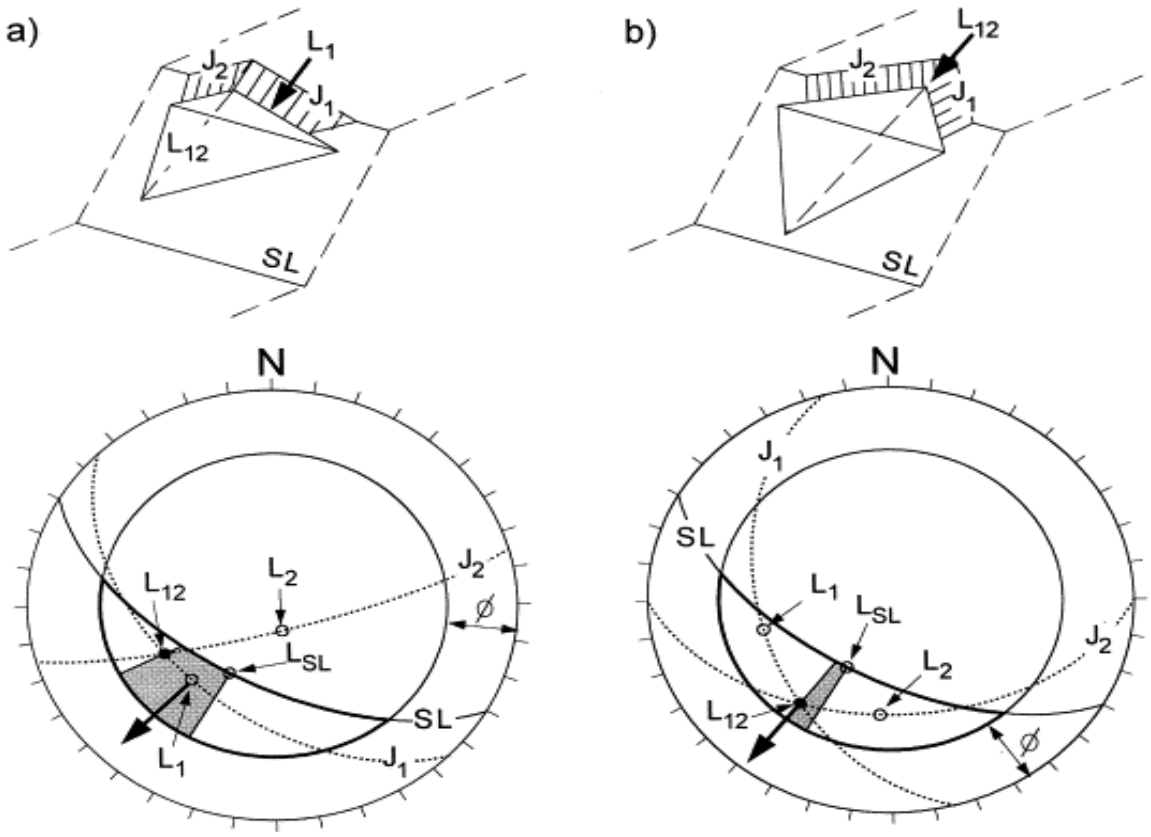

Figure 6. Single and double plane sliding

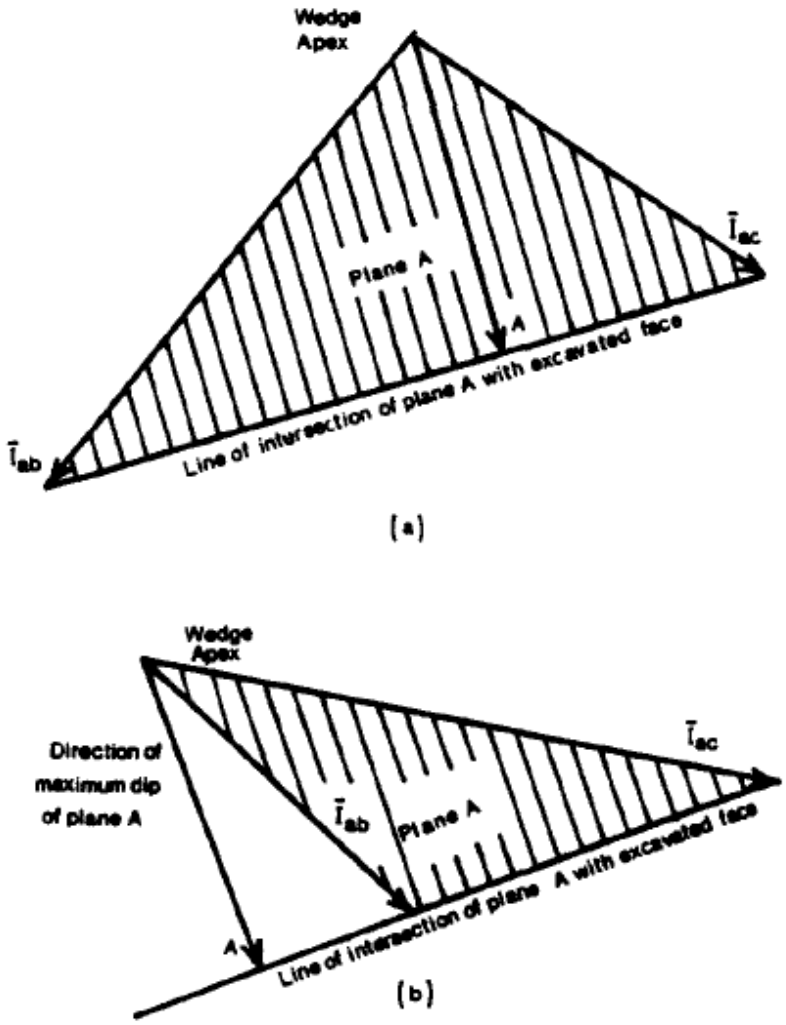

Figure 7. Conditions for sliding on one and two planes

Figure 7 illustrates, from a bird's eye view, the physical difference between sliding along one plane or both planes (Lucas, 1980). In (a) condition required for sliding on one plane, the dip direction of the plane lies between the azimuths of the two intersection lines between the apex of the wedge and the excavated slope face, resulting in sliding along the plane. In (b) condition required for sliding on the intersection of two planes, the dip direction of the plane lies outside of the two intersection lines and therefore sliding has to occur along both planes in the direction of the keel of the wedge.

A simple analogy would be to release a ball at the apex of the wedge to see which way it would roll. If the ball rolls straight down, only making contact with one plane then it is planar sliding. If the ball hits the other plane it is forced to roll down the trough, making contact with both planes.

While an initial generalized assessment for the potential planar failure can be done to identify whether wedges are formed, calculations are required to determine the stability. In practice, this step of checking for potential wedges is skipped and calculations are done regardless because of the ease and speed with which they can be performed. All data is processed at once and then filtered afterwards.

2.1.4 Stability Calculation of a Rock Wedge

Stability assessments of the wedge failure condition, like planar failure, can be done using stereographic projection techniques or commercially available software such as Rocscience's SWedge. Alternatively, the full equation for the solution of a wedge, as provided by Hoek, Bray and Boyd (1973), can be completed by hand or by using spreadsheet or scripted programs. However, given the increased complexity of the wedge solution, computational methods are the most practical and widely used methods.

Stereographic Techniques

Stereographic techniques for stability assessments of wedge failure are also limited to identifying the critical modes, provided the conditions are dry and cohesionless and the strength along the two sliding planes are the same (commercial software requires the strengths to be the same; other

situations require doing the stereonets by hand). The resulting answer is limited to FOS < 1 (unstable), FOS = 1 (at equilibrium), or FOS > 1 (stable).

The process involves drawing a friction cone and a plane for the slope face. But instead of looking at poles of structures, the plunge and direction of the intersection are plotted. In DIPS a Critical Zone for Wedge Sliding is identified, which is the area inside the friction cone and outside the slope plane area. Intersections inside the slope plane area are steeper and do not daylight. Intersections outside the friction cone, like with planar sliding, are stable.

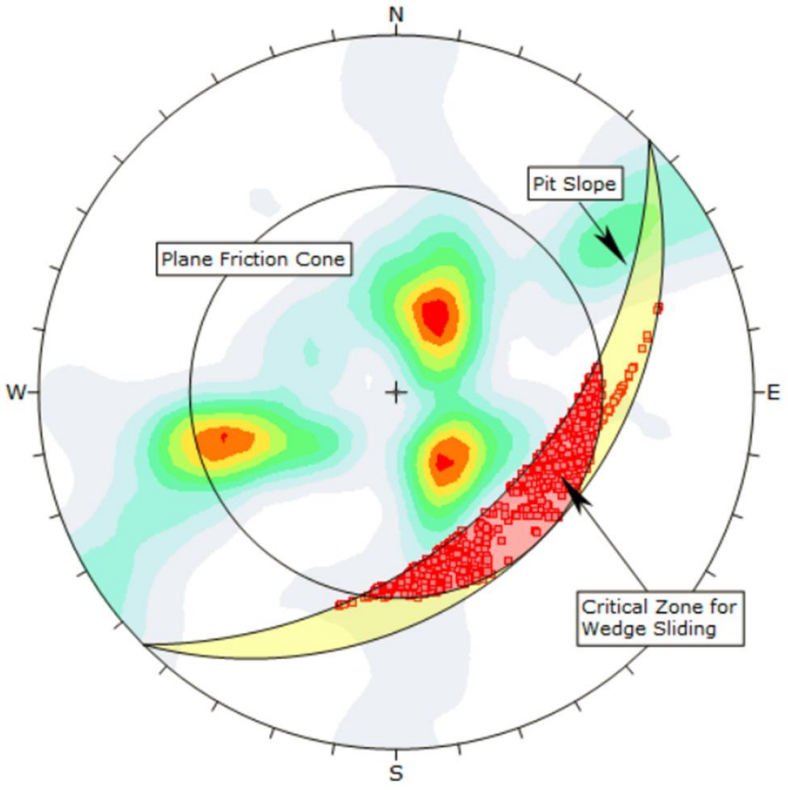

Figure 8. Sliding on one or two planes within primary and secondary critical zones

Figure 8 from Rocscience is a helpful visualization with regards to sliding on one or two planes (further discussion later): within the primary critical zone (red), wedges can slide on either two planes or one plane, but in the secondary critical zone (yellow), wedges always slide on one plane.

Calculations

The wedge is also the solution to the free body diagram but the tetrahedral block results in a more complex equation, the full solution of which is presented in Hoek, Bray, and Boyd (1973). The following assumptions in bold that are made during the course the analyses are presented in Hoek, Bray, and Boyd (1973):

i) **The wedge remains in contact with both discontinuity surfaces while sliding.**
   a. This assumption is somewhat similar to the previously stated assumption for planar failure, in that if the wedge were to lose contact either through floating from excessive pore pressures or a result of toppling occurring, then the failure mode would be changed.
   b. This assumption / requirement means that sliding is in direction of the line of intersection (refer to Section 2.1.6 for further discussion of this)

ii) **The influence of moments are neglected, i.e. it is assumed that all forces act through the centroid of the wedge**
   a. Introduction of moments requires additional calculation of forces and if resultant moments led to tipping about an edge then contact with the planes being lost changing the failure mode to block rotation (e.g., toppling) or involving rolling (e.g., rock fall)

iii) **The shear strength of the sliding surfaces is defined by a linear relationship**

$$\tau = c + \tan\ tan\ \varphi$$

where *c* is the cohesive strength and φ the angle of friction of the surface.

a. Since Hoek, Bray, and Boyd presented their original work in 1973 advancements in computational methods have allowed for other failure criteria to be considered. The assumption is that the strength conditions of the sliding surfaces are going to behave according to a specified relationship, of which there are multiple options (e.g., Mohr-Coulomb, Barton-Bandis, or Power Curve) to consider and the validity of those options in relation to the problem being assessed needs to be considered. For further discussion on these shear strength of discontinuities refer to Chapter 5 of Rock Slope Engineering (Wyllie, 2018)

iv) **Sliding of the wedge is kinematically possible, i.e. the line of intersection of the two planes on which sliding occurs daylights in the face of the slope.**

a. This assumption states that the wedge has to be removable and that sliding can occur. For this assumption to be true, the two planes are assumed to be continuous enough to intersect each other as well as the face of the slope. The intersection is typically assumed to occur at the toe of the slope so the structure can occur anywhere in the rock mass, but for this calculation it is assumed to be at the toe. Effectively, the discontinuities are fully continuous through the rock mass and ubiquitous.

The solution to the wedge problem is presented utilizing both engineering graphic and stereographic methods and was found to be accurate within a few percent. Granted these

methods were done by hand and great care had to be taken to ensure accuracy of the results. An analytical solution is also presented that replaces the hand-drawn graphical methods, removing the inaccuracy of hand measurements. Using a computer or scientific calculator eliminates rounding errors, providing a more accurate solution to the wedge equation. While stability charts were presented at the time and in later publications to aid in approximation solutions, current computational capabilities allow for extensive use of the analytical solution which is used in commonly available commercial software such as Rocscience's SWedge, which is widely used in industry.

Anyone creating their own computational solution using the equations provided by Hoek is cautioned to take care in applying the assumptions and to validate the solution against the worked examples in Hoek, Bray, and Boyd (1973) and later versions of *Rock Slope Engineering*.

2.1.5 The Influence of Dry and Cohesionless Conditions

As mentioned with the plane equation, when the conditions along the sliding surface are dry and cohesionless then the problem simplifies to a ratio of the friction angle to slope angle. Consequently, the mass and volume of the block and the size of the contact area become irrelevant and the solution is the same regardless of these parameters. Conversely, if there is water involved or cohesion along the sliding surface then the block's mass, volume, and contact area are required to define the problem. In the case of plane failure mentioned previously if the geometry can be assumed to be uniform along the length of the plane then a two-dimensional representation can be made, otherwise a wedge geometry must be considered (further discussion of this in Section 2.1.6). As shown in Table 1, the FOS calculations for an equivalent 2D plane

(i.e., infinite plane case) as shown in Figure 9 results in a lower FOS than that of a 3D wedge (i.e., finite tetrahedral block) as shown in Figure 10, involving sliding on one plane only.

Table 1. Comparison of FOS for 2D planar vs 3D wedge for a 40° dipping plane vs a wedge formed by 40°/350° and 70°/035°

Example Case	Planar FOS (RocPlane)	Wedge FOS (SWedge)
Cohesionless (φ=35°, c'= 0 kPa)	0.83	0.83
Nominal Cohesion (φ=35°, c'= 10 kPa)	0.97	1.02

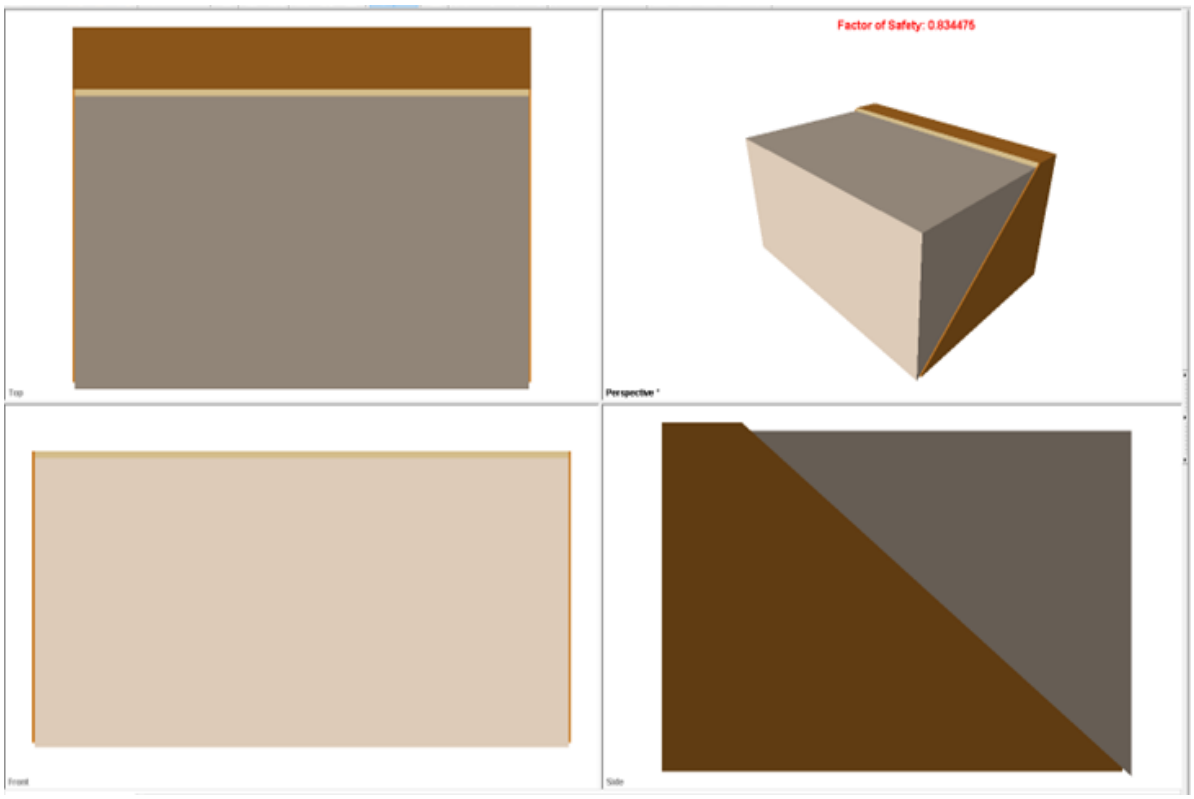

Figure 9. Rocplane analysis

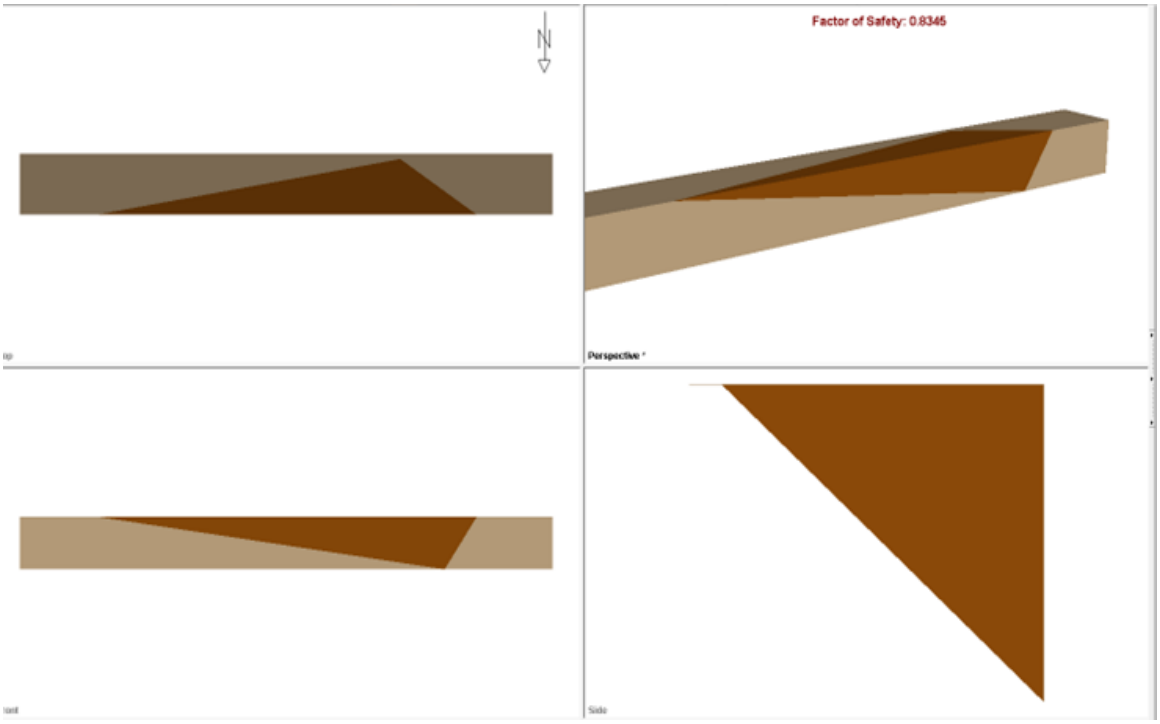

Figure 10. SWedge analysis

The same is true for the wedge condition. If both sliding surfaces are dry and cohesionless then the solution reduces to a ratio of the friction angles to the dip angles of the sliding planes. The height of the wedge or its overall size do not affect the final FOS (a height still needs to be specified to allow for computation); whereas if water or cohesion are present then the scale of the problem needs to be defined. When establishing a calculation, it is important to change default input parameters, especially those that will contribute to the solution, for example using a 15 metre or an 18 metre bench height will provide different answers once cohesion or water are involved.

2.1.6 The Importance of Sliding Direction for a Wedge Failure

As mentioned in Section 2.1.3, a wedge failure has the potential to slide along one plane or both planes. This is an important consideration because it distinguishes whether an assessment needs to be considered as sliding occurring on one plane vs sliding along two planes, which will be discussed next.

For planar failure the sliding direction is simply along the dip vector of the plane, but for a wedge formed by two planes there are three possible scenarios:

1) Sliding along the line of intersection (a classic wedge)
2) Sliding along one plane only (a planar wedge)
3) Sliding along either plane (also a planar wedge)

Understanding the scenario is important because "if sliding down the line of intersection is always assumed, then the stability of the wedge will be overestimated for cases in which sliding down a single plane actually occurs" (Hocking, 1976).

When two planes combine to form a wedge geometry it does not mean that the wedge will behave as a "true wedge" or a "classic wedge" with sliding occurring along both planes with movement in the direction of the line of intersection. The wedge could behave like a "plane" with sliding occurring along only one of the planes.

With this scenario, there are two implications:

1. How will the FOS be calculated? Is it a wedge or is it a plane?

2. How will the results be tabulated? Based along the plunge of the line of intersection of the wedge or the dip vector of the plane along which sliding occurs?

The scenario of sliding along one plane is analogous to a plane failure with the block now being tetrahedral. As mentioned previously, if the conditions are dry and cohesionless then the size of the block does not matter and the planar equation simplifies to a ratio of the friction and slope angle tangents. Sliding direction is in the direction of the dip vector of the plane. For a wedge undergoing sliding along one plane, the direction of movement would also be in the direction of the dip vector of the plane and not along the line of intersection of the wedge. If the second plane is changed to be a "perfect release" (i.e., dip of 90° and a DIPDIR equal to the DIPDIR of the first plane minus 090°) then the resulting tetrahedral wedge produces results in the same FOS as the plane equation because the second plane is vertical.

If the original wedge geometry is maintained and the direction of sliding is assumed to be along the line of intersection, then utilizing the wedge equation results in a higher FOS due to the other plane contributing to the resisting forces. As noted by Hocking (1976), this results in an overestimation of the FOS. Some early versions of computational software did not make this distinction and it was up to the user to be aware of it. Current versions of software, like SWedge, provide details whether the mode of sliding is along plane 1, plane 2, or both.

For scenarios involving cohesion or water pressures along the planes, the wedge equation must be used because the tetrahedral 3D geometry is not analogous to an infinite 2D plane; the volume of the tetrahedral block is required.

The general nomenclature when referring to the planes is to call them Plane 1 and Plane 2 or Plane A and Plane B, with Plane 1 or A typically being the flatter dip of the two planes, but this is not always the case nor a requirement. For this document, the Plane 1 and 2 convention will be used to be consistent with other literature and Rocscience.

In Table 2, the sliding scenarios associated with a classic wedge, planar wedges 1 and planar wedge 2 are defined.

Table 2. Sliding Scenarios

Scenario	Sliding along Plane 1 is…	Sliding along Plane 2 is…	Results in sliding along	Figure
Classic Wedge	Restricted by Plane 2	Restricted by Plane 1	The line of intersection	Fig 11(i)
Planar Wedge 1	Unrestricted	Restricted by Plane 1	The dip vector of Plane 1	Fig 11(ii)
Planar Wedge 2	Restricted by Plane 2	Unrestricted	The dip vector of Plane 2	Fig 11(iii)
Planar Wedge 1 or 2	Unrestricted	Unrestricted	The steeper dip vector of Plane 1 or 2	Fig 11(iv)

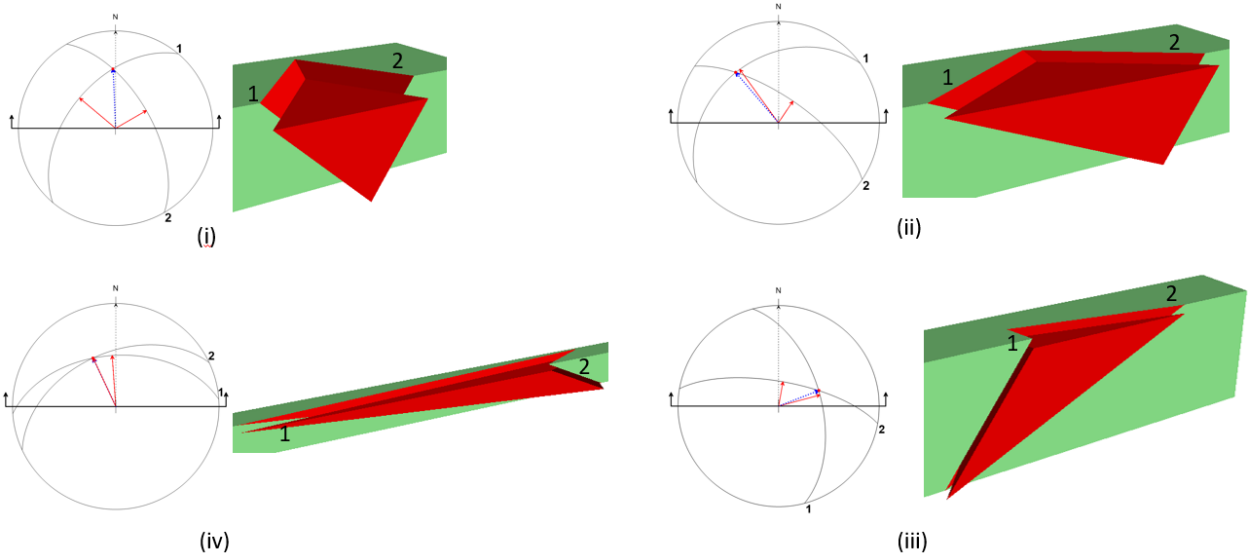

Figure 11. Stereonet and perspective views of double and single plane sliding scenarios

In Figure 11, the stereonet and perspective views of sliding scenarios indicate: (i) double plane sliding, a “wedge” where sliding along either plane is restricted by the other; (ii) and (iii) single plane sliding, a “planar wedge” where sliding along one plane is restricted by the other which is unrestricted; and (iv) resultant geometry is “planar wedge” but both planes are unrestricted.

2.1.7 Polyhedral Block Kinematics

Representing potential failure mechanisms as polyhedral blocks rather than an idealized plane or wedge failure addresses the concerns regarding any assumptions that are made as a result of the size of block or how sliding is occuring (Sections 2.1.5 and 2.1.6). A polyhedral wedge is a fully defined 3D rock block that has a single resultant vector defining the exit geometry and there is one resultant FOS for the block.

As described in Goodman and Shi (1985), the main concept of block theory is that when conducting stability analyses for an excavation it is not necessary to look at all the possible combinations. It is possible to ignore many of the irrelevant blocks and proceed directly to analysis of the critical blocks, also called key blocks.

Identifying key blocks is made possible through the theorem on the finiteness of blocks. This is similar conceptually to plane failure analysis in that only planes that fall within the plane window are assessed for stability and planes outside of the plane window are ignored. Or in the case of wedge failures, if the wedge is non-daylighting, stability assessments are not required. For polyhedral blocks, only the removable blocks need to be assessed for stability.

As shown in Figure 12, Goodman and Shi (1985) provide the following classification systems for polyhedral blocks:

- Type V – Infinite block: assuming that there is no internal cracking or degradation of the rock mass, these blocks provide no hazard to an excavation surface because the block cannot move, it is non-removable.
- Type VI – Tapered block: finite blocks that are non-removable due to their shape; they require a change in the excavated slope face in order to become removable.
- Type III – Stable without friction: a non-tapered finite removable block that has a favourable orientation relative to the resultant force and will remain stable even without mobilizing frictional forces. It is possible to lift the block, but under gravitational forces alone the block will remain at rest (for example a block in the floor of a tunnel or in the berm of the bench slope). Another way to consider this type of block is one where the resultant force is away from the excavation.
- Type II – Stable with friction: also a non-tapered finite removable block, but one where the resultant force of the block is towards the excavation. This type of block has the potential to be a key block, but only if the frictional resistance to sliding is exceeded, either due to a change in the resisting forces or driving forces (e.g., strain softening, pore pressures, loading, etc.). While Type II blocks are indicated to be stable, a FOS calculation would still need to be performed to see if it meets acceptance criteria.
- Type I – Unstable without support: a true key block. In addition to being non-tapered finite and removable, this block is oriented in an unsafe manner such that it can freely slide or fall into the excavation.

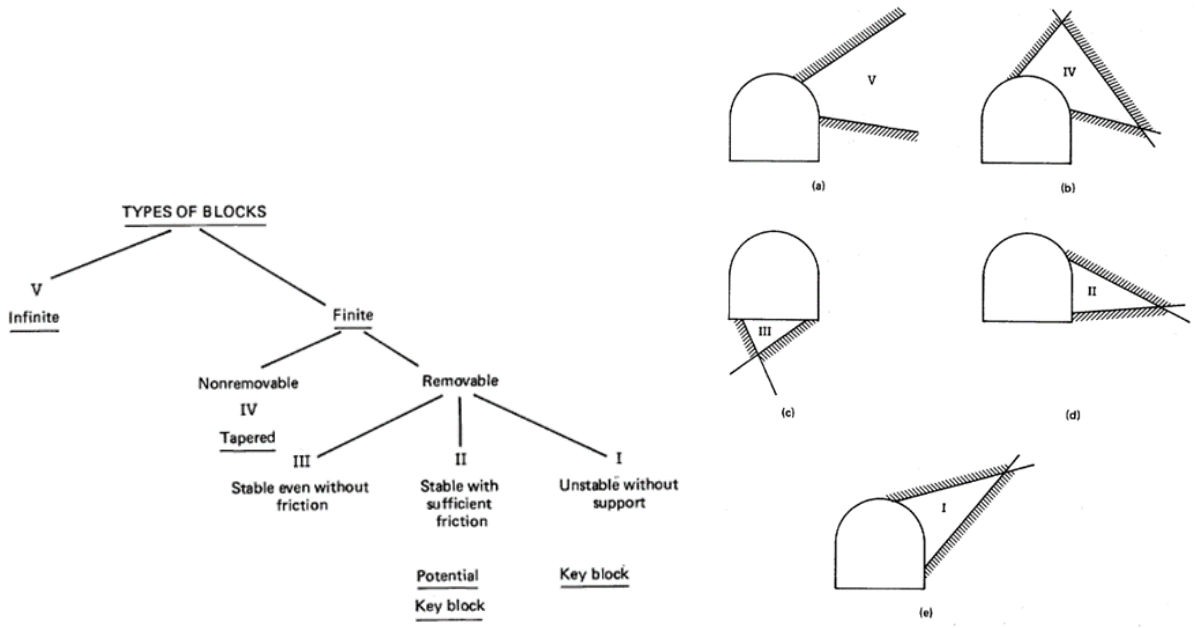

Figure 12. Types of blocks: (a) infinite; (b) tapered; (c) stable; (d) potential key block; (e) key block

The modes of failure for a removable polyhedral block are:

a) sliding along one joint (i.e., planar failure);

b) sliding along multiple planes (if only two planes it is a wedge failure, otherwise it is a polyhedral failure); and

c) falling, which is unlikely to occur in surface excavations unless there is a progressive failure (shown in Figure 13, from Goodman and Shi (1985)) of a series of blocks that results in a void into which a rock block could fall.

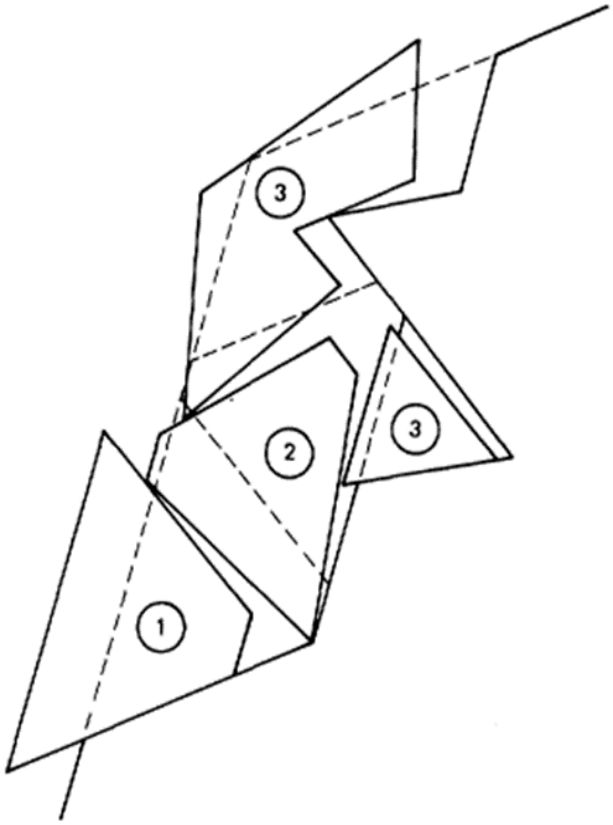

Figure 13. Example of progressive slope failure, blocks numbered according to order in which they fail

Progressive failure is not considered for plane or wedge failure because the structures are assumed to be continuous for the entire slope geometry therefore the resulting failure is a block volume of the entire height of the slope. However, with polyhedral blocks and block theory, the failure of a key block creates a space and the blocks located behind the key block may become removable. If they are unstable they would then fail into the vacated space.

The consideration of polyhedral wedges or blocks as presented in block theory by Goodman and Shi (1985) and using the modelling algorithm method described by Elmouttie and Poropat (2010) results in the generation of polyhedral (rock blocks) that have no limitation to their

complexity with respect to the number of faces or shape that make up the block (Open Pit Simulator (OPS), called SIROMODEL (CSIRO, 2020). Refer to the authors listed previously in this paragraph for more details.

2.2 Discrete Fracture Networks

As the primary focus of this thesis is on the use of a discrete fracture network (DFN) in the context of kinematic analysis at the bench scale in open pit mining applications, a discussion of DFNs is required.

DFNs were introduced in the late 1970s. Within the hydrogeological community there has been much debate regarding the value of the DFN approach compared to the stochastic continuum approach (Dershowitz et al., 2004). Modelling groundwater flow through fractured rock mass systems and fractured reservoirs was one of the early applications of DFNs (Elmo et al., 2015). DFNs originated from the areas of study that deal with subsurface rock, not rock that is exposed on the surface, making it difficult to determine the validity of a DFN if one cannot see the rock that is being modelled. Since then, DFN modelling has been applied to other rock engineering problems including surface mining applications.

The method proposed by the ISRM (1978) indicates the following parameters when collecting information on structural discontinuities in rock masses from field observations: orientation (dip and dip direction), spacing, persistence, roughness, wall strength, aperture, filling, seepage, number of sets, and block size. In addition to this list, the number of features per set (i.e., quantity) should also be recorded as well as the location (easting, northing, and elevation or

x,y,z), it is generally assumed that one would record the location of the mapping outcrop from which the measurements were made.

In the context of conventional kinematics, the only parameters required are orientation and those affecting discontinuity strength. Continuity of the structure is not required because of the assumption that structures are fully continuous and ubiquitous, which means that location is also not required. The number of features (i.e., quantity) is only needed if allowing for counting of the same failure more than once in a statistical assessment. However, for polyhedral and DFN-based kinematics, additional parameters are required (i.e., location X, Y, Z and radius) which are determined stochastically through statistical distributions of the DFN input parameters. Parameters that describe the surface conditions (roughness, filling, wall strength) are assessed separately and in a DFN a single strength is assigned to features (or sets of features). Aperture or gap distance of a feature is not physically modelled in a DFN; there are not two surfaces 1 cm apart representing an open joint. The strength of the single feature would be adjusted based on the parameters mentioned.

The main parameters of importance in a DFN are:

- Orientation – the dip and dip direction are easily mapped in the field from surface outcrops or exposed rock cuts or collected from subsurface drilling data. The orientation of structures can have a lot of variability depending on the geological conditions, which are generally addressed through sufficient field data to describe the main sets.
- Location – a DFN generates a spatial distribution of the structures based on an assumed distribution model and using the measured spacing of the structures from field

observations to inform that model. Spacing is more challenging to determine and generally requires the assumption of an average orientation from which to base the spacing.

- Continuity – is the most difficult to determine because it is not possible to directly map the 3D spatial extent of a feature. Without a slope failure exposing features and bounding features, only the surface trace length of a feature can be observed. Whether this trace length represents the longest or shortest portion of the features depends on the true representation of the feature. Refer to works by Mauldon (1998) or Zhang and Einstein (2000) for more discussion on continuity.

A common way in which DFNs are generated, assessed, compared, or validated is through the various measures of fracture density and intensity. Figure 14, modified from Dershowitz and Herda (1992), demonstrates the measures for fracture intensity.

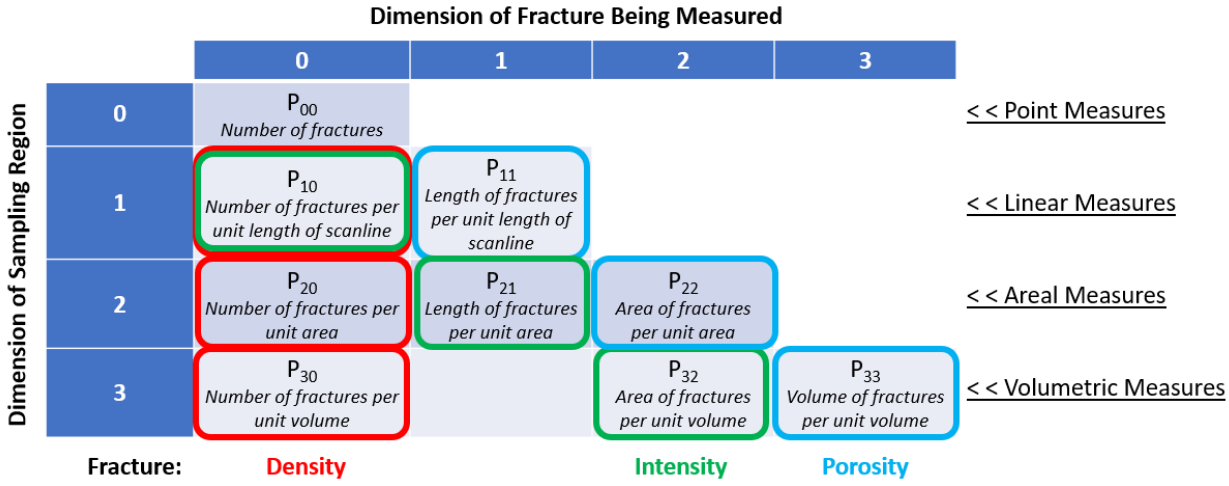

Figure 14. Nomenclature for fracture density, intensity, and porosity of a DFN

The nomenclature is to use "Pij" where i and j are numbers ranging from 1 to 3. The first number refers to the dimension of the measurement region (i.e., P1 for a line, P2 for an area, and P3 for a volume) and the second number refers to the dimension of the structures (i.e., P#1 for trace

length, P#2, for area, P#3 for volume). The most commonly used parameters are those which describe the intensity of the DFN:

- P10: number of fractures per unit length of scanline; comparable to fracture count crossing a scanline in surface mapping or fractures intercepted by a drillhole.
- P21: length of fractures per unit area; comparable to the length of fracture traces observed on a rock face such as outcrop mapping or photogrammetry.
- P32: area of fractures per unit volume; this parameter cannot currently be measured in the field.

A method for determining P32 based on P21 and the dimensionless constant of proportionality (C21) using the linear relationship P32=C21 x P21 is proposed by Dershowitz and Herda (1992). The value for which depends on the orientation and size distributions of the joint set and the orientation of the slope face (Havaej, 2015). An alternative method by Staub et al. (2002) is to determine P32 from P21 using a series of simulated models to determine C21. For more details, refer to the referenced sources.

As discussed by Elmo and Stead (2010), a DFN is a tool allowing for simulation of more realistic geological models. A stochastic DFN creates a realistic geometric model of the discontinuities that reflects the heterogeneous nature of a fractured rock mass. The alternative is to create a model containing each fracture explicitly for a true representation of the observed conditions. This task would be incredibly difficult and still have limitations and assumptions associated with it. As presented by Steve Rogers (2023), a DFN is meant to create a representation of features that we know exist but are too difficult or too time consuming to model individually. DFNs are

not intended to be a copy of reality but rather a proximate representation of real-world conditions.

The validity of this representation or how accurately the model represents real-world conditions is an area requiring further study. DFNs are generated using an assumed spatial distribution model and statistical distributions of input data. As discussed by Elmo et al. (2015) data uncertainty and variability need to be addressed otherwise it perpetuates into the model. Currently, validation of DFNs involves sampling of the modelled DFN and comparing the distributions of the sample synthetic data to the input data. This type of validation merely confirms that the DFN was generated as expected (i.e., in compliance with statistical distribution of the input parameters). It does not check whether the synthetic data reproduces the field measurements.

Reliable validation of DFNs is difficult because a DFN is based on a small subset of data intended to be representative of the structural fabric for a larger area in a specific region. The DFN is used to create a larger set of data that represents the remainder of the structural fabric; however, the DFN cannot be thoroughly checked without collecting a large dataset. Additionally, multiple realizations of the DFN can be generated from the input parameters and still be statistically valid. Consequently, multiple realizations of a particular DFN are required; how many are required is unknown, but a sufficient number would be where additional DFNs do not change the outcome of the analyses from the prior DFNs.

2.3 Evolution of Kinematic Theory

Figure 15 shows the progression of kinematic assessments of rigid blocks, which originated with simple, to potentially complex, stereographic projections allowing for a graphical solution and later computational solutions were derived to allow for more precise assessments. These methods continued to be used as the primary means of analysis until the late 1990s when computers allowed for more complex assessments, but still based on the original derivations, which have become standard industry practice. The introduction of DFNs presents a new advancement in kinematic assessments for the present and for the future, the inclusion of step-path failure through rock-bridges would bring kinematic theoretical analyses closer to reality.

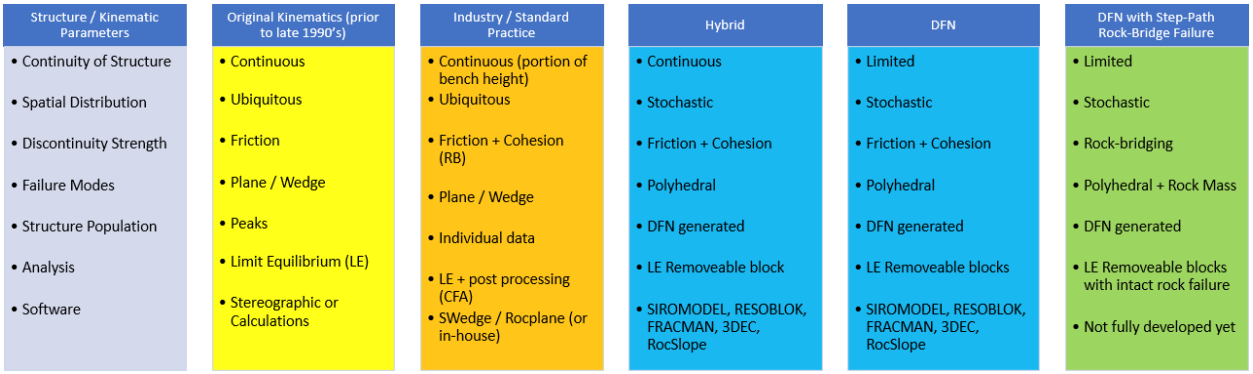

Figure 15. Summary of the evolution of kinematic theory and computational abilities

Early kinematic analyses required certain assumptions to reach a solution. Two of the main assumptions concerned the continuity of the structural discontinuities and their spatial location:

1. Ubiquity – this assumption asserts all structures can occur anywhere in space and therefore any structure can combine with any other structure; and
2. Fully continuous – this assumption avoids the need to assess rock-bridging because the structures in question are fully continuous for the scale of the problem being assessed.

A result of these two assumptions means that any wedges formed during kinematic analyses are assumed to have a line of intersection connected with the toe of the slope, thus creating the largest possible combination of those two structures. Essentially conventional kinematics analyses always assume the largest possible geometry or worst-case scenario (i.e., largest possible rock block) that can result from the combination of any two structural discontinuities. The shear strength of discontinuities were assumed to behave following the Mohr-Coulomb failure criterion (i.e., linear strengths) consisting of friction, generally without cohesion to allow for stereographic analysis. Early failure modes were limited to just simple planar or wedge failure for ease of calculation. The datasets historically were small and calculations limited to an assessment of only the peak structural orientations. Analyses consisted of stereographic projections, vector analysis, and calculation of FOS.

Approximately 15 to 20 years ago, kinematic analyses advanced due to improvements in computing methods. The assumption of ubiquitous fully continuous joints remained, but shear strengths could include cohesion or alternative failure criterion options and the datasets analyzed could consist of the full data set (i.e., individual measurements) not just the peak orientations. Stereographic analyses were still performed to develop an understanding of the underlying structural conditions, but FOS calculations were carried out for all the data because computational time was no longer a restriction. A new step was added to the analysis process involving the post-processing of all FOS data to determine what was relevant. Instead of assessing the FOS of a few key critical wedges, the entire population of wedges can be assessed and the results presented as a cumulative frequency distribution so that designs can be determined statistically.

While the kinematic theory for polyhedral kinematics and block theory has existed for nearly 40 years, it has not been widely applied in industry as part of the standard design process. A number of possible factors can be attributed to this, including the extent of the computational effort required to determine multiple polyhedral blocks, and the large database of georeferenced structures from which the blocks could be determined. It was not until discrete fracture networks (DFNs) became more common that polyhedral kinematics could be paired with DFNs allowing for the assessment of multiple polyhedral blocks without the need for explicit modelling of all the input structures. However, the topic is still relatively new as evidenced by the 5th edition of the "Rock Slope Engineering" book, published in 2018. This text contains a brief discussion of DFNs under "Special Topics", a sub-heading of Chapter 12 - Numerical Analyses.

A DFN provides a stochastic representation of the structural discontinuities in a manner that is meant to simulate reality. This addresses the assumption of ubiquity because structures are no longer allowed to occur anywhere and everywhere, they occur at a specific location in space. Additionally the assumption of fully continuous structures is addressed because the features represented in the DFN have a specific continuity. The resulting failure modes become a case of removable blocks, which may or may not be tetrahedral wedges. The shear strength conditions assessed continue to be Mohr-Coulomb or other failure criterion supposed by the analysis software. The population of potential blocks is now a matter of only if the structures combine to form a block that is removable. Unlike the simple plane and wedge kinematic assessments where everything combines and is always removable because the rock mass is assumed to be ubiquitous and fully continuous, with a DFN, if the features are not spatially located nor continuous, then

there is no block produced. A rock-bridge is all that is required to result in a block that cannot move or to result in a block not being formed. Therefore if a rock mass is too discontinuous no blocks will be formed.

However, the DFN approach, as will be discussed later, needs to have a validation of the original input DFN to confirm that it is an accurate representation of real-world conditions. A DFN that is developed based on statistical inputs from real-world data does not necessarily generate structural fabric that matches the features from which the data was collected.

Additionally with DFNs, polyhedral blocks, and block theory there is the potential for progressive failure following the removal of key blocks. The removal of a single block creates spaces for more blocks to move, with a domino or cascading effect of additional blocks failing until there are no more blocks to remove, resulting in the final geometry.

2.4 Previous Applications of Discrete Fracture Networks to Bench Scale Kinematics

Prior to 2010 there were almost no papers presented at the main open pit mining conferences that included DFNs (Lorig, 2015). Between 2012 and 2015, these conferences saw on average six such papers per conference, most of which were on the topic of using DFNs for synthetic rock mass models. Lorig mentions the development of the advanced algorithms by Elmouttie, Poropat, and Krähenbühl (2010), and the SIROMODEL software but only as a tool that can be used; no case study is presented.

Ortiz (2009) presented one of the early applications of SIROMODEL to open pit mining and compared the results to a probabilistic analysis based on conventional kinematics. The model was limited in size to 50 m wide by 3 benches tall and the input parameters were not provided in the paper. The results of this work were variable with model predictions that failed to predict the observed conditions when compared to documented slope profiles.

Weir and Fowler (2016) developed a DFN using only drilling data for a planned starter pit. DFN and kinematic analyses were performed using the FracMan software code (Golder, 2018). The modeled pit slope was 500 m in width and 480 m in height. The analyses indicated the number of failed blocks ranged from 43 to 298 and 117 to 771 for two separate domains. As there are no exposed benches these results cannot be validated against real-world data.

Veillette et al. (2018) present a design approach for slope steepening at an open pit mining operation that applied a DFN to identify whether adverse joint persistence could impact bench stability during excavation of 30 m high double benches. The DFNs were generated based on photogrammetry data from exposed benches above the working level of the open pit. Analyses were conducted using 3DEC modelling code to determine if potential planar or wedge failures existed on future double benched slopes.

Valerio et al. (2020) and Montiel et al. (2020) each present examples for the application of DFNs in open pit mining with data derived from surface mapping; however, both of these cases focus on the interramp to overall pit-slope scale to investigate multi-bench kinematic mechanisms.

Rogers et al. (2020) present a theoretical case of bench-scale kinematic analysis utilizing FracMan to demonstrate that a DFN approach results in steeper expected breakback compared to results obtained from SWedge. The structure modelled involves two sets oriented 45° oblique to the slope resulting in the formation of only perfect wedges. The structure in these analyses was modelled with an average length of 25 m. If the modelled bench height was 20 m, this would result in a large number of the fractures being the equivalent of fully continuous at the scale of the bench. Based on the results of the hypothetical inputs it should be possible to model steeper bench face angles using a DFN approach, in theory.

From the literature reviewed at the time of writing, while there are varying aspects that have been completed in various parts by others, there have not been any publications where DFNs have been used as the primary tool for widespread kinematic analysis and bench design in an open pit mining environment. Applications to date of DFNs to open pit mining have been either small multi-bench areas or assessments at the interramp scale.

The primary objective of this thesis document is to determine the applicability or viability of a DFN approach to bench design.

CHAPTER 3: METHODOLOGY

Based on the industry experience of the author and others, it is common to observe less breakback than what is predicted using conventional kinematic analysis. While steeper slopes are frequently observed when compared to the initial designs, it is difficult to justify steeper design slopes until there are excavated slopes that prove steeper angles can be achieved. The conventional kinematic analysis method uses conservative assumptions such as ubiquity and full continuity of structures, which does not reflect the true nature of a rock mass. A discrete fracture network (DFN) provides a more realistic representation of the structural conditions.

The hypothesis to be tested is whether a DFN, with its more realistic representation of structure, would provide a more accurate prediction of the expected breakback when compared to the conventional kinematic approach. To test this hypothesis, DFNs were generated at both the pit scale and bench scale for an assumed excavation geometry. The analyses were conducted using SIROMODEL and involved generation of the DFN, a block analysis to form polyhedral blocks and assess their stability, and an assessment of the breakback. Additionally, given that there is uncertainty associated with the data input into the generation of a DFN, a separate sensitivity analysis of the continuity of structures was performed on existing DFNs.

3.1 Continuity

Continuity of structures is a difficult parameter to measure in the field and is commonly represented as a circular disc during photogrammetric mapping of structures. In DFNs the structures are further simplified through representation as a triangle, square, or hexagon (due to computational constraints), as shown in Figure 16 from the SIROMODEL manual (2020). When

considering 6-sided polygons compared to 3-sided there is a computational run-time penalty of ~400% in SIROMODEL.

In most applications, four-sided representations are used to balance between computational efficiency and accurate representation of the structural features. It should be noted that depending on the polygonal representation, an upscaling of the radius may be required to maintain the P32 relationship to field data, due to the data collection methods or assumed representations. Data collected using photogrammetric techniques represents structures as a planar disc. An exposed joint with a trace length of 20 metres would be mapped as a disc with a radius of 10 metres and an area of 314.16 metres. Representing this same feature as a square reduces the area to 200 metres, or a triangle reduces the area to 129.9 metres. Consequently, the input radii for modelling within a DFN may need to be increased from field observations such that the modelled equivalent joint areas match the observed joint areas in the field so that the modelled P32 will more accurately reflect the observed P32.

The newly released RocSlope software by Rocscience overcomes this issue by representing the structures as circular discs at apparently little to no computational penalty. Representing structures as discs also addresses the variability of rotation of the structures when using 3, 4, or 6-sided polygons.

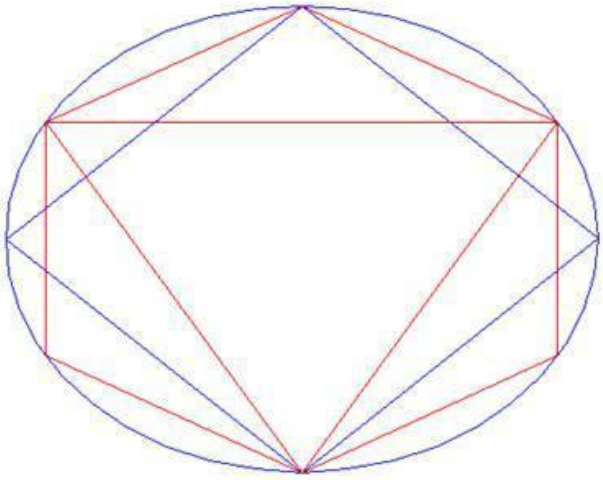

Figure 16. Triangle, square, and hexagon joint representations defined on the circle of specified radius

To develop a better understanding of the influence of continuity, a sensitivity analysis on continuity was carried out on two separate DFNs. These DFNs are referred to as DFN Mountain Large and DFN Mountain Small for confidentiality reasons. They had been previously developed during prior research conducted by others and were deemed to be valid in that the DFNs sufficiently represented the exposed rock faces.

Using SIROMODEL, the continuity of the structures was scaled using a range of factors (i.e., 1.1 for a 10% increase or 2.0 for 100%). The upscaled DFNs were then assessed on a sectional basis to determine the influence on fracture parameters such as P20 or P21.

3.2 Kinematics

The comparative analysis between the kinematic design of benches using conventional methods (e.g., SWedge) - where structures are assumed to be ubiquitous, fully continuous, and daylight at

the toe of the bench forming simple wedges - versus a discrete fracture network approach - where structures are stochastic, discontinuous, and can combine to form complex block geometries - was carried out using two different approaches.

The first approach involved generating a DFN at the same scale of the intended pit slopes and conducting the stability assessments across all the benches in the model (i.e., at the pit scale). This allowed for a representation of the complete bench stack and created a model representing the planned overall slope heights with the potential to consider both single and multi-bench controls. The results of the stability assessments were compared to the bench documentation data of the as-built conditions and the parameters were adjusted as required until calibration was achieved. Additional realizations would be assessed during the stability assessments. Based on the differences in results between successive iterations, the total number of realizations required to achieve a repeatable answer was determined. By conducting a large model there should not be a need to conduct numerous realizations since it is expected that sufficient kinematic combinations would be observed as part of the large model. This approach provides a direct approximation of the real-world conditions (i.e., a full pit slope height) in terms of the scale of the problem to be a comparable model to the conditions for which slope documentation data exists.

The second approach involved developing a DFN model at the scale of a single bench to assess the stability conditions for a single bench. This approach would require running numerous realizations to develop a representative database of failure geometries. Similar to the other approach, the apparent plunge of the breakback would then be compared to the documented

bench breakback data. This approach is similar to conventional kinematics in that the analyses are conducted at the scale of a single bench.

The stability assessments of the DFN models will only consider failure of the initial blocks. A key block analysis involving progressive failure is not being considered at this time based on field observations over the past 17 years where structurally controlled bench breakback demonstrates that the main structures involved are generally continuous enough to form a single resultant wedge. Pending the outcome of the above assessments, the need for progressive failure analysis will be revisited during the analysis process.

CHAPTER 4: CASE STUDY

For this thesis, a series of DFN models and realizations were developed using the Open Pit Simulator (OPS), also known as SIROMODEL, developed by CSIRO. The data used came from real-world data from anonymized data sources or data from published literature.

4.1 Effect of Scaling Continuity in a DFN

The sensitivity analyses for continuity were carried out using two relatively small validated and anonymous DFNs. The two DFNs are referred to as “DFN Mountain Large” and “DFN Mountain Small”.

The variability of the DFNs was assessed with respect to scaling of the diameter along two-dimensional (2D) cross-sections. The two DFNs contained both deterministic and stochastic features and had undergone a rigorous validation process during their development to confirm their accuracy. The imported data consisted of: dip, dip direction, x, y, and z coordinate and radius. The features were represented as four-sided planes when imported into SIROMODEL and the rotation of the features was randomized (the rotations of the original features were not available).

The DFNs were imported directly into SIROMODEL as “Deterministic Joint Polygons” using a square or four-sided polygonal representation. Rotation of the polygons was the only parameter that could not be reproduced from the original dataset; the influence of rotation on the dataset was not assessed but is discussed in the conclusions. To assess the sensitivity of continuity an inference was made that the continuity of a structure could be approximated based on the

observed continuity and the end condition of the structure. If only one end is visible then the continuity could be double but if no ends are visible then it could be tripled. Subsequently for the sensitivity assessment the structures were scaled up from 1.0 to 2.0 (i.e., doubled) in increments of 0.1 and then from 2.0 to 3.0 (i.e., tripled) in increments of 0.2 for scaling factor. The “Use existing joints” feature in SIROMODEL was used to scale the joints while keeping the same joint rotation so as not to introduce a new degree of uncertainty. Figure 17 provides an example of the original model and the model after a scaling factor of 2.8 has been applied.

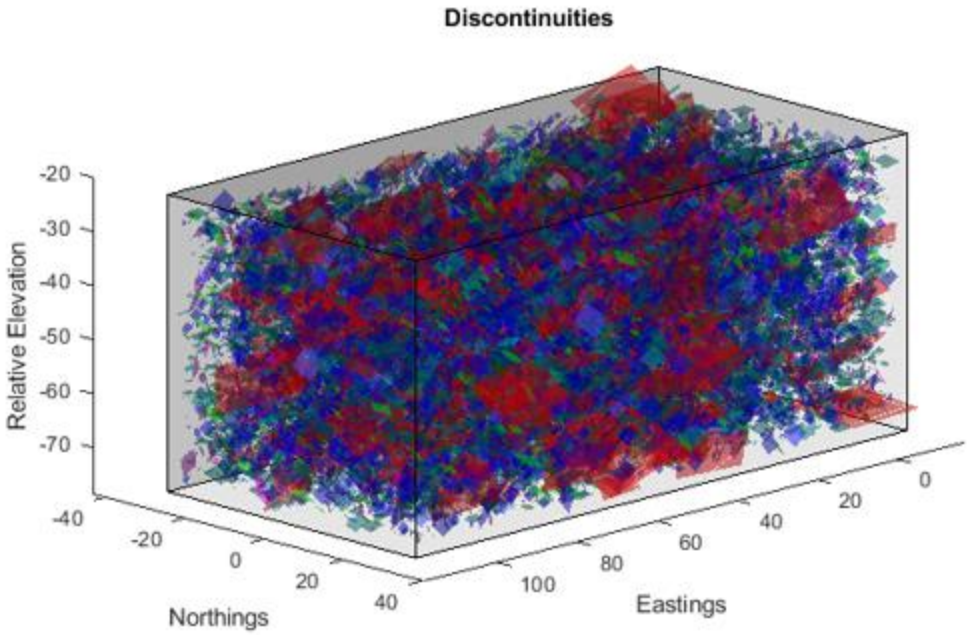

(a)

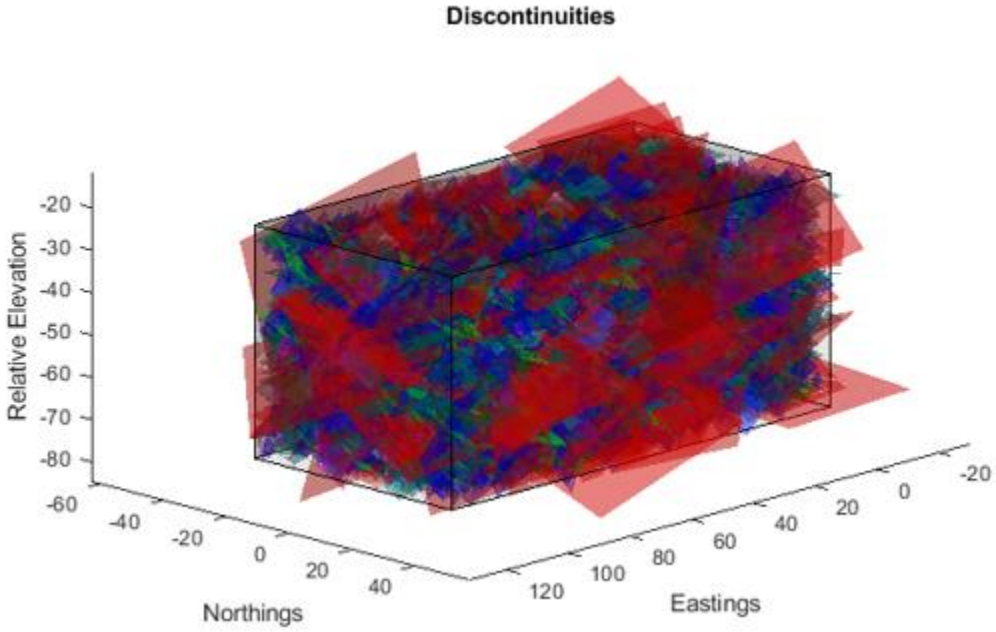

(b)

Figure 17. Isometric view from SIROMODEL of DFN Mountain Large (a) without scaling and (b) with a scale factor of 2.8

The standard output figures from SIROMODEL are included in Appendix A. The figures show the original DFN setup in the model view, and figures of the fracture statistical analysis and isopleths which are a visual representation of fracture intensity.

It is common practice to assess rock engineering problems with 2D analysis sections. This is often done for practical reasons as a 3D model of a full open pit is more time consuming and not required for general assessments. Also, the geology or geometry conditions may be, or are considered to be, adequately represented by a single 2D section. However, for a DFN that consists of discontinuous features distributed spatially in 3D, there may be a component of variability when trying to represent it in two dimensions. To address this variability, a series of cross-sections both parallel and perpendicular to the long axis of the DFN (i.e., North-South and East-West sections) were generated and are presented in Figure 18, with additional iterations in Appendix A.

(a) Sections of original DFN Mountain Small

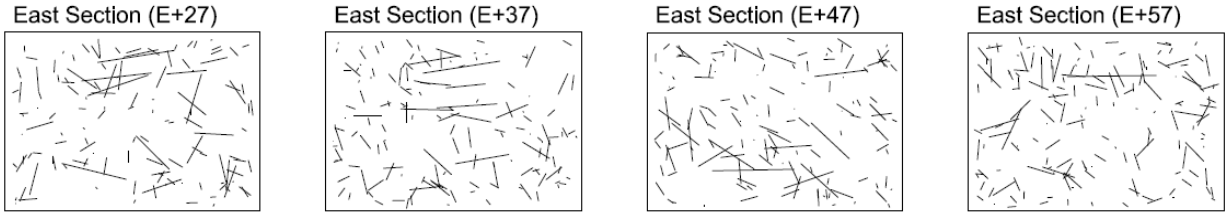

(b) Sections of DFN Mountain Small with a scale factor of 2.8

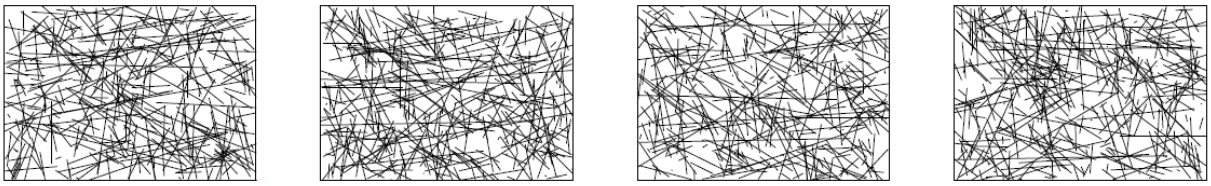

Figure 18. Cross-sections through DFN Mountain Small (a) without scaling and (b) with scaling

The sections were then compared based on the fracture count and fracture length (P20, P21) and the intersections (count, per area, and network connectivity) graphs, which are included in Appendix A.

The main observations drawn from this assessment are:

1) The variability between the sections for a given DFN model (e.g. Small or Large) is quite significant, depending on the parameter assessed. The variability between sections for a DFN can be -30% to +70% of the average for the parameter from all the sections (shown in Figure 19).

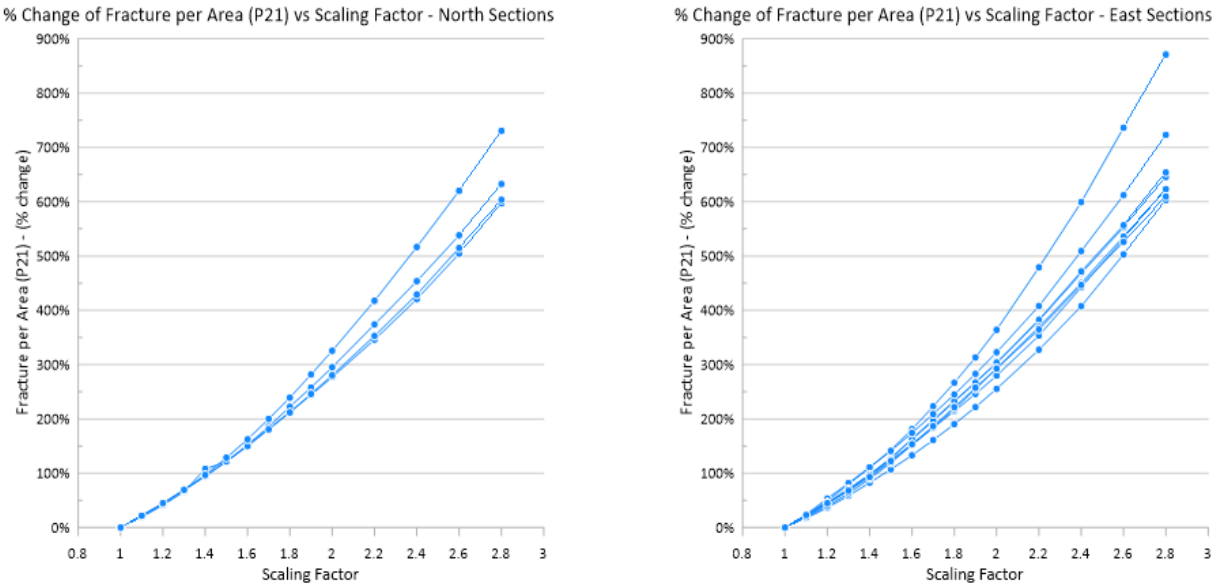

Figure 19. Graph of the percent change in P21 for the North and East facing sections for DFN Mountain Small

2) The scaling factor has a different and non-linear effect on each of the parameters as shown in Figure 20 (e.g. increasing by 10% does not equate to increasing length by 10%).

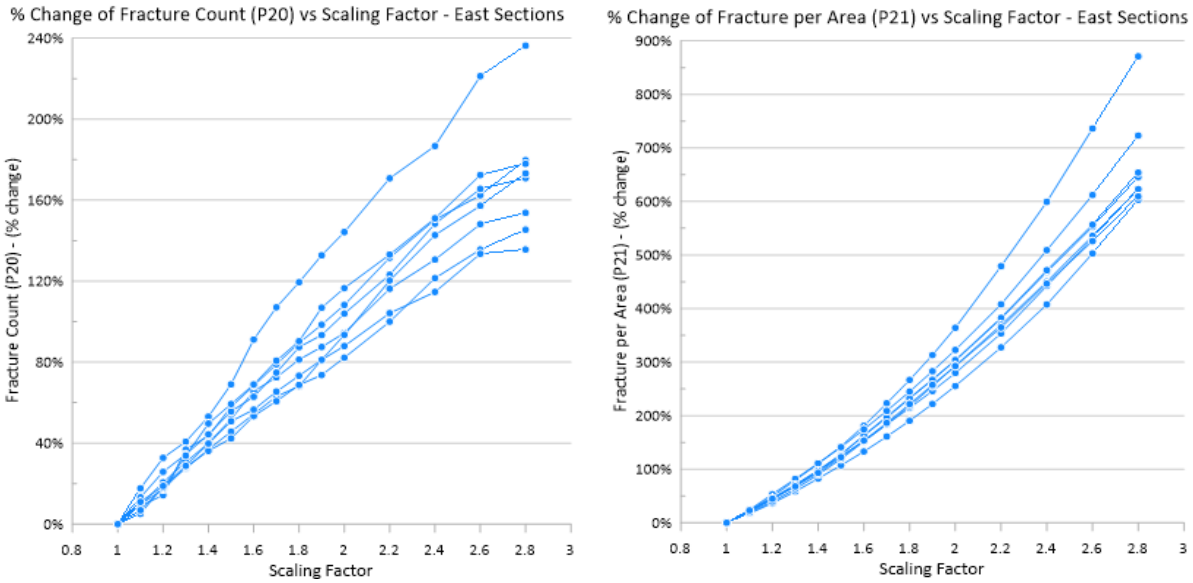

Figure 20. Graphs of the percent change in P20 and P21 for the DFN Mountain Small versus scaling factor of the fractures

3) There is a similarity in the general shape of the curves between the Large and Small DFNs. The DFNs are from the same site location, but they were developed using data from different areas and the two DFNs are of different sizes; however, in comparing the results of the two as a percentage change, the curves are quite similar (see Figure 21).

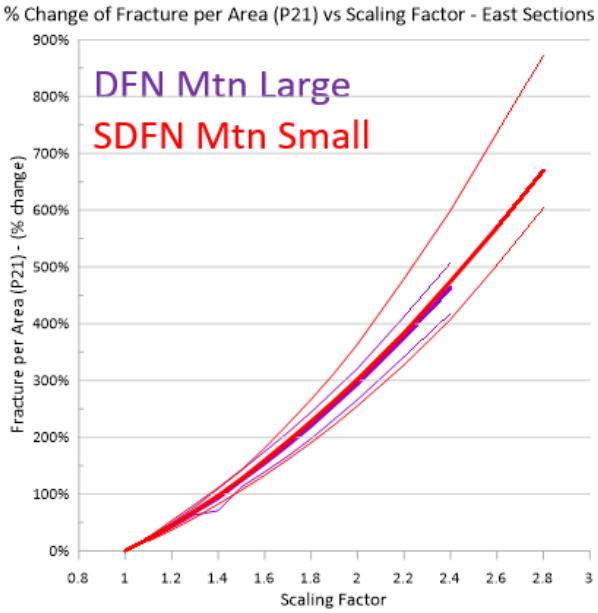

Figure 21. Comparison of the percent change in P21 between the DFNs Mountain Large and Mountain Small versus scaling factor of the fractures

4.2 DFN Attempts

The second set of analyses focused on kinematic failure assessments of a single bench across a range of model configurations ranging from pit-scale to single bench. The dataset used is based on the results presented in Veillette et al. (2018).

The first DFN model spanned 1,015 m by 990 m by 505 m (del X, del Y, del Z) and is representative of the entire pit slope conditions for a quadrant of a pit containing multiple wall orientations. This DFN model had approximately 1.45 million stochastic structures, which proved to be too large for the software / hardware used for the assessments.

The initial model was reduced in area to span 500 m by 500 m by 505 m (del X, del Y, del Z) representing a single wall orientation, but still kept at a pit scale modelling an overall slope height of 315 metres (21 benches). This model had approximately 234,000 stochastic structures. This model was able to be solved by the software but resulted in only 1 block being generated. Based on the previous assessments of scaling with the smaller DFN, the DFN was scaled using a factor of 2, 3, 5, and 10. The scale factors of 5 and 10 failed to compute whereas the factors for 2 and 3 resulted in the generation of 33 and 465 blocks, respectively, as shown in Figure 22.

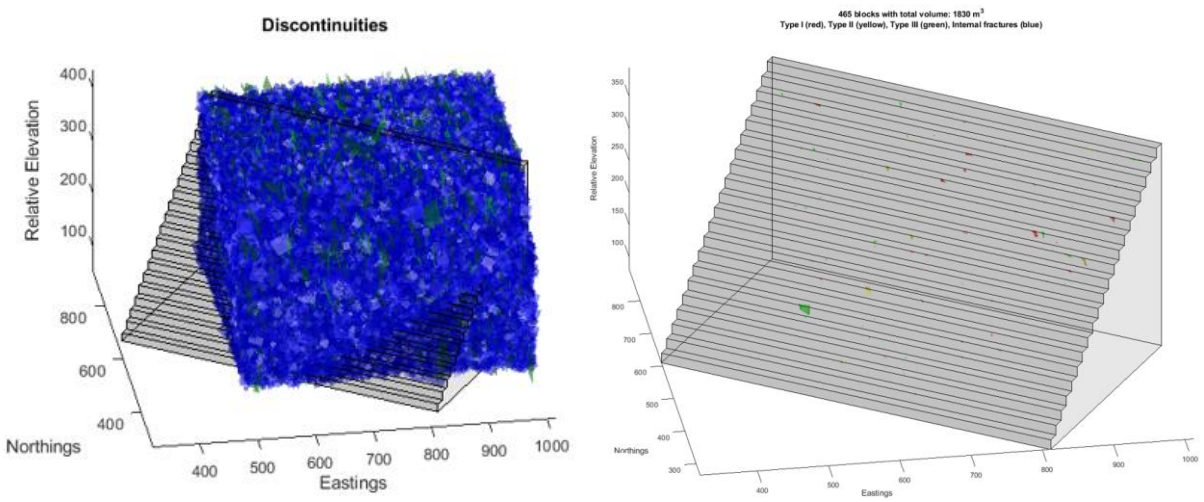

Figure 22. DFN scaled at a factor of 3 and resulting blocks

Attempts were also made using a smaller DFN model: 300 m, 90 m, 45 m cubed at the original structure size and with scaling that provided similar results. Through the course of the analyses it was concluded that attempting to model individual benches comprising an overall slope, while conceptually providing the best attempt at modelling the real-world conditions from which the slope documentation data was collected proved to be more complex than desired. Additionally, the assessment of breakback would need to be performed for each bench level and then the results combined, a time intensive approach. Consequently, the analysis approach was changed to be a model consisting of a single bench, which would provide a comparison to how conventional kinematic analyses are performed.

The conventional approach to kinematic analyses using software such as SWedge involves the analysis of a single bench. This approach was replicated in SIROMODEL using a 15 m by 16.7 m by 15 m cube to represent a single bench geometry. However, with the smaller model more realizations of the DFN are required in order to develop a statically representative dataset

for comparison. Similar to the large-scale DFNs, as would be expected given the results, the single bench model failed to produce blocks across the realizations.

As an alternative to running multiple DFN realizations for single bench analyses and then combining the results, it was decided that a similar end result could be achieved by extruding the bench geometry to make a sufficiently long bench to create a large enough geometry for the blocks to be formed. Subsequently, DFN models were generated for bench lengths of 150 m, 450 m, and 1200 m. Based on the results from the earlier models, where they were not able to produce the number of failed blocks to match the observed bench documentation data, it was determined that there needed to be more structures with greater continuity. Consequently, the input parameter for average continuity was doubled and the fracture intensity increased, essentially simulating structures that are mostly or fully continuous at the scale of the bench but allowing for spatial variability in the location of the structures.

As expected, the longer bench models of 1200 m or 450 m generated more predicted failures and a relatively smoother CFA, as shown in Figure 23. However, the total count of failed blocks was still relatively low and the shape of the CFA did not match that of the slope documentation. The next step was to increase the fracture density by adding more fractures to the DFN with the expectation for more blocks to be formed. The DFN models did result in more blocks but again the CFA of expected bench breakback from the DFN continued to be steeper than the observed slope documentation.

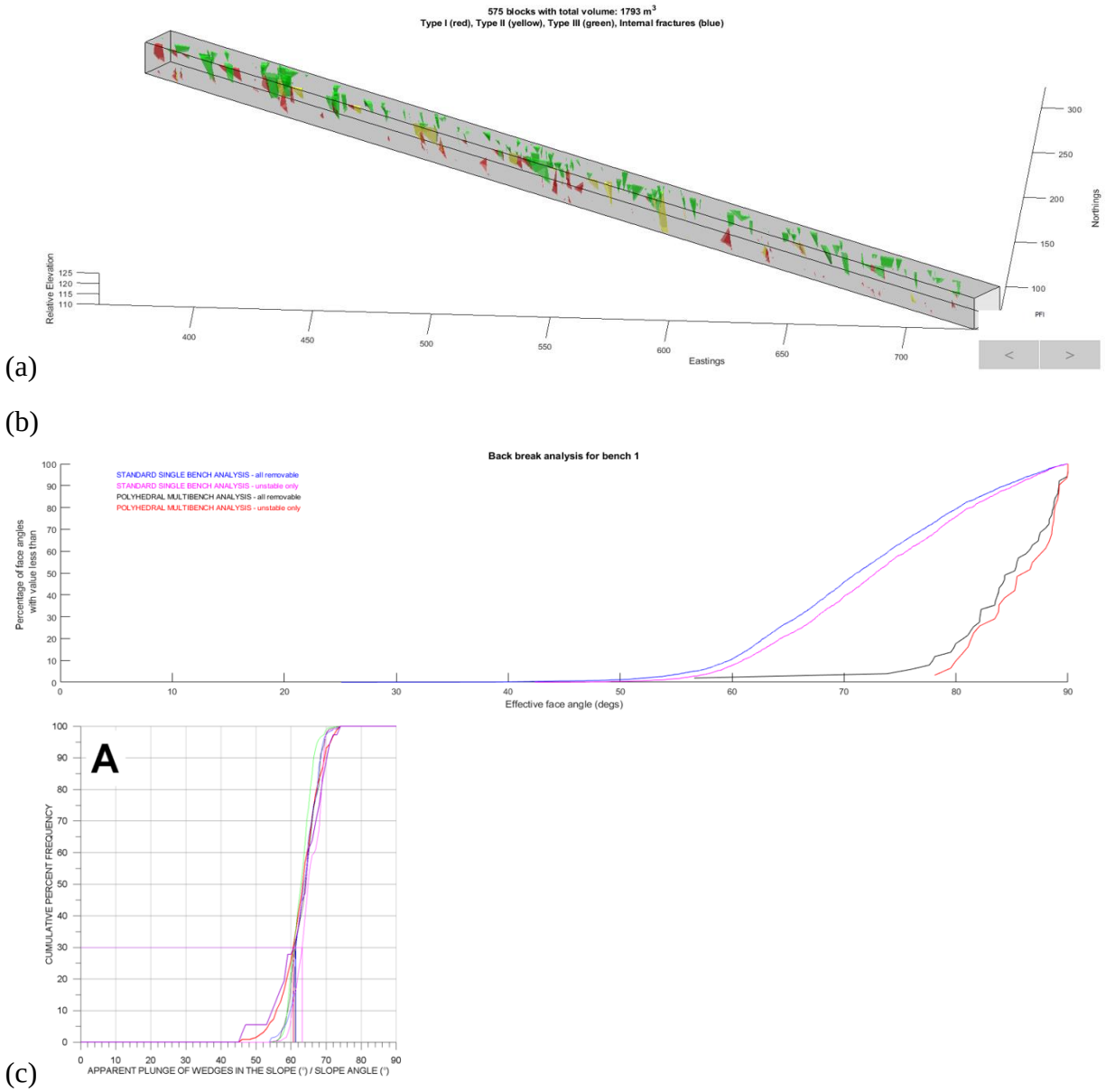

Figure 23. Results of single bench model 450 metre long (a) visualization of blocks formed and (b) CFA of expected bench face angle (c) CFA from Veillette (2018) with slope documentation

From these analyses it is evident that there is a component of the real-world slope behaviour that is not being modelled correctly or properly taken into account as the results were unable to reproduce the observed slope performance. Further study is required to identify and address the discrepancy.

CHAPTER 5: CONCLUSIONS AND RECOMMENDATIONS

5.1 Research Conclusions

The application of DFNs to rock engineering problems has increased significantly over the past 10 to 15 years. Early development of computational algorithms was by researchers, research groups, or industry leading experts and produced software that was either proprietary or had a limited group of users. With more commercially available software, such as Rocscience's newly released RocSlope (27 June 2023), the use of DFNs in rock engineering will become more commonplace. The main objective of this research was to determine if a DFN approach involving polyhedral kinematics could produce a distribution of expected breakback that matched that of observed slope conditions. Essentially: could the current conventional kinematic analysis approach be replaced by a DFN approach?

The benefit of a DFN is that it provides a structural model that closely resembles that of the real world. The alternative, to model every structure explicitly, is impracticable. With a DFN, only enough structures need to be mapped to be representative of the entire population of structures within the structural domain. How many is enough varies for each case, but it would be when additional data no longer provides new information and falls within the bounds of the existing dataset. For the current discussion, 200 measurements is assumed to be sufficient. Statistical distributions from this small dataset provide the input parameters for the DFN, which can then generate thousands or tens of thousands of structures to represent the structural fabric throughout the rock mass.

A key question that follows is “Does the DFN accurately represent the real-world conditions?” and perhaps more importantly “How do we determine the validity of the DFN?” This question is one that requires further research to be able to answer. Currently, there is no consensus in the industry as to what defines a valid DFN. Considering that the inputs are derived from statistical distributions of data, the DFN output will have variability within it and between different realizations of the same input parameters.

In geological engineering it is commonplace to use representative cross-sections to help with visualization of the subsurface conditions and for analytical purposes. The assessment of continuity in Chapter 4 reveals that caution needs to be exercised when trying to apply a fracture network in 2D. There was considerable variability between cross-sections generated from the same DFN; therefore, a 2D cross-sectional approach is likely not a good candidate for validation of a DFN generated in 3D. Furthermore, the effects of scaling structures in 3D has different implications than scaling structures in 2D. In 3D the structures are simply made bigger, but in 2D (because it is derived from 3D) there is also an increase in the number of fractures as well as the continuity.

The SIROMODEL software was used to conduct kinematic analyses at the bench scale utilizing a DFN developed based on data from an operating open pit mine. Full pit-scale models were found to exceed the computational capabilities of the computers being used. With future advances in both computing power and algorithms, full pit-scale models will likely be possible. Smaller scale models of portions of the pit or representative models were successfully computed with relatively short model run times (in minutes). An analysis of the initial input parameters,

however, failed to generate rock blocks and eventually required modelling of the structures as nearly fully continuous and with a greater intensity than indicated by the source data. The new results produced kinematically failing rock blocks, but the breakback indicated was steeper than that observed in the slope performance data and steeper than the results indicated by conventional analysis methods, which were calibrated to the slope performance data.

To fully explain the discrepancy between the breakback from the DFN compared to the conventional kinematics and observed breakback would require a detailed comparison of the inputs into the respective breakback CFAs. The conventional kinematic approach results in more rock blocks because all structures are combined with each other. In a DFN the structures are spatially distributed so not all structures are combined, even with a larger population of stochastic structures there are fewer resultant blocks than in a conventional kinematic analysis. In the DFNs modelled and observed in the literature, the number of blocks identified were relatively low (<1000) whereas conventional kinematics using fewer overall fractures results in combinations of 10,000 to 500,000 or greater depending on the size of the input database. From a statistical perspective, the conventional kinematics look at all possible blocks and therefore a larger population for analysis, whereas DFNs only look at the blocks that are formed by the structures, which puts a high demand on the need for an accurate DFN. The combinations generated in a DFN may be missing or are underrepresented compared to real-world conditions.

An assessment of which structural orientations contributed to the rock blocks could be performed and then those orientations compared to the conventional kinematics to identify similarities or differences in structural features that contribute to the formation of rock blocks. Because DFNs

do not allow all structures to combine with others, the DFNs are missing combinations that the conventional kinematics have. Whether these combinations are the reason for the discrepancy requires further analysis.

The structural continuities considered during the assessments were increased to be almost fully continuous and therefore should have had combinations at the bench scale that would be sufficiently large to match the field-documented bench breakback. However, this was not the case. The resulting combinations were relatively small in size and not the full height of the bench as is assumed in conventional kinematics. One possibility for this is progressive failure. If the first round of blocks were removed from the model and additional blocks failed, this would result in more breakback in the model.

Based on general field observations of wedge or planar failures at the scale of the bench from the author's experience at multiple open pit mining operations, where there are structural controls the resulting bench breakback is generally continuous for the portion of the bench and there is not a rough geometry indicating a direct need for progressive failure. However, progressive failure would be expected where the slope profile is more blocky and irregular. For the models assessed with continuous structures, there should not have been a need for progressive failure; however, it is something that would require further analysis before discounting.

Further work is required to address the observed discrepancies and concerns regarding validation before the DFN approach is adopted in lieu of the conventional kinematic analysis approach.

Presently DFNs seem most applicable to complex site specific analysis of smaller areas rather than a widespread application for bench design.

5.2 Other Considerations and Recommendations for Future Work

DFNs are generally validated by performing a statistical analysis of the data generated and checking it against the input statistical distributions. This type of validation process merely confirms that the DFN was generated as expected. Alternatively, comparison of the DFN parameters against each other e.g., P32 vs P21 plots compare a sampling of the data against itself which is simply a check of "does this particular DFN realization seem reasonable". What these validation methods fail to do is check whether the DFN is an accurate representation of the real-world conditions.

DFN generators assume a spatial distribution model to determine the centers (i.e., X, Y, Z or Easting, Northing, Elevation) of the fracture discs or polygon shapes that represent the joints. The SIROMODEL software currently only supports one spatial distribution model as indicated in the manual (2020):

> The joint set generator currently only supports the Baecher Model (Baecher & Einstein 1977) and slight variants thereof. This model assumes circular joints are distributed uniformly throughout the simulation volume with their total number adhering to a Poisson process (i.e. a binomial distribution tailored for large numbers of low probability events).

Considering the uniqueness of different geological and structural environments the applicability of that spatial distribution model to the site-specific geological conditions requires further study

to aid in ensuring that the generated DFN provides a spatial distribution of structures that matches that of the observed field conditions.

For DFN validation, generating statistical distributions of the DFN and comparing them against the inputs only validates that the generated DFN conforms to the input parameters that were specified. One potential method to try for validation would be to assess the DFN for how many of the stochastic structures are close to the explicit field measurements. With photogrammetric mapping data, it would be a case of comparing the mapped discs to the stochastically generated ones and identifying the nearest matches. If the stochastic discs are not similar to the mapped discs, then even though the stochastic DFN represents the structure as a whole, that particular realization may not be representative of the site-specific conditions. A new realization, one that provides a better match to field measurements, would be required. For drilling data it is a case of assessing the DFN with ‘drillholes’ at the same location as the real-world measurements and then comparing stochastic borehole log to the actual borehole log. Without a validation showing that the DFN realization matches the real-world conditions, the DFN is just one representation and additional DFN realizations should be made and assessed until the results between additional realizations are consistent.

Representation of structures using 3-, 4-, or 6-sided polygons introduces an additional parameter of uncertainty: the rotation of the polygon. The uncertainty is really only relevant to rock masses with discontinuous structures that are not very blocky. If the rock mass has persistent structure and is blocky, then the uncertainty can be addressed through increasing the continuity of the structures within the DFN to ensure that any rotations still result in the formation of the desired

blocks. As the newly released RocSlope software represents structures as discs, the computational problem has been addressed and other DFN software codes should be looking toward algorithms that utilize circular disc representation of structures as well.

A 2D representation of a DFN has notable variability between sections and sensitivity assessments by considering more or less continuous structures in 2D, for example to simulate rock-bridging effects, and has a different scaling effect when compared back to 3D. Furthermore in a rock mass with a higher fracture intensity, the effect of variability between sections is greater than in a rock mass with fewer features. This intuitively makes sense because a "massive" rock mass with few fractures in it should show relatively low variability across sections. If the rock mass is more blocky, then depending on section location, the results are going to diverge from the assumed average parameters.

A typical sensitivity approach is to simply assess structures as being more or less continuous. In 3D this is a simple task; however, the implication on a 2D representation is that by increasing continuity of a structure in 3D additional features are going to intersect the cross-section that previously did not. Therefore 2D representations need to have the fracture intensity increased in addition to the fracture length. This example illustrates one of the limitations of doing a 2D representation of a DFN. While 3D models increase the overall complexity of the system there are aspects of variability that are reduced or eliminated for the assessments. If choosing to proceed with 2D models then the modelling needs to bracket the variability of representing the 3D model with 2D sections.

A coupled analysis including the effects of blasting was outside of the scope of this thesis but the impacts of blasting are important to discuss in relation to kinematic design benches due to the influence that blasting can have on the final slope geometry. The following information regarding blasting is, or should be, part of any introductory blasting course. The implications for kinematic bench design are as follows:

Blasting has the following consequences:

1. Generation of new fractures: The rock adjacent to a blasthole is crushed as a result of the detonation. Outside of the crushing zone, hoop tensile stresses propagate and these can result in the generation of new cracks at the bench face. Consequently a block that was assumed to be large and intact during the kinematic analysis process may end up being broken into smaller blocks as a result of the blasting process. The orientation(s) of the new cracks may or may not follow the existing structural discontinuities. Therefore there is the possibility for new adversely oriented blocks to form at the bench face as a result of blasting.
2. Propagation of cracks: The shock wave generated by the blast moves through the rock mass at very high velocities. Crack propagation along any existing features follows in the wake of this shock wave. This occurs farther away from the blast hole. Consequently a structural feature of a specified or limited continuity prior to a blast has the potential to lengthen as a result of the blast energy.
3. Gas pressure: Pressurized gas from the detonation in the hole flows through the cracks and enhances the fragmentation process. Depending on the continuity of structures and whether a trim shot or a pre-split shot has been fired in advance of the main blast to

create a cut-off surface within the rock mass, blast gases can propagate great distances along structures. This pressure wave of gases results in the dilation of structures and consequently a lowering of the shear resistance along the surface (either a loss of cohesion along the structure or by physically dilating the structures through movement of the rock blocks so there is less contact along the surfaces).

While the impact of blasting was not modelled explicitly through the analysis process, some of the implications of blasting were considered through sensitivity assessments. When continuity and fracture intensity were increased, more rock blocks were formed relative to the base model conditions.

A general observation is that bench performance does not equate to structural continuity. If blasting damage does not occur or is minimized and cohesion of structures is maintained, then rock blocks will remain stable and slope performance will be positive as a result. If the original strength of structures can be preserved through controlled blasting efforts, then fully continuous adversely oriented structures can exist at the bench scale and design bench angles can be achieved. Similarly, a positive bench performance does not mean the absence of structure either through it not being present or it being of limited continuity; the existence of structure and continuity should be determined from field mapping.

The comparison of conventional kinematic analyses to bench documentation involves comparing the apparent plunge of the wedges, or dip of planes, to bench documentation data. The bench documentation data is either averaged over a mapping window, likely equal in width to the

height of the bench, or perhaps more commonly, measured along profiles. These profiles are typically spaced on the order of 10 or 15 metres and from a sampling perspective will not always capture the steepest portion of the wedge. Conventional kinematics always samples the flattest angle because there is no spatial distribution of the wedges. To perform a more accurate comparison between DFN kinematics and real-world conditions, the DFN should be analyzed for the scale of the pit wall in question and then all removable blocks subtracted from the pit surface. This adjustment results in the generation of a surface topography following breakback and this modelled as-built geometry can then be documented similar to the real-world bench documentation process. This type of approach would provide for comparison of modelled results to real-world data as they were both generated in the same fashion.

A limitation of block theory, DFNs, and polyhedral kinematics is that the potential for shearing through intact portions of rock (i.e., rock-bridges) is currently not allowed for in the analysis process. The blocks need to be fully formed, which means that even a small rock bridge has the potential to keep blocks in place, while in reality these small rock bridges would either be lost as a result of blasting or shear over time as a result of strain softening. Therefore, future iterations of software need to be able to model shear failure of the intact rock for the non-removable blocks.

One of the risks of new numerical modelling techniques and software is being narrowly focused on the output such that the fundamental failure mechanisms are ignored and the limitations of the model are not thoroughly questioned or addressed. Engineering design is at risk of being too reliant on the output of the model, without a deep understanding of what went into the model

generation or how its outputs were created. The newer software makes it quite easy to conduct analyses, but the analysis process still should require querying the individual results for a deeper understanding. Users of the software should conduct a query of the individual blocks for verification analysis and confirmation of the results.

The answer to the initial research question of, “Can a DFN approach be used to conduct kinematic analyses at the bench scale to more accurately predict the expected breakback?” would be “it depends on the validity of the DFN.” Utilizing a DFN approach to kinematic analyses did result in steeper predictions to the expected breakback, which agrees with other research done using theoretical data; this time it was shown to also be true with a DFN based on real-world data. However, the results were 10° to 20° steeper than observed breakback conditions, potentially the result of the DFN generated not having been validated at the bench scale, or the influence of progressive failure of key blocks.

Further work is required to explain the discrepancies between the kinematic failure predictions made using conventional kinematics versus DFN polyhedral kinematics versus observed slope performance. Analysis of open pit slopes using DFNs has been demonstrated by others to be successful for specific cases or pit areas requiring more detailed analysis but as a general design tool more work is required before conventional kinematics is replaced by DFN analyses for widespread design of benches.

REFERENCES

Ashby, J.P. (1971). Sliding and Toppling Modes of Failure in Models and Jointed Rock Slopes. *M.Sc. Dissertation in Engineering Rock Mechanics,* Department of Mining, Imperial College of Science & Technology, University of London.

Baecher, G.B., Lanney, N.A. and Einstein, H.H. (1977). "Statistical description of rock properties and sampling" in *18th US Symp. on Rock Mech.*, Colorado School of Mines, Golden, CO, 5Cl, 1-8.

Barton, N.R. and Choubey, V. (1977). The shear strength of rock joints in theory and practice. *Rock Mech*., *10*(1-2), 1-54.

CSIRO (2020). Open Pit Simulator (OPS), also known as SIROMODEL. *Manual*. https://research.csiro.au/msci/projects/mining/siromodel/manual/ (retrieved on 14 Aug 2023).

Dershowitz, W.S., Herda, H.H. (1992). Interpretation of fracture spacing and intensity. *Proc. 33rd U.S. Rock Mech. Symp.*, Santa Fe, New Mexico, 3-5 June, 757-766.

Dershowitz, W., La Pointe, P., Doe, T. and Golder Associates. (2004). Advances in discrete fracture network modeling.

Elmo, D. and Stead, D. (2010). An Integrated Numerical Modelling–Discrete Fracture Network Approach Applied to the Characterisation of Rock Mass Strength of Naturally Fractured Pillars. *Rock Mechanics and Rock Engineering*, *43*(1), 3–19. https://doi.org/10.1007/s00603-009-0027-3

Elmo, D., Stead, D. & Rogers, S. (2015). Guidelines for the Quantitative Description of Discontinuities for Use in Discrete Fracture Network Modelling. *13th Int. Congress of Rock Mech.* Montreal, Canada, 10-13 May.

Elmo, D., Yang, B., Stead, D., & Rogers, S. (2021). A Discrete Fracture Network Approach to Rock Mass Classification. In M. Barla, A. Di Donna, & D. Sterpi (Eds.), *Challenges and Innovations in Geomechanics, 125*, 854–861.

Elmouttie, M.K., Poropat, G.V. and Krähenbühl, G. (2010). Polyhedral modelling of rock mass structure. *Int. J. Rock Mech. Min. Sci., 47*, 544-552

Goodman R.E. and Shi, G. (1985). *Block Theory and Its Application to Rock Engineering*. Englewood Cliffs, N.J: Prentice-Hall.

Havaej, M. (2015). Characterisation of High Rock Slopes using an Integrated Numerical Modelling - Remote Sensing Approach. *PhD Thesis*. Simon Fraser University, Burnaby, Canada.

Hocking, G. (1976). A method for distinguishing between single and double plane sliding of tetrahedral wedges. *Int. J. Rock Mech. Min. Sci. Geomech. Abstr., 13*, 225-226.

Hoek, E. and Bray, J.W. (1981). *Rock Slope Engineering*, Revised 3rd Ed., The Institution of Mining and Metallurgy, London.

Hoek, E., Bray, J.W. and Boyd, J.M. (1973). The stability of a rock slope containing a wedge resting on two intersecting discontinuities. *Q. J. Engng Geol., 6*, 1-55.

International Society for Rock Mechanics, Commission on Standardization of Laboratory and Field Tests. (1978). Suggested methods for the quantitative description of discontinuities in rock masses. *Int. J. Rock Mech. Min. Sci. Geomech. Abstr., 15*, 319-368.

Lorig, L.J., Darcel, C., Damjanac, B., Pierce, M. & Billaux, D. (2015). Application of discrete fracture networks in mining and civil geomechanics. *Mining Technology*, *124*(4), 239-254.

Lucas, J.M. (1980). A General Stereographic Method for Determining the Possible Mode of Failure of Any Tetrahedral Rock Wedge. *Int. J. Rock Mech. Min. Sci. & Geomech., 17,* 57-61.

Martin, D. and Piteau, D. (1977). Slope Stability Analysis and Design Based on Probability Techniques at Cassiar Mine. *CIM Bulletin, 70*(779), 139-150.

Mauldon, M. (1998). Estimating mean fracture trace length and density from observations in convex windows. *Rock Mech. Rock Eng., 31*, 201-216.

Montiel, E., Varona, P., Fernandez, C. & Espinoza, Z. (2020). "Use of discrete fracture networks in 3D numerical modelling for stability analysis in open pits" in PM Dight (ed.), S*lope Stability 2020: Proc. 2020 Int. Symp. Slope Stability in Open Pit Mining and Civil Eng,,* Australian Centre for Geomechanics, Perth, 913-926: https://papers.acg.uwa.edu.au/p/2025_60_Montiel/

Ortiz, R. & Silva-Mandiola, R. (2009). Probabilistic Analysis of Bench Scale Stability through Diverse Analytical Tools. *Slope Stability,* Santiago, Chile, November.

Piteau D.R. (1970). Geological factors significant to the stability of slopes cut in rock. *S. Aft. Inst. Min. Metall. Symp.*, Plannino Open Pit Mines, Johannesburg, 33-53.

Read, J. and Stacey, P. (2009). Guidelines for Open Pit Slope Design. *CSIRO Publishing,* Clayton. DOI:10.1071/9780643101104

Rocscience. (2019). *Verification Manual*. https://static.rocscience.cloud/assets/verification-and-theory/RocPlane/RocPlane-Theory-Manual-Factor-of-Safety-Calculations-Planar-Failures.pdf (retrieved on 14 Aug 2023).

Rogers, S. (2023). Evaluation of inter-ramp scale slopes using a discrete fracture network-based method. Webinar presented 14 Jun 2023. https://www.youtube.com/watch?v=sXSCOrBUFBg (last accessed on 7 Aug 2023).

Rogers, S. and Valerio, M., Yetisir, M., Lawrence, K.P. (2020). Bench Scale Stability Analysis Using Discrete Fracture Networks. *ARMA Proc. 54th US Rock Mechanics/Geomechanics Symp.*, Golden, Colorado, US, 28 Jun-1 Jul.

Sagaseta, C. (1986). Technical Note on the Modes of Instability of a Rigid Block on an Inclined Plane. *Rock Mech. and Rock Eng., 19*, 261-266.

Staub, I., Fredriksson, A. & Outters, N. (2002). Strategy for a rock mechanics site descriptive model development and testing of the theoretical approach. *SKB Report R-02-02*. Golder Associates AB.

Valerio, M., Rogers, S., Lawrence, K.P., Moffitt, K.M., Rysdahl, B. & Gaida, M. (2020). Discrete fracture network based approaches to assessing inter-ramp design. Slope Stability 2020 - PM Dight (ed.), Australian Centre for Geomechanics, Perth, 1017-1030. doi:10.36487/ACG_repo/2025_67

Veillette, M., Rose, N., King, M.N. (2019). Slope Steepening Investigations for the Valley Pit at the Teck Highland Valley Copper Mine using Pre-split Blasting. *Society for Mining, Metallurgy and Exploration (SME)*. February 25.

Warburton P. (1981). Vector stability analysis of an arbitrary polyhedral rock block with any number of free faces. *Int. J. Rock. Mech. Min. Sci. & Geomech. Abstr*., *18*, 415-427.

Weir, F.M. and Fowler, M.J. (2016). Discrete fracture network modelling for hard rock slopes. APSSIM 2016 - PM Dight (ed.), Australian Centre for Geomechanics, Perth, 157-168. https://papers.acg.uwa.edu.au/p/1604_06_Weir/

Wyllie, D.C. (2018). “Rock Slope Engineering: Civil Applications, 5th. Ed.” CRC Press: Boca Raton: Taylor & Francis.

Zhang, L. and Einstein, H.H. (2000). Estimating the intensity of rock discontinuities, *Int. J. Rock Mech. and Min. Sci. 37*(5), 819-837.

APPENDIX A: ASSESSMENT OF SCALED EFFECTS OF CONTINUITY IN A DFN

APPENDIX A
ASSESSMENT OF SCALED EFFECTS OF CONTINUITY IN A DFN

A.1 Sensitivity of Continuity – DFN Mountain Small

Model views from SIROMODEL of DFN Mountain Small – no scaling

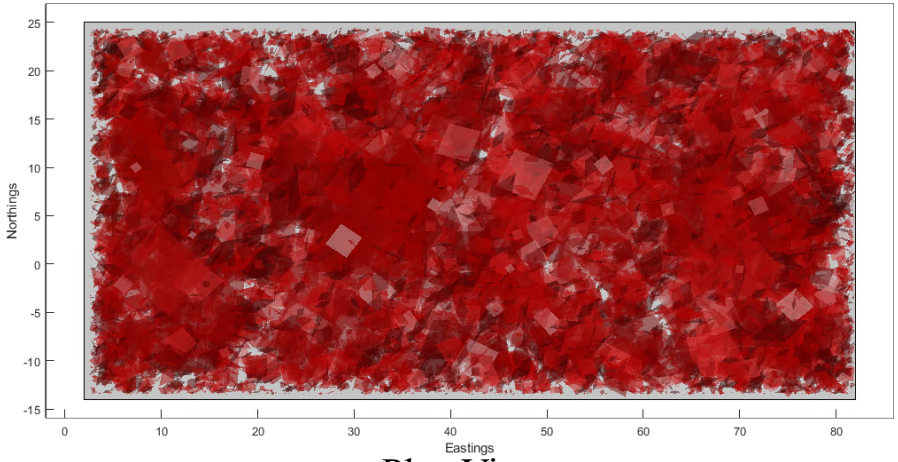

Plan View

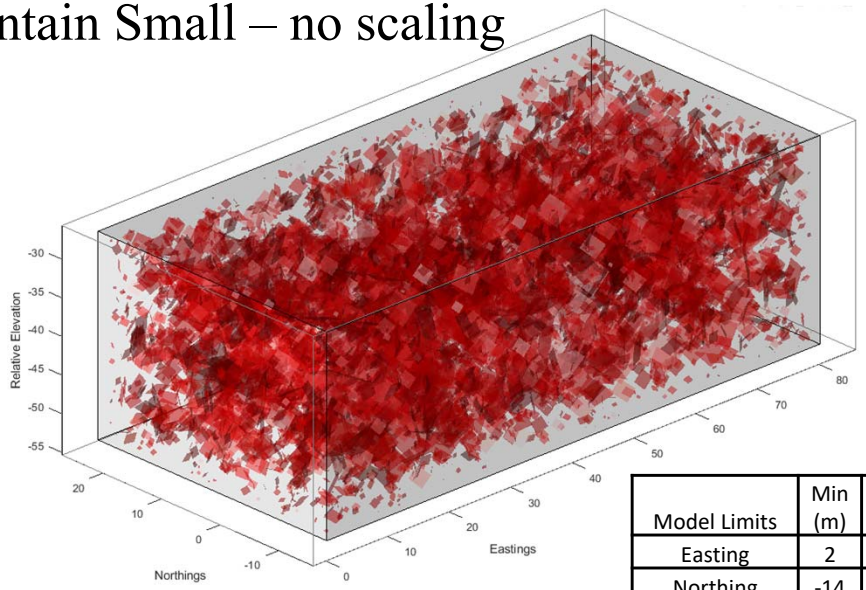

Isometric View

Model Limits	Min (m)	Max (m)
Easting	2	82
Northing	-14	25
Elev	-54	-27

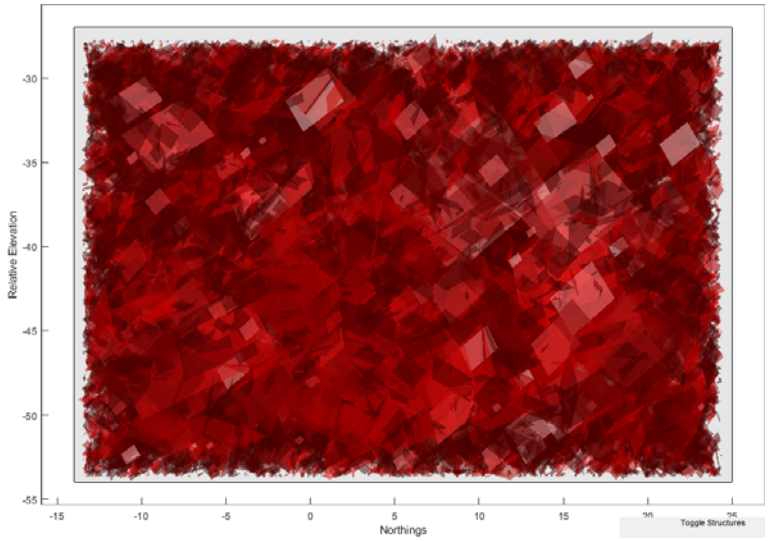

East View

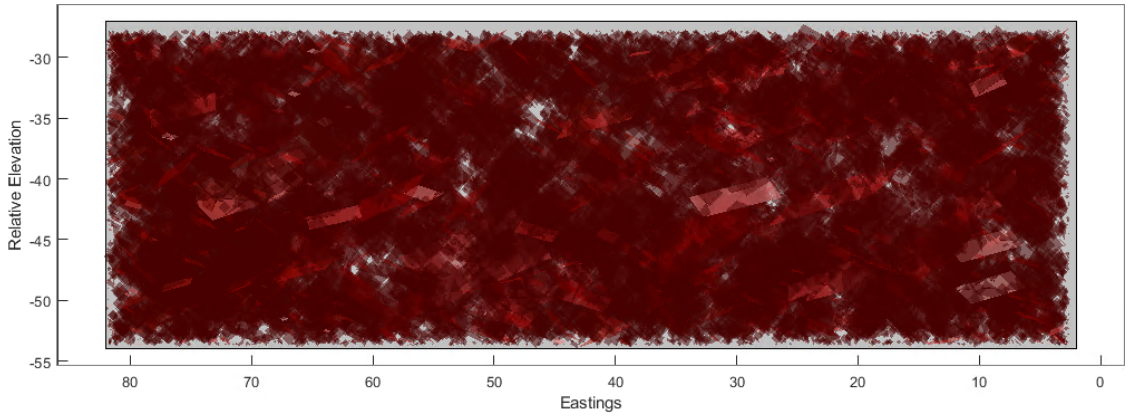

North View

Structural Analysis from SIROMODEL of DFN Mountain Small – no scaling (Scale Factor=1)

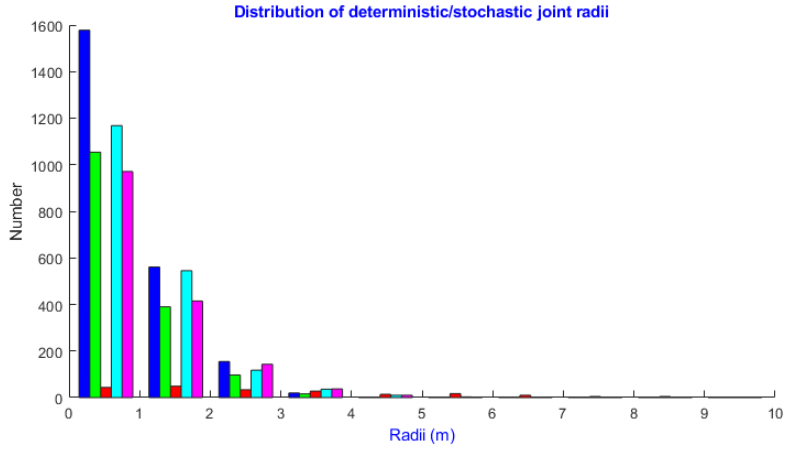

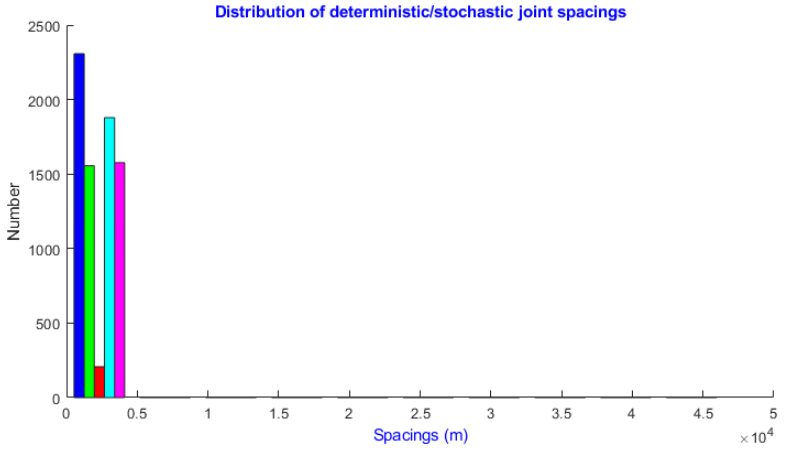

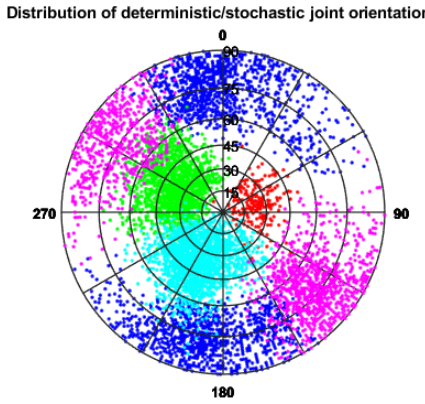

Stereonet Plot of Dip Vectors

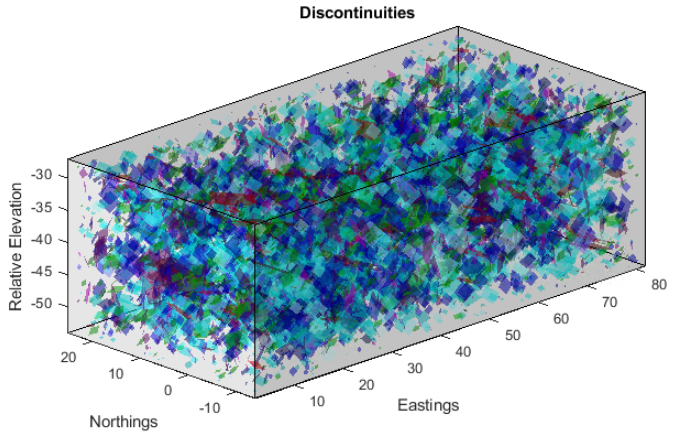

Isopleths of Fracture Statistical Analysis: DFN Mountain Small – no scaling (Scale Factor=1)

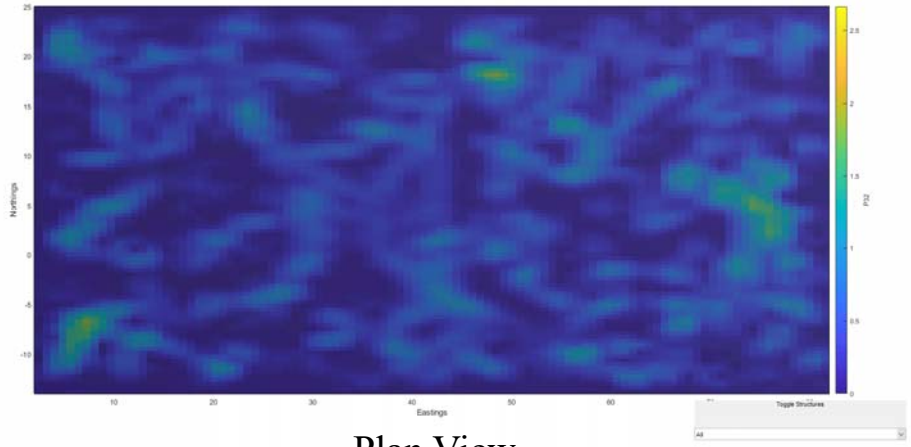

Plan View

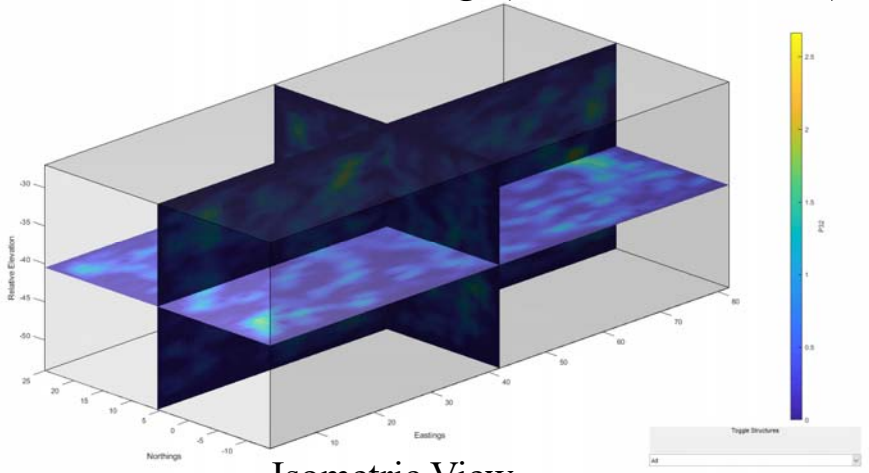

Isometric View

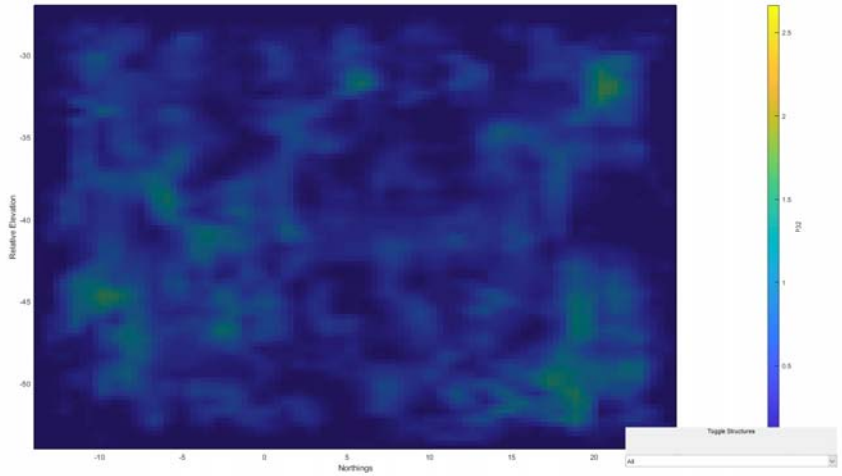

East View

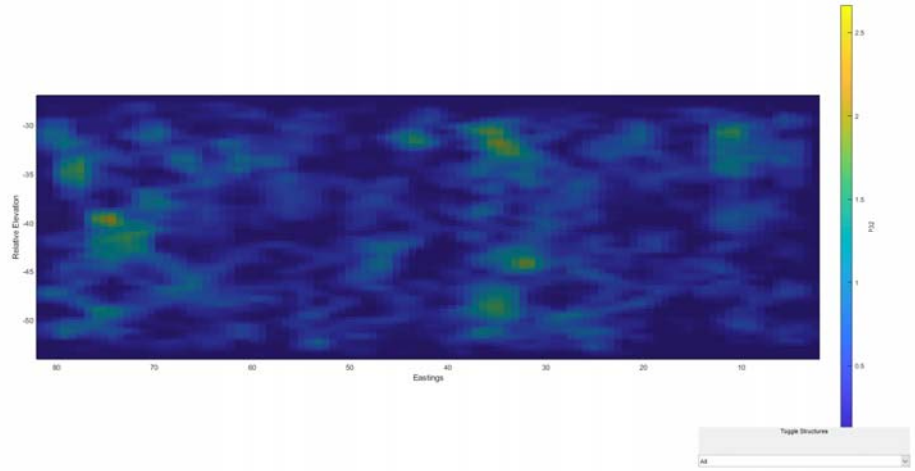

North View

Structural Analysis from SIROMODEL of DFN Mountain Small – Scale Factor=1.1

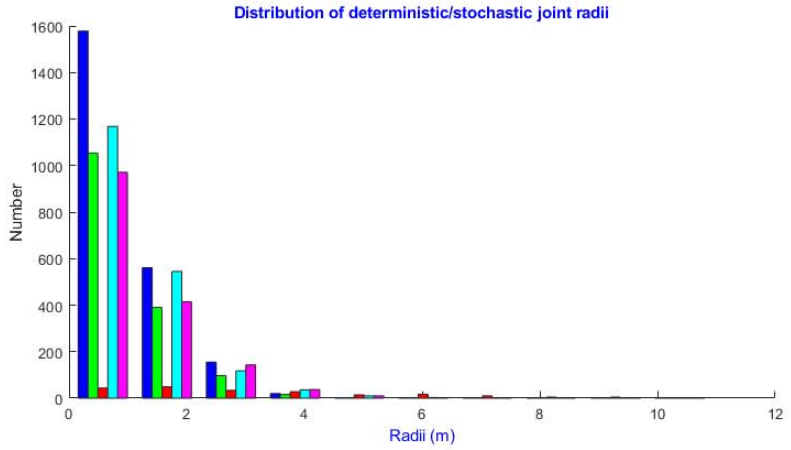

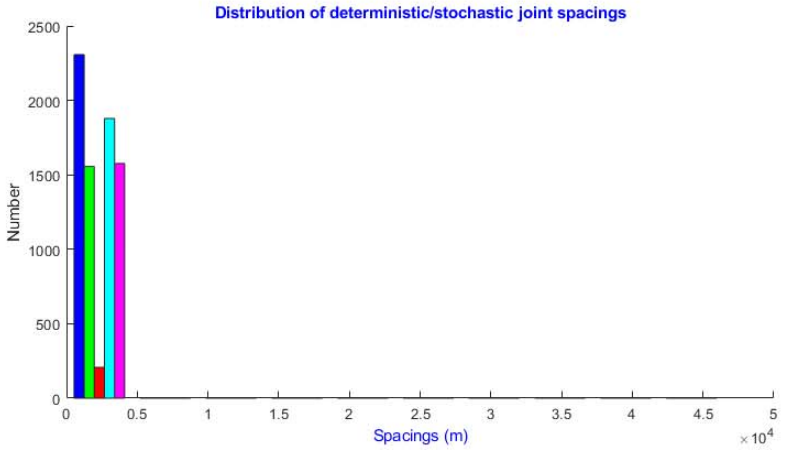

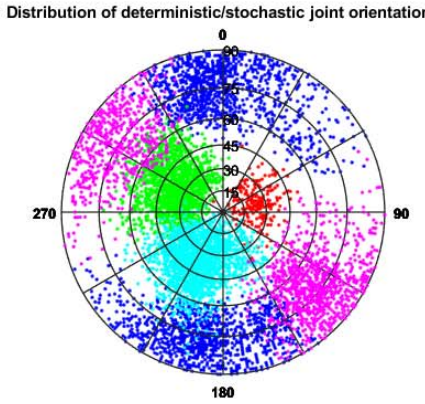

Stereonet Plot of Dip Vectors

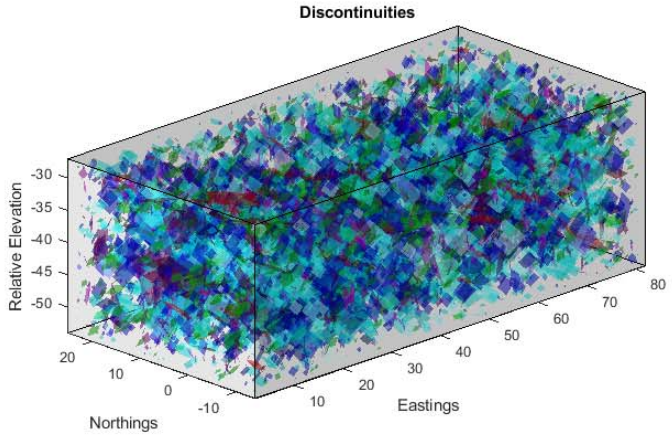

Isopleths of Fracture Statistical Analysis: DFN Mountain Small – Scale Factor=1.1

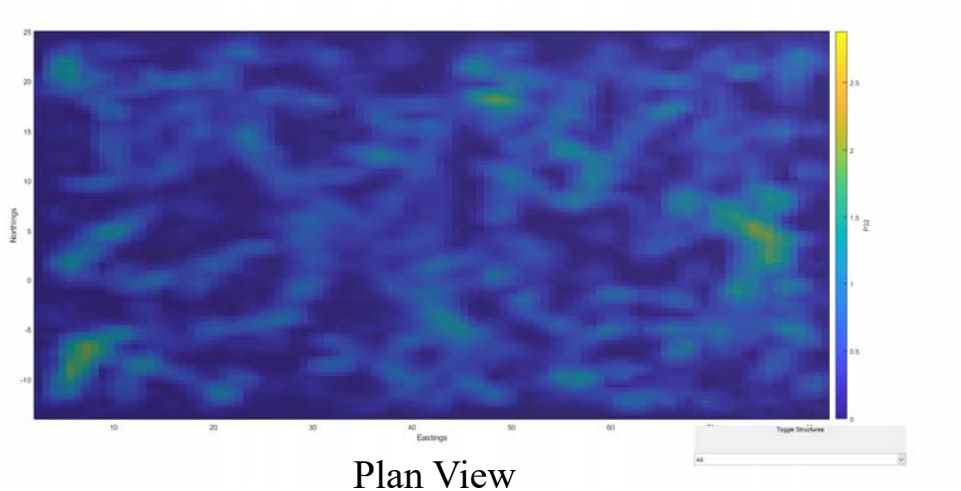

Plan View

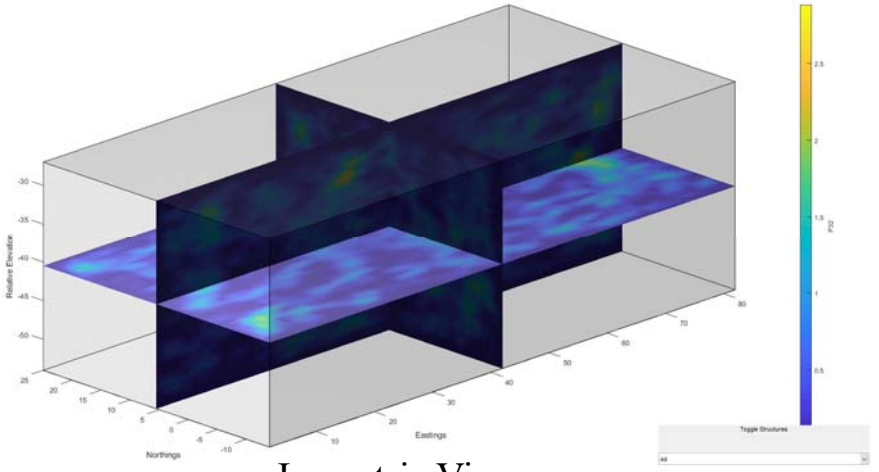

Isometric View

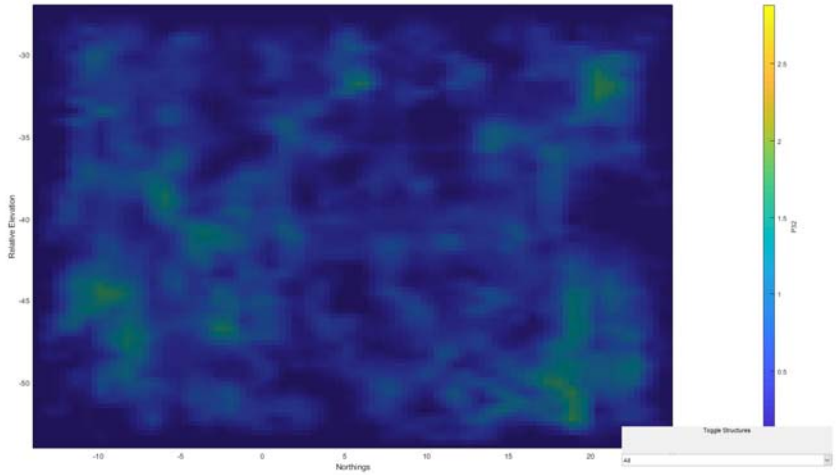

East View

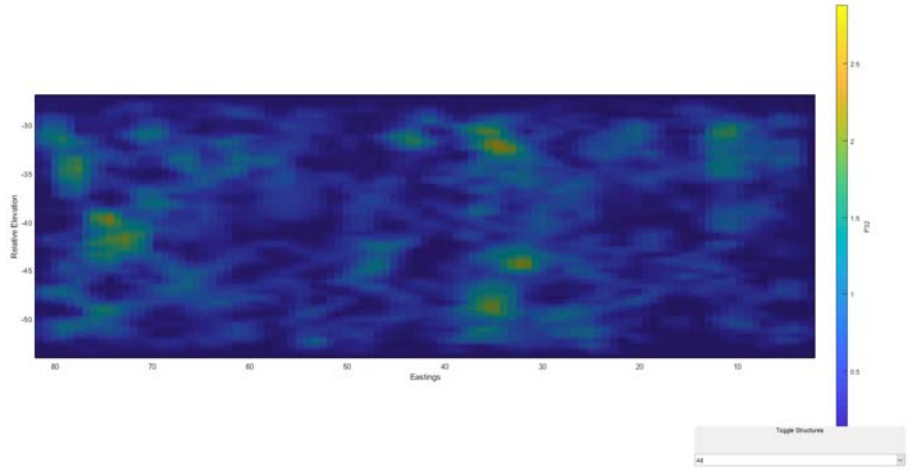

North View

Structural Analysis from SIROMODEL of DFN Mountain Small – Scale Factor=1.2

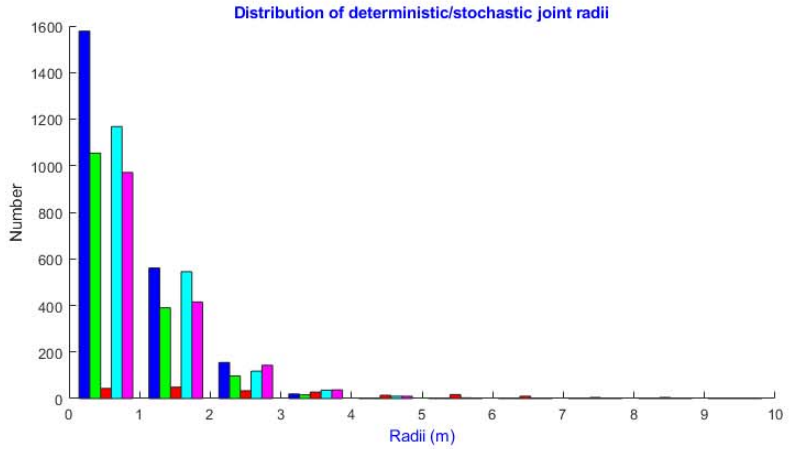

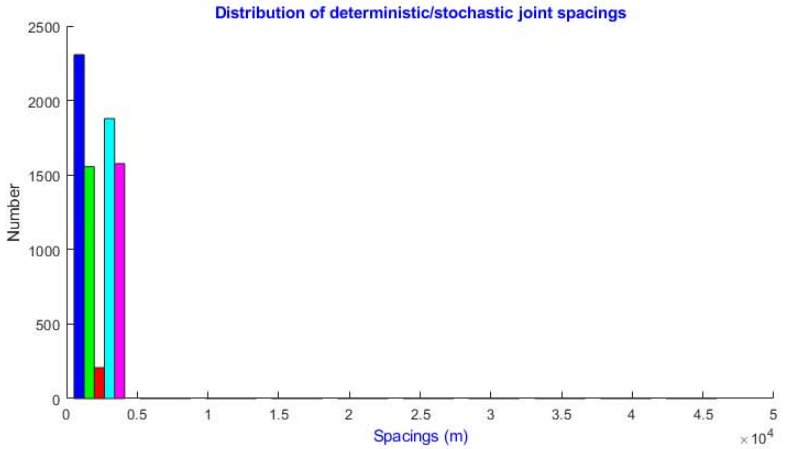

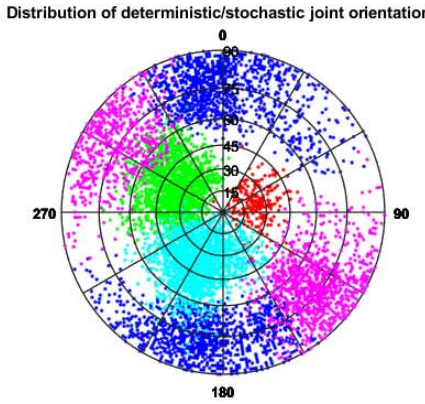

Stereonet Plot of Dip Vectors

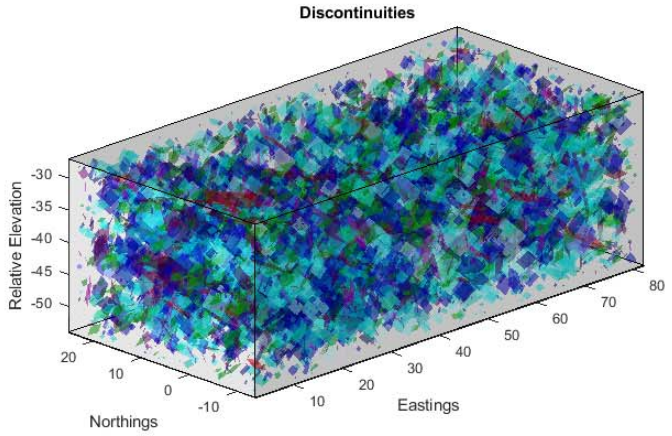

Isopleths of Fracture Statistical Analysis: DFN Mountain Small – Scale Factor=1.2

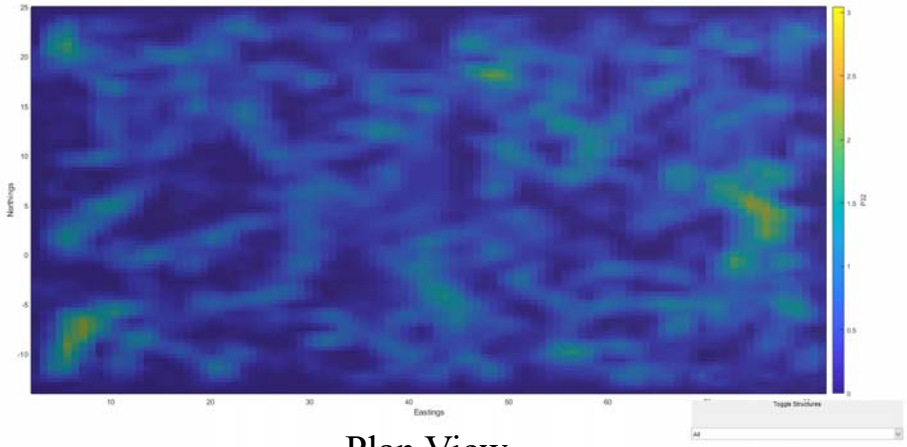

Plan View

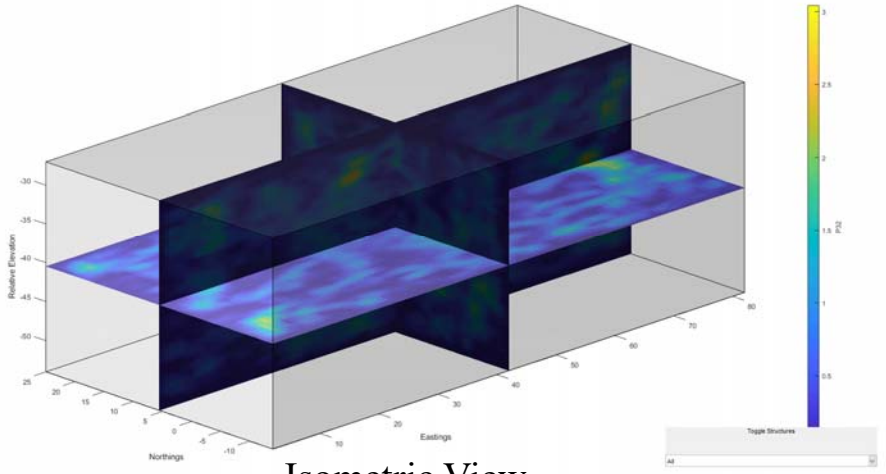

Isometric View

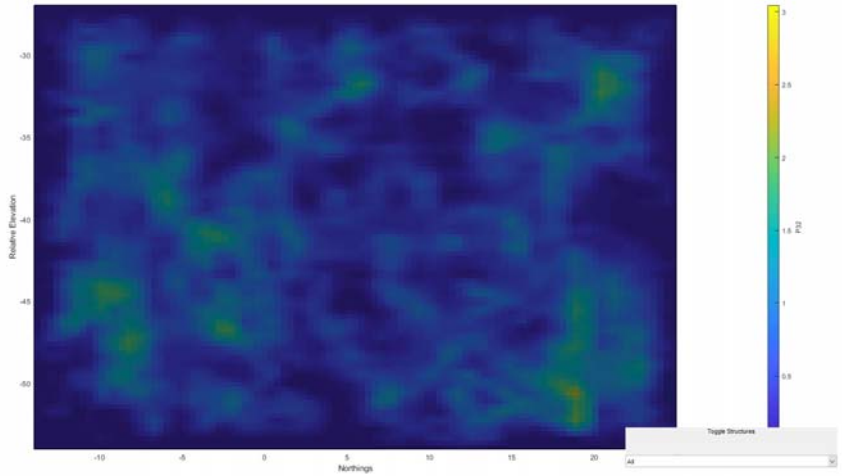

East View

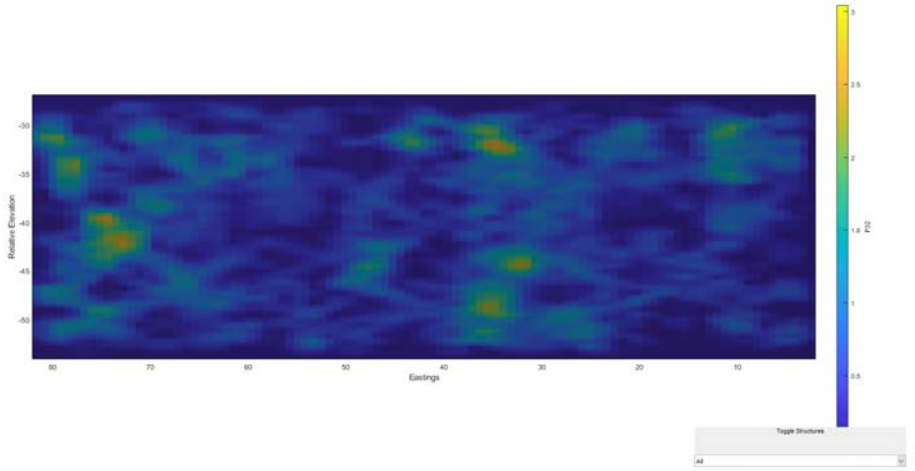

North View

Structural Analysis from SIROMODEL of DFN Mountain Small – Scale Factor=1.3

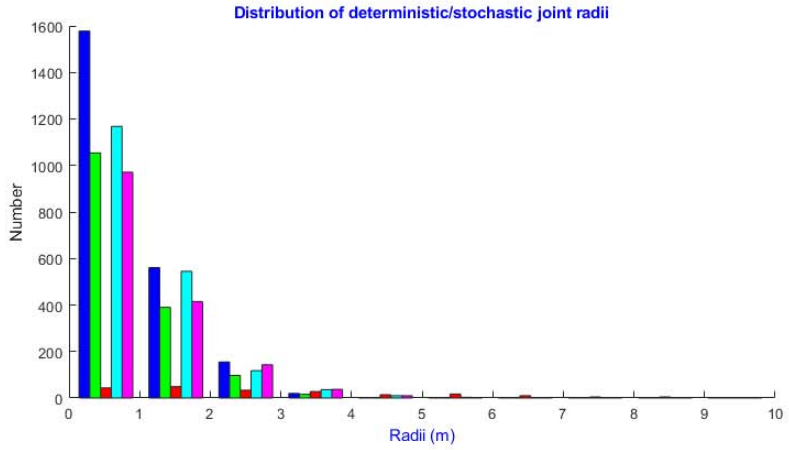

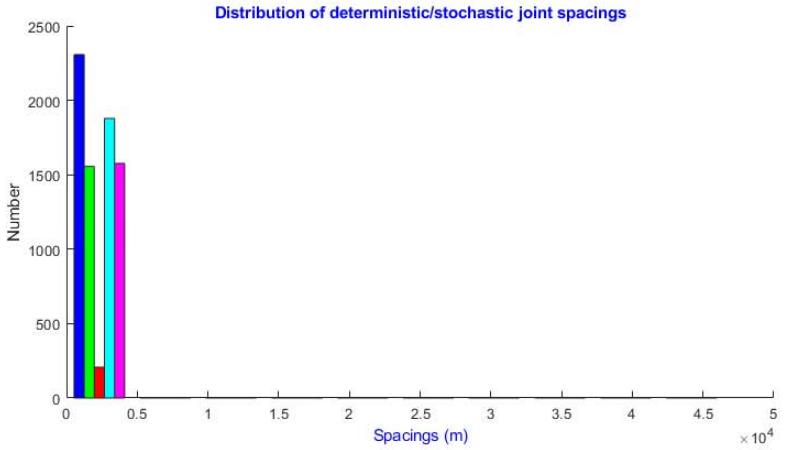

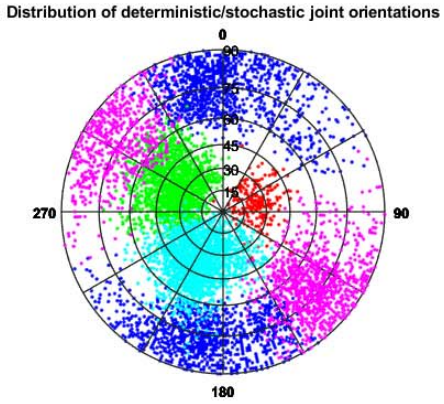

Stereonet Plot of Dip Vectors

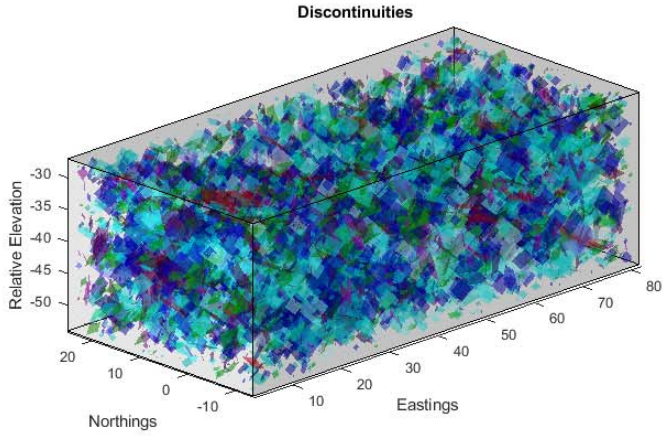

Isopleths of Fracture Statistical Analysis: DFN Mountain Small – Scale Factor=1.3

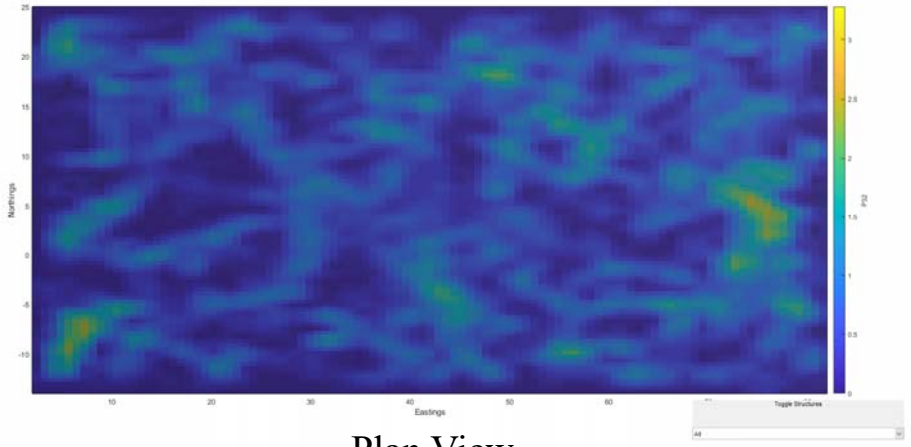

Plan View

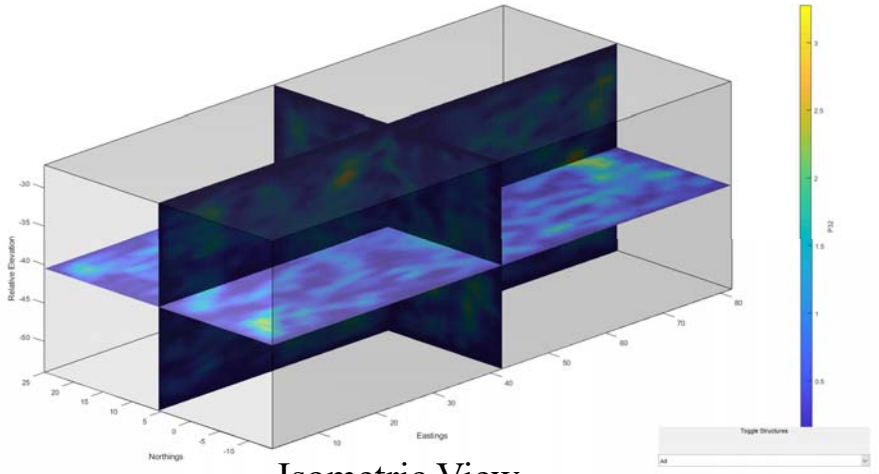

Isometric View

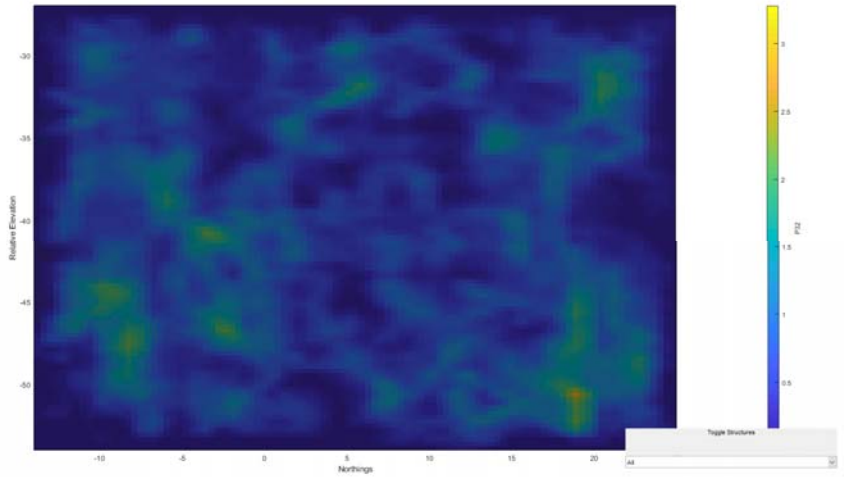

East View

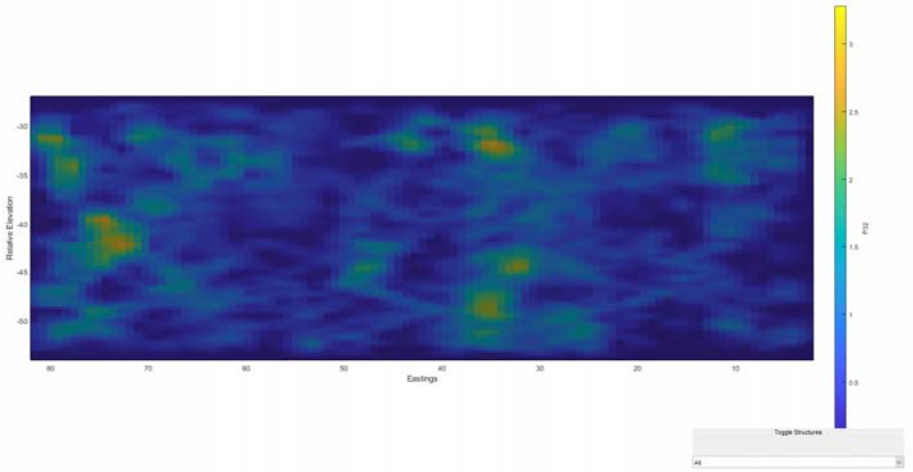

North View

Structural Analysis from SIROMODEL of DFN Mountain Small – Scale Factor=1.4

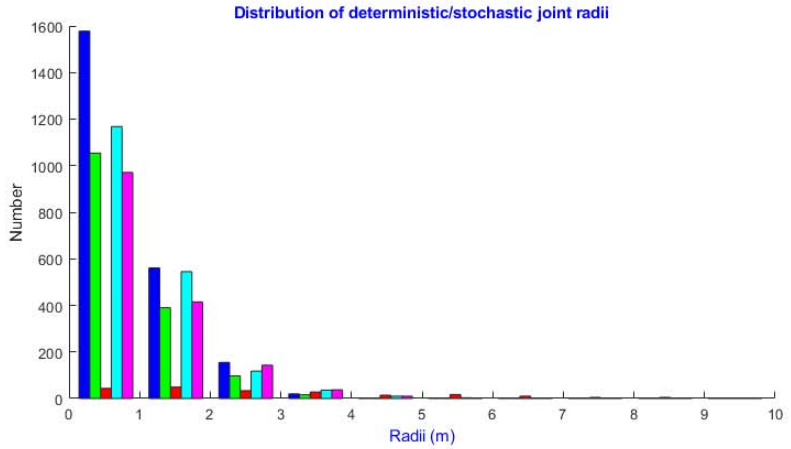

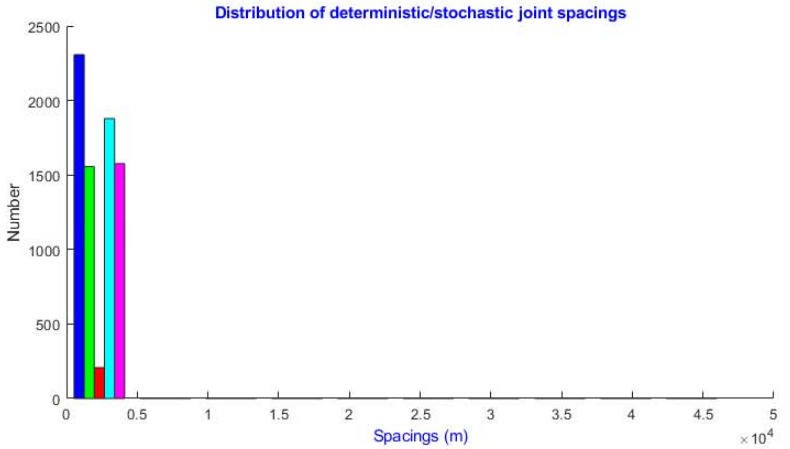

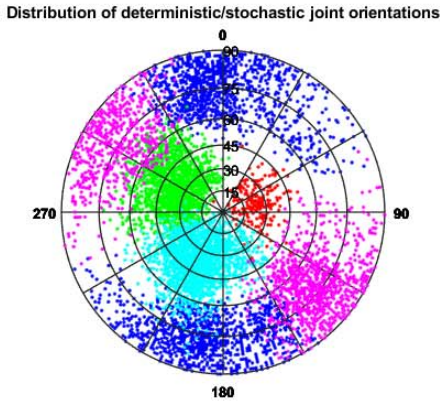

Stereonet Plot of Dip Vectors

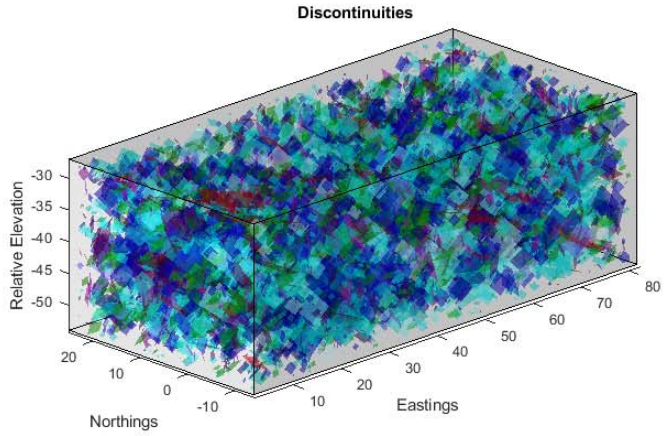

Isopleths of Fracture Statistical Analysis: DFN Mountain Small – Scale Factor=1.4

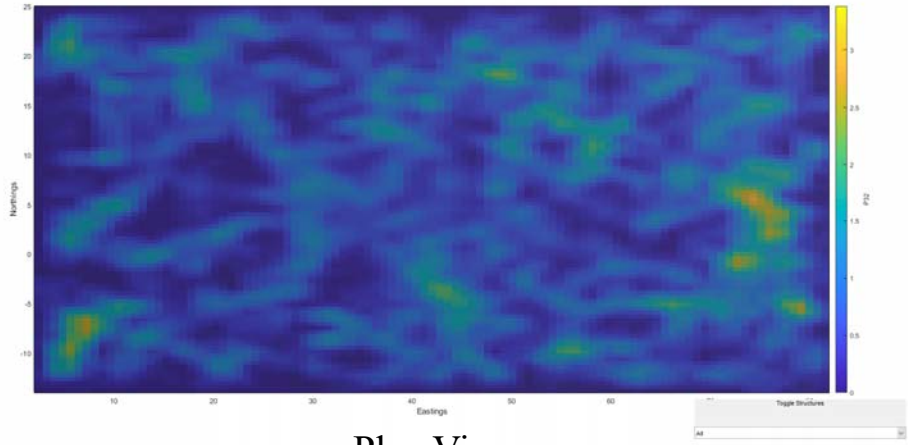

Plan View

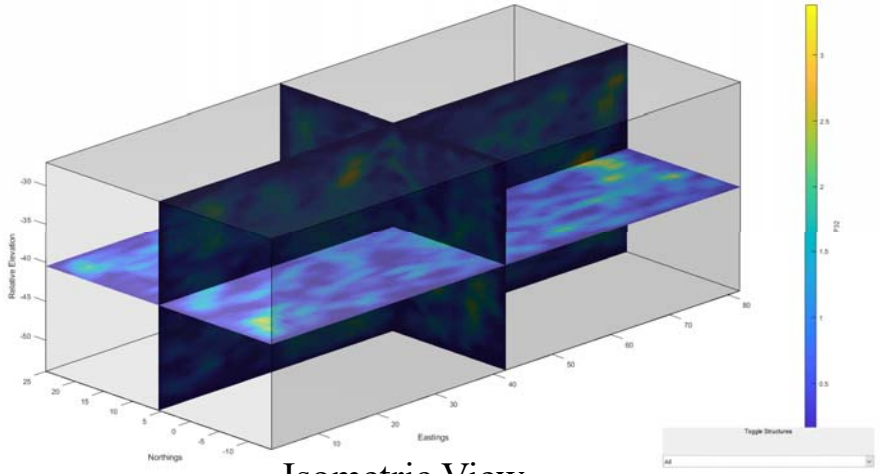

Isometric View

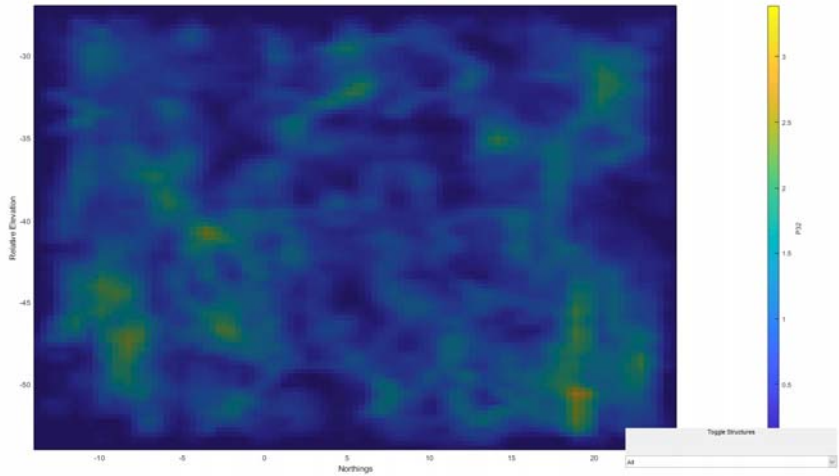

East View

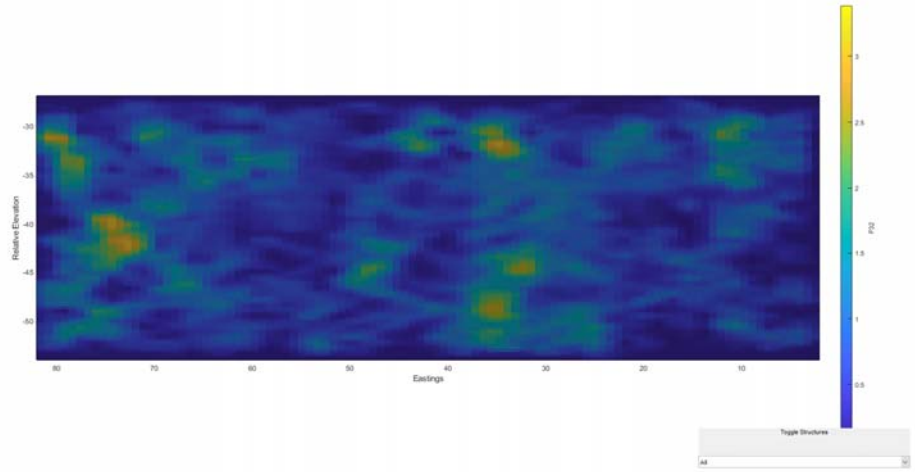

North View

Structural Analysis from SIROMODEL of DFN Mountain Small – Scale Factor=1.5

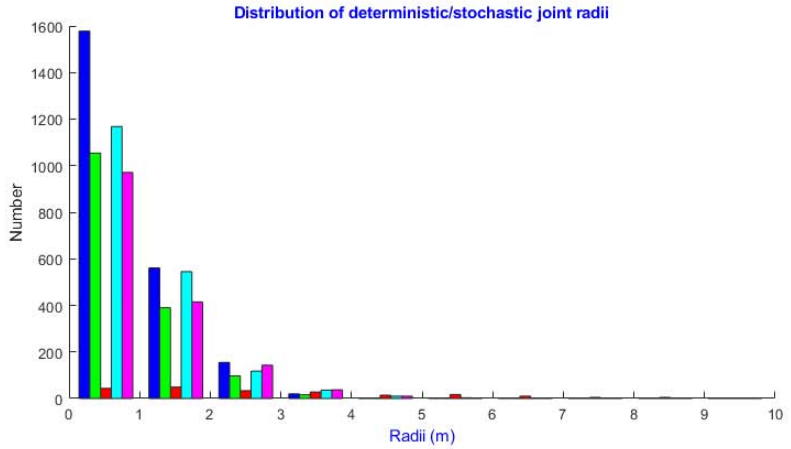

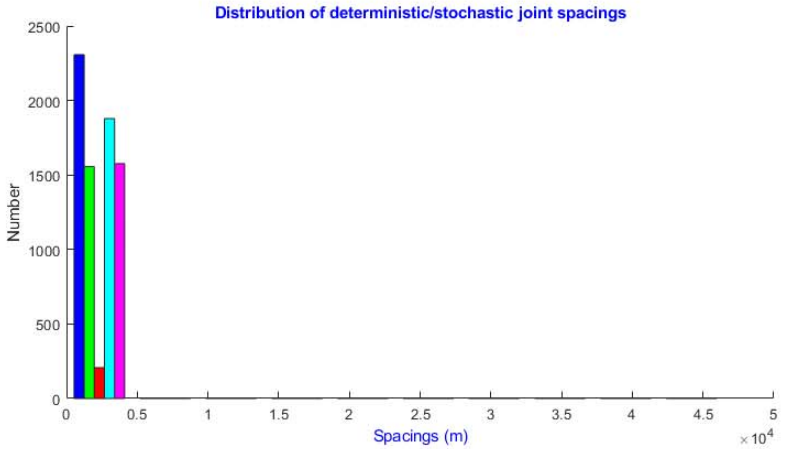

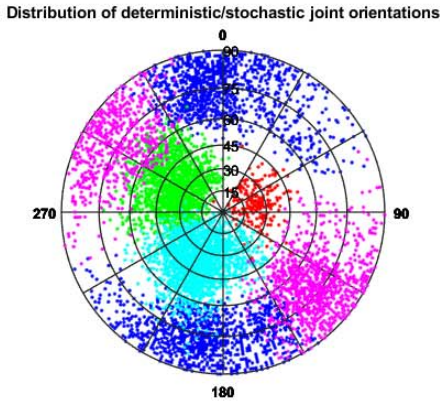

Stereonet Plot of Dip Vectors

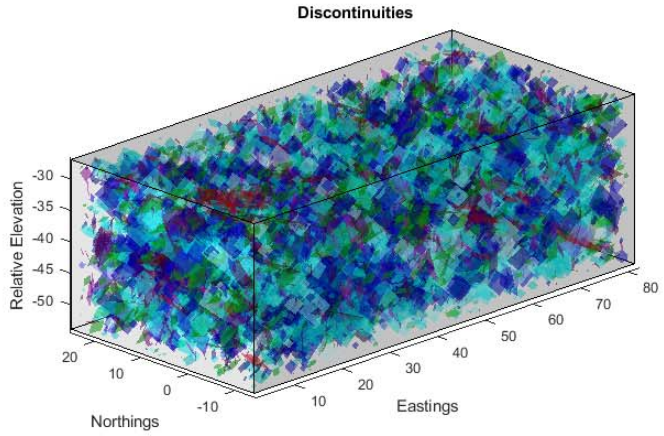

Isopleths of Fracture Statistical Analysis: DFN Mountain Small – Scale Factor=1.5

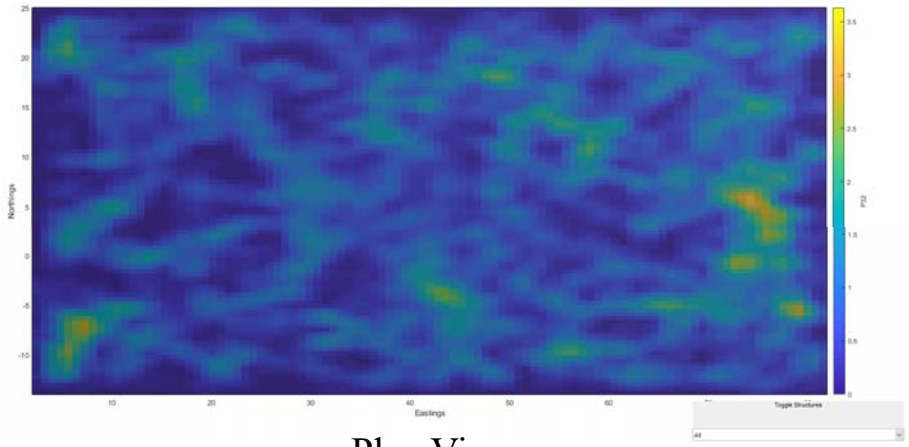

Plan View

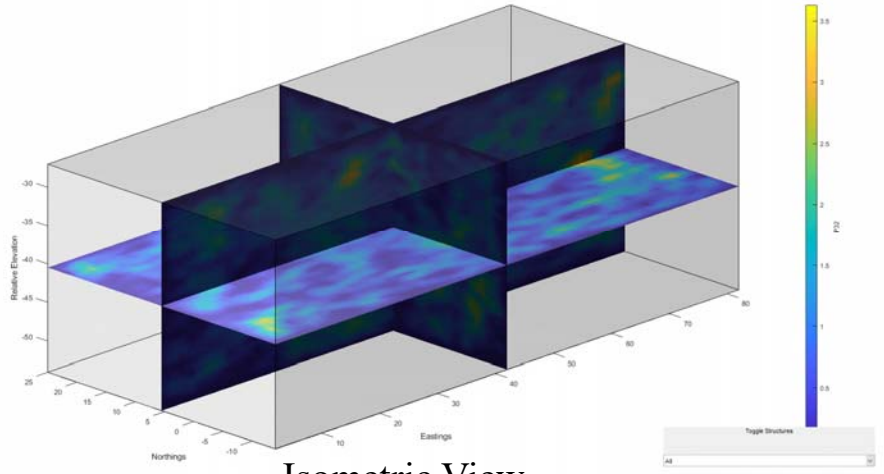

Isometric View

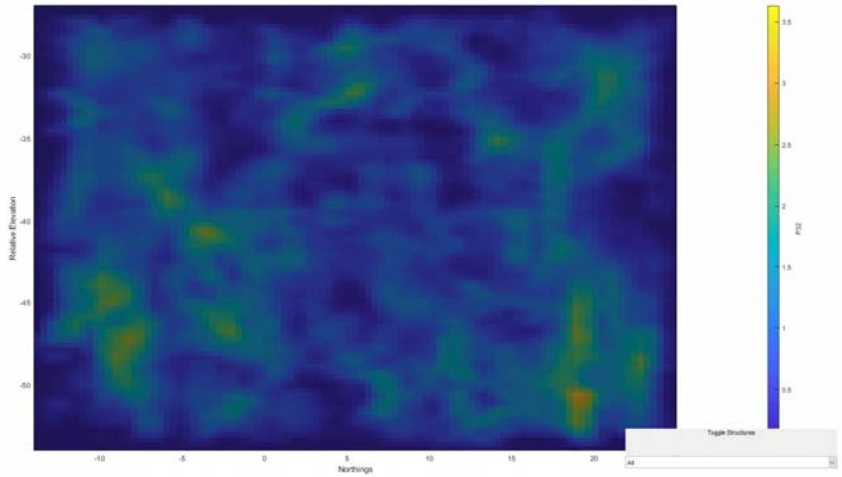

East View

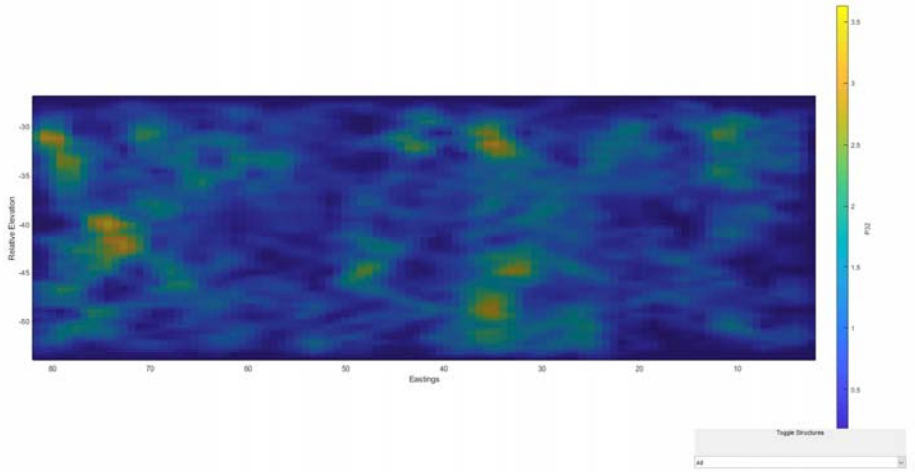

North View

Structural Analysis from SIROMODEL of DFN Mountain Small – Scale Factor=1.6

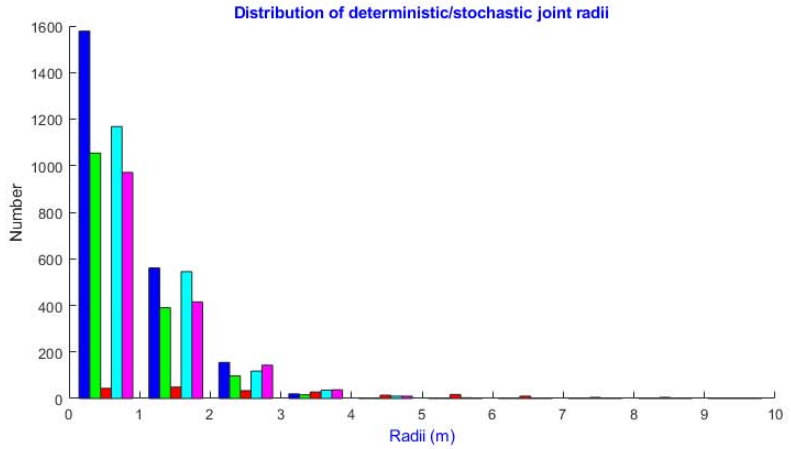

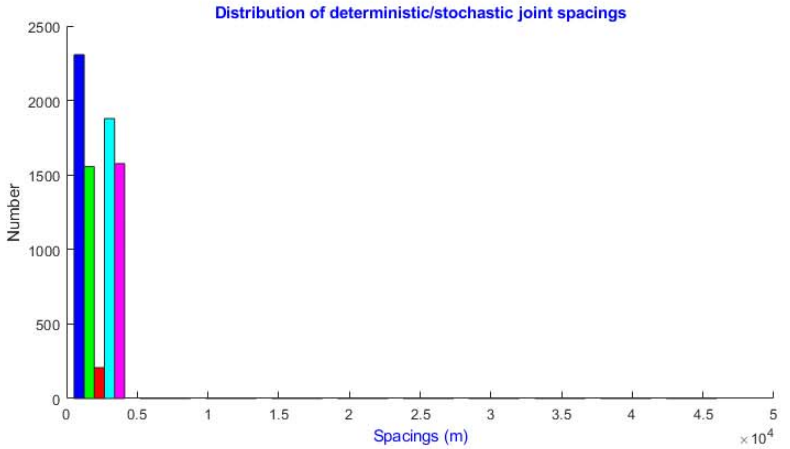

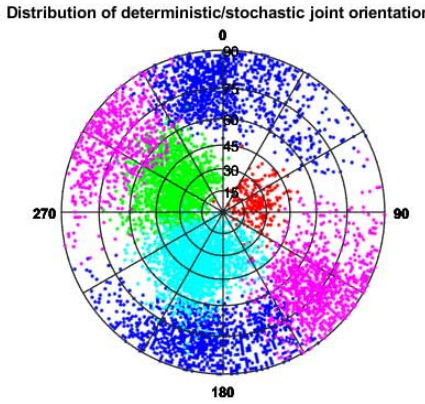

Stereonet Plot of Dip Vectors

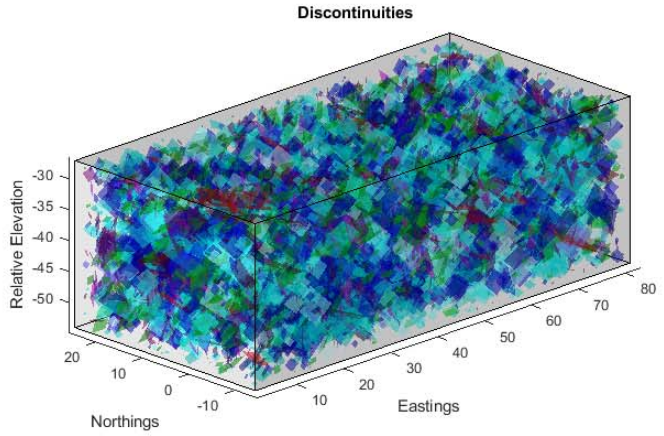

Isopleths of Fracture Statistical Analysis: DFN Mountain Small – Scale Factor=1.6

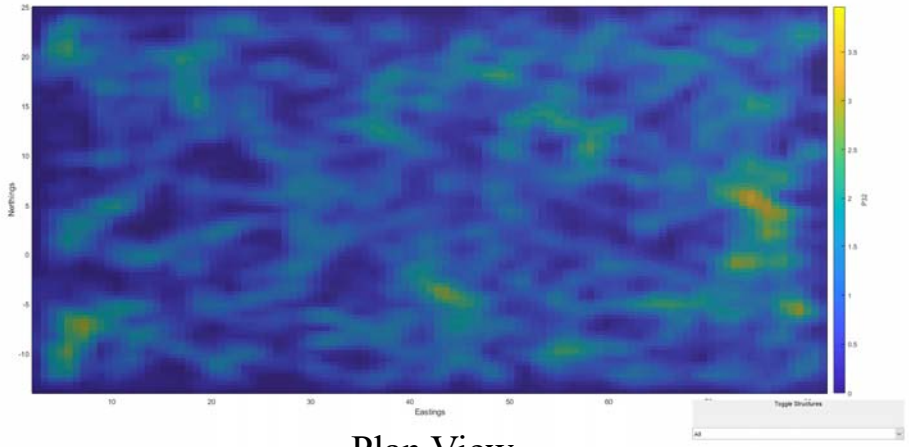

Plan View

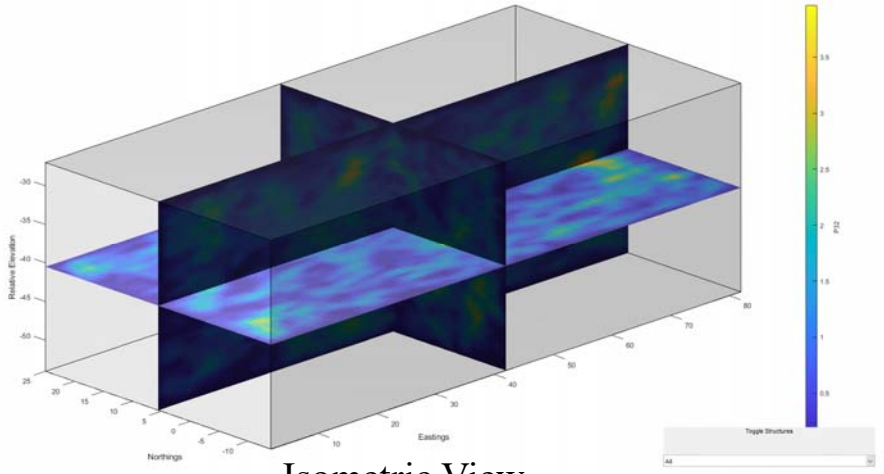

Isometric View

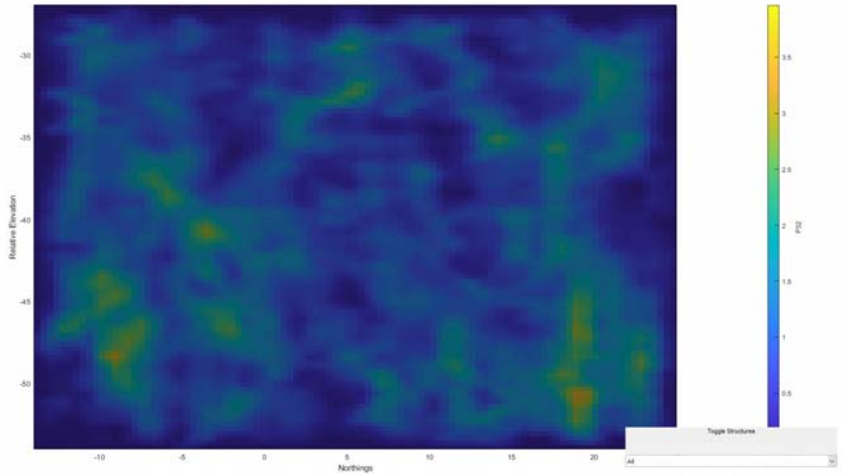

East View

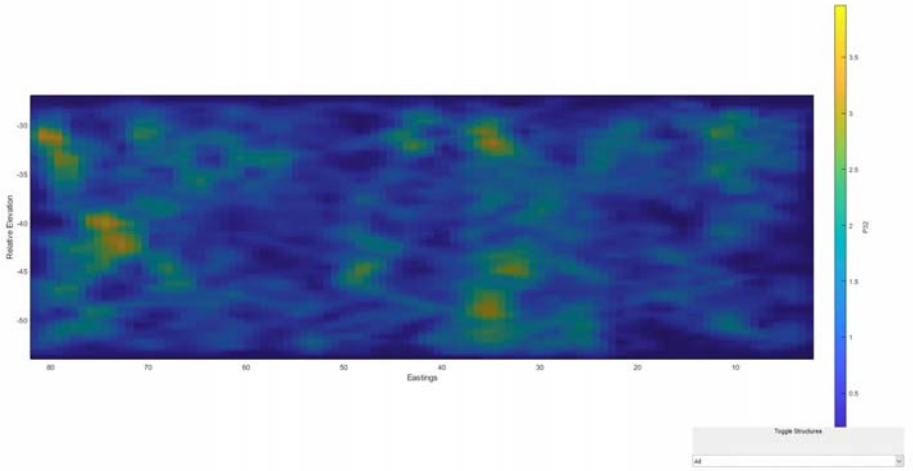

North View

Structural Analysis from SIROMODEL of DFN Mountain Small – Scale Factor=1.7

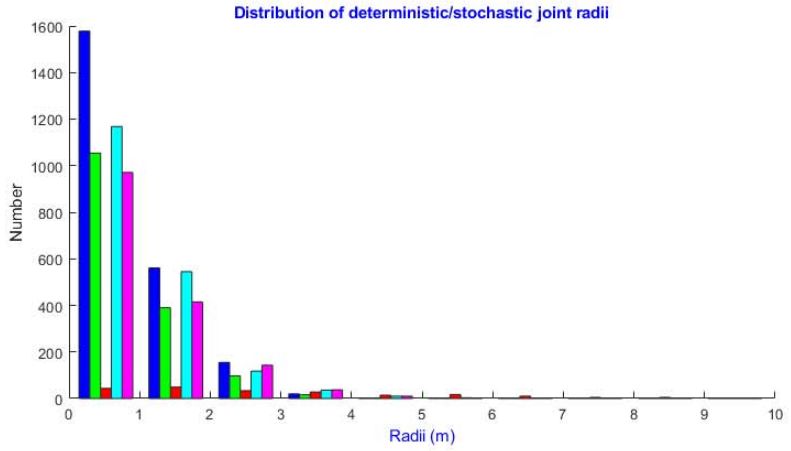

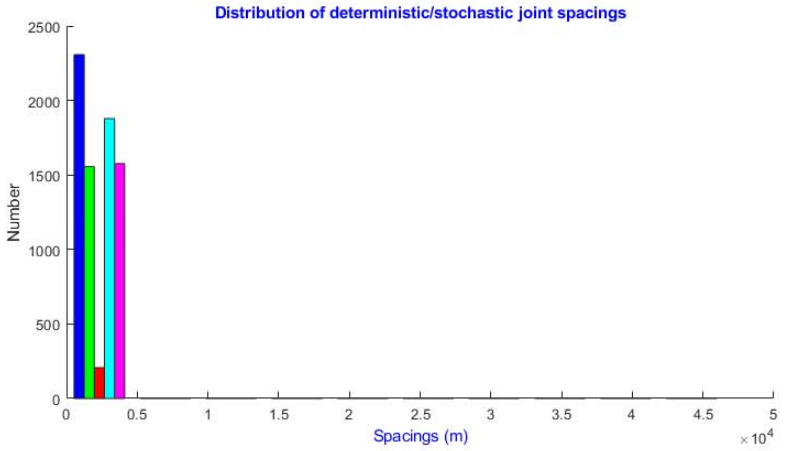

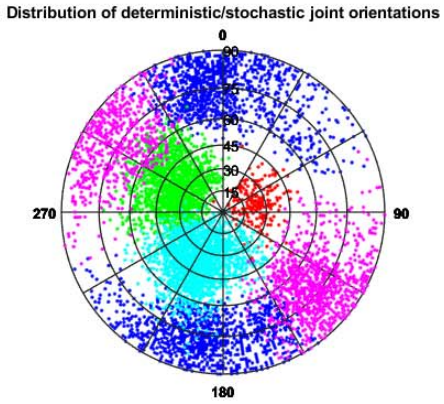

Stereonet Plot of Dip Vectors

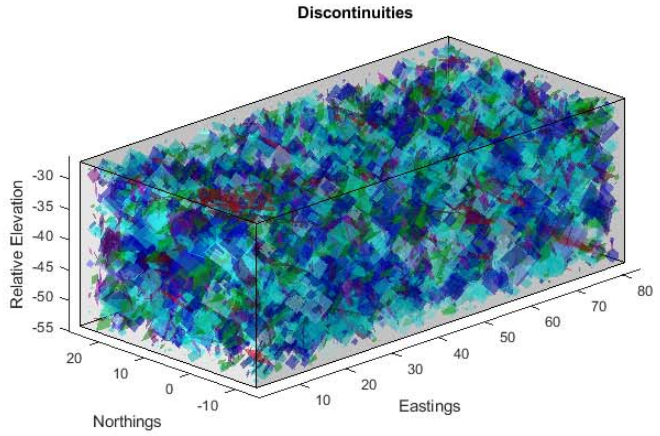

Isopleths of Fracture Statistical Analysis: DFN Mountain Small – Scale Factor=1.7

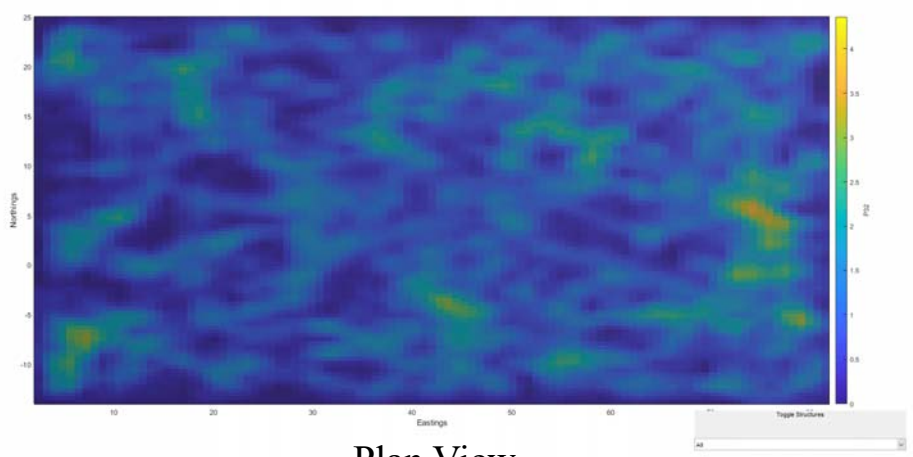

Plan View

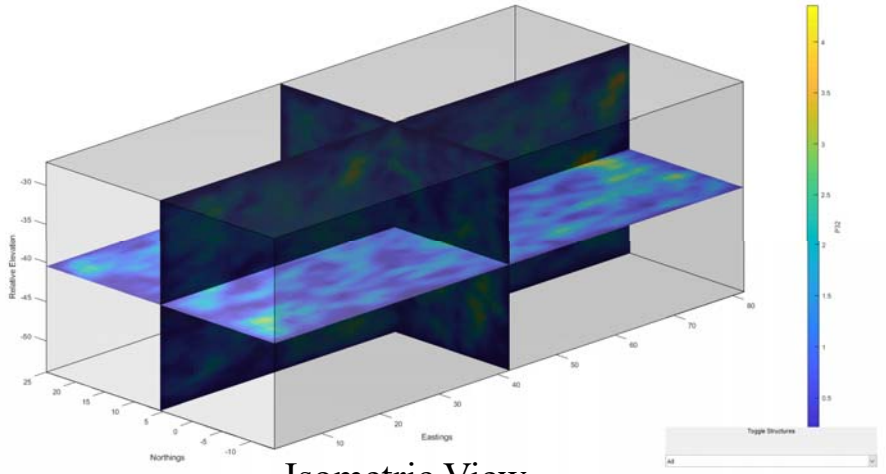

Isometric View

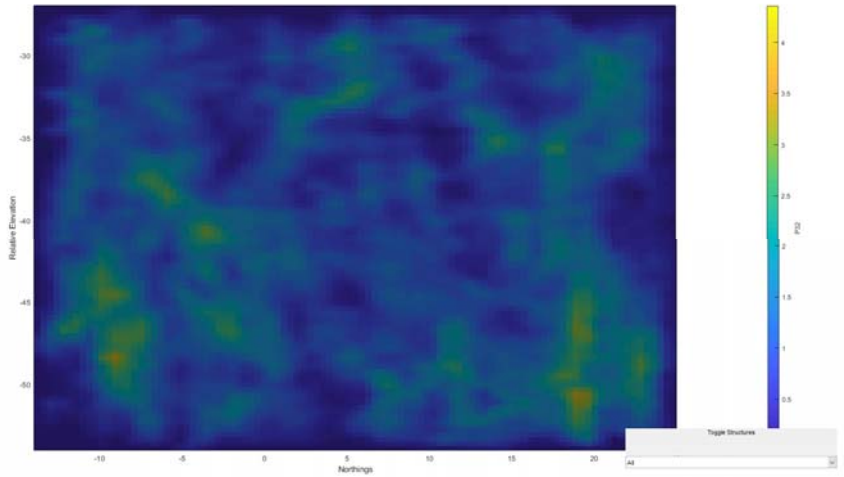

East View

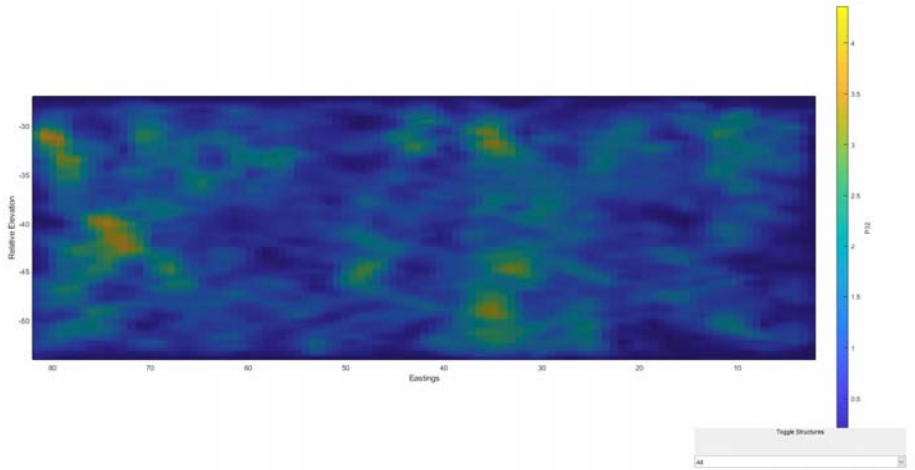

North View

Structural Analysis from SIROMODEL of DFN Mountain Small – Scale Factor=1.8

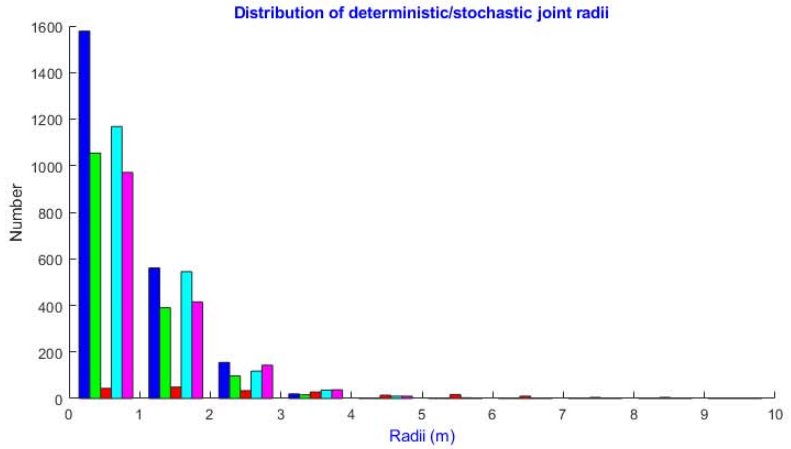

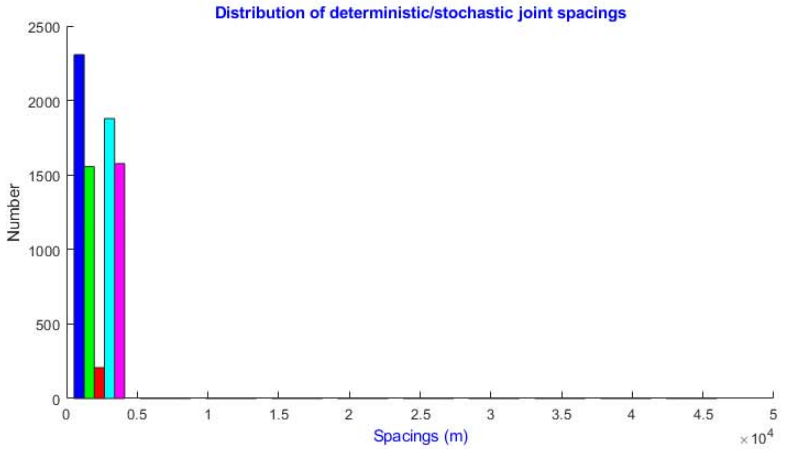

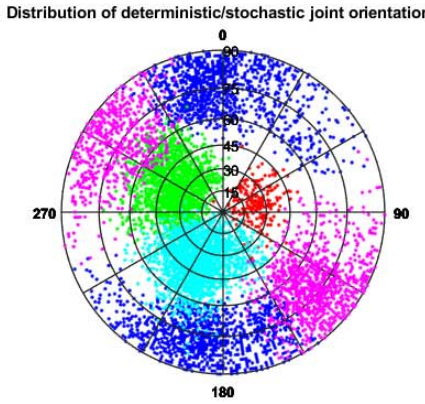

Stereonet Plot of Dip Vectors

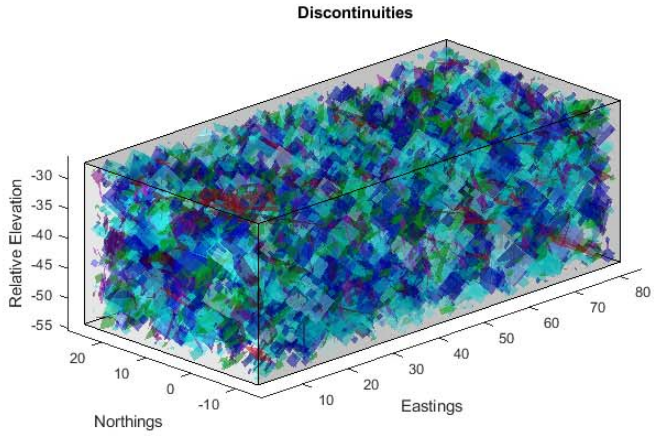

Isopleths of Fracture Statistical Analysis: DFN Mountain Small – Scale Factor=1.8

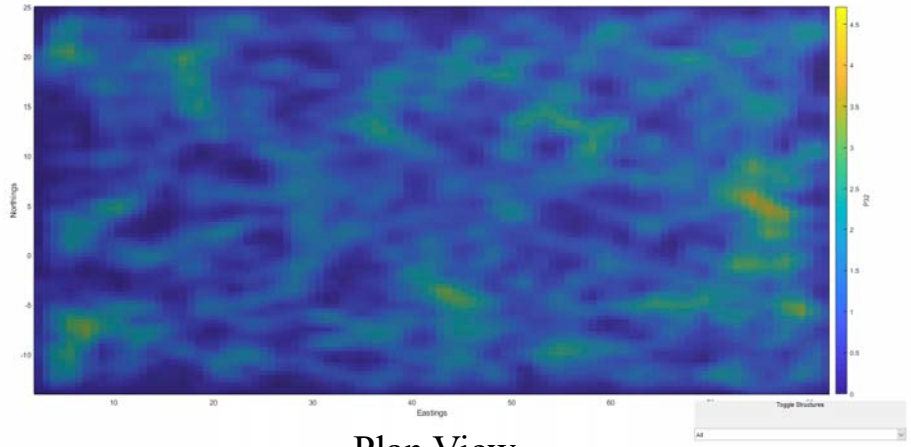

Plan View

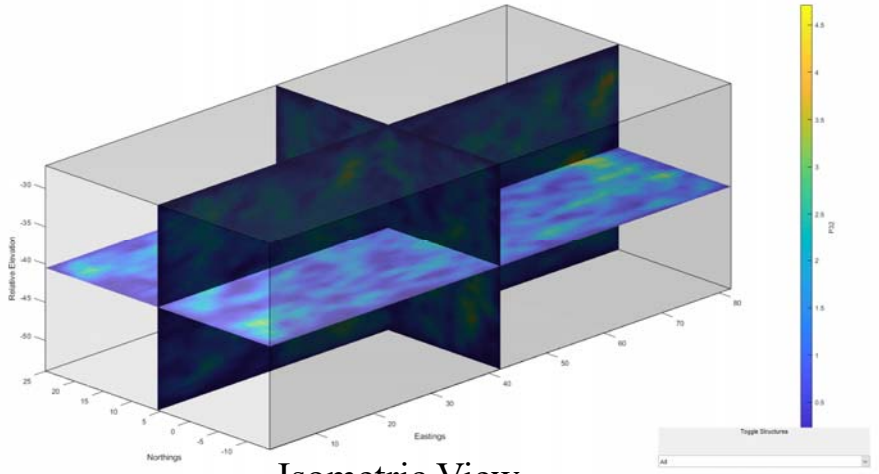

Isometric View

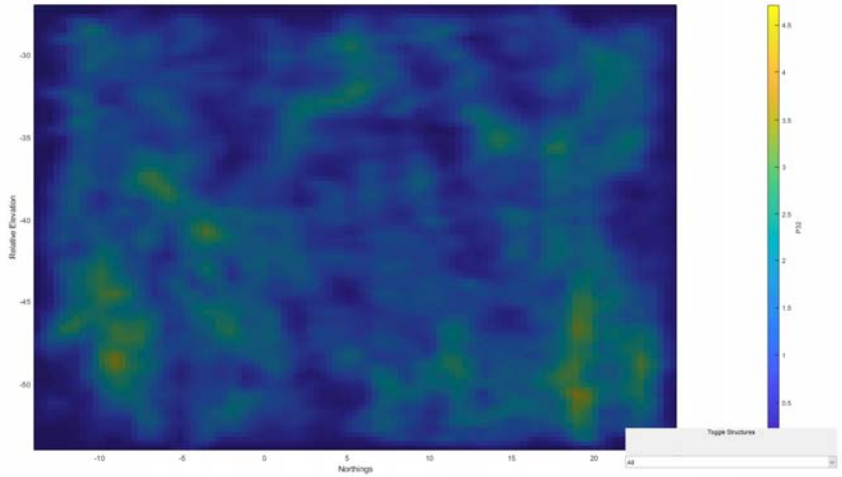

East View

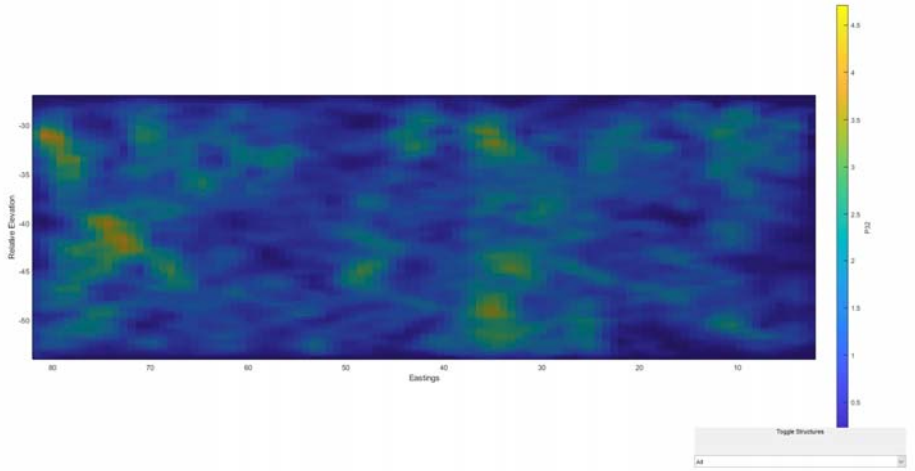

North View

Structural Analysis from SIROMODEL of DFN Mountain Small – Scale Factor=1.9

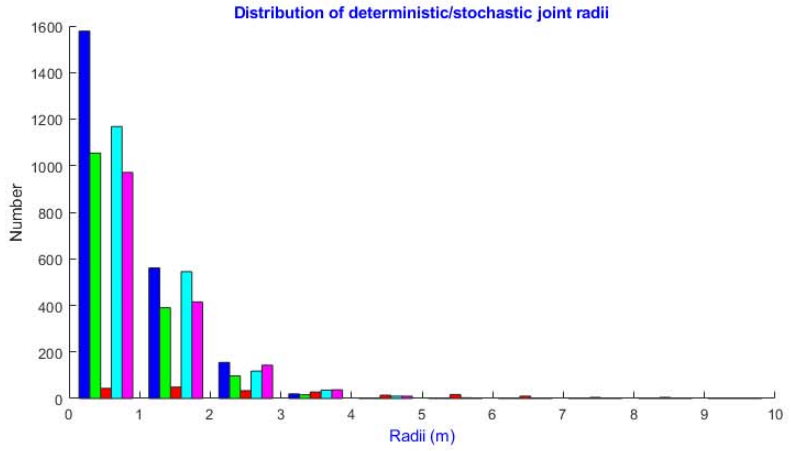

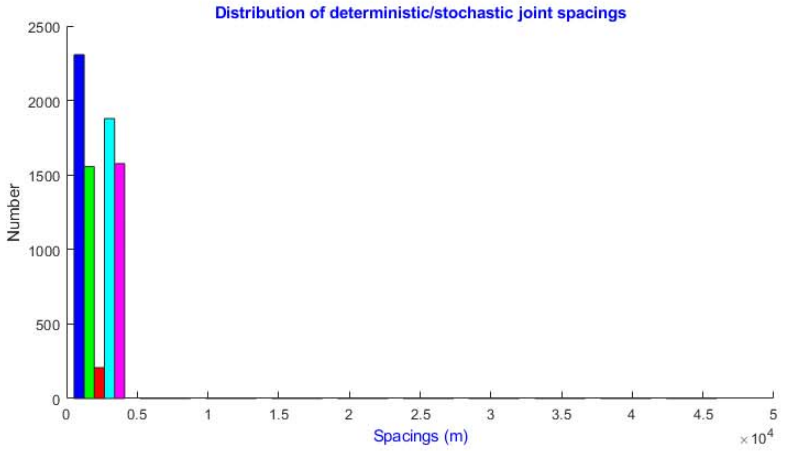

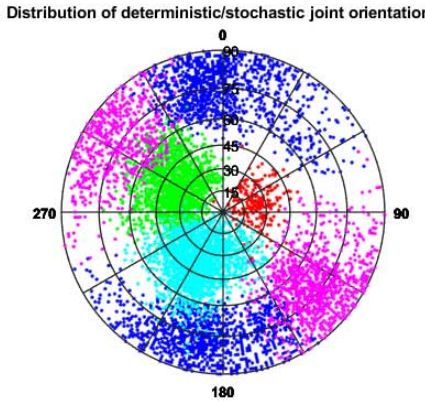

Stereonet Plot of Dip Vectors

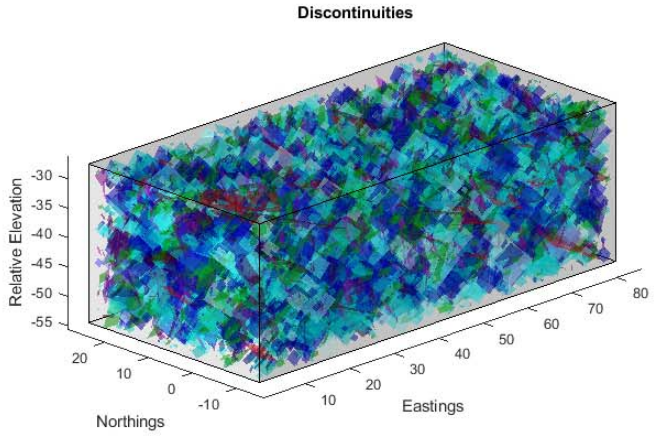

Isopleths of Fracture Statistical Analysis: DFN Mountain Small – Scale Factor=1.9

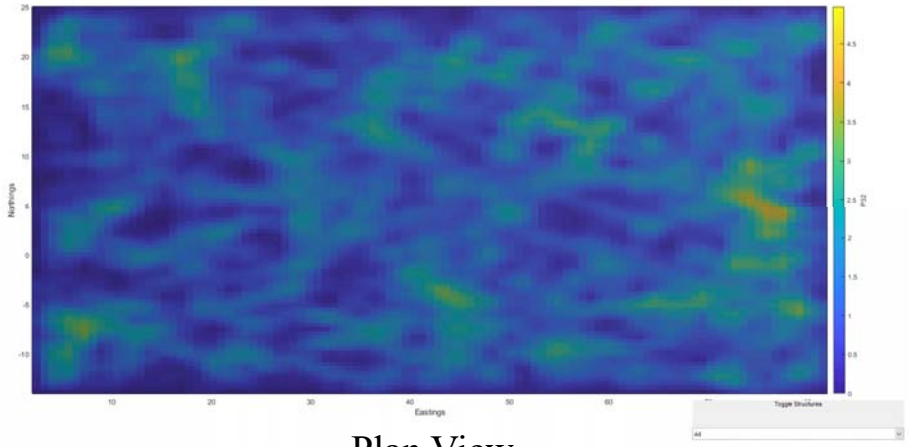

Plan View

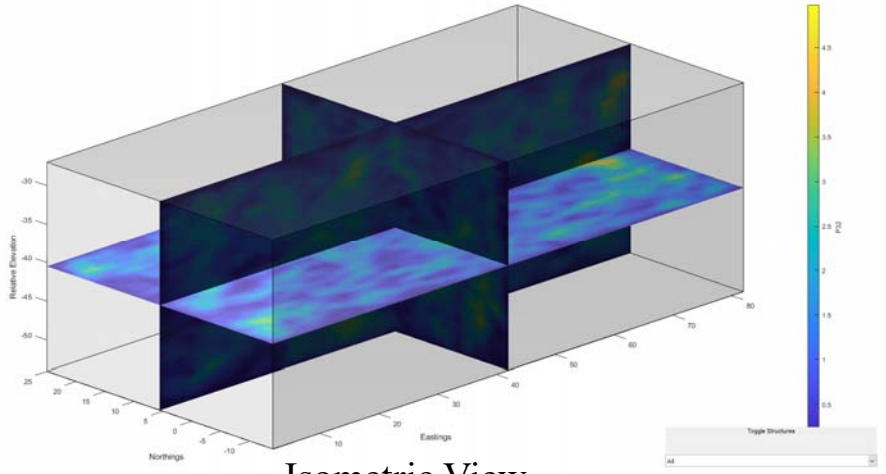

Isometric View

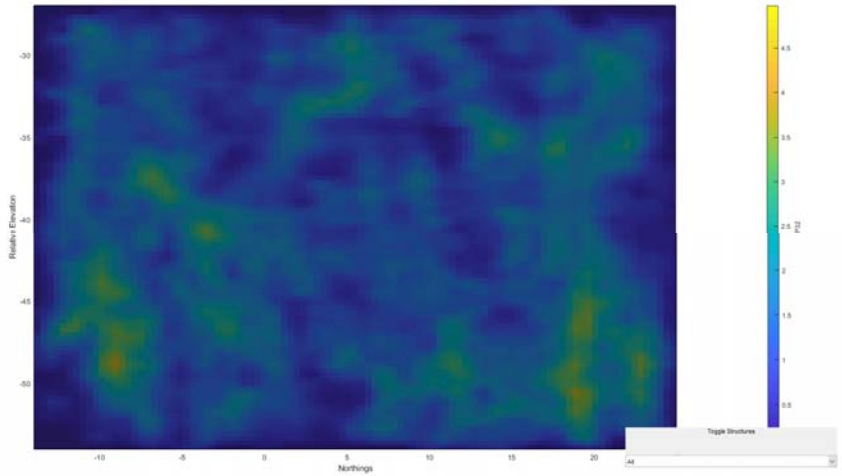

East View

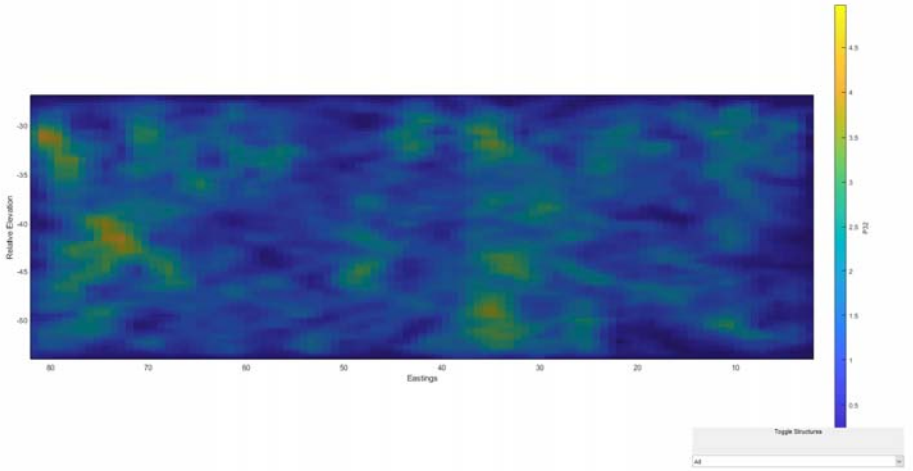

North View

Structural Analysis from SIROMODEL of DFN Mountain Small – Scale Factor=2

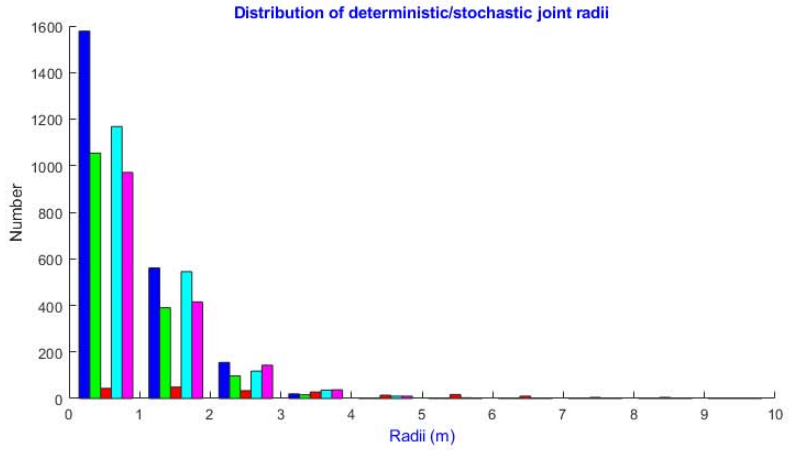

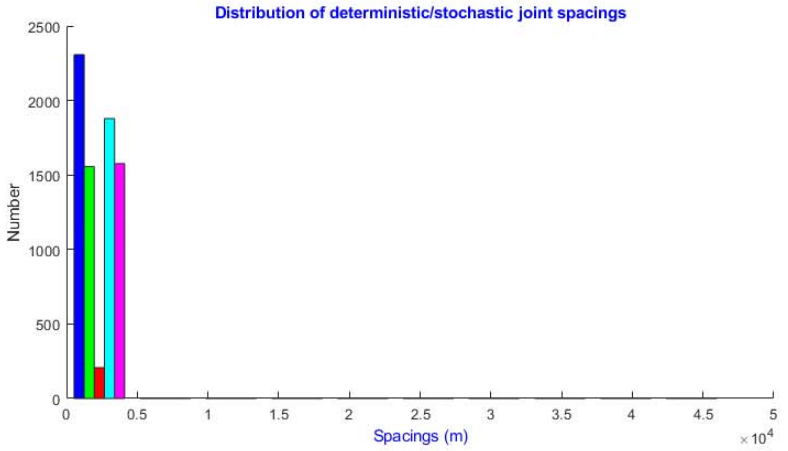

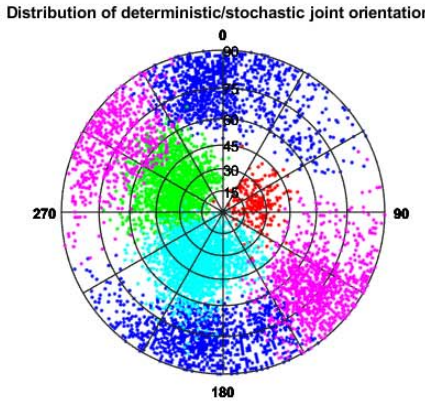

Stereonet Plot of Dip Vectors

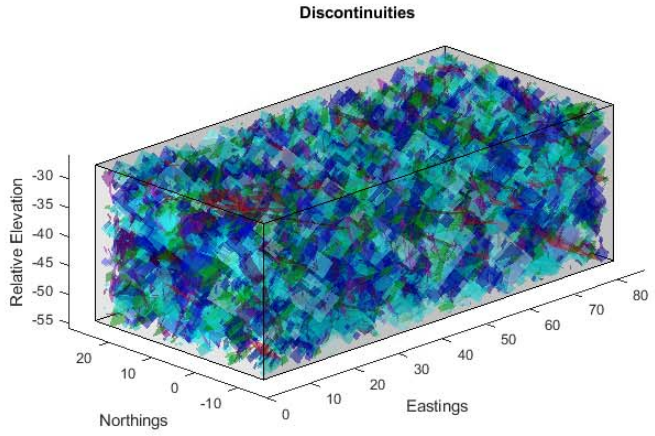

Isopleths of Fracture Statistical Analysis: DFN Mountain Small – Scale Factor=2

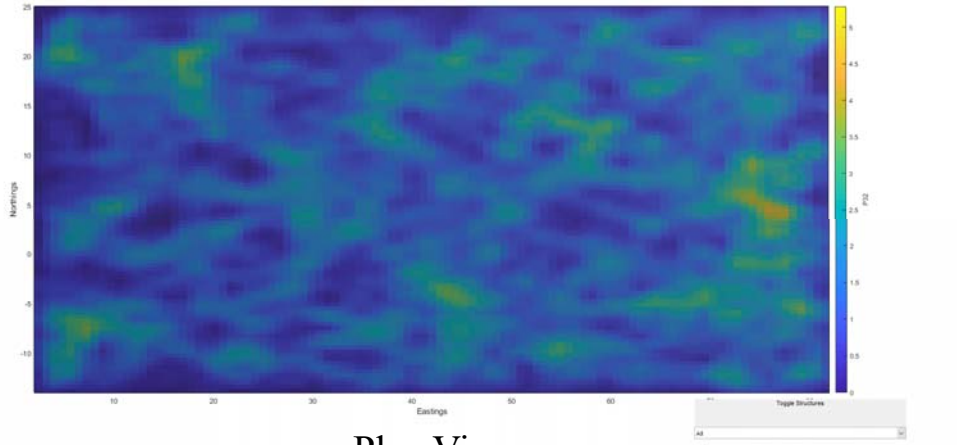

Plan View

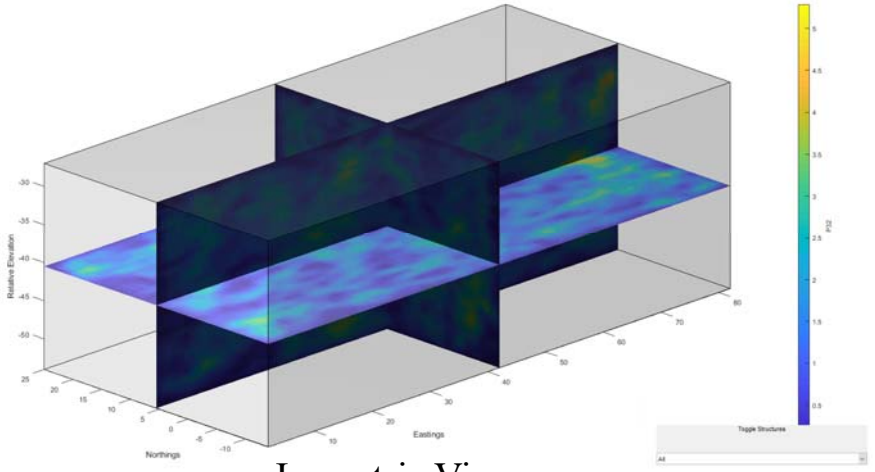

Isometric View

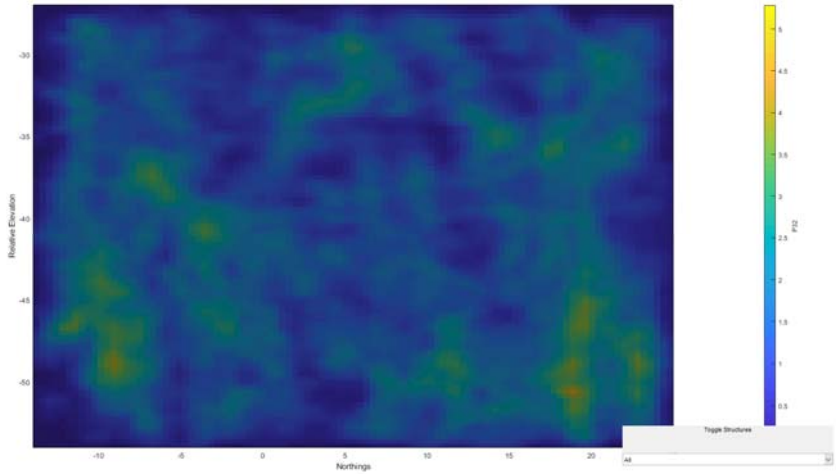

East View

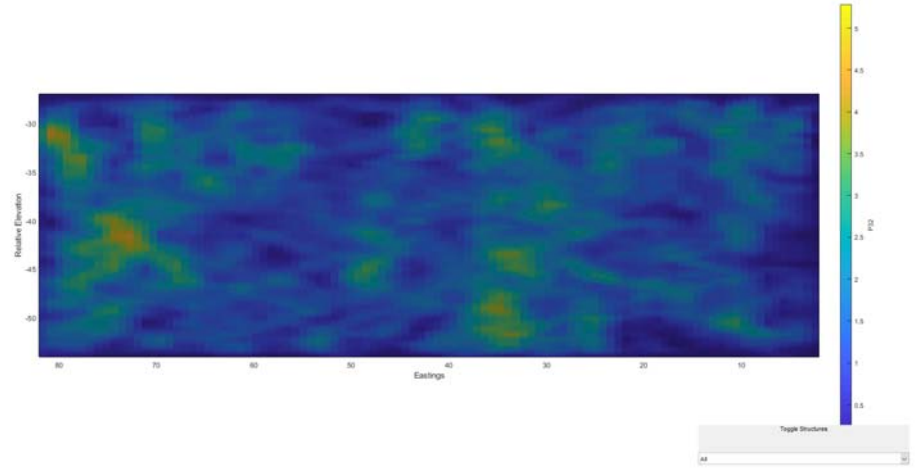

North View

Structural Analysis from SIROMODEL of DFN Mountain Small – Scale Factor=2.2

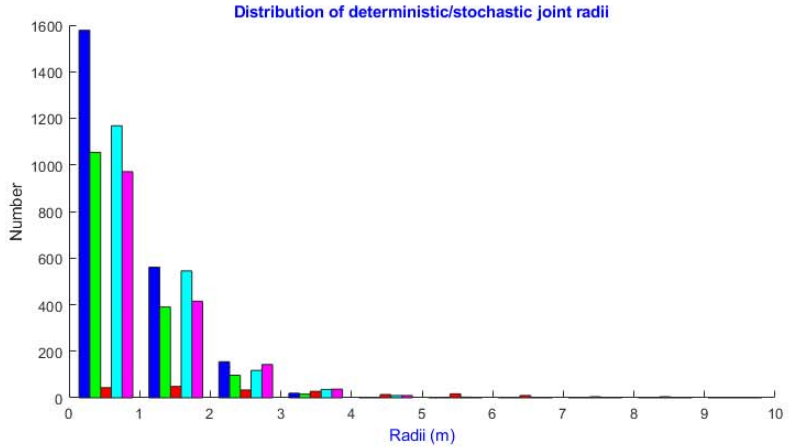

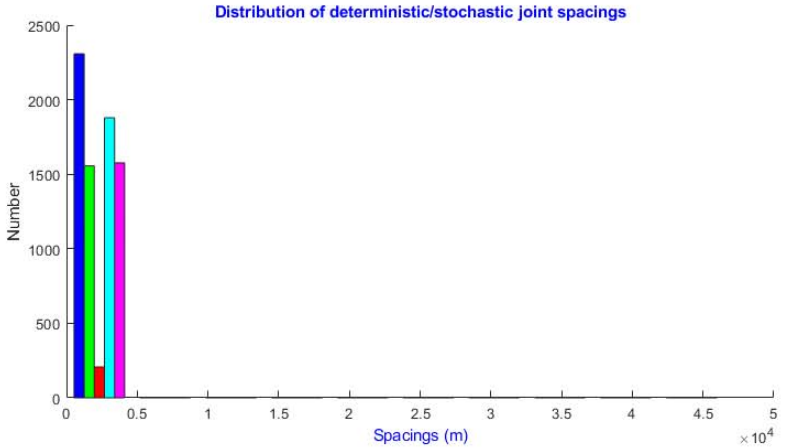

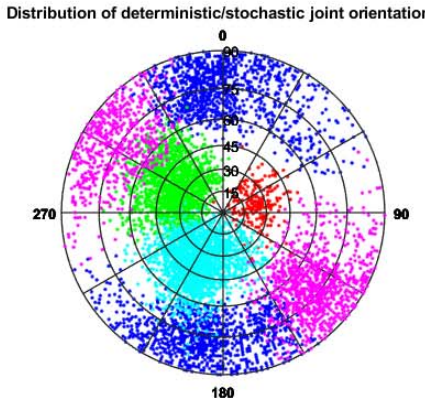

Stereonet Plot of Dip Vectors

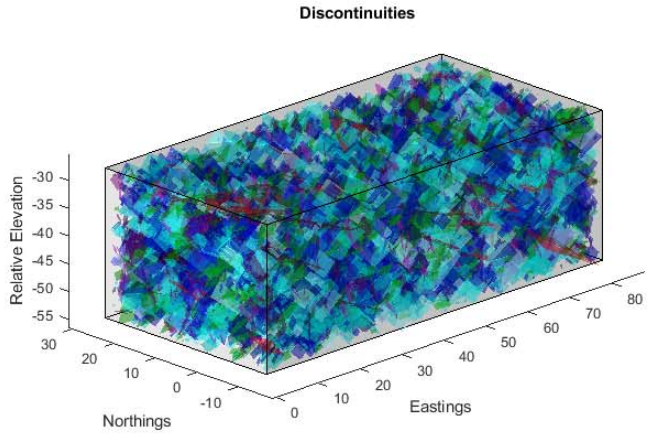

Isopleths of Fracture Statistical Analysis: DFN Mountain Small – Scale Factor=2.2

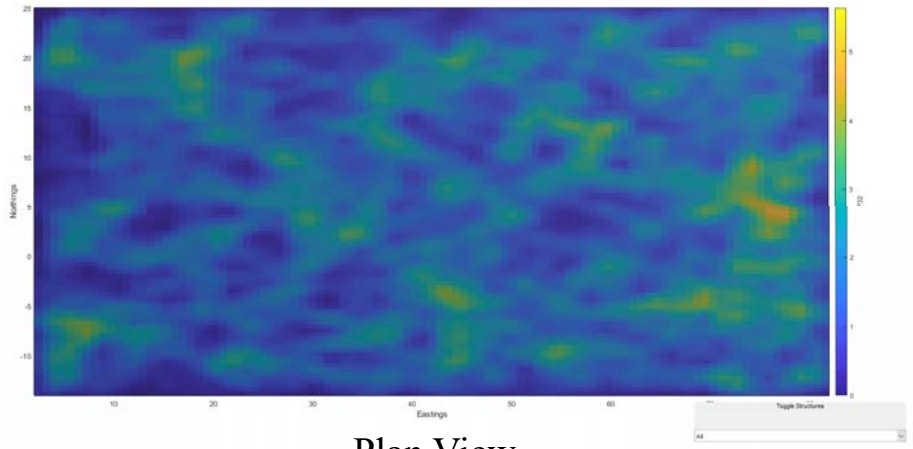

Plan View

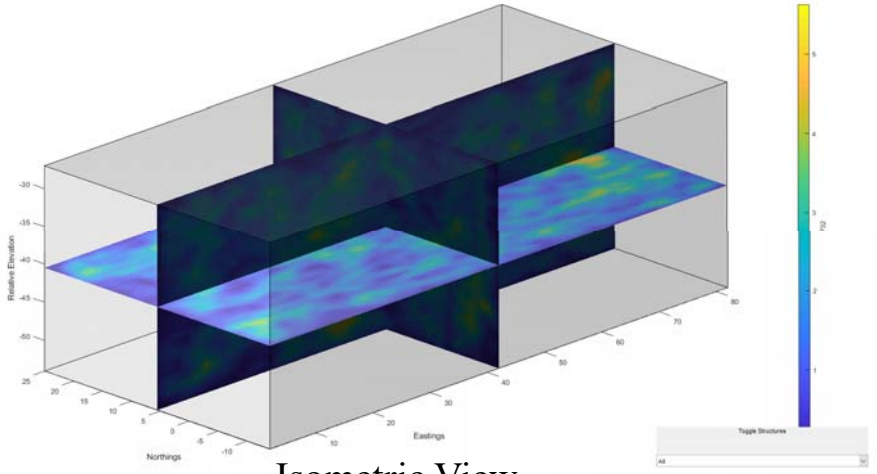

Isometric View

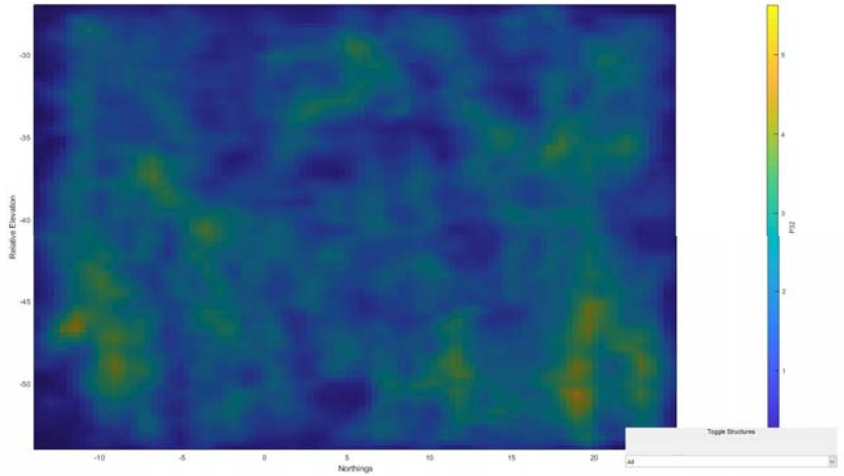

East View

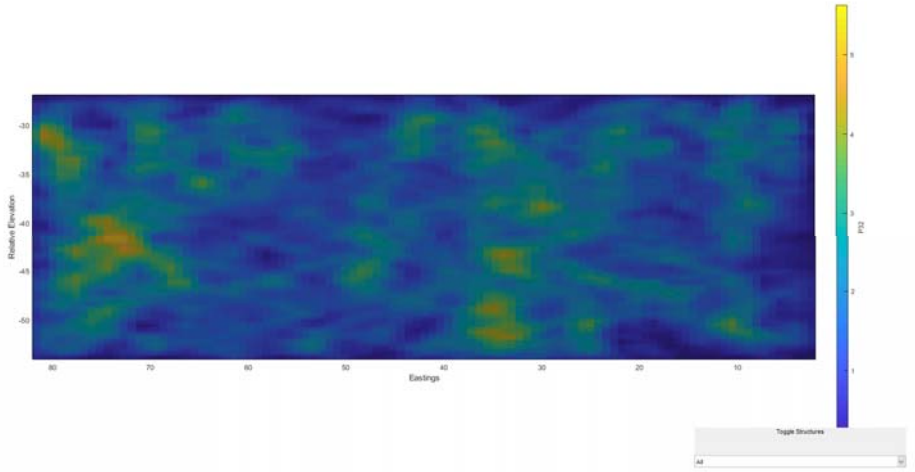

North View

Structural Analysis from SIROMODEL of DFN Mountain Small – Scale Factor=2.4

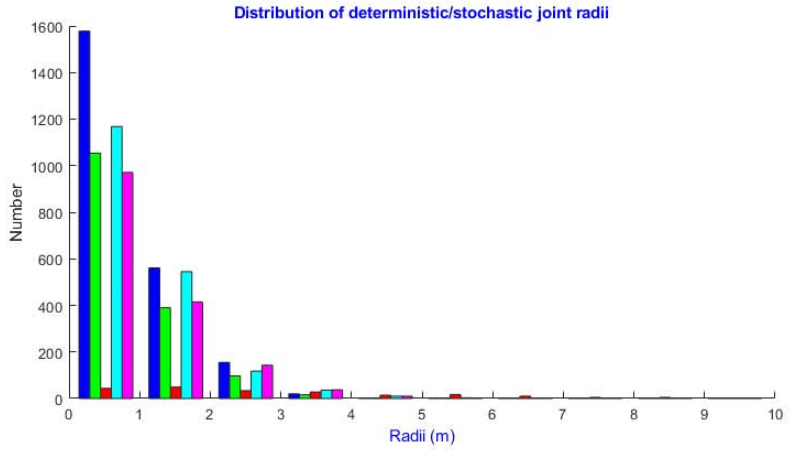

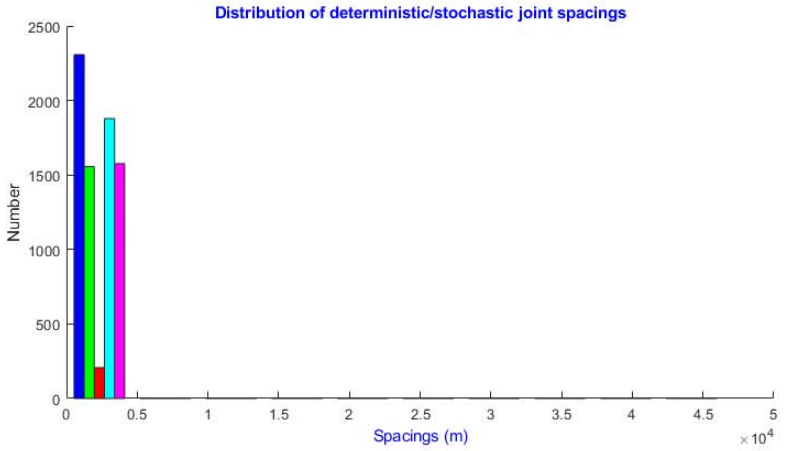

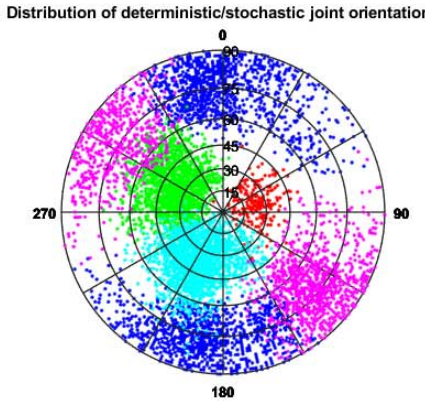

Stereonet Plot of Dip Vectors

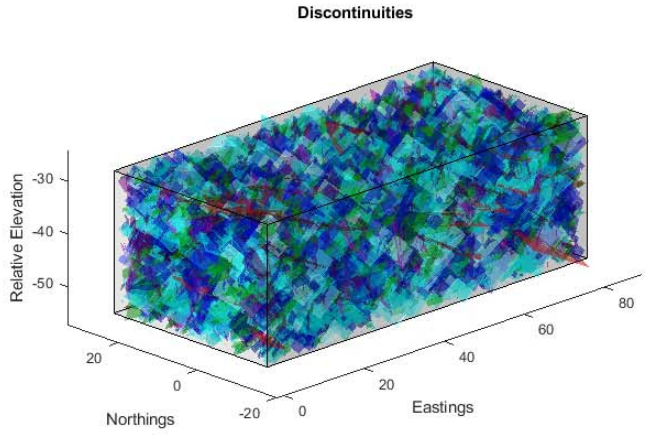

Isopleths of Fracture Statistical Analysis: DFN Mountain Small – Scale Factor=2.4

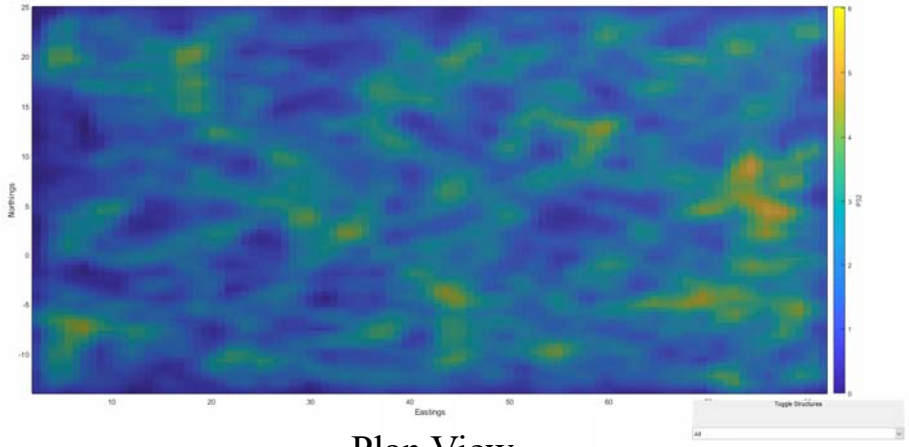

Plan View

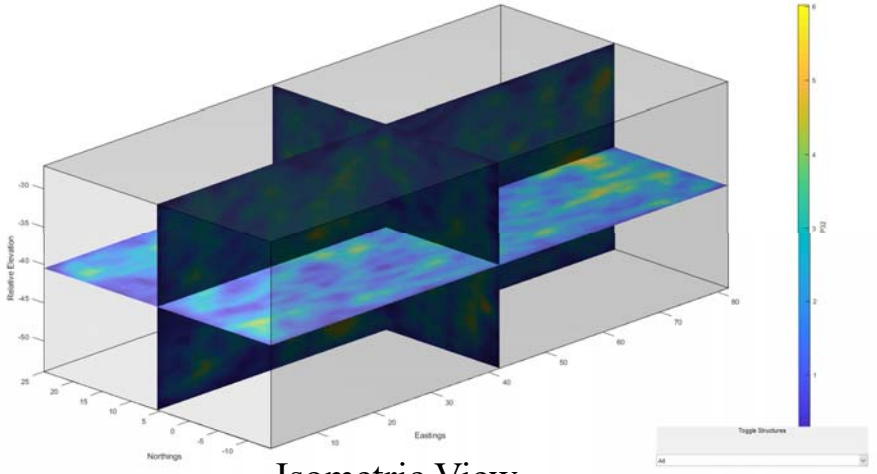

Isometric View

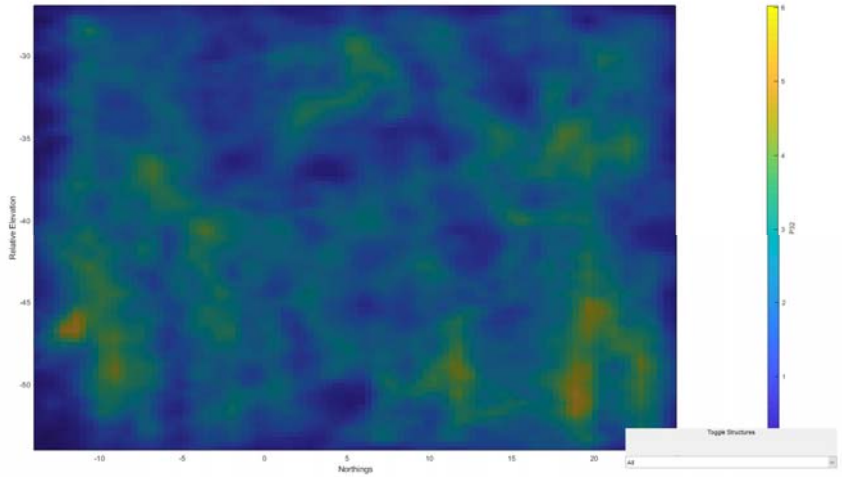

East View

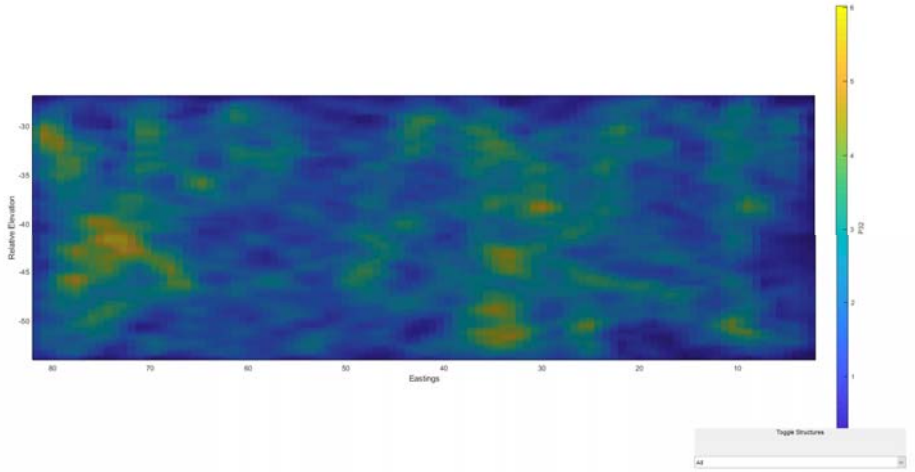

North View

Structural Analysis from SIROMODEL of DFN Mountain Small – Scale Factor=2.6

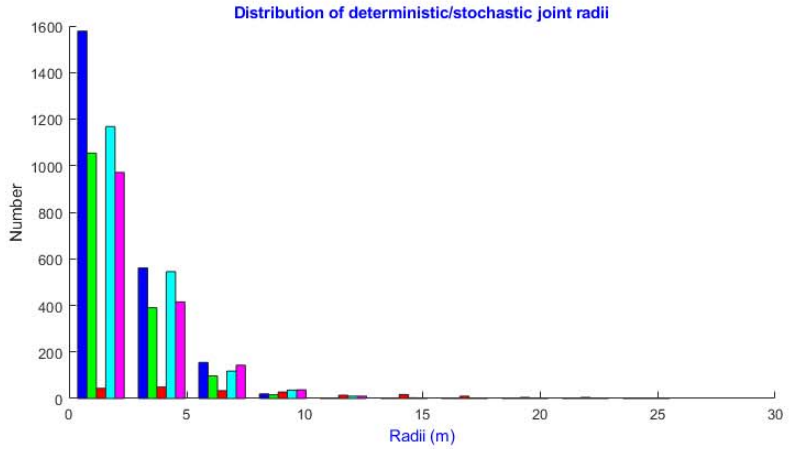

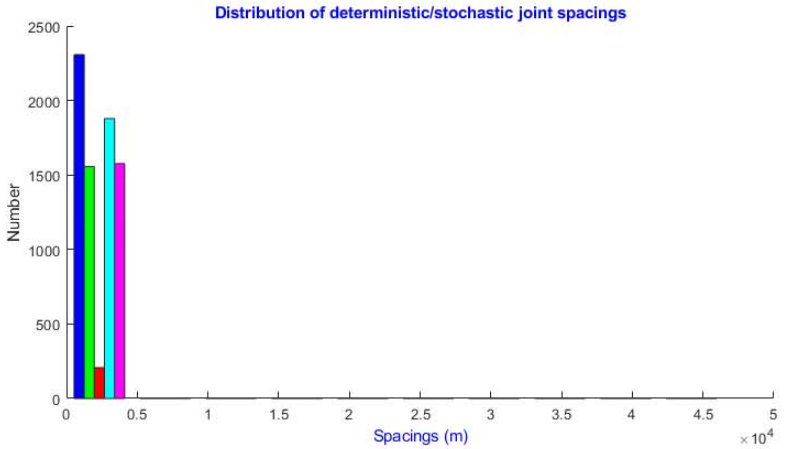

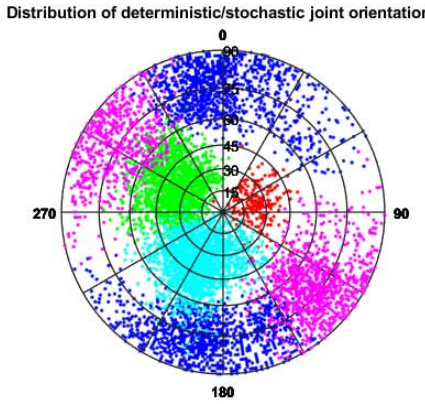

Stereonet Plot of Dip Vectors

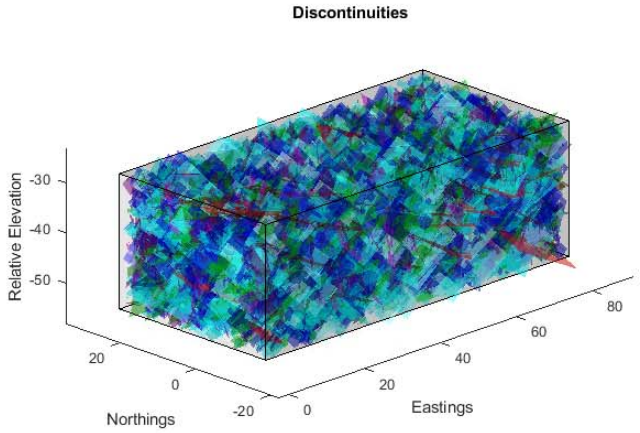

Isopleths of Fracture Statistical Analysis: DFN Mountain Small – Scale Factor=2.6

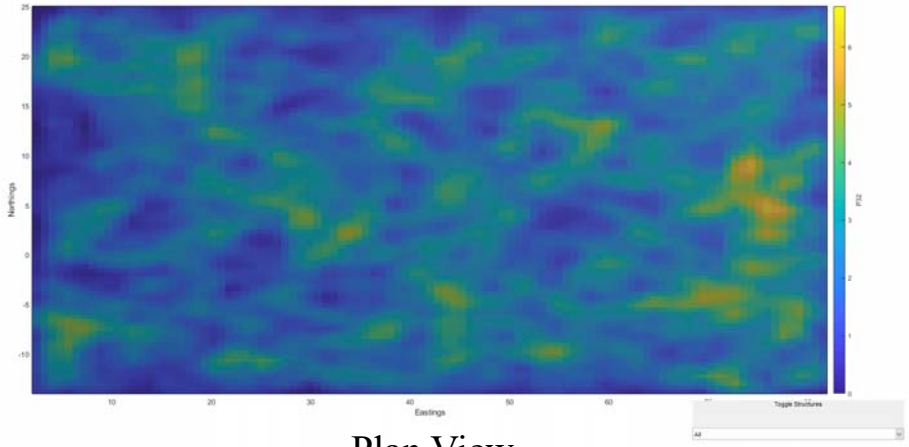

Plan View

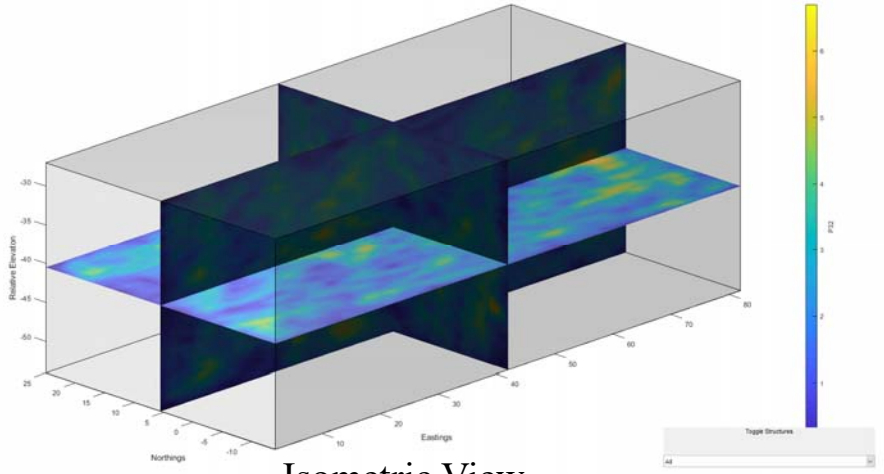

Isometric View

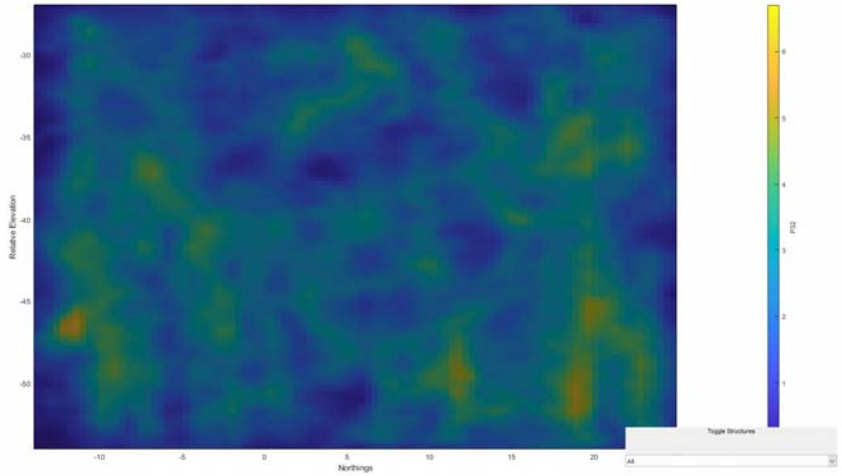

East View

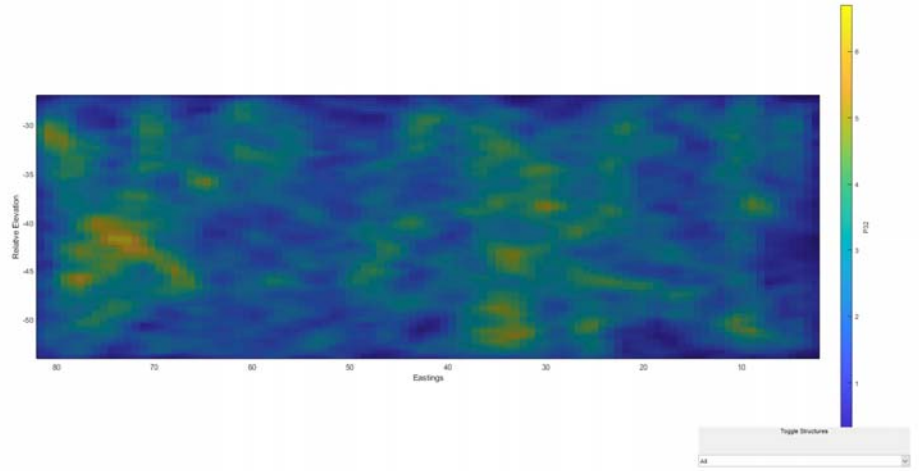

North View

Structural Analysis from SIROMODEL of DFN Mountain Small – Scale Factor=2.8

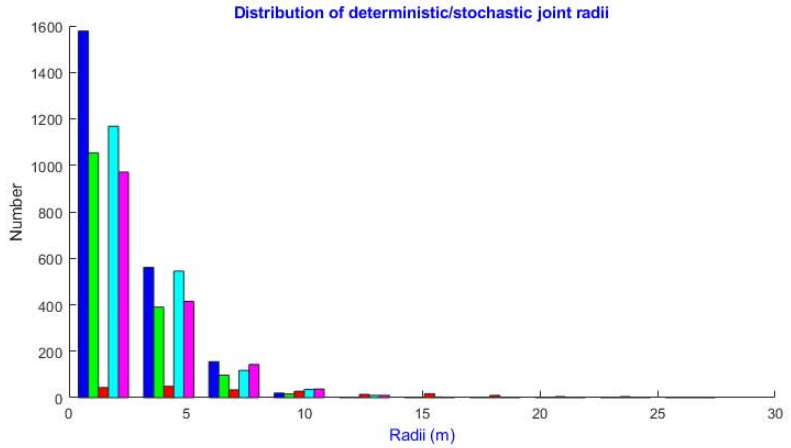

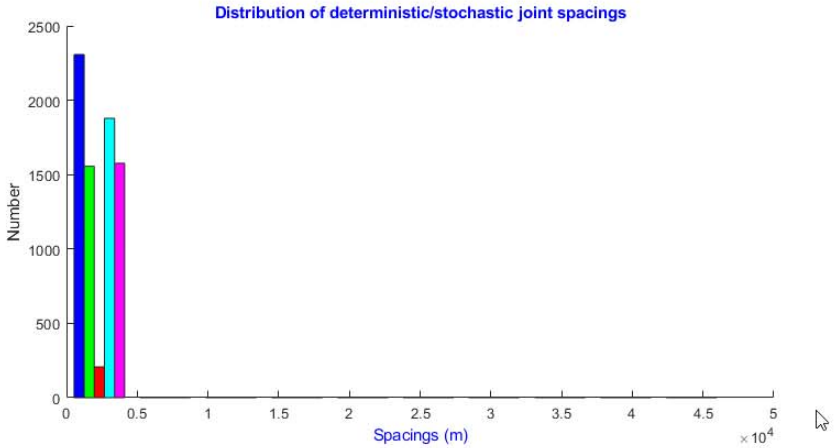

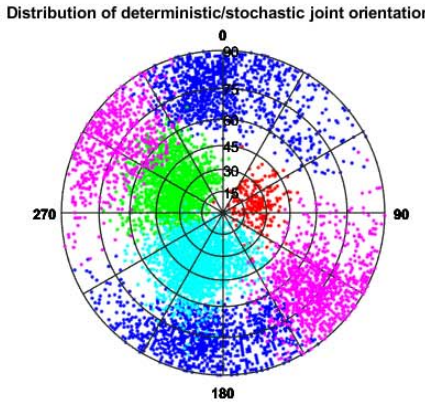

Stereonet Plot of Dip Vectors

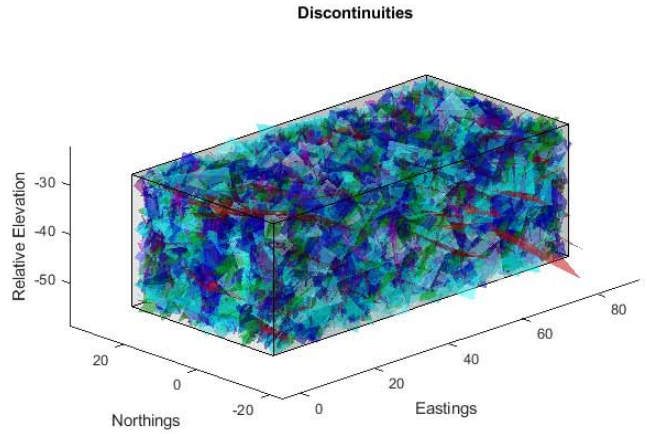

Isopleths of Fracture Statistical Analysis: DFN Mountain Small – Scale Factor=2.8

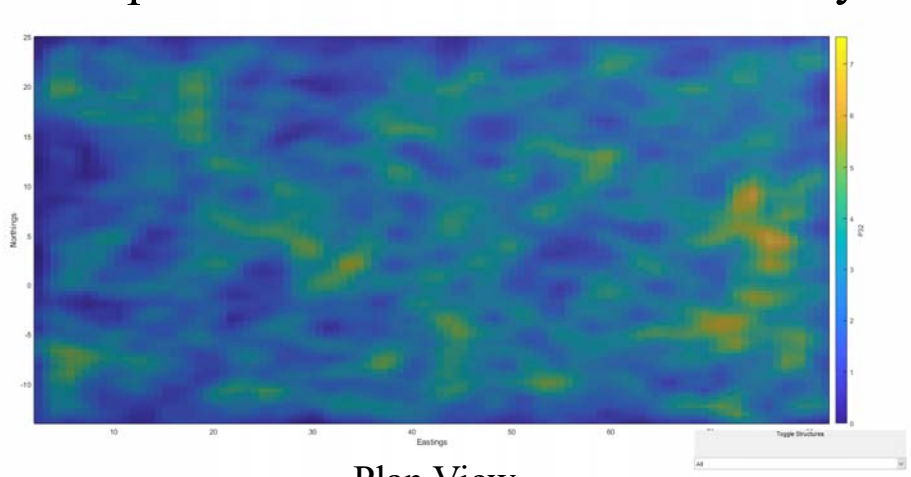

Plan View

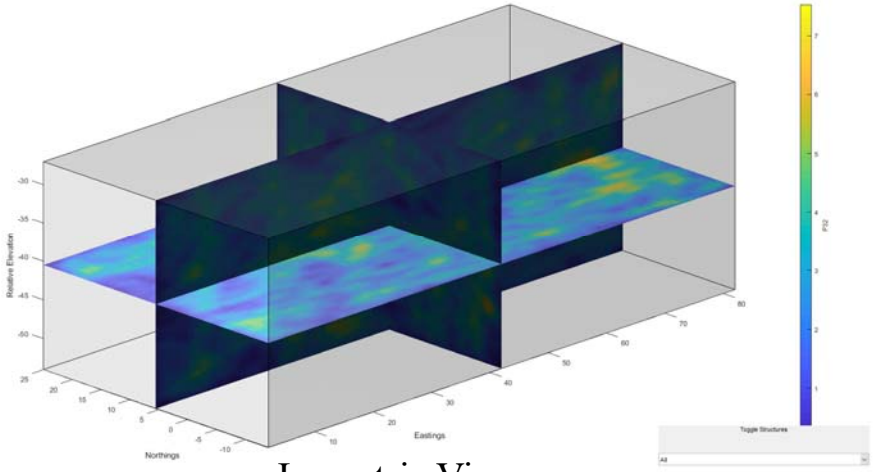

Isometric View

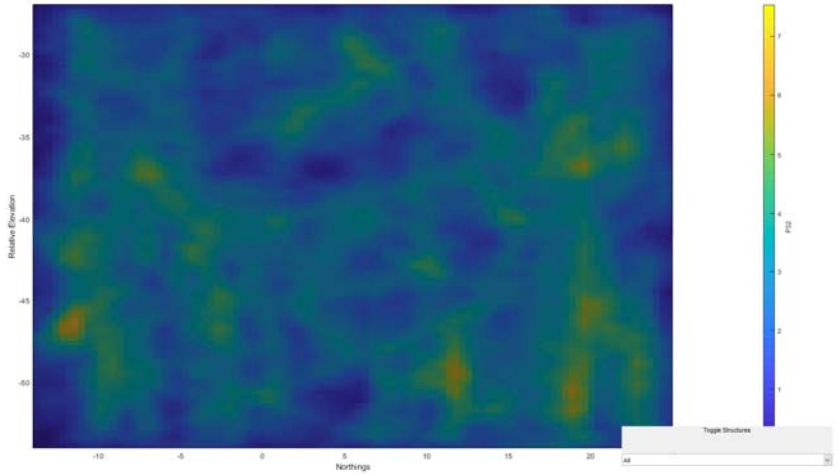

East View

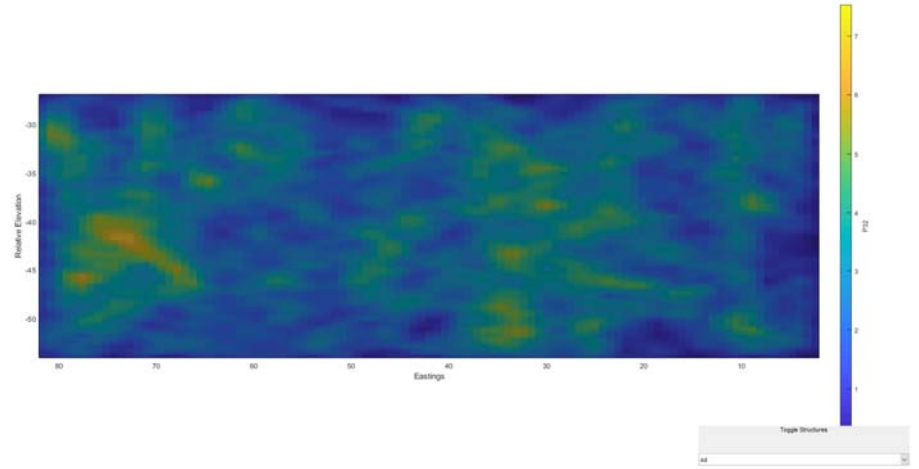

North View

Structural Analysis from SIROMODEL of DFN Mountain Small – Scale Factor=3

SIROMODEL application crashed and failed to complete assessments of a scale factor of 3

APPENDIX A
ASSESSMENT OF SCALED EFFECTS OF CONTINUITY IN A DFN

A.2 Sensitivity of Continuity – DFN Mountain Large

Model views from SIROMODEL of DFN Mountain Large – no scaling

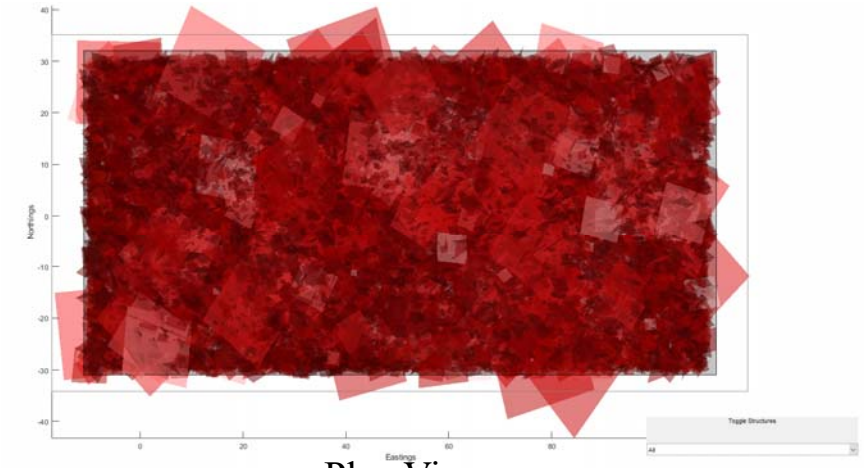

Plan View

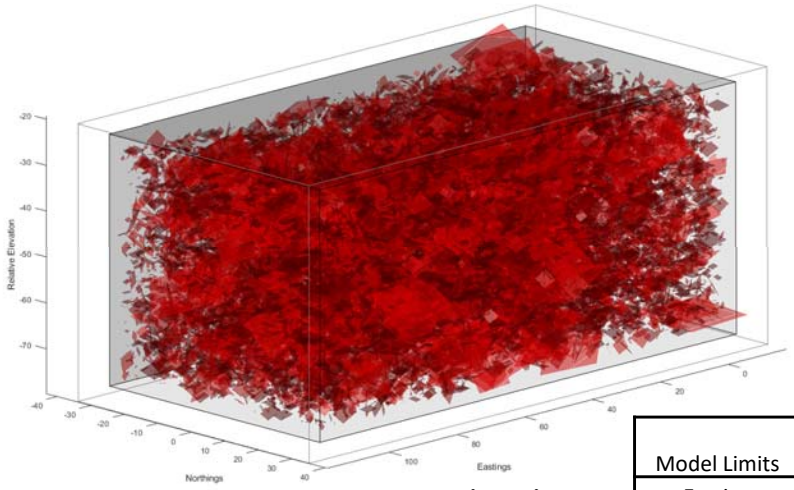

Isometric View

Model Limits	Min (m)	Max (m)
Easting	-11	112
Northing	-31	32
Elev	-77	-22

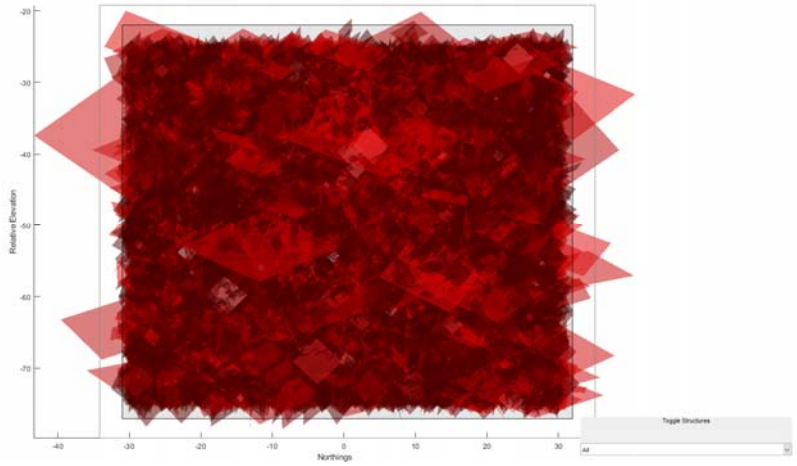

East View

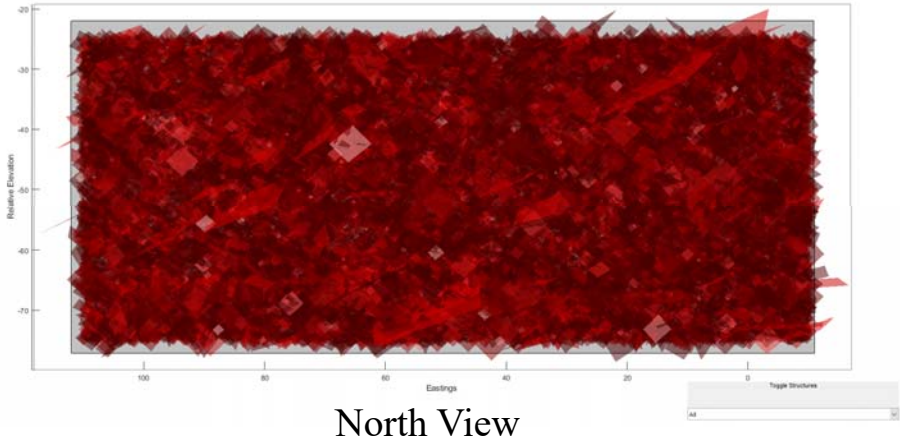

North View

Structural Analysis from SIROMODEL of DFN Mountain Large – no scaling (Scale Factor=1)

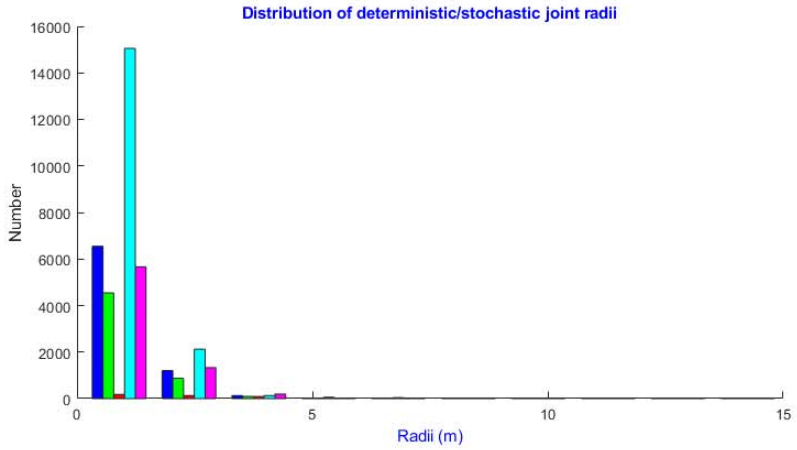

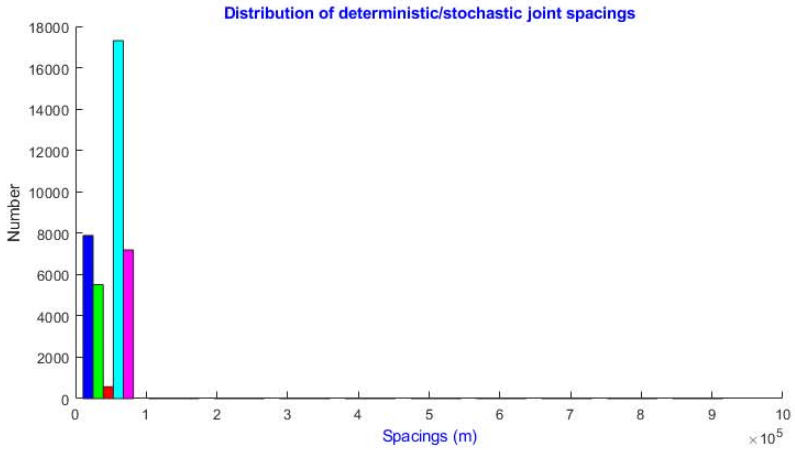

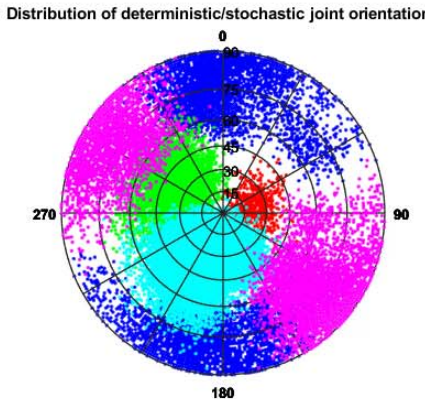

Stereonet Plot of Dip Vectors

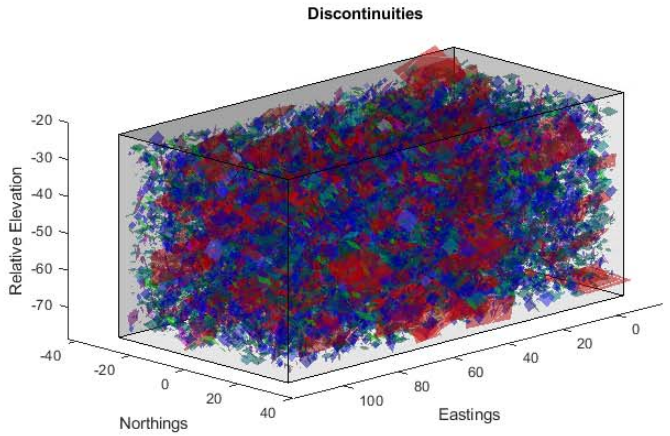

Isopleths of Fracture Statistical Analysis: DFN Mountain Large – no scaling (Scale Factor=1)

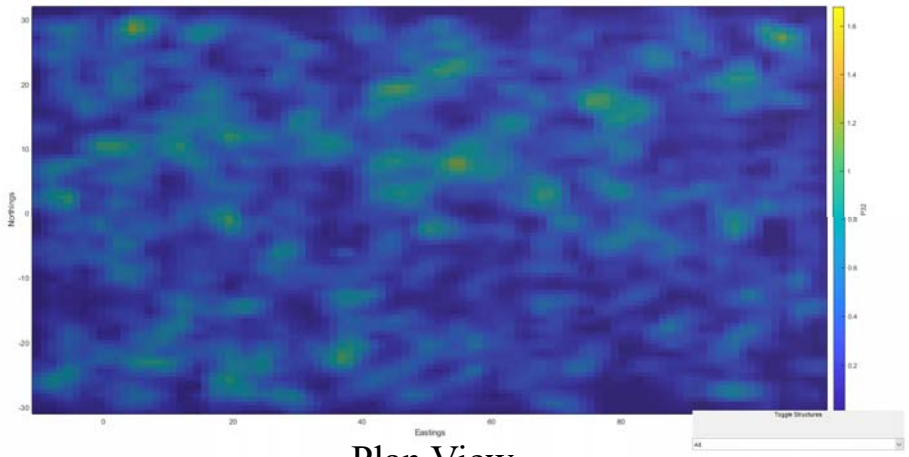

Plan View

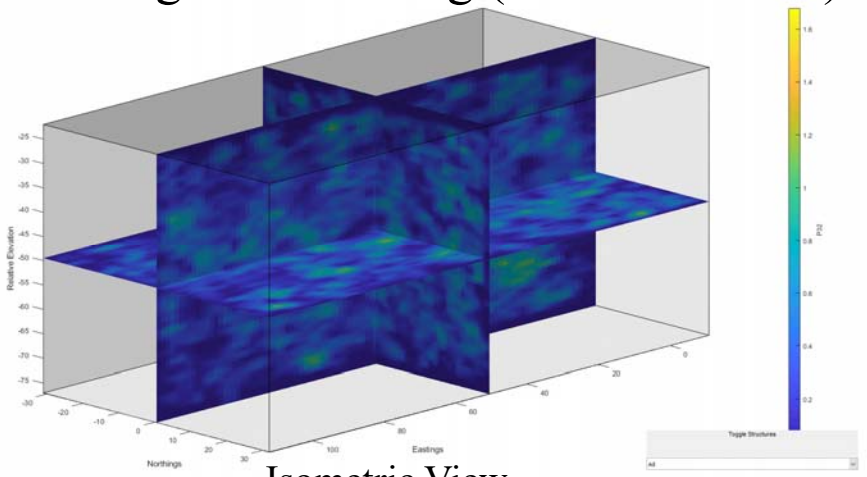

Isometric View

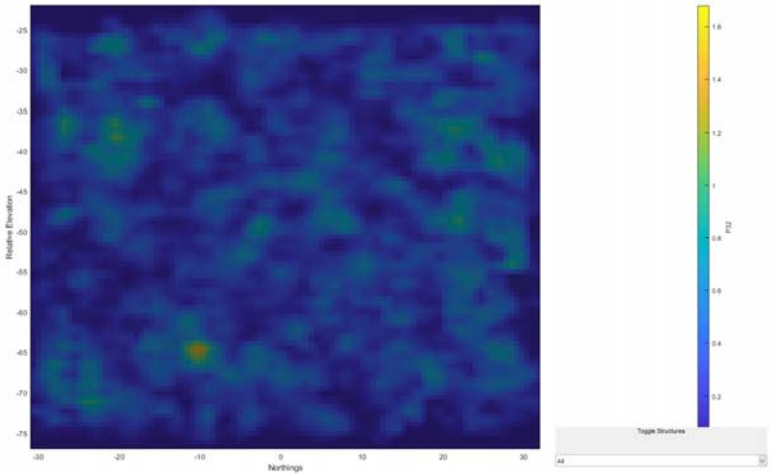

East View

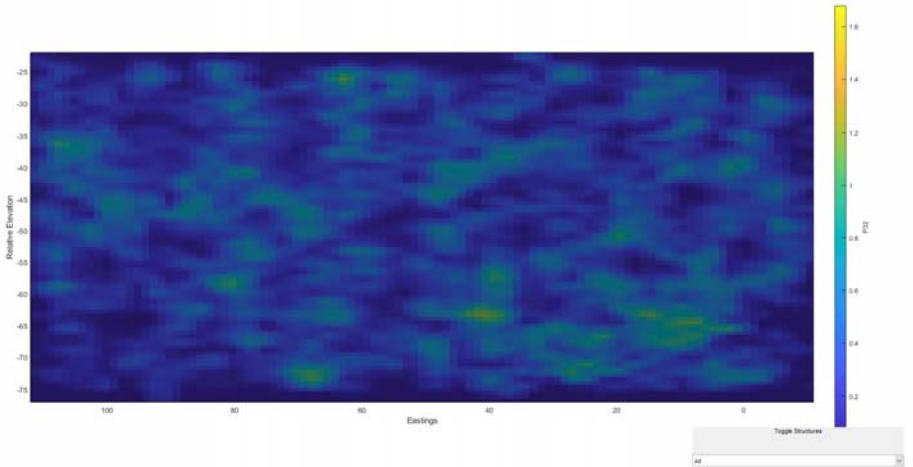

North View

Structural Analysis from SIROMODEL of DFN Mountain Large – Scale Factor=1.1

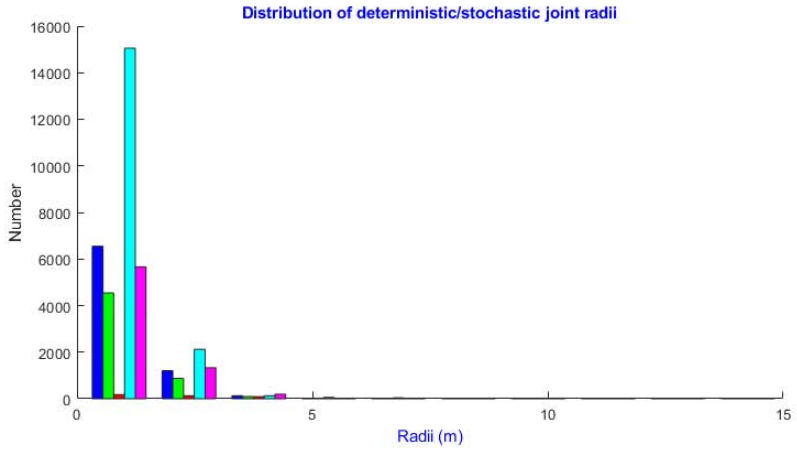

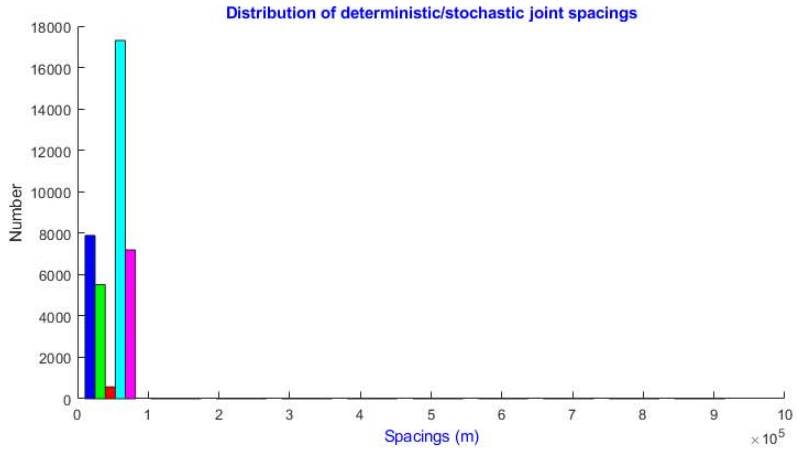

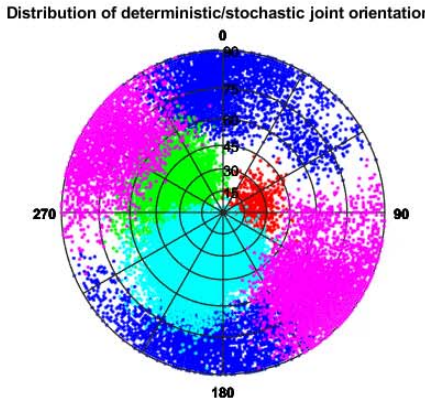

Stereonet Plot of Dip Vectors

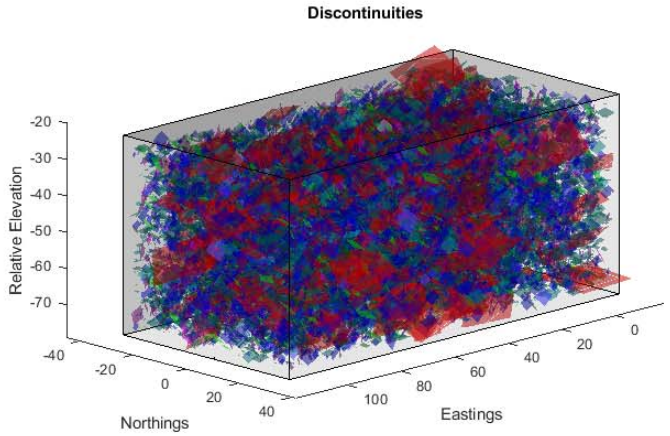

Isopleths of Fracture Statistical Analysis: DFN Mountain Large – Scale Factor=1.1

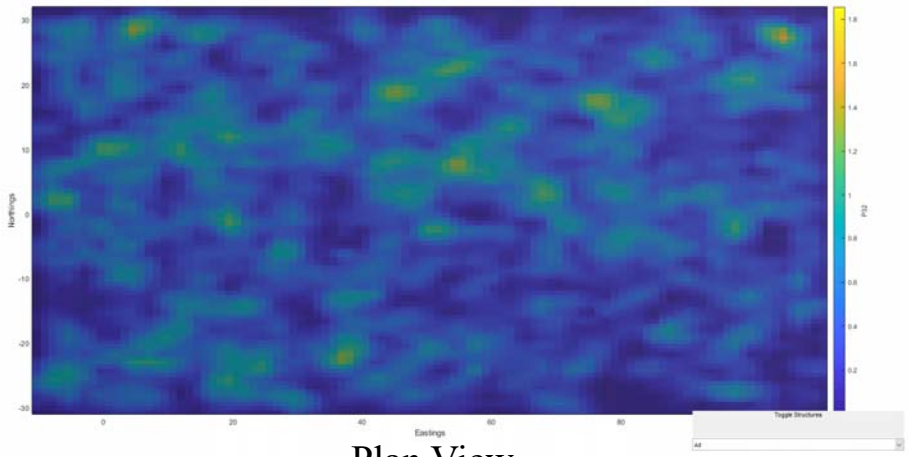

Plan View

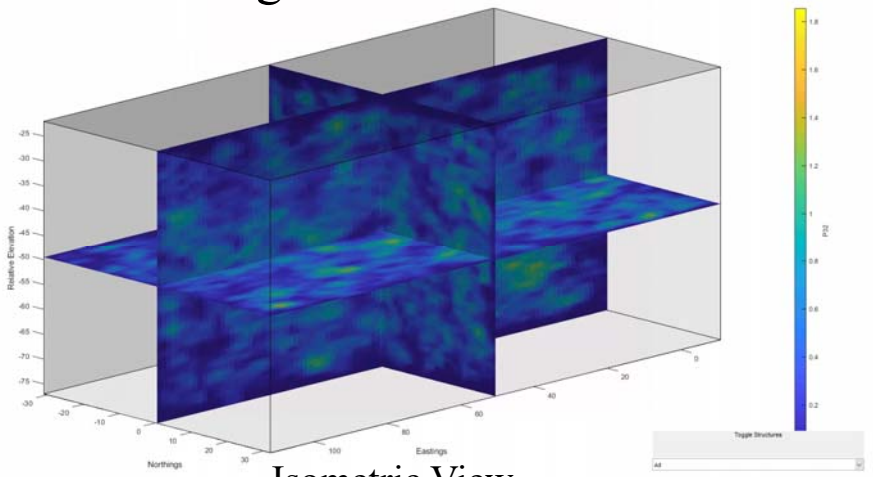

Isometric View

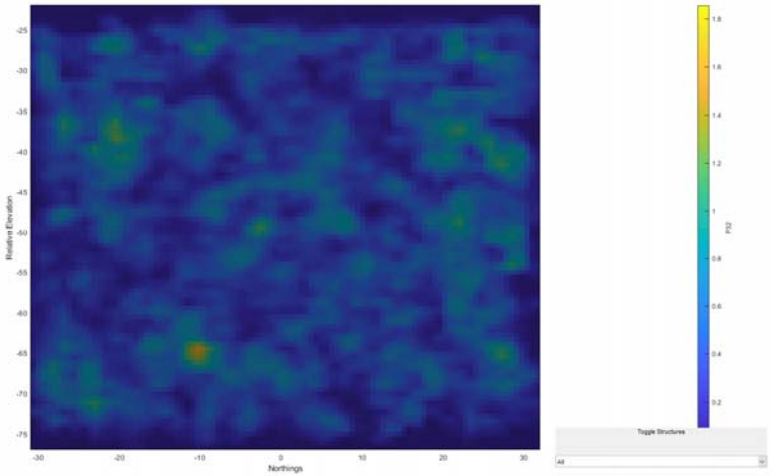

East View

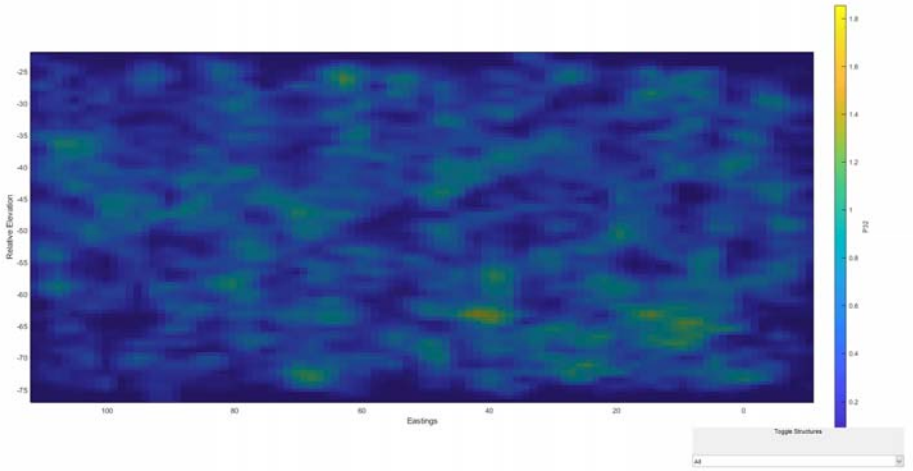

North View

Structural Analysis from SIROMODEL of DFN Mountain Large – Scale Factor=1.2

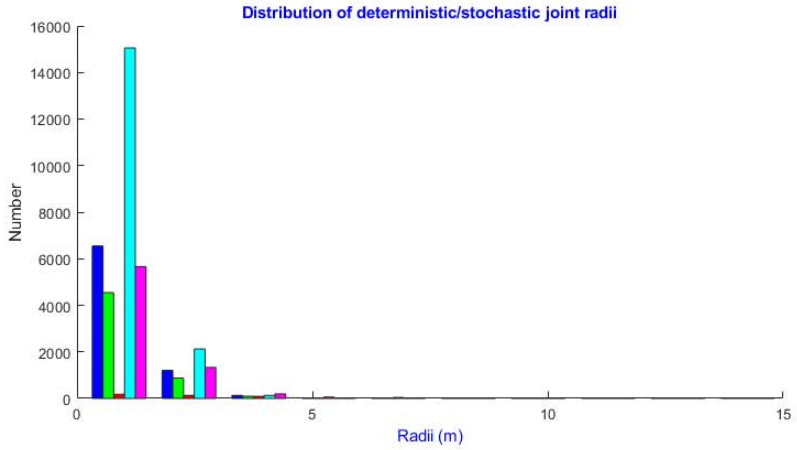

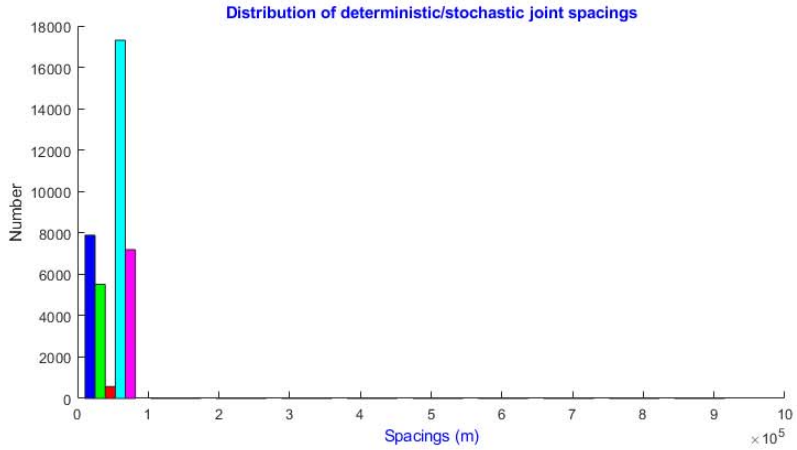

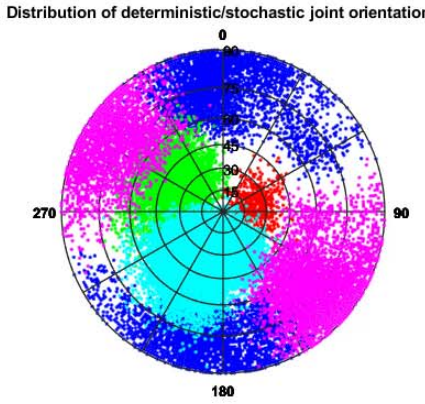

Stereonet Plot of Dip Vectors

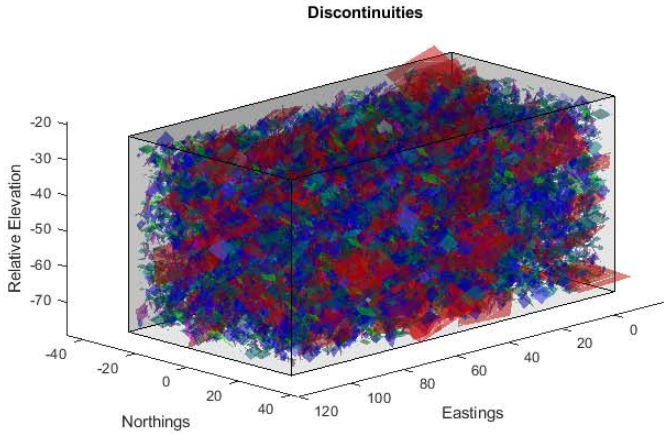

Isopleths of Fracture Statistical Analysis: DFN Mountain Large – Scale Factor=1.2

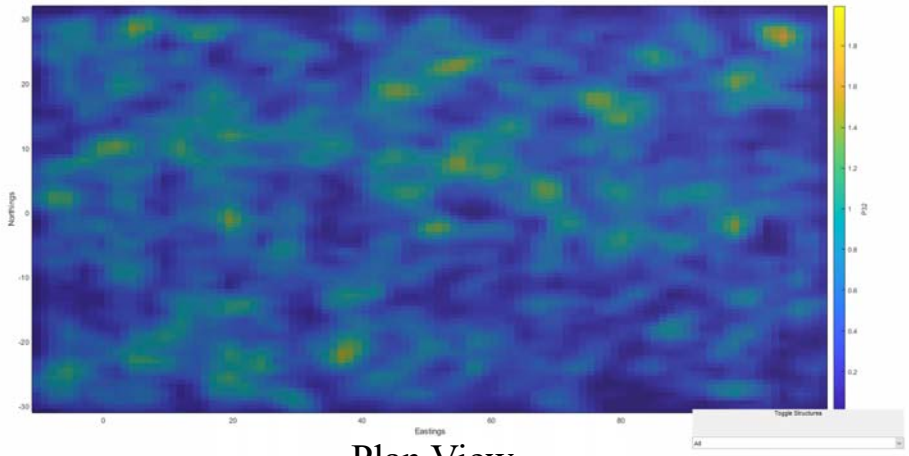

Plan View

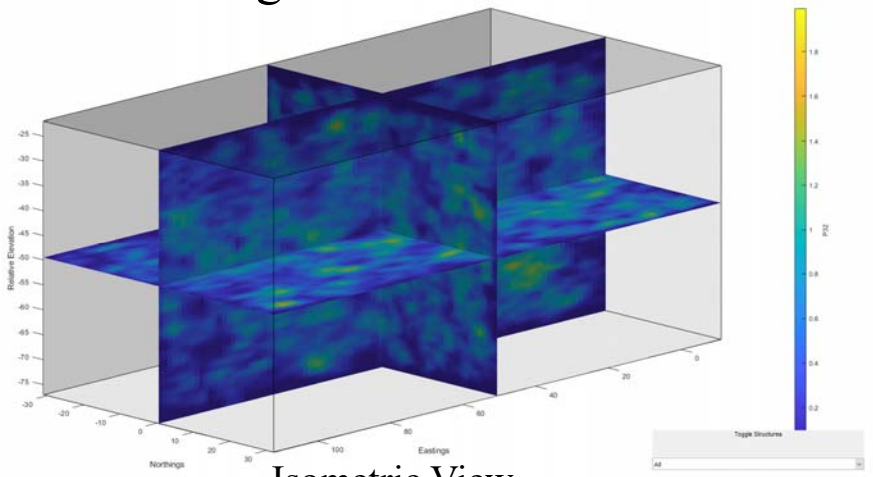

Isometric View

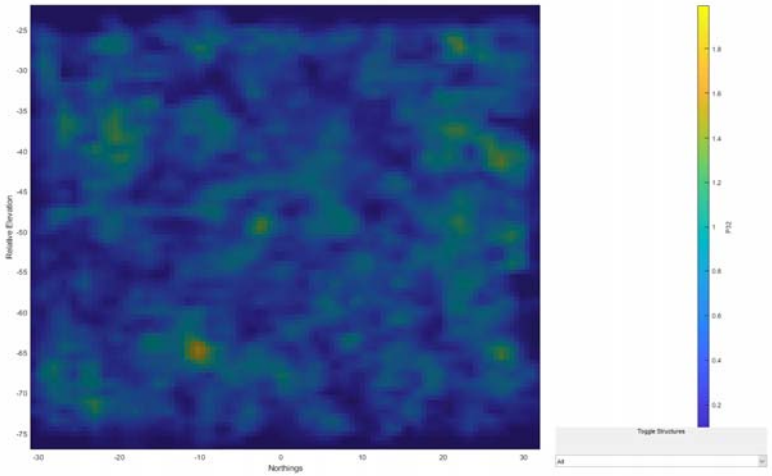

East View

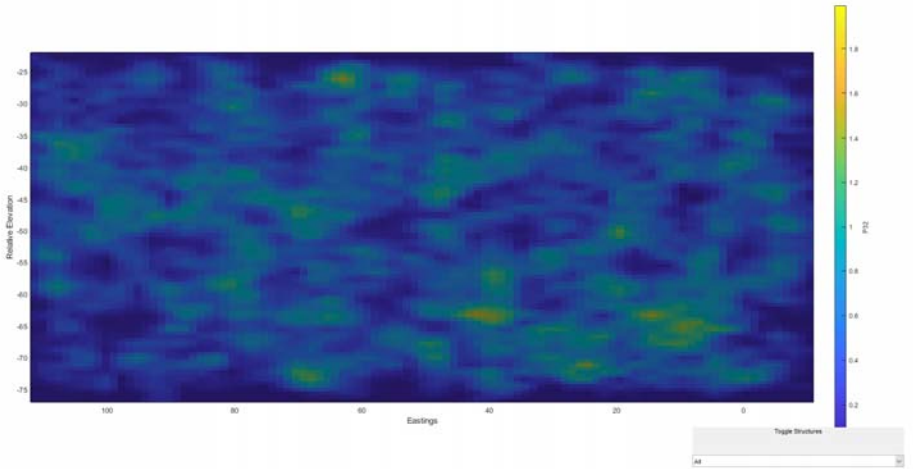

North View

Structural Analysis from SIROMODEL of DFN Mountain Large – Scale Factor=1.3

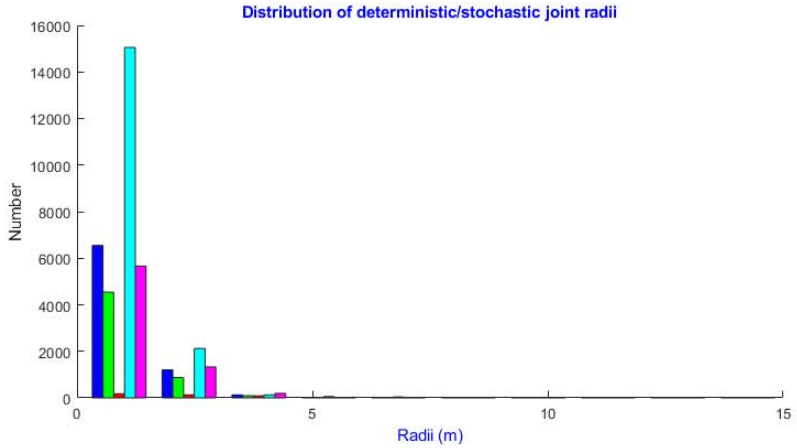

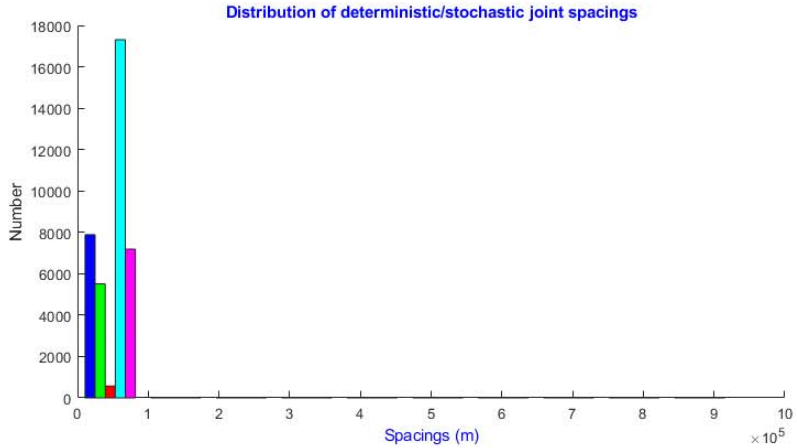

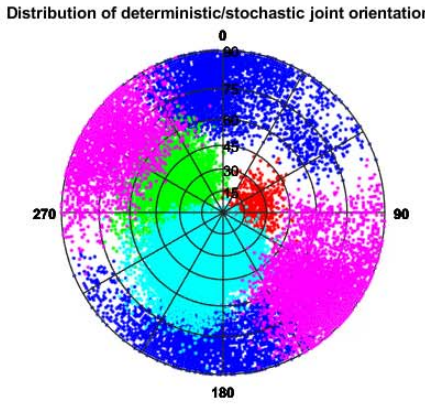

Stereonet Plot of Dip Vectors

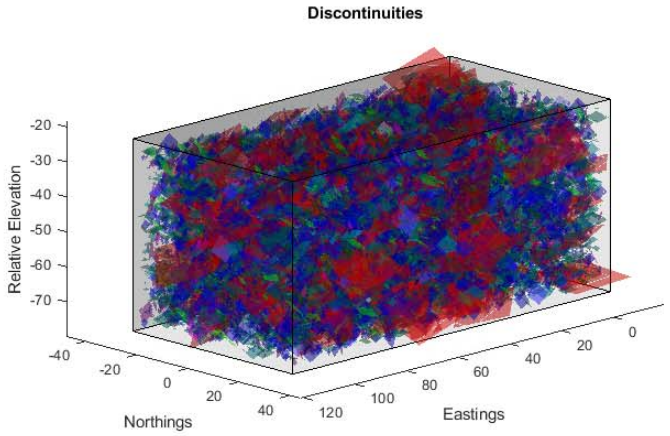

Isopleths of Fracture Statistical Analysis: DFN Mountain Large – Scale Factor=1.3

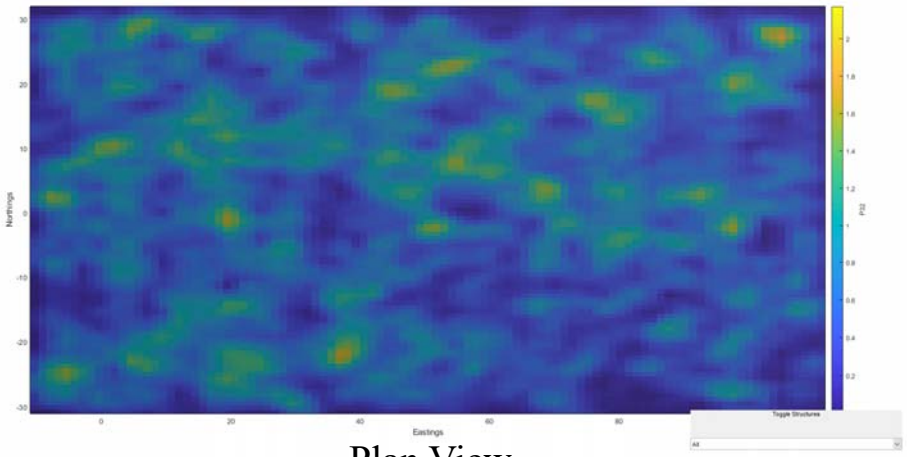

Plan View

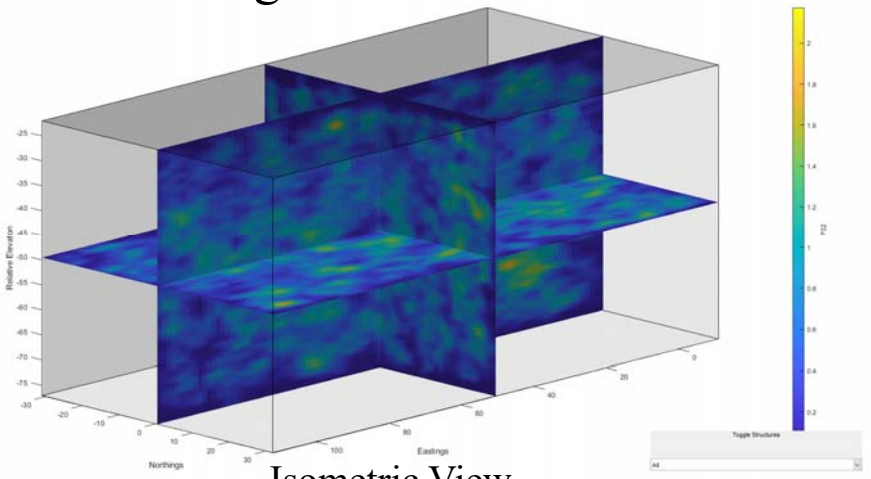

Isometric View

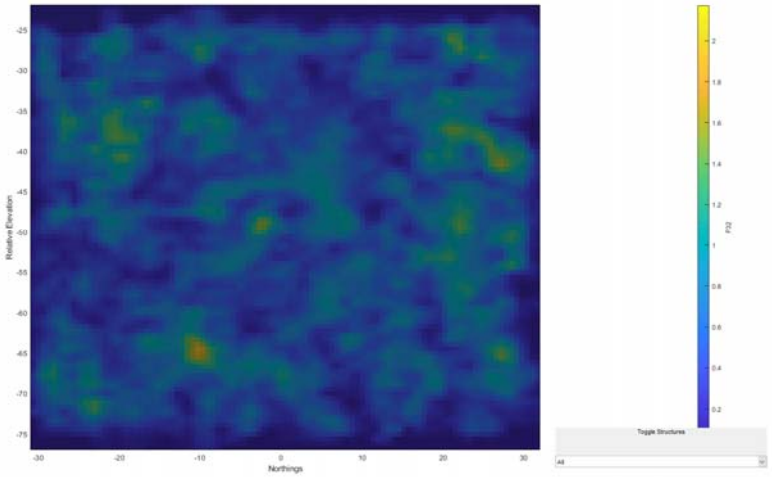

East View

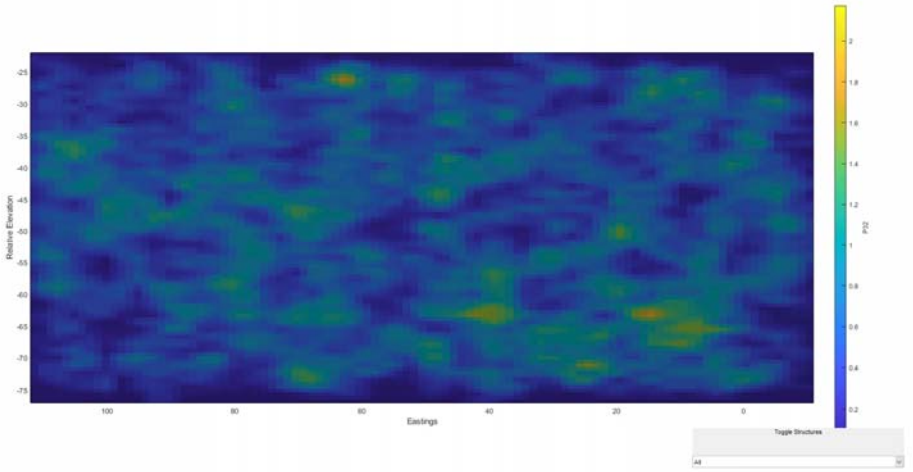

North View

Structural Analysis from SIROMODEL of DFN Mountain Large – Scale Factor=1.4

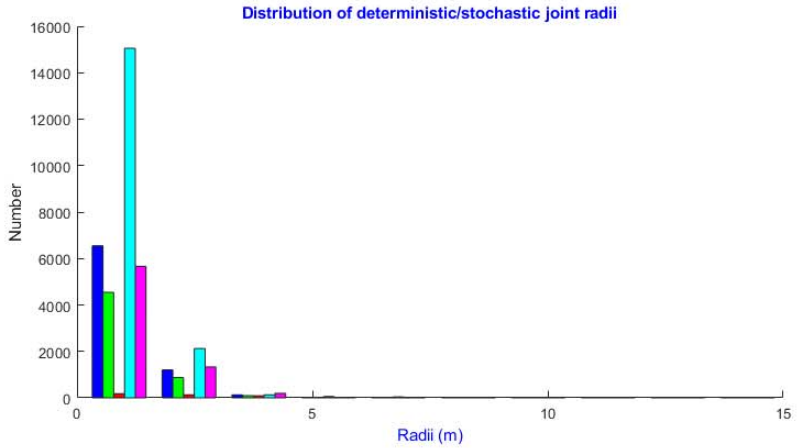

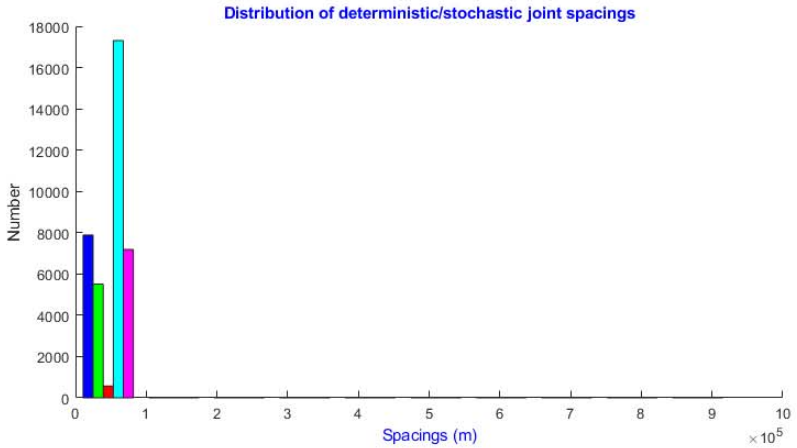

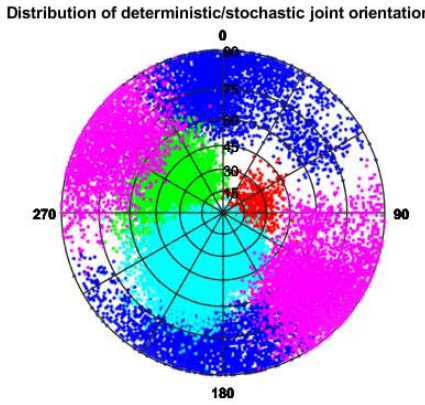

Stereonet Plot of Dip Vectors

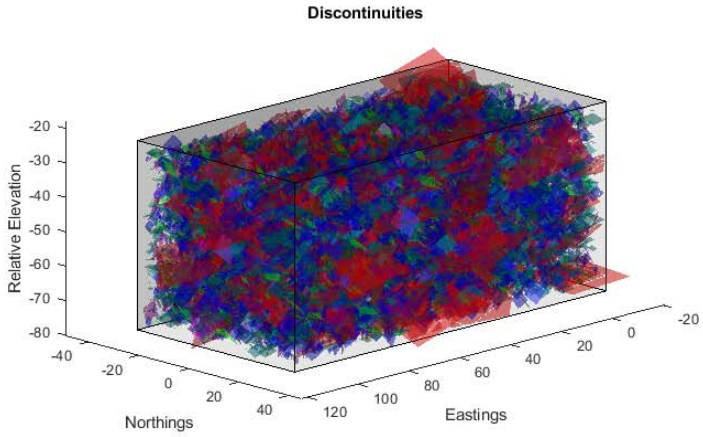

Isopleths of Fracture Statistical Analysis: DFN Mountain Large – Scale Factor=1.4

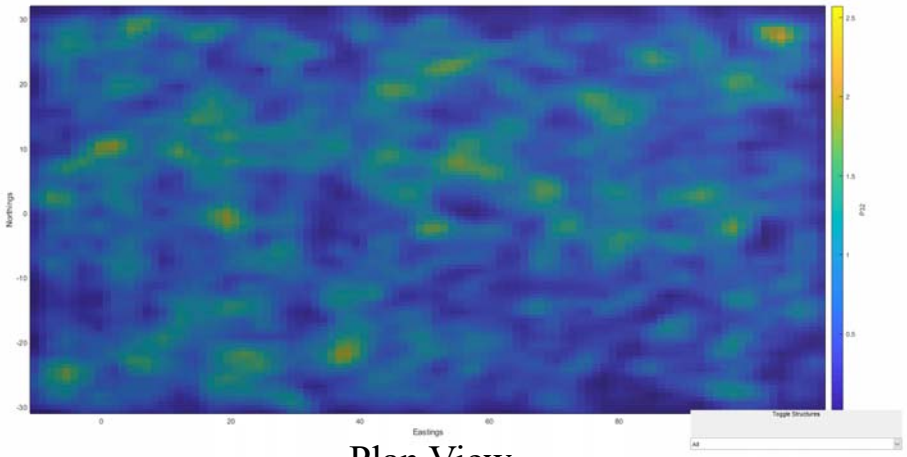

Plan View

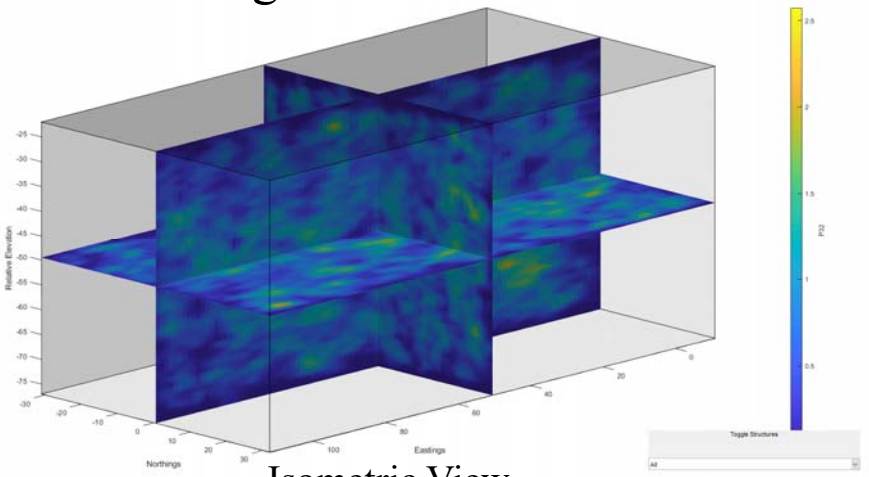

Isometric View

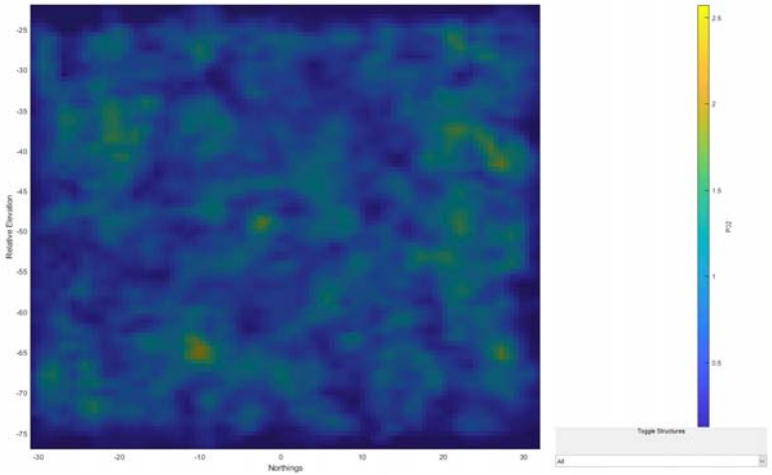

East View

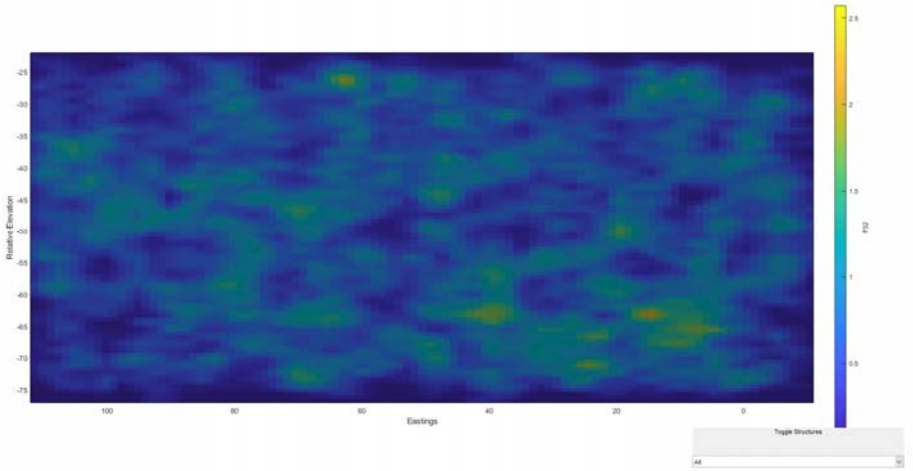

North View

Structural Analysis from SIROMODEL of DFN Mountain Large – Scale Factor=1.5

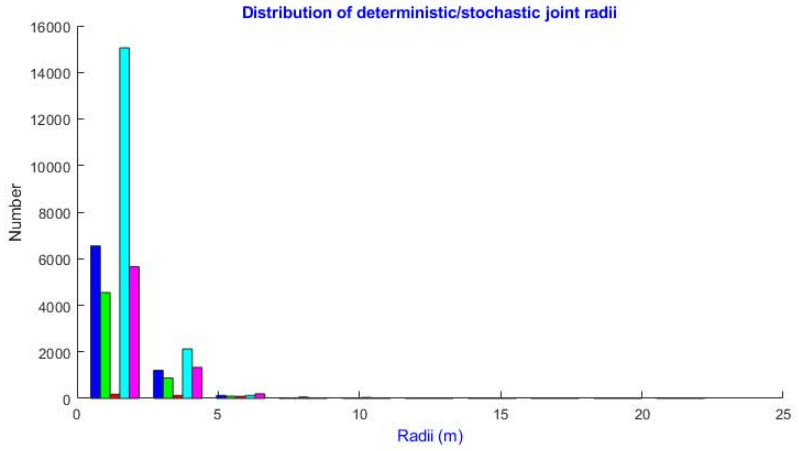

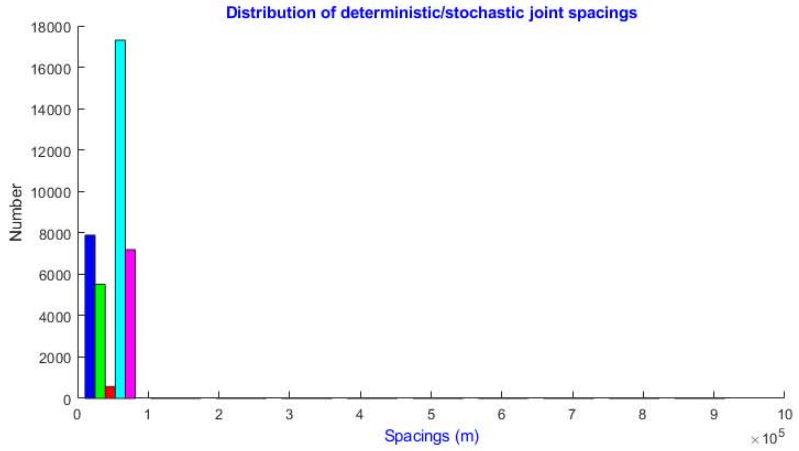

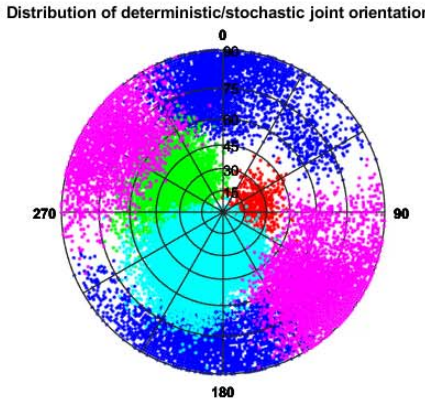

Stereonet Plot of Dip Vectors

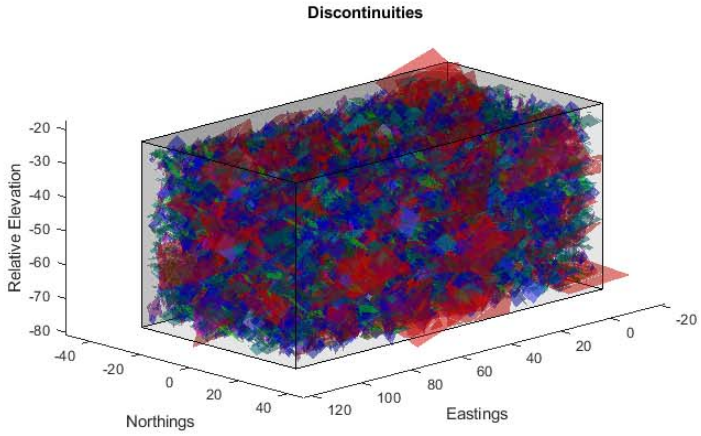

Isopleths of Fracture Statistical Analysis: DFN Mountain Large – Scale Factor=1.5

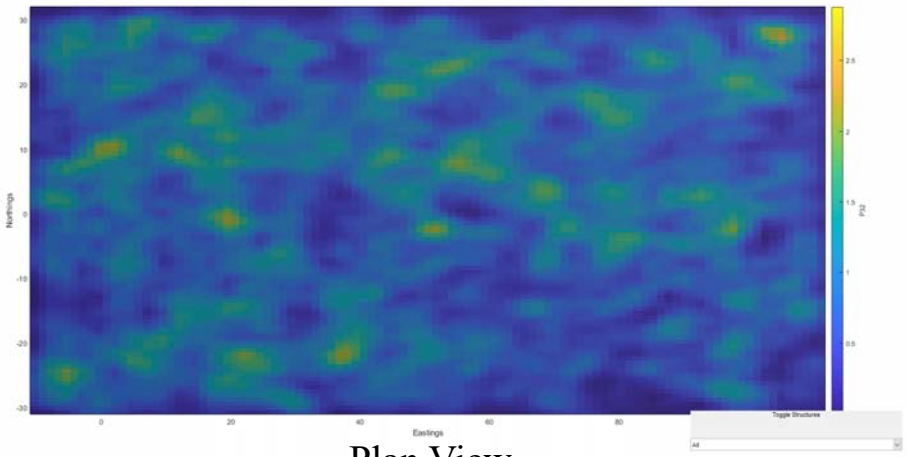

Plan View

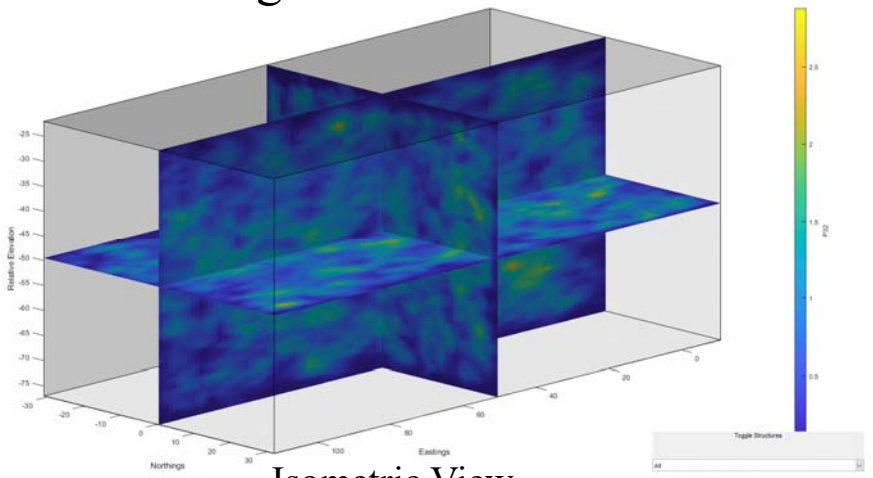

Isometric View

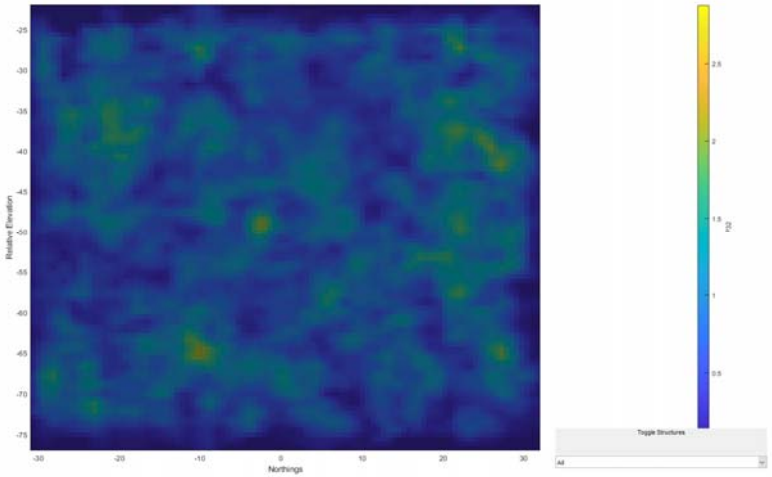

East View

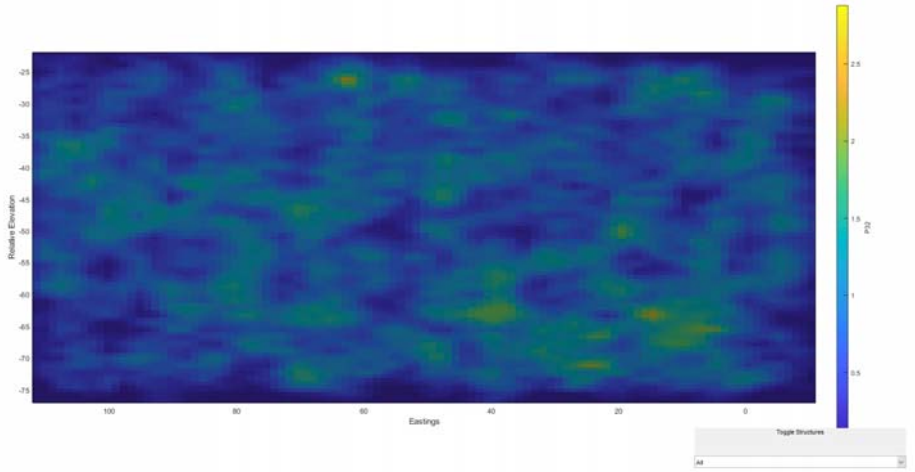

North View

Structural Analysis from SIROMODEL of DFN Mountain Large – Scale Factor=1.6

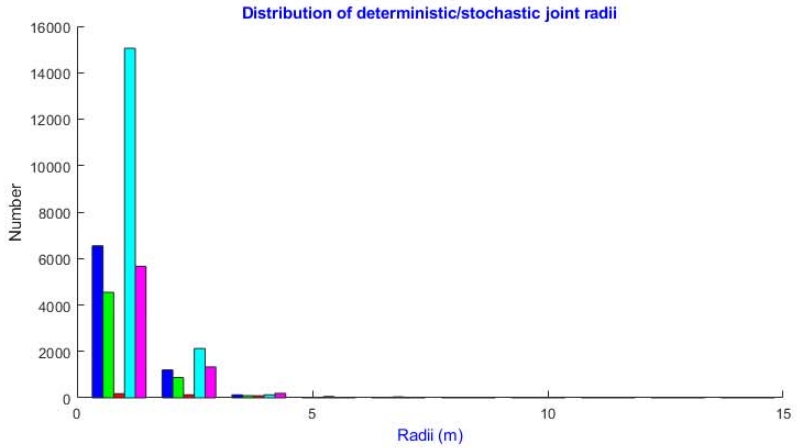

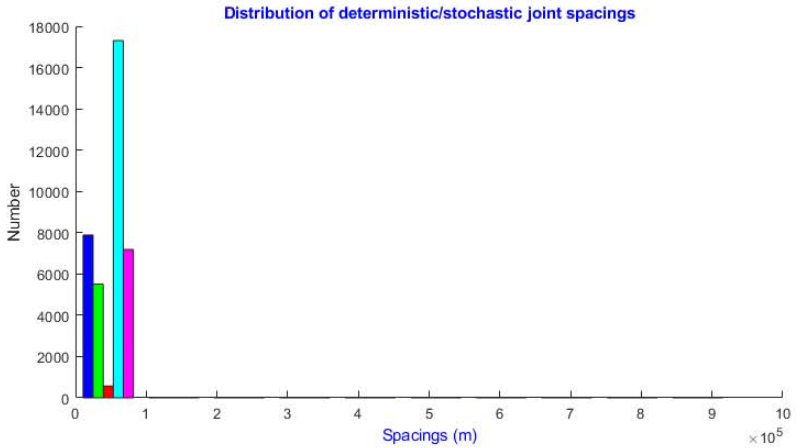

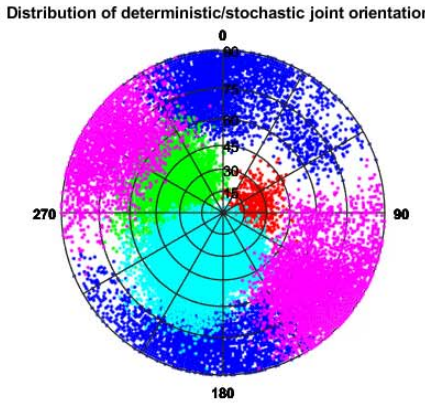

Stereonet Plot of Dip Vectors

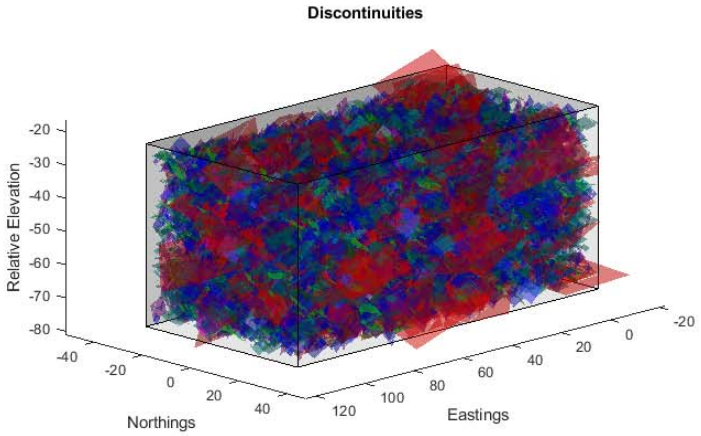

Isopleths of Fracture Statistical Analysis: DFN Mountain Large – Scale Factor=1.6

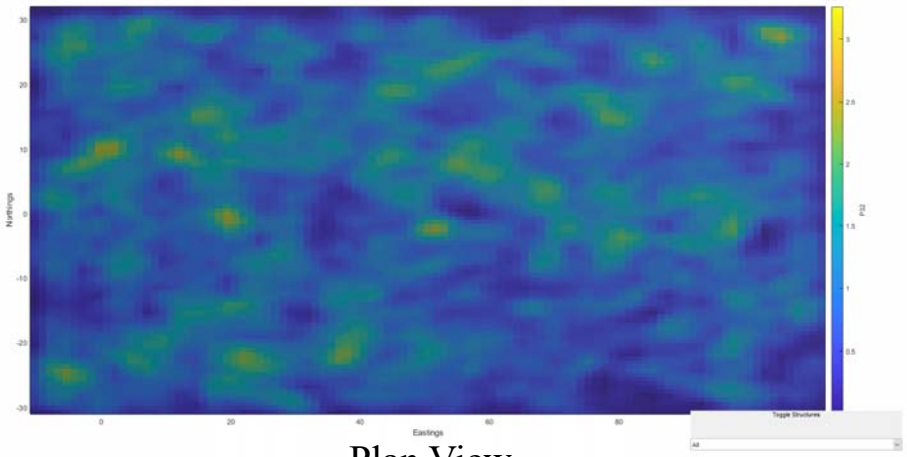

Plan View

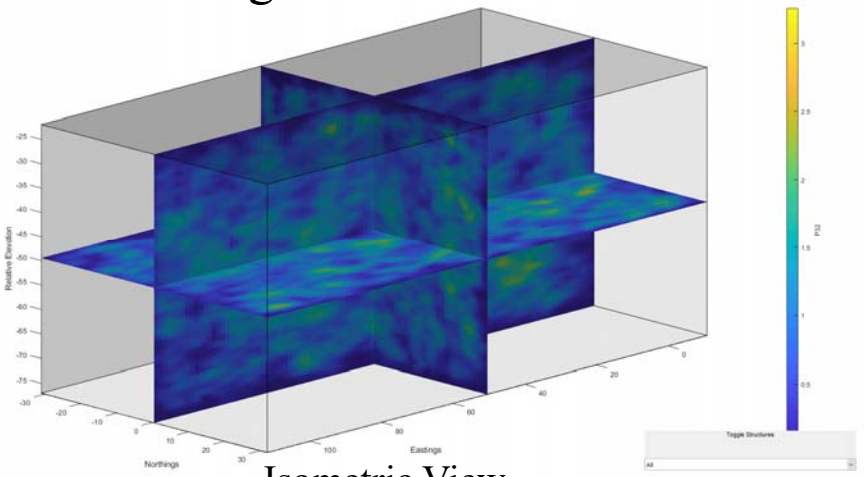

Isometric View

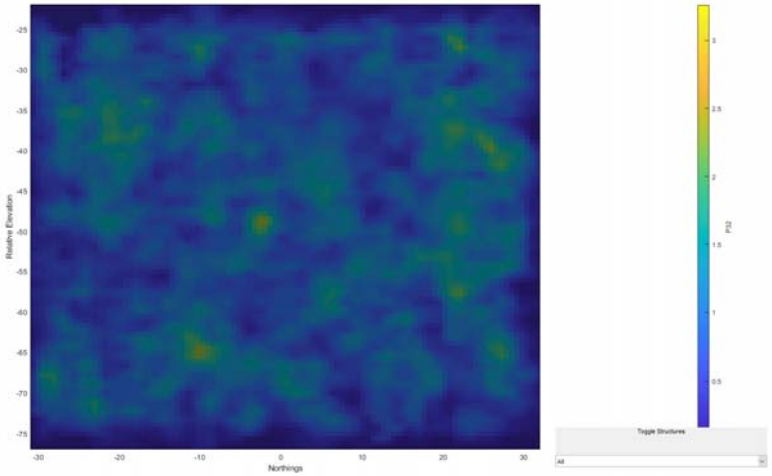

East View

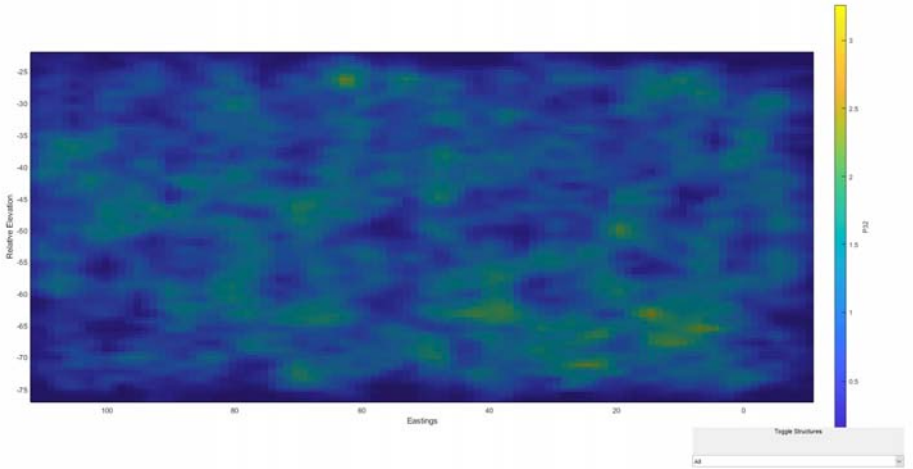

North View

Structural Analysis from SIROMODEL of DFN Mountain Large – Scale Factor=1.7

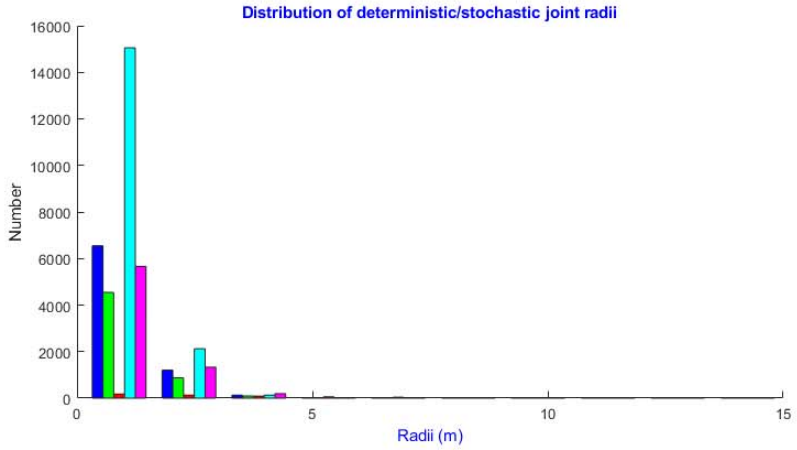

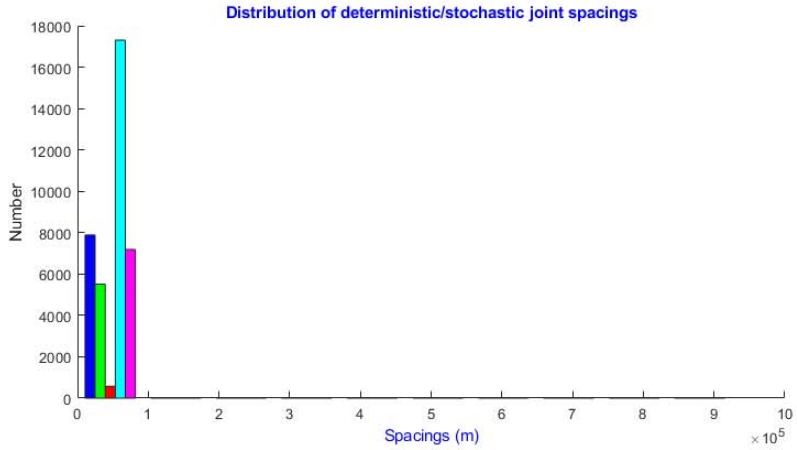

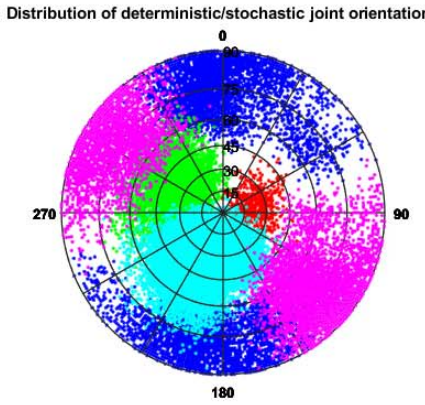

Stereonet Plot of Dip Vectors

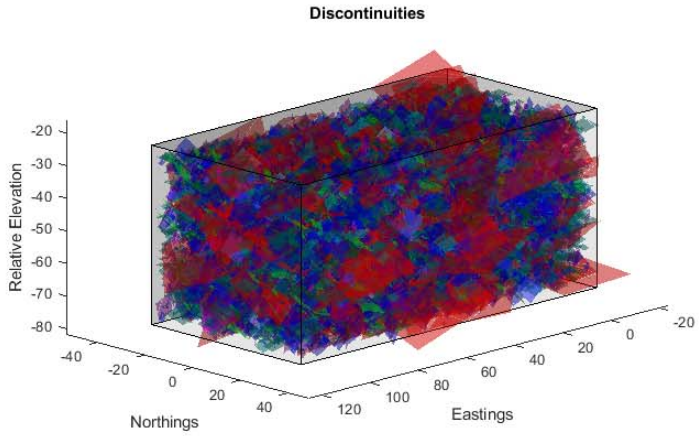

Isopleths of Fracture Statistical Analysis: DFN Mountain Large – Scale Factor=1.7

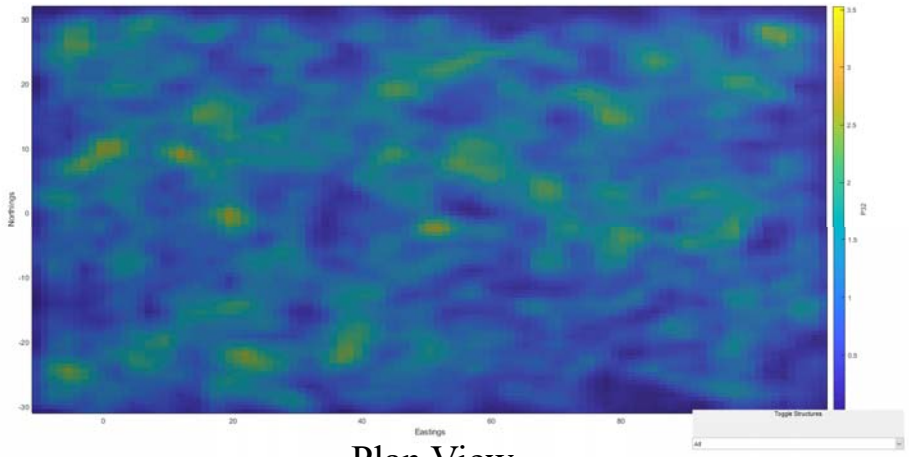

Plan View

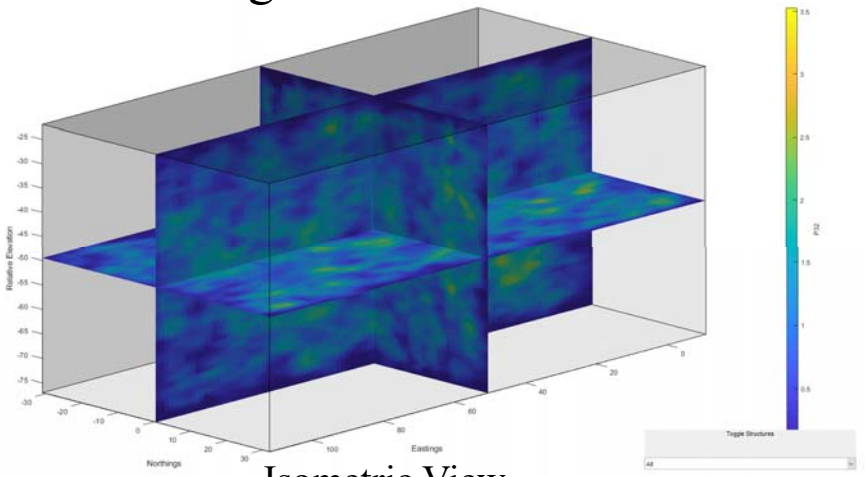

Isometric View

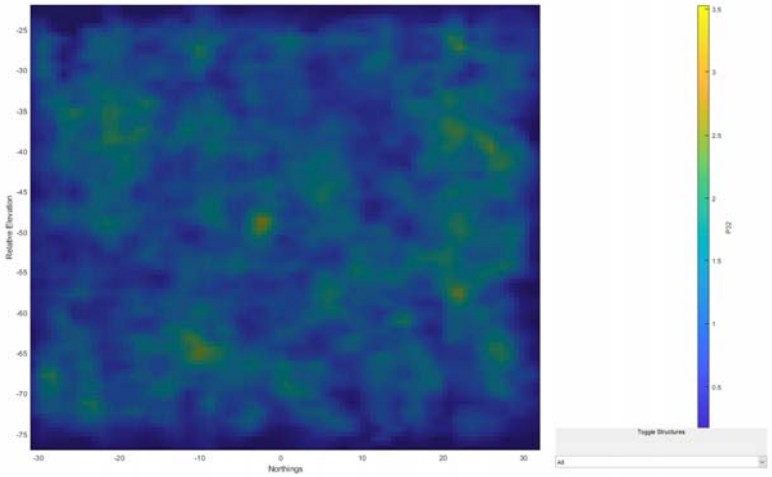

East View

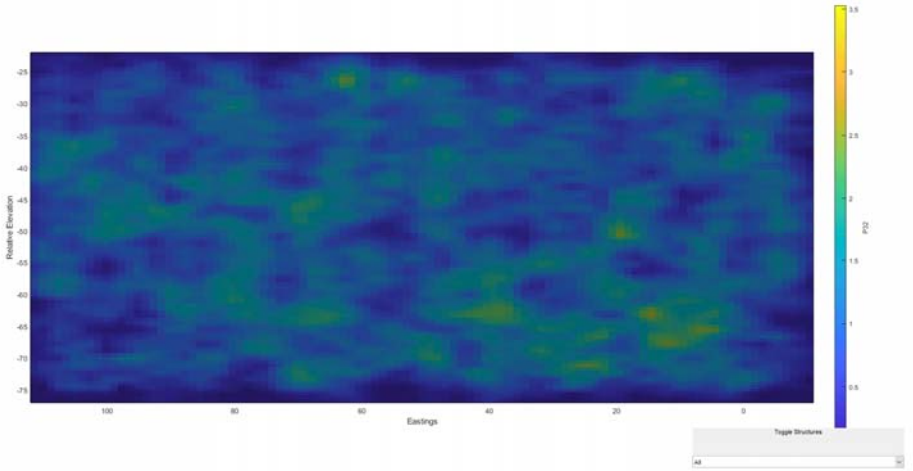

North View

Structural Analysis from SIROMODEL of DFN Mountain Large – Scale Factor=1.8

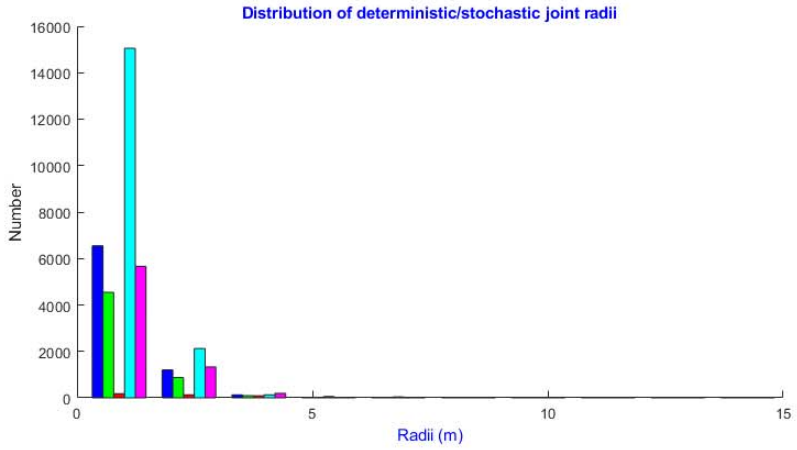

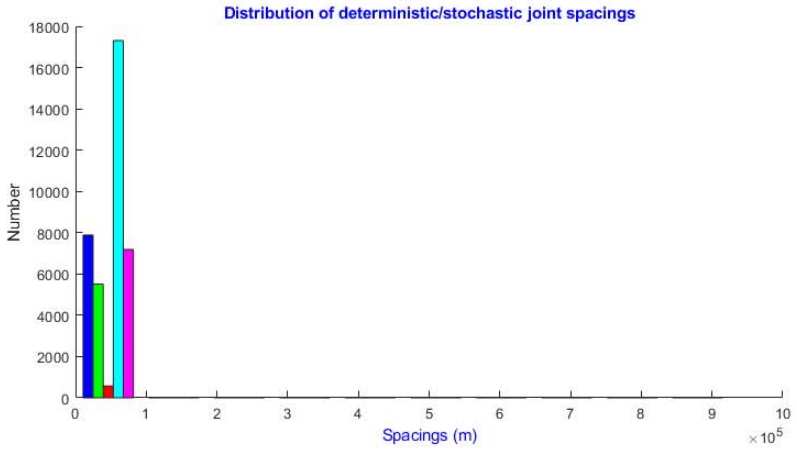

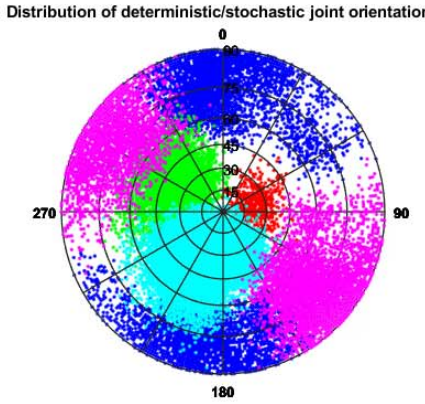

Stereonet Plot of Dip Vectors

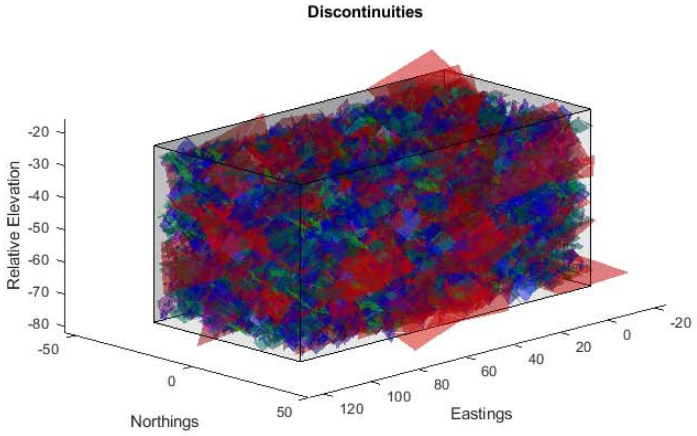

Isopleths of Fracture Statistical Analysis: DFN Mountain Large – Scale Factor=1.8

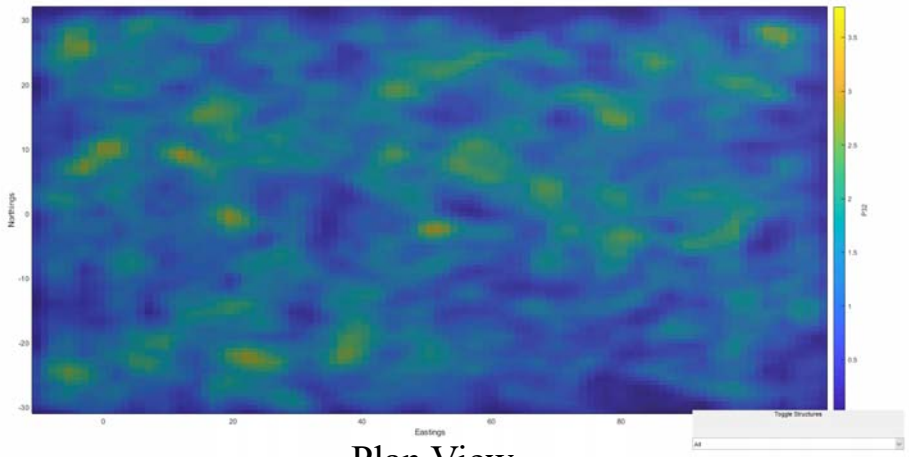

Plan View

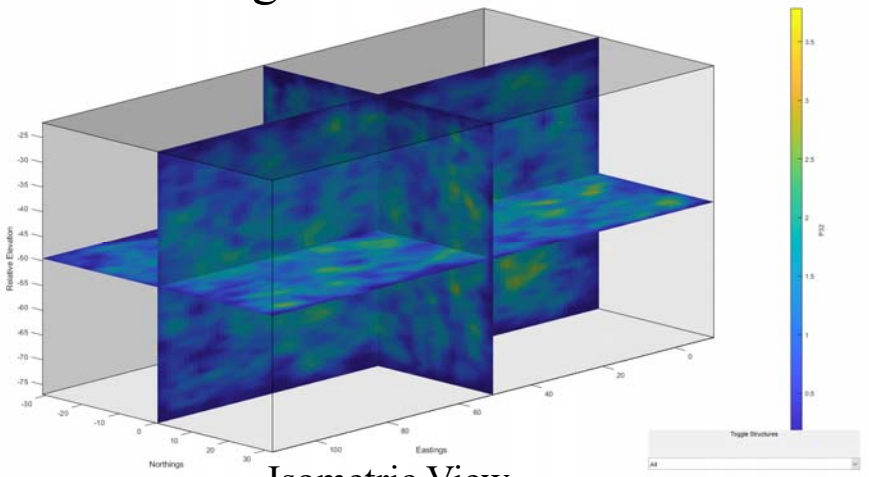

Isometric View

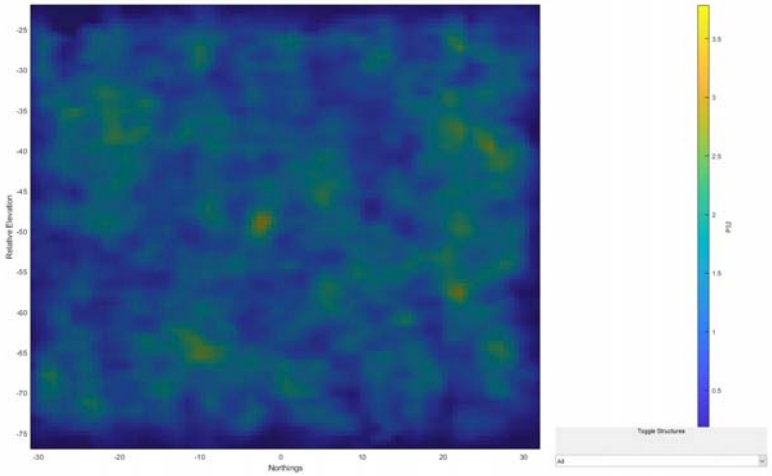

East View

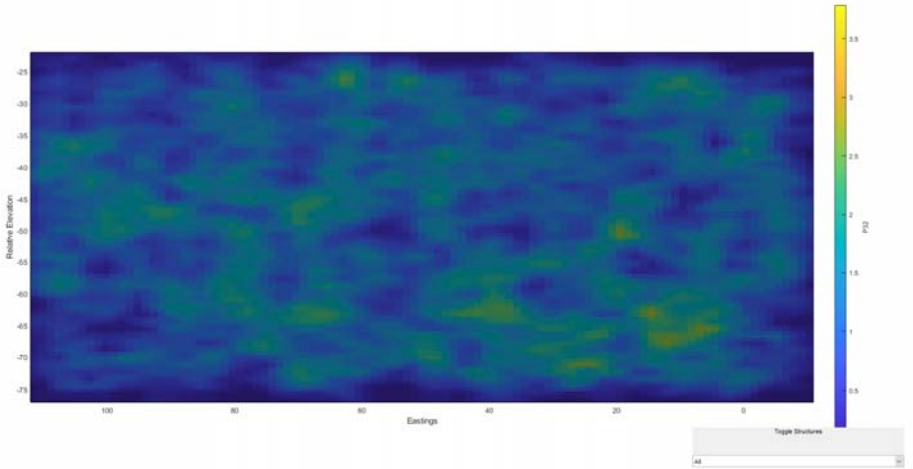

North View

Structural Analysis from SIROMODEL of DFN Mountain Large – Scale Factor=1.9

SIROMODEL application crashed and failed to complete assessments of a scale factor of 1.9

Structural Analysis from SIROMODEL of DFN Mountain Large – Scale Factor=2

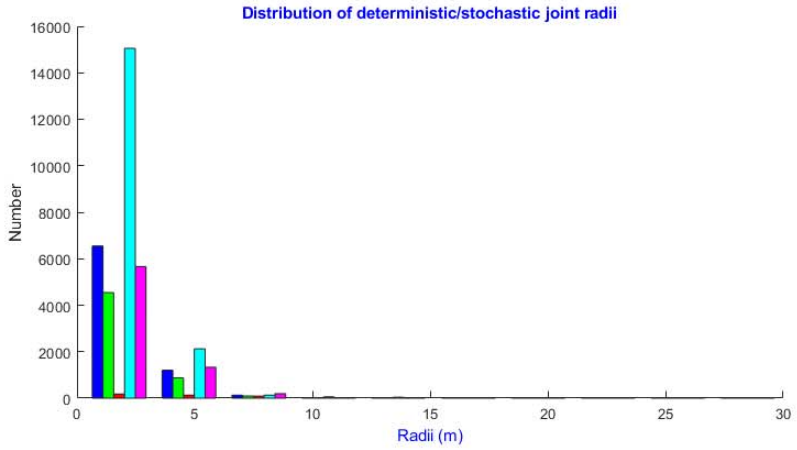

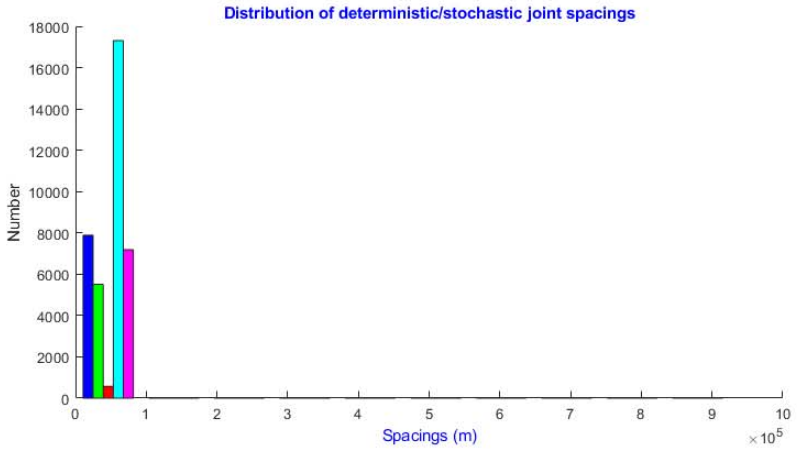

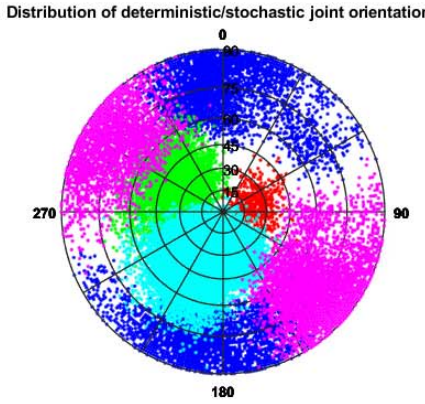

Stereonet Plot of Dip Vectors

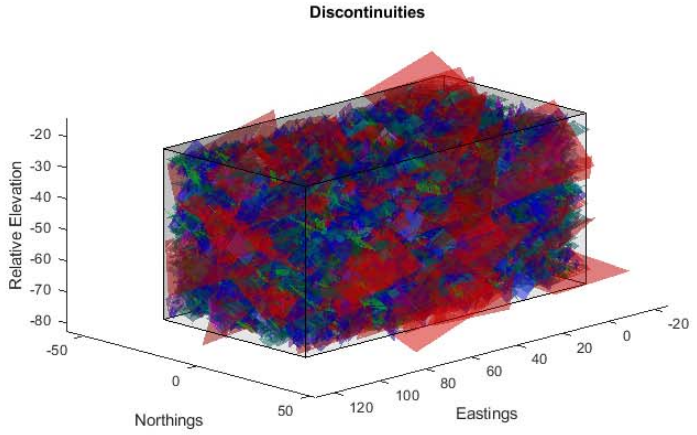

Isopleths of Fracture Statistical Analysis: DFN Mountain Large – Scale Factor=2

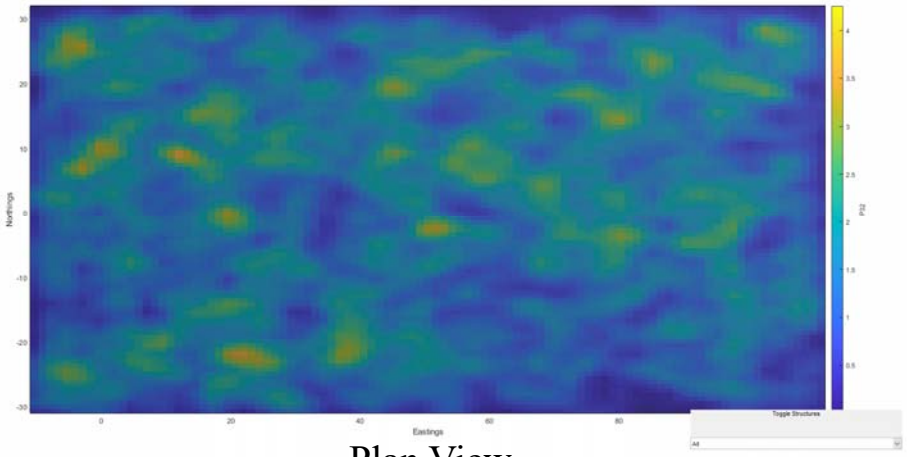

Plan View

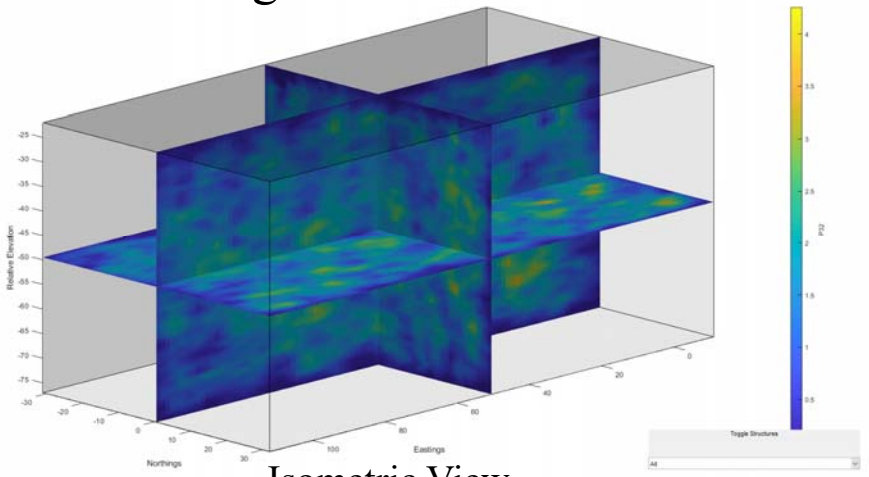

Isometric View

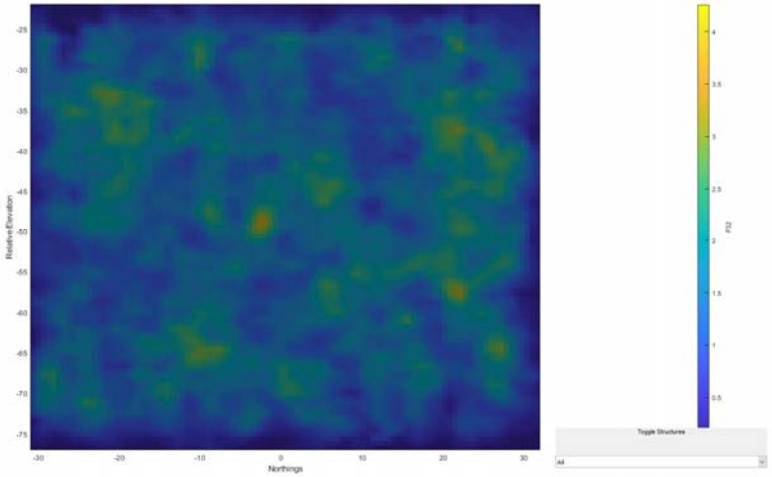

East View

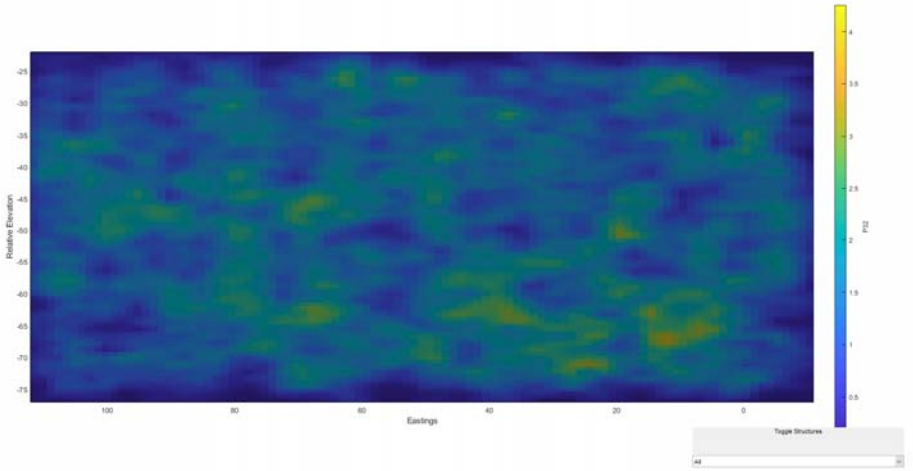

North View

Structural Analysis from SIROMODEL of DFN Mountain Large – Scale Factor=2.2

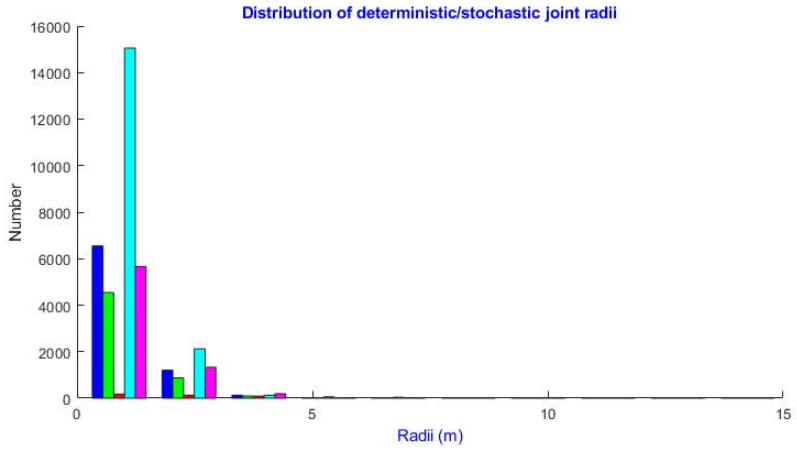

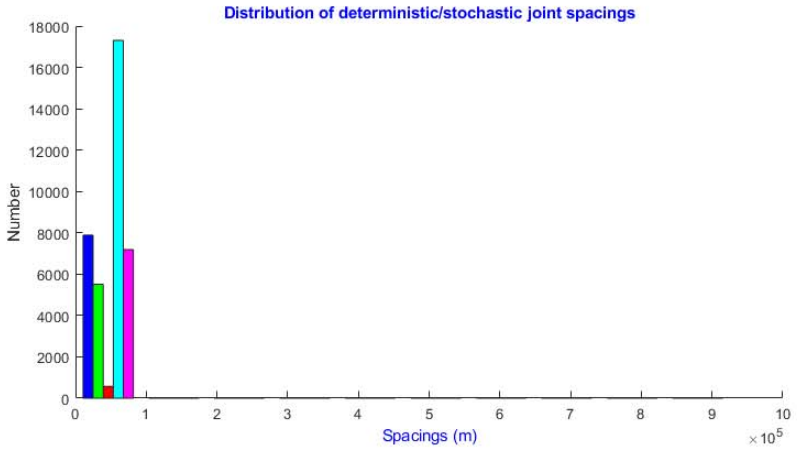

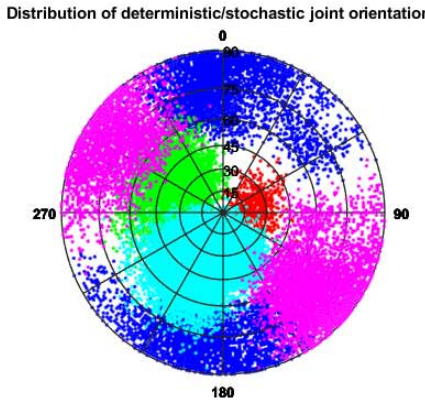

Stereonet Plot of Dip Vectors

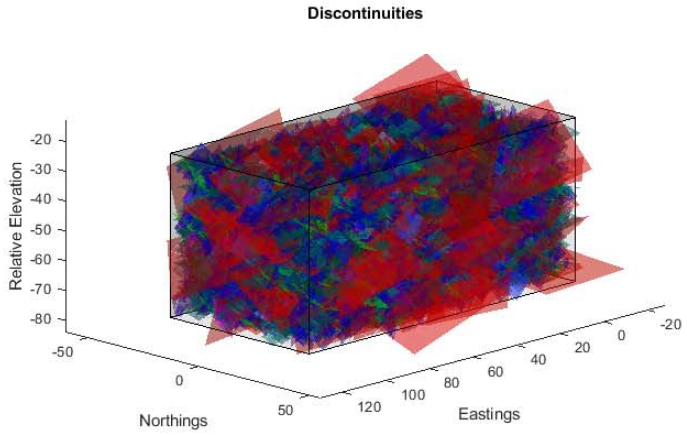

Isopleths of Fracture Statistical Analysis: DFN Mountain Large – Scale Factor=2.2

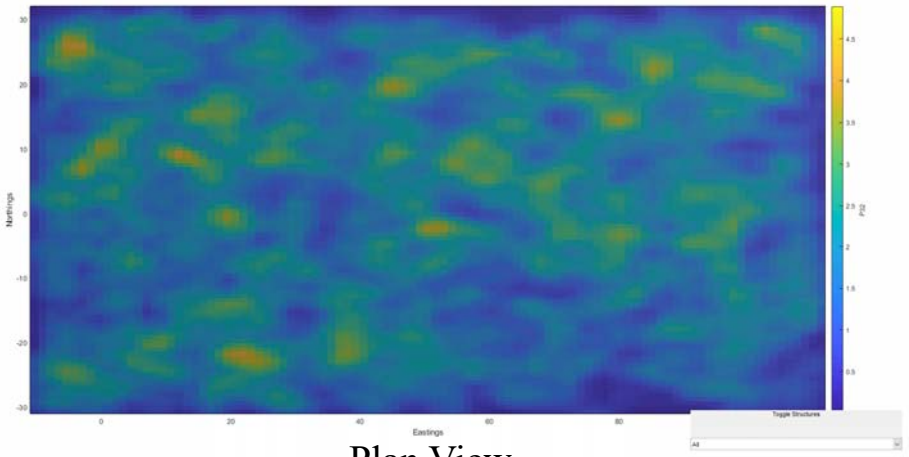

Plan View

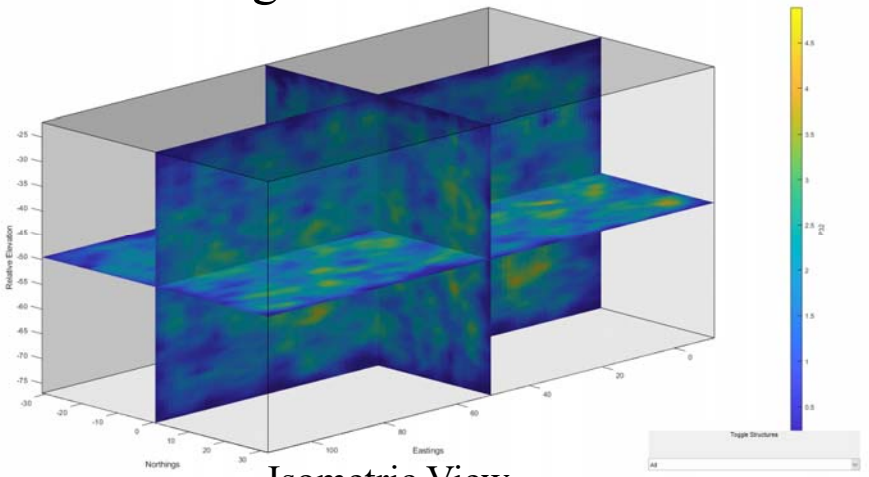

Isometric View

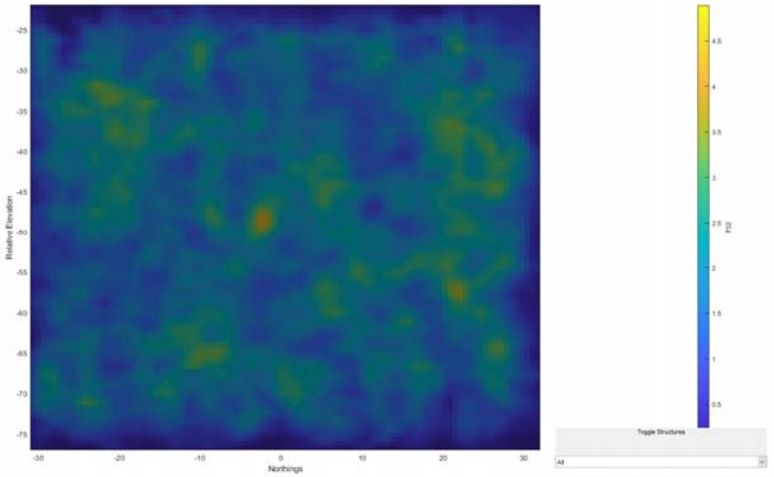

East View

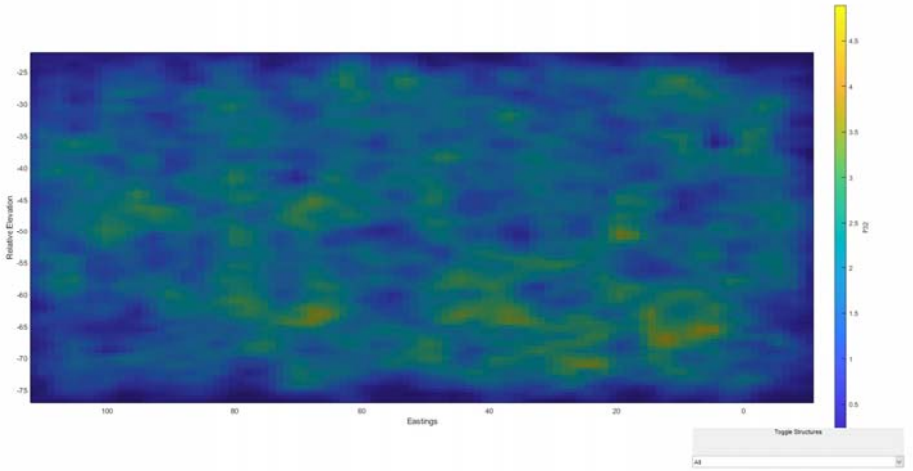

North View

Structural Analysis from SIROMODEL of DFN Mountain Large – Scale Factor=2.4

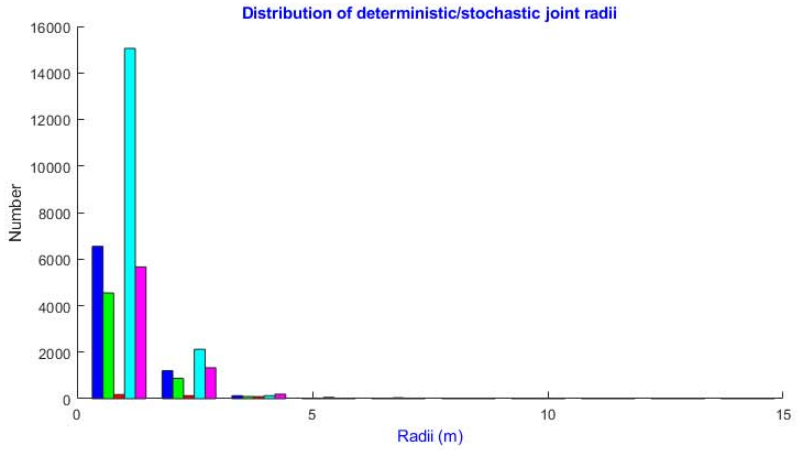

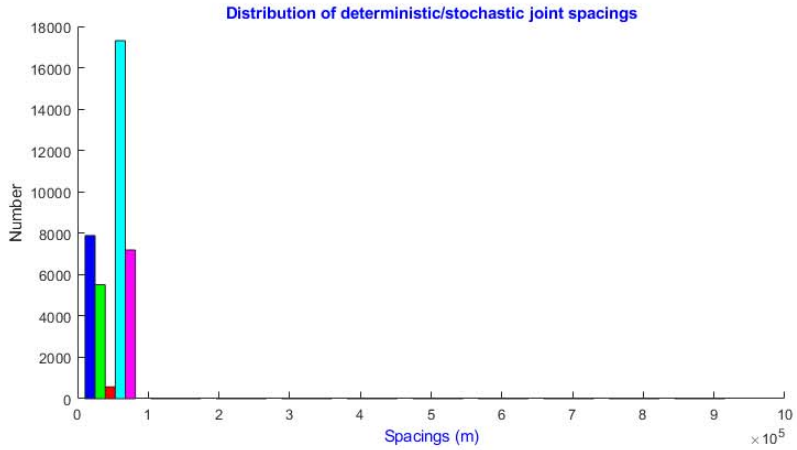

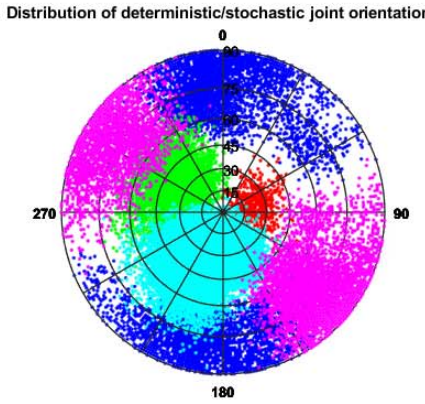

Stereonet Plot of Dip Vectors

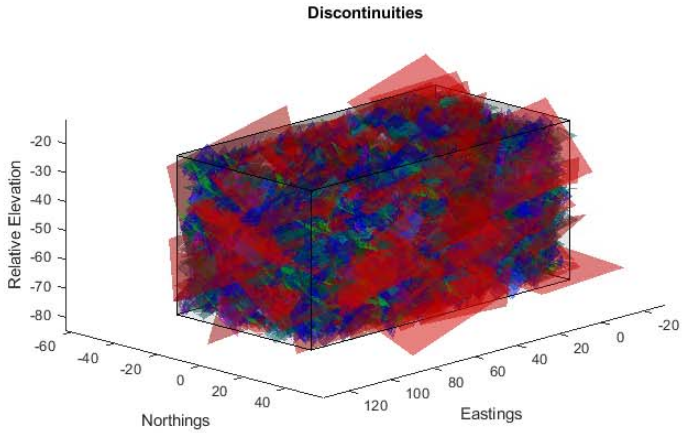

Isopleths of Fracture Statistical Analysis: DFN Mountain Large – Scale Factor=2.4

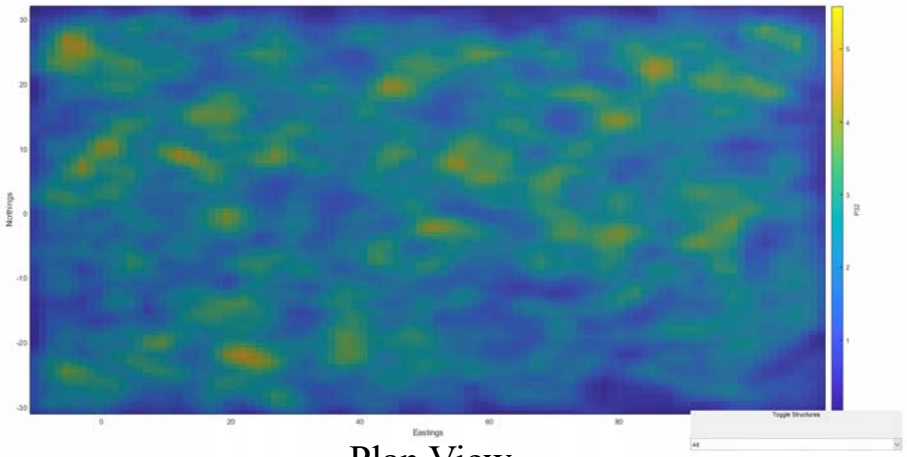

Plan View

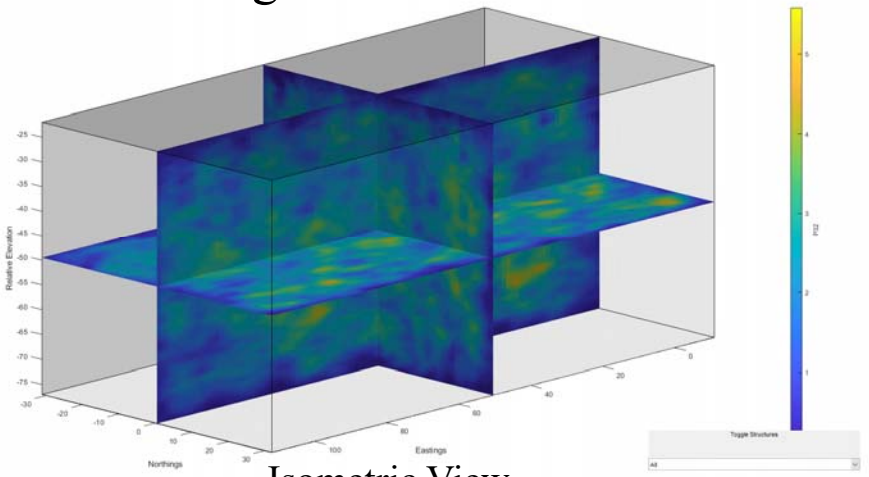

Isometric View

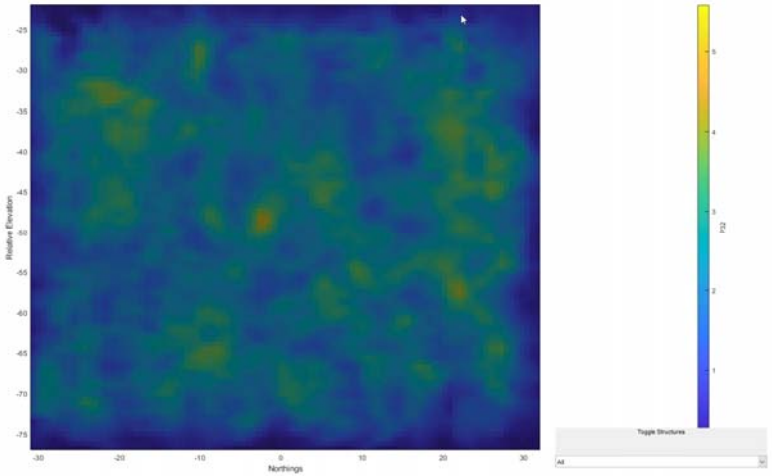

East View

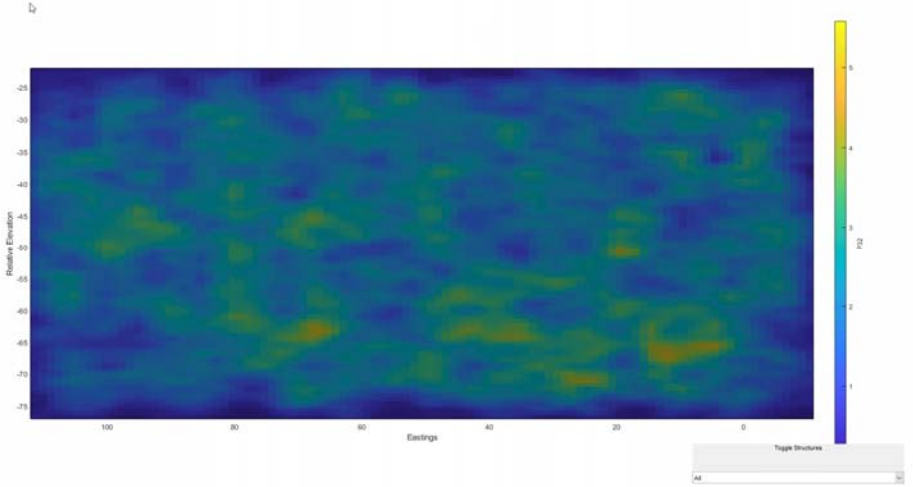

North View

Structural Analysis from SIROMODEL of DFN Mountain Large – Scale Factor=2.6, 2.8, 3

SIROMODEL application crashed and failed to complete assessments of a scale factor of 2.6, 2.8, and 3

APPENDIX A
ASSESSMENT OF SCALED EFFECTS OF CONTINUITY IN A DFN

A.3 Cross Sectional Comparison of Scaled Continuity for DFN Mountain Large and Small

East and North scaled cross sections of DFN Mountain Small

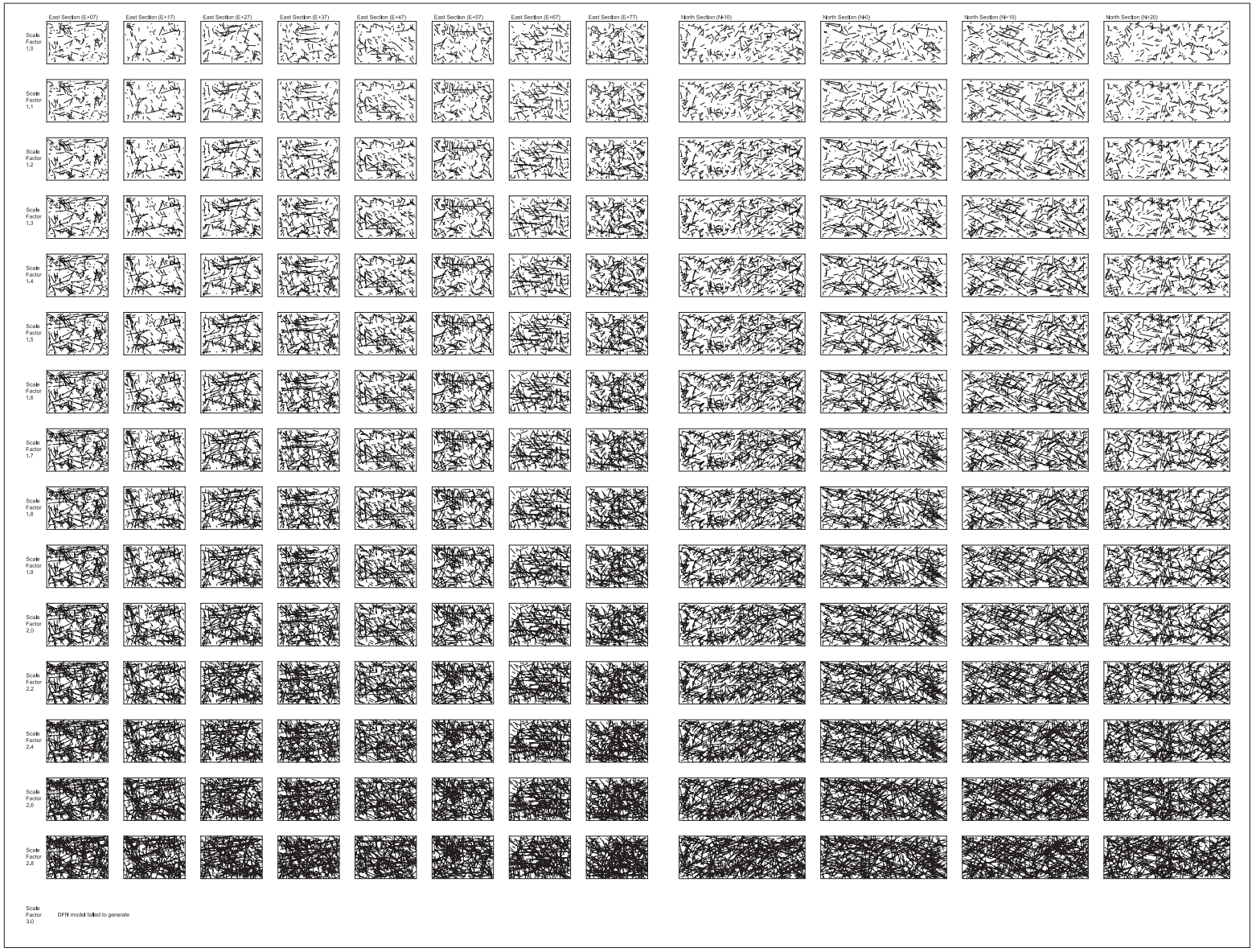

Fracture Count vs Scaling Factor for DFN Mountain Small

Fracture count (P_{20}) is the number of fractures sampled from the cross sections

Each curve represents a cross-section:
North cross-sections (x 4)
East cross-sections (x 8)

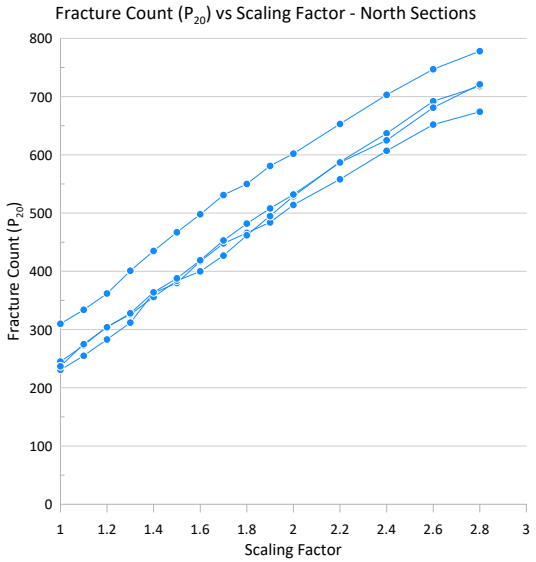

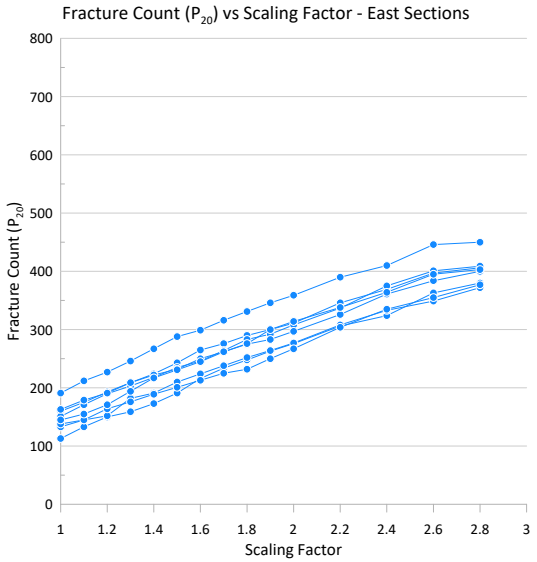

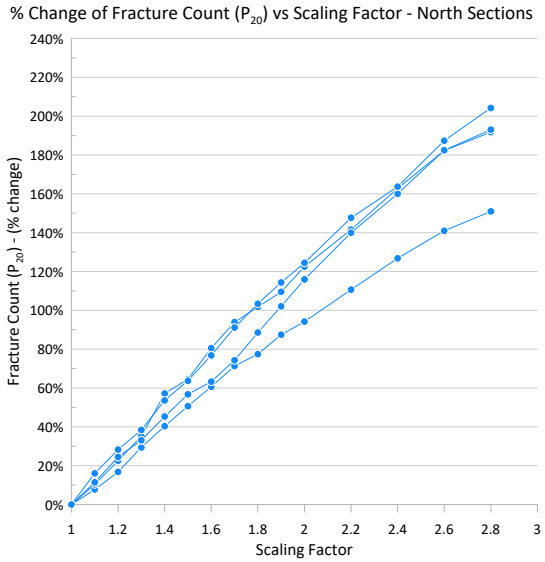

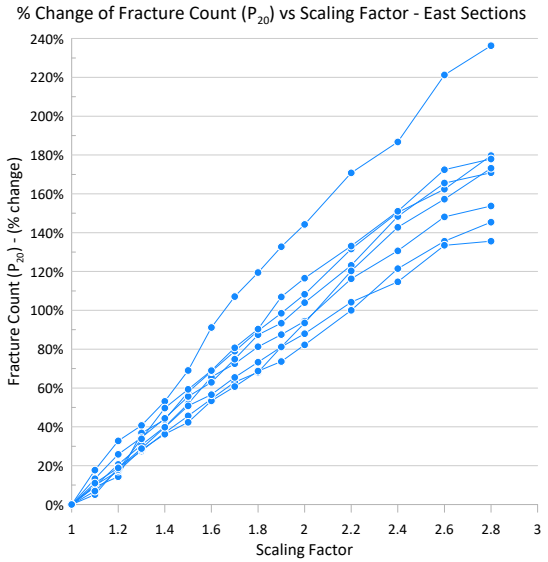

Fracture Count per unit area vs Scaling Factor for DFN Mountain Small

Fracture count per unit area (P_{21}) is the number of fractures sampled from the cross sections divided by the area

Each curve represents a cross-section:
North cross-sections (x 4) Area = 2160 m^2
East cross-sections (x 8) Area = 1053 m^2

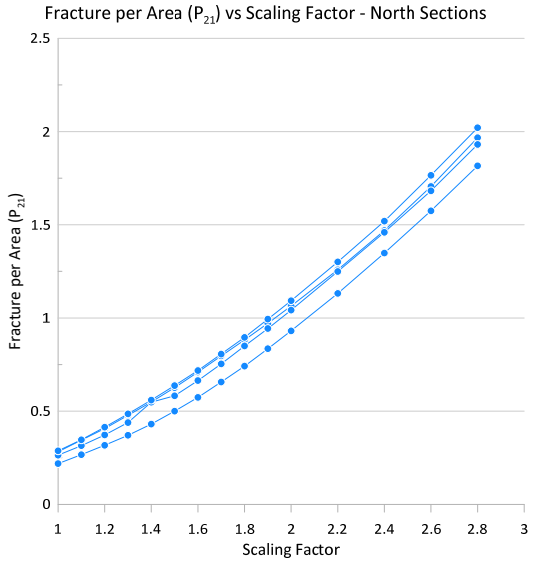

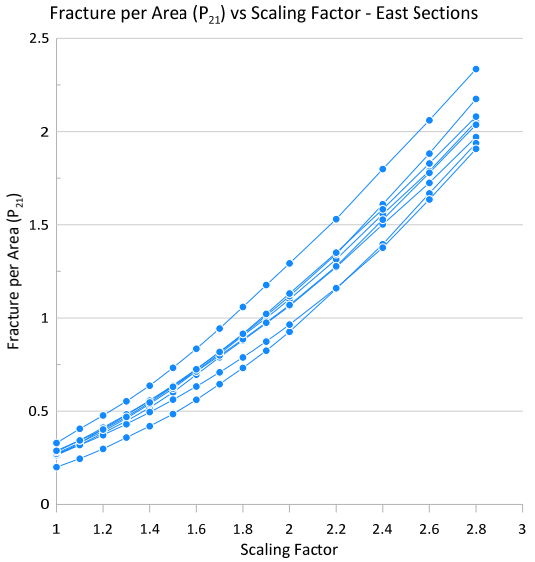

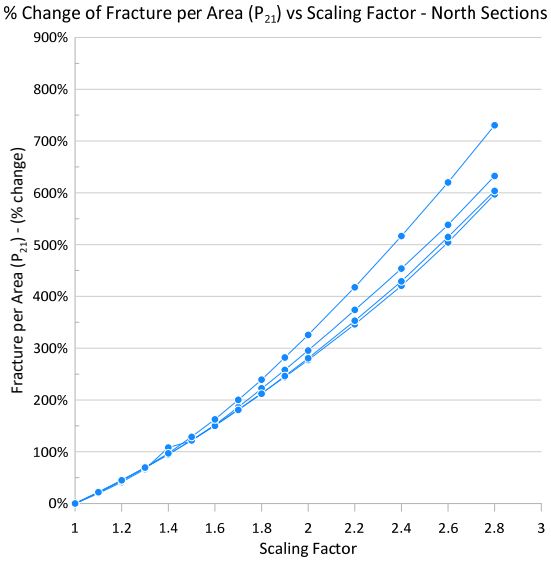

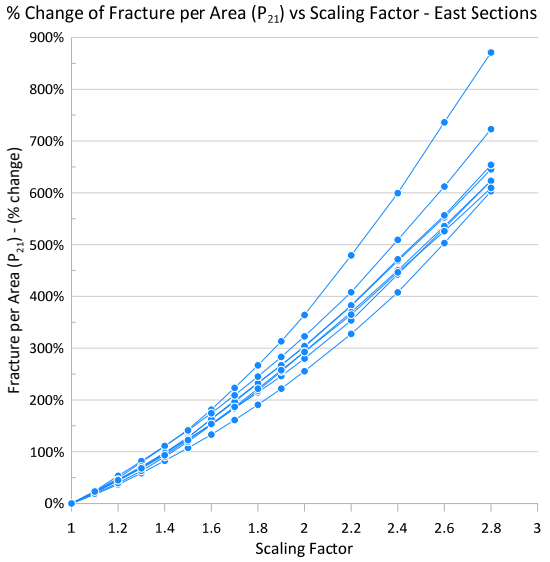

Intersection Count vs Scaling Factor for DFN Mountain Small

Intersection count (I_{20}) is the number of intersections between structures based on assessment of cross sections

Each curve represents a cross-section:
North cross-sections (x 4)
East cross-sections (x 8)

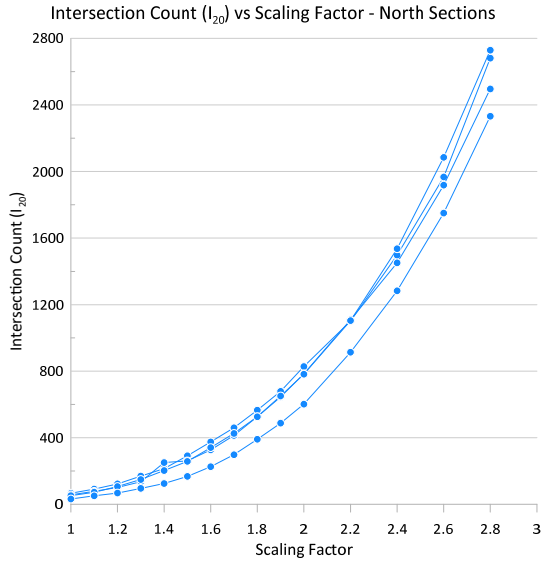

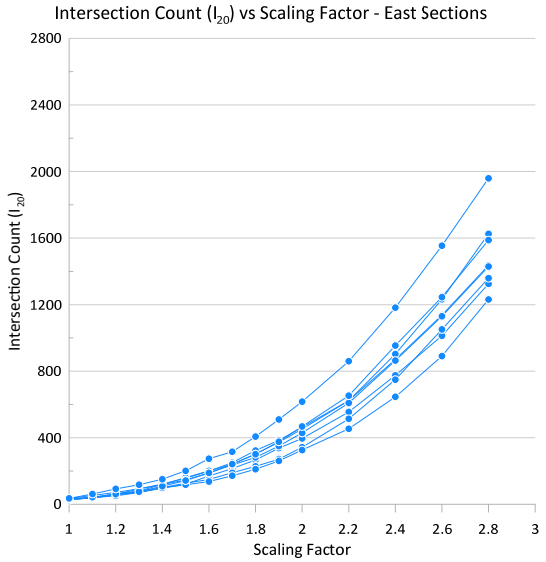

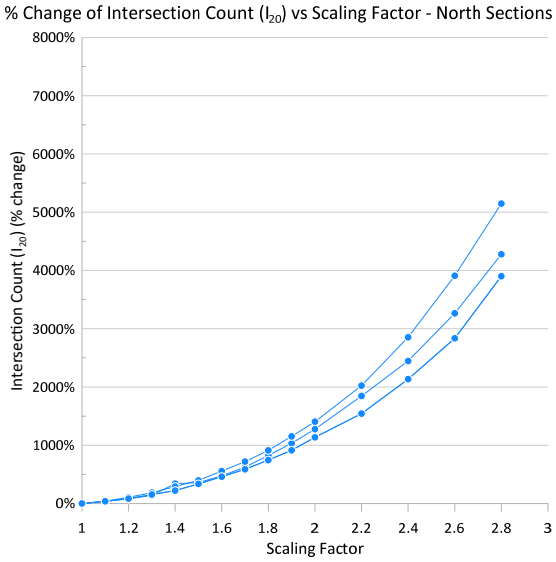

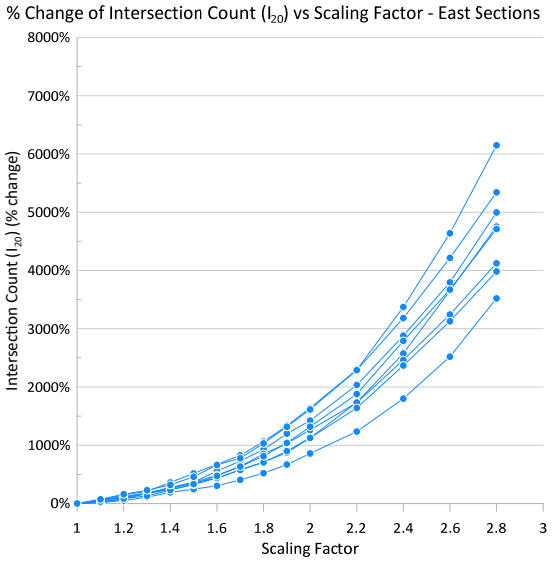

Intersection Count per unit area vs Scaling Factor for DFN Mountain Small

Intersection count per unit area (I_{21}) is the number of intersections between structures based on assessment of cross sections

Each curve represents a cross-section:
North cross-sections (x 4) Area = 2160 m^2
East cross-sections (x 8) Area = 1053 m^2

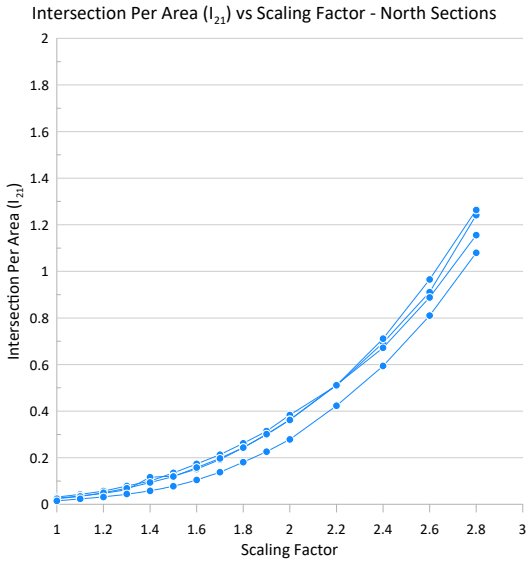

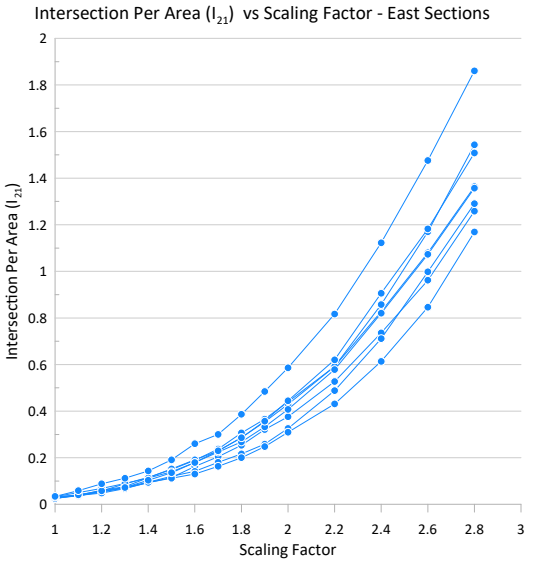

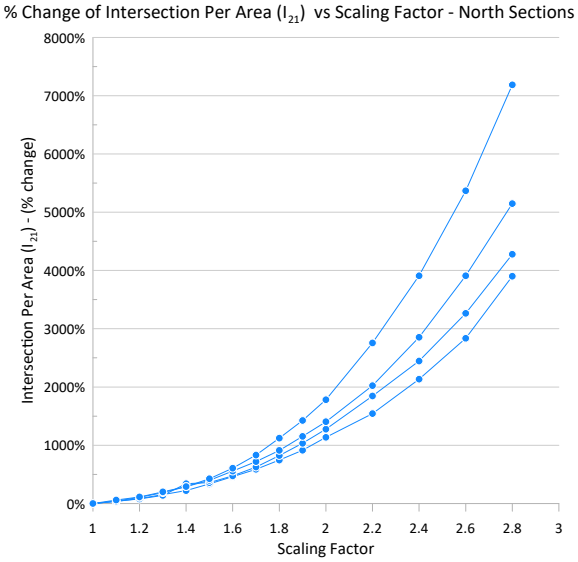

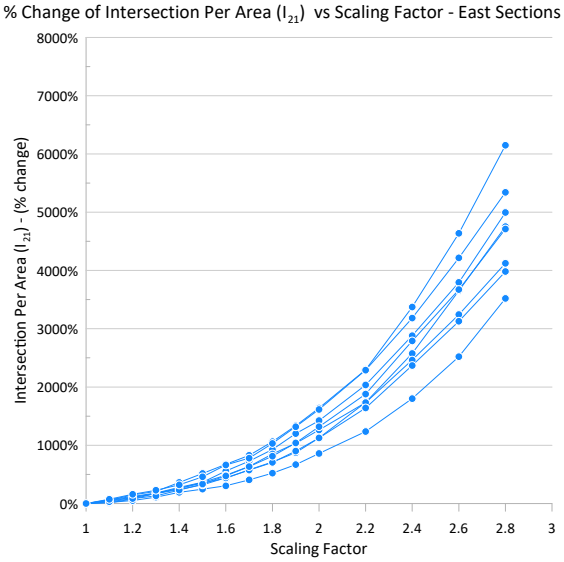

Network Connectivity vs Scaling Factor for DFN Mountain Small

Network connectivity (Elmo, et al. 2021) is an alternative rock mass quality indicator and is determined by $P_{21}/P_{20} * I_{20}$

Each curve represents a cross-section:
North cross-sections (x 4)
East cross-sections (x 8)

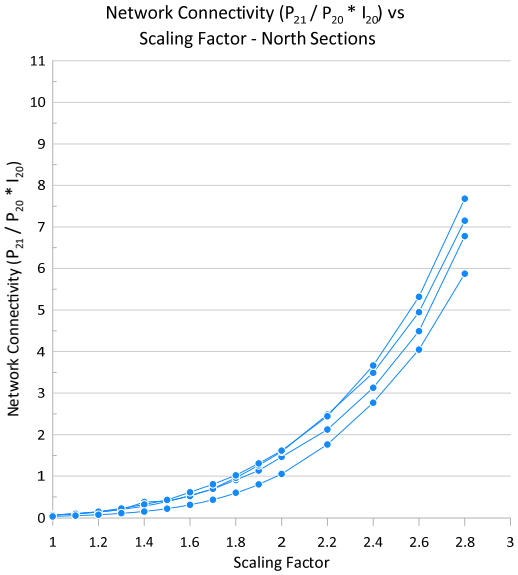

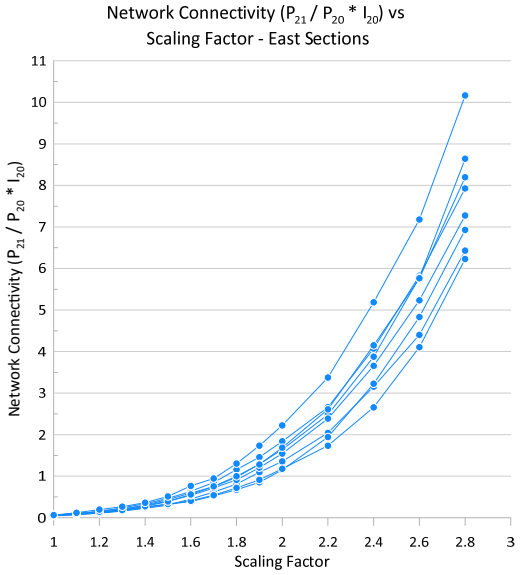

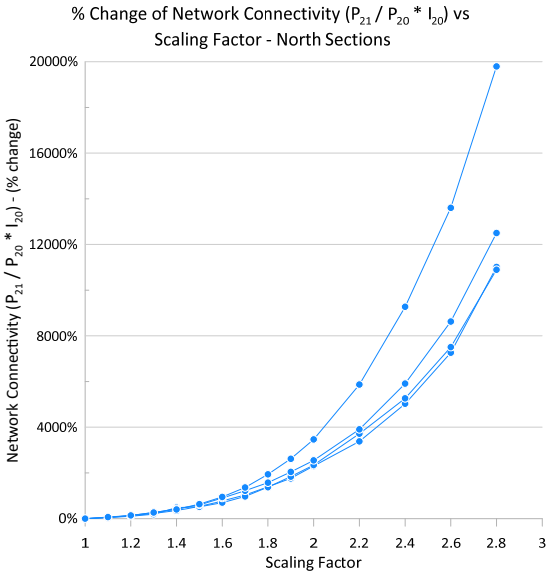

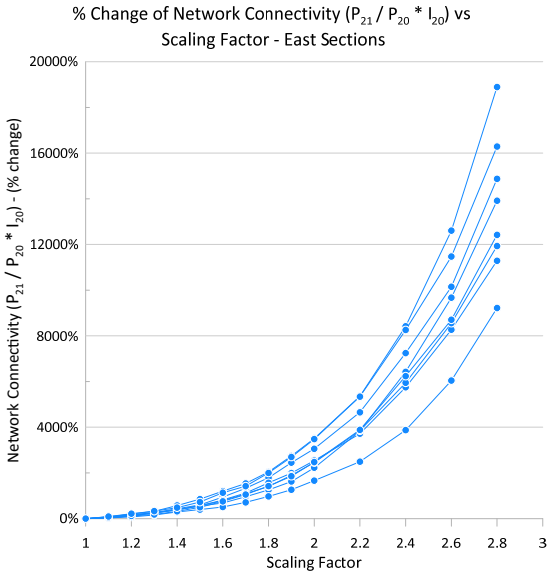

East and North scaled cross sections of DFN Mountain Large

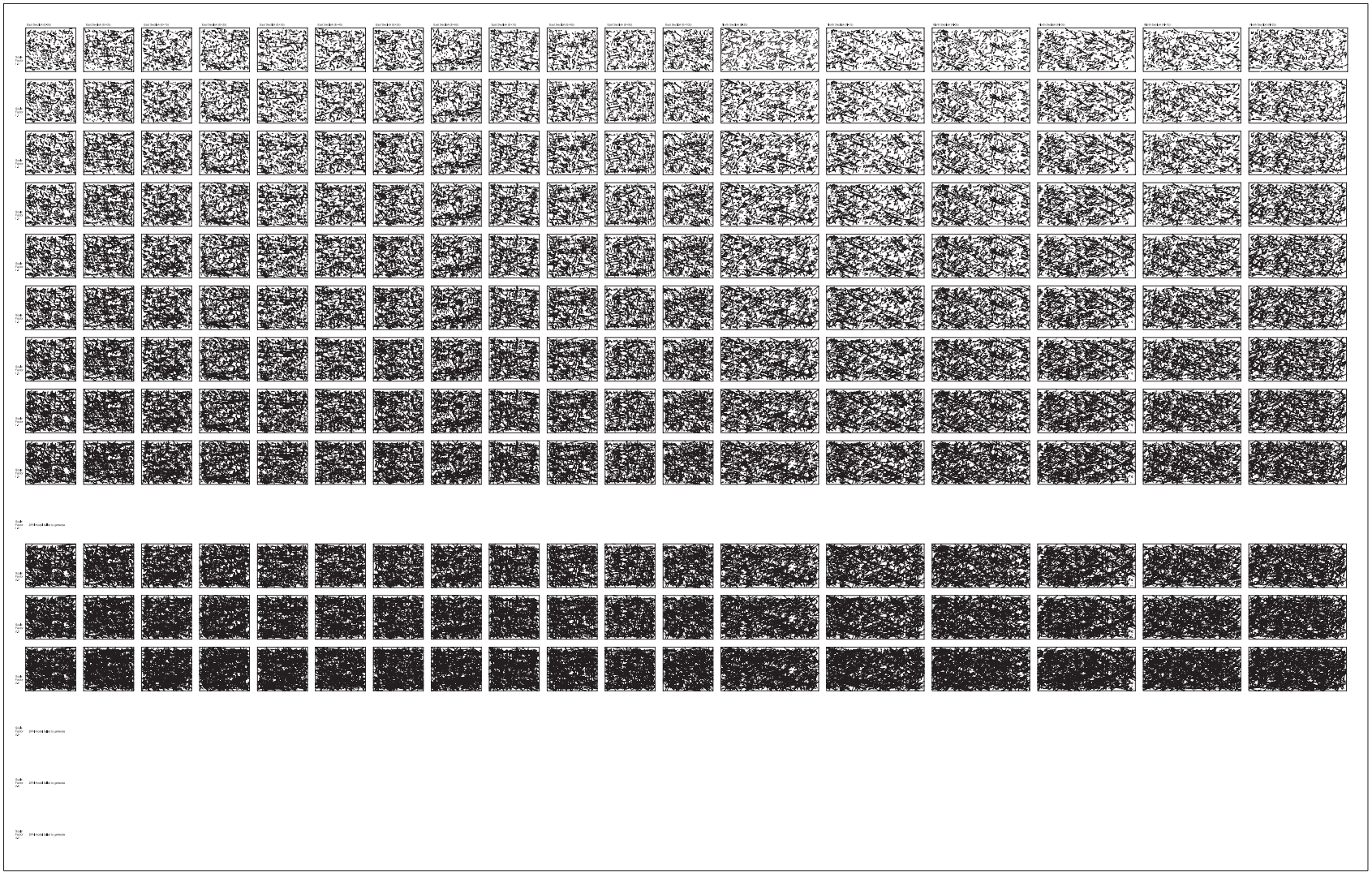

0 50 100 150 200 250 m

SCALE 1:5000

Fracture Count vs Scaling Factor for DFN Mountain Large

Fracture count (P_{20}) is the number of fractures sampled from the cross sections

Each curve represents a cross-section:
North cross-sections (x 6)
East cross-sections (x 12)

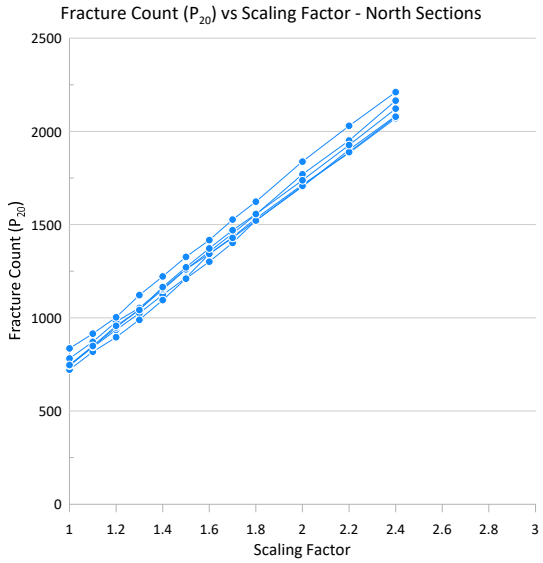

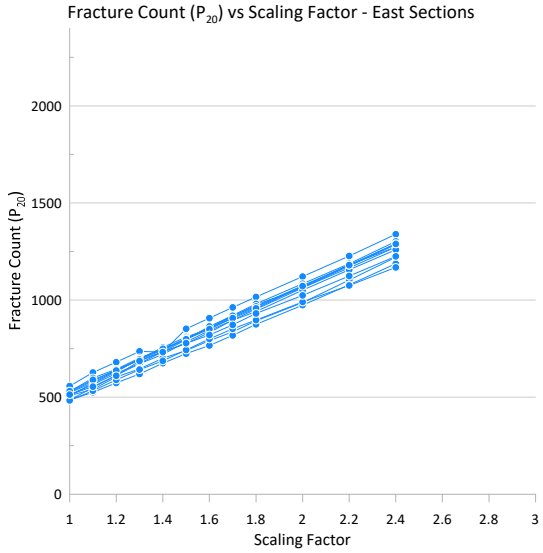

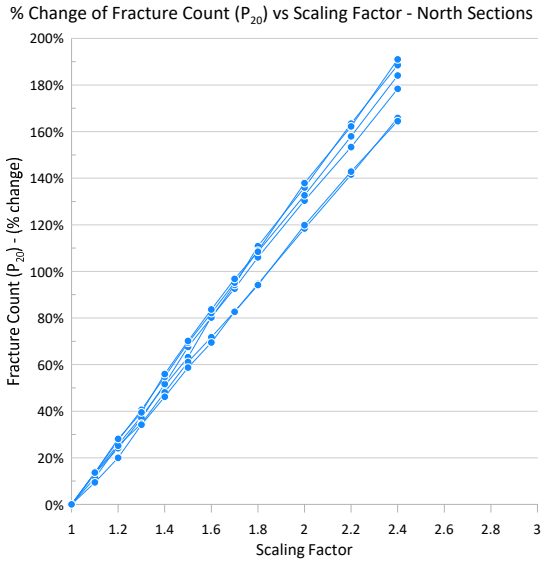

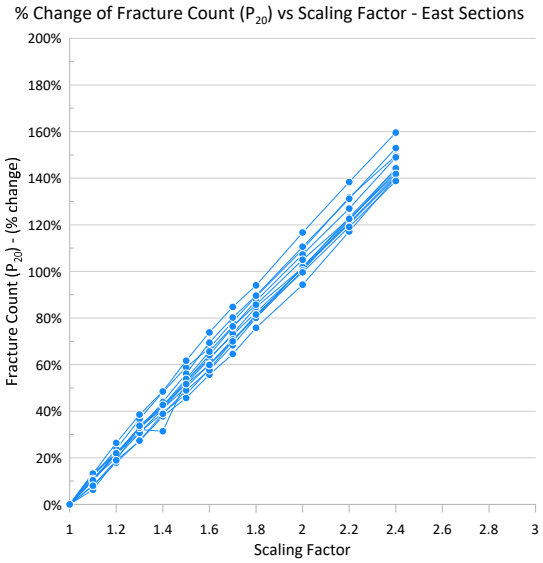

Fracture Count per unit area vs Scaling Factor for DFN Mountain Large

Fracture count per unit area (P_{21}) is the number of fractures sampled from the cross sections divided by the area

Each curve represents a cross-section:
North cross-sections (x 6) Area = 6765 m^2
East cross-sections (x 12) Area = 3465 m^2

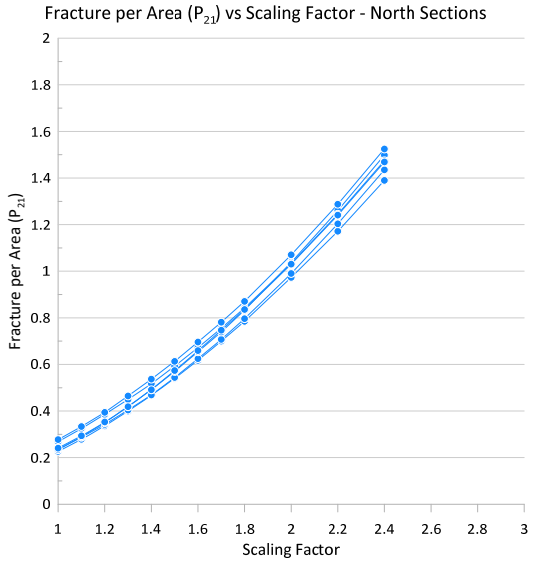

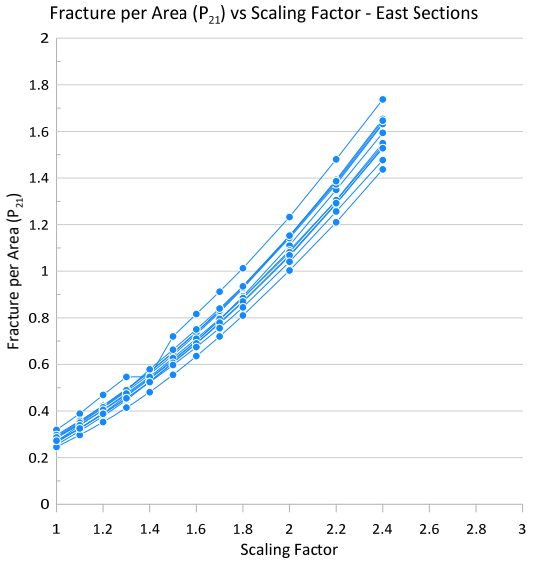

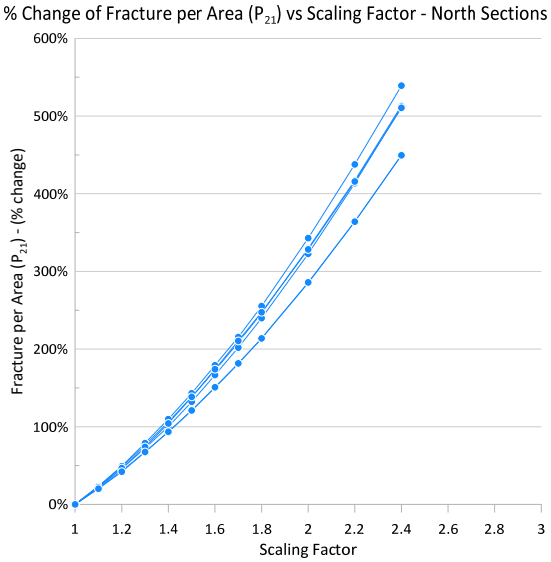

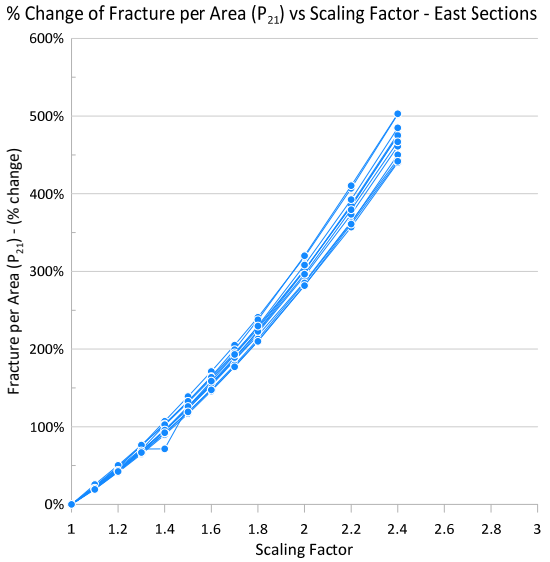

Intersection Count vs Scaling Factor for DFN Mountain Large

Intersection count (I_{20}) is the number of intersections between structures based on assessment of cross sections

Each curve represents a cross-section:
North cross-sections (x 6)
East cross-sections (x 12)

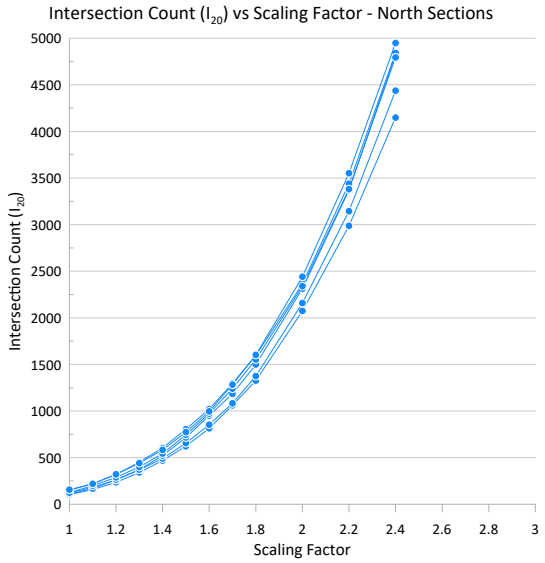

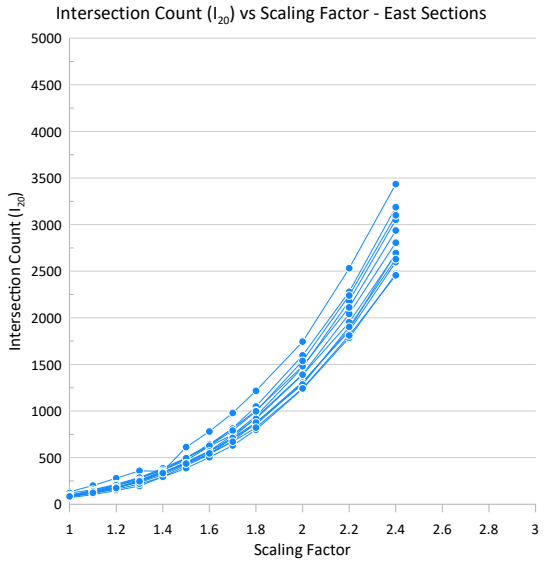

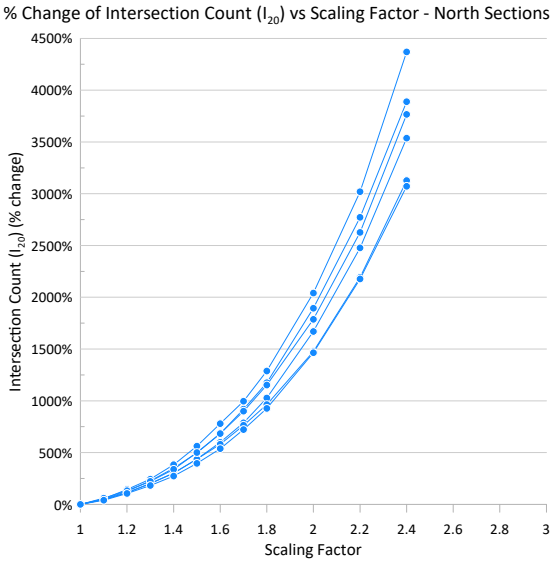

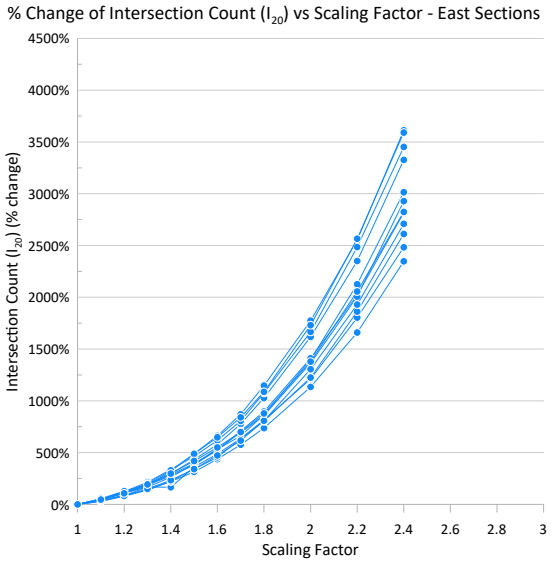

Intersection Count per unit area vs Scaling Factor for DFN Mountain Large

Intersection count per unit area (I_{21}) is the number of intersections between structures based on assessment of cross sections

Each curve represents a cross-section:
North cross-sections (x 6) Area = 6765 m^2
East cross-sections (x 12) Area = 3465 m^2

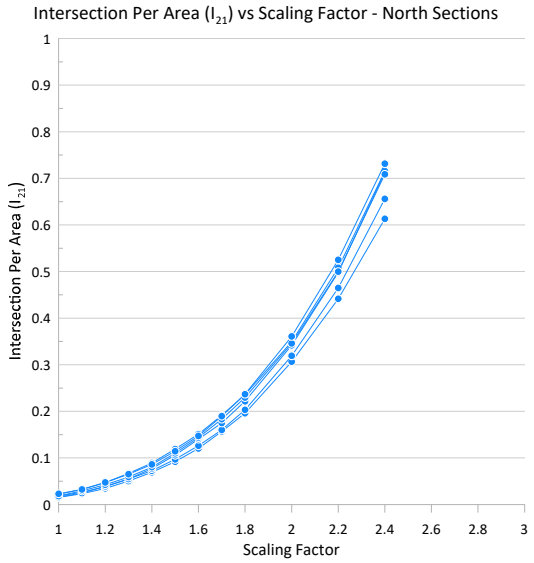

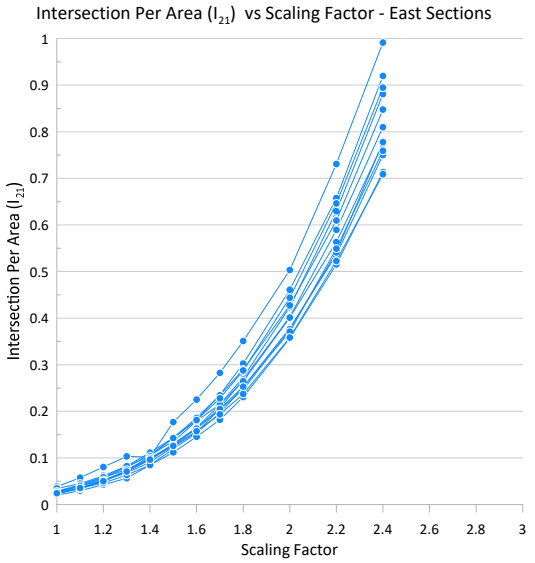

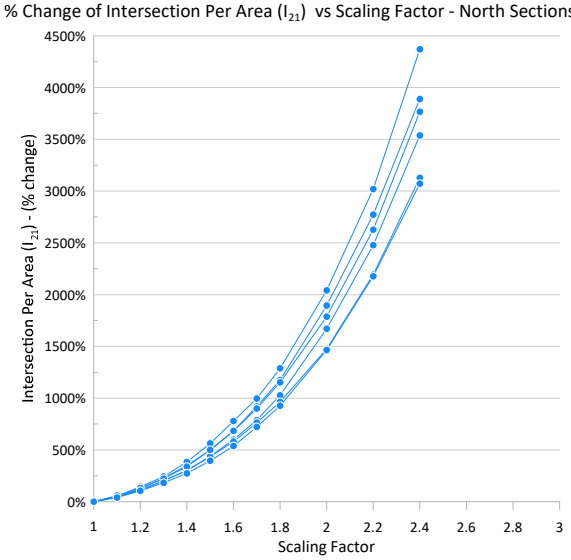

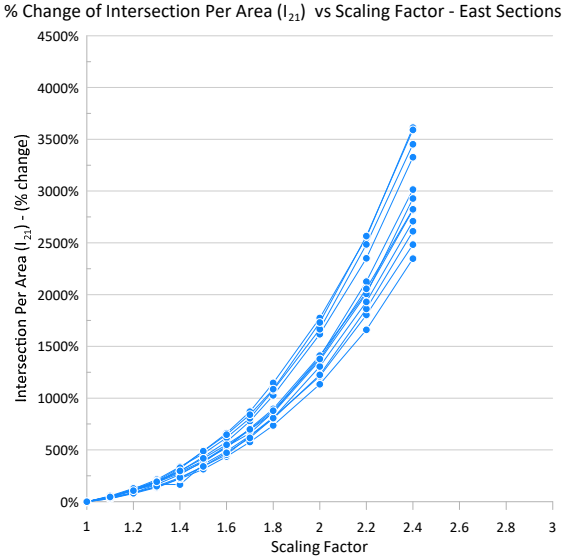

Network Connectivity vs Scaling Factor for DFN Mountain Large

Network connectivity (Elmo, et al. 2021) is an alternative rock mass quality indicator and is determined by $P_{21}/P_{20} * I_{20}$

Each curve represents a cross-section:
North cross-sections (x 6)
East cross-sections (x 12)

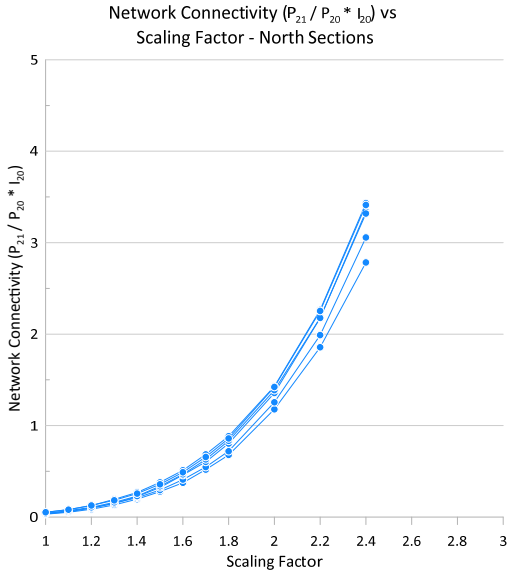

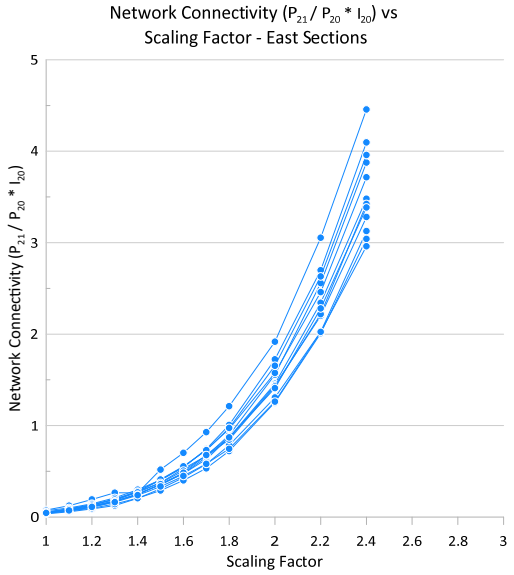

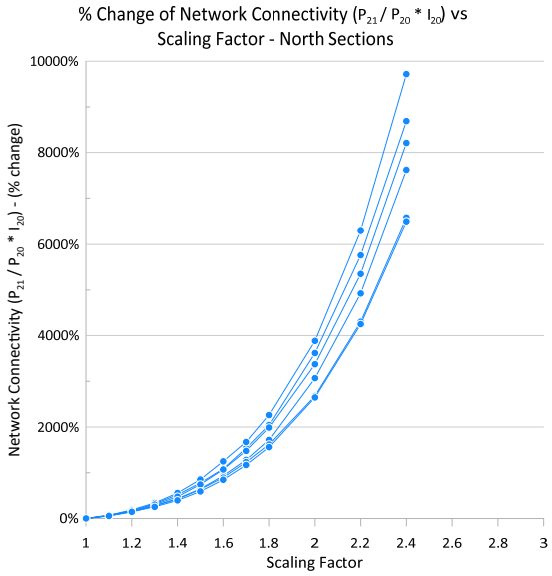

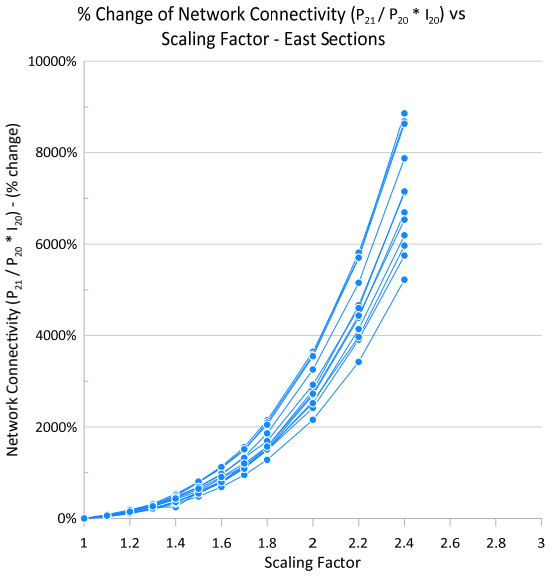

Fracture Count vs Scaling Factor

Comparison of DFN Mountain Large and Small (normalized as % change)

Top graphs:
Each curve represents a cross-section
4 & 6 North cross-sections for Small & Large
8 & 12 East cross-sections for Small & Large

Bottom graphs:
Based on the data plotted above the minimum and maximum curves (thin line) were made for each model, as well as an average curve (thick line)

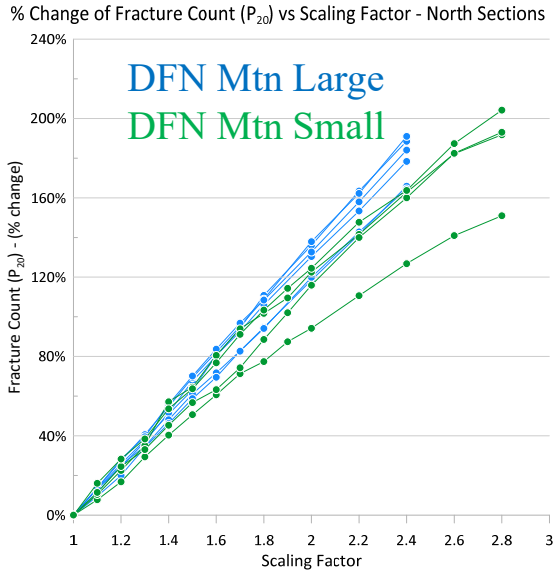

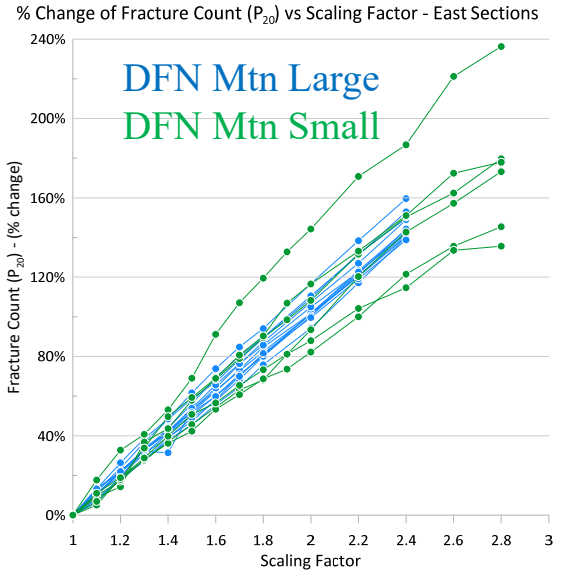

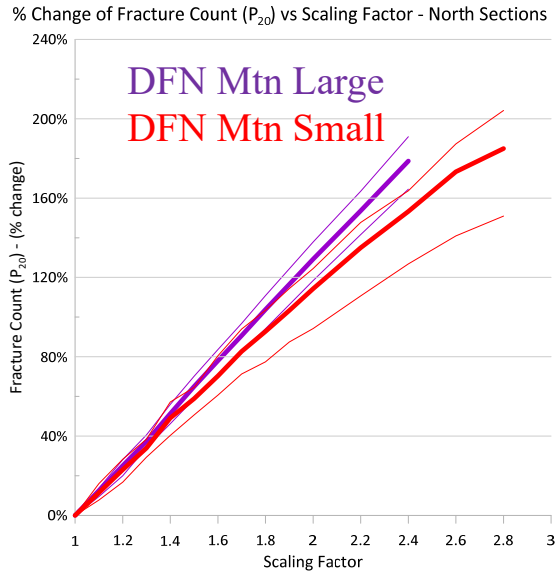

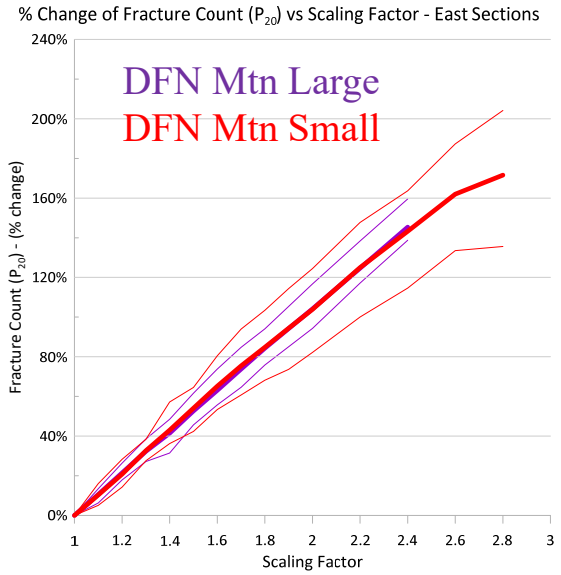

Fracture Count per unit area vs Scaling Factor

Comparison of DFN Mountain Large and Small (normalized as % change)

Top graphs:
Each curve represents a cross-section
4 & 6 North cross-sections for Small & Large
8 & 12 East cross-sections for Small & Large

Bottom graphs:
Based on the data plotted above the minimum and maximum curves (thin line) were made for each model, as well as an average curve (thick line)

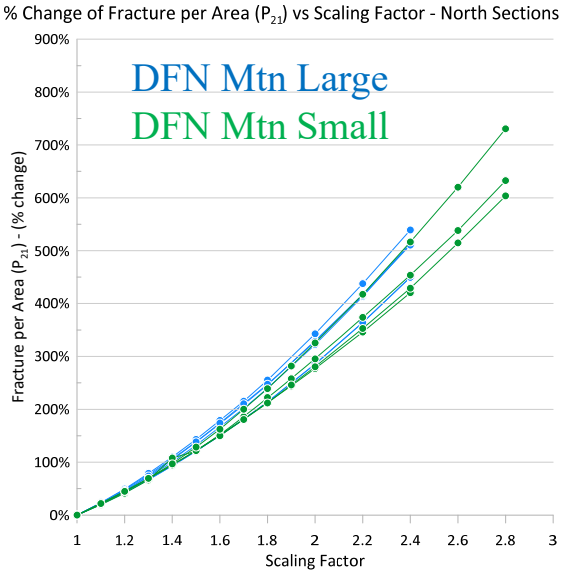

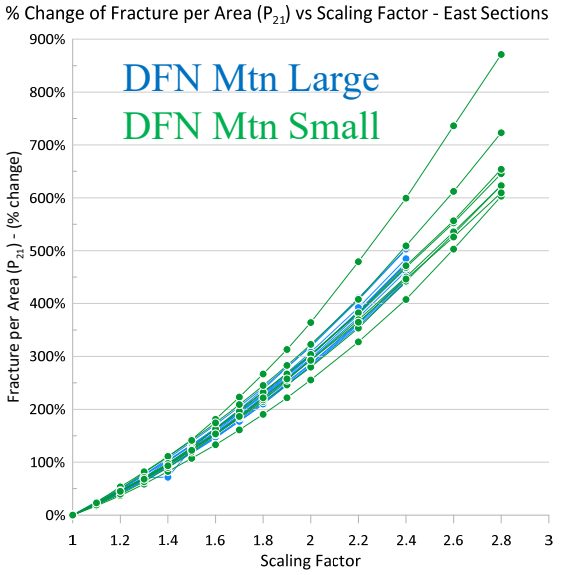

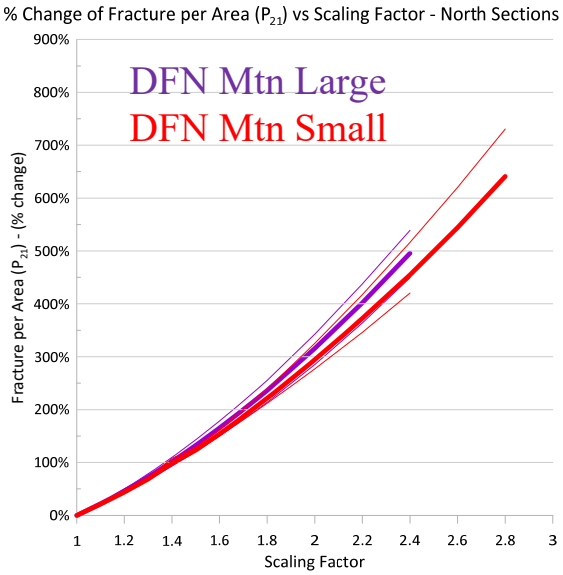

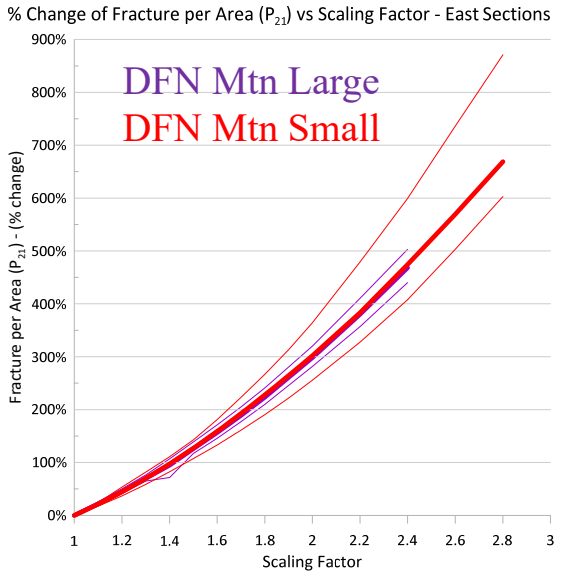

Intersection Count vs Scaling Factor

Comparison of DFN Mountain Large and Small (normalized as % change)

Top graphs:
Each curve represents a cross-section
4 & 6 North cross-sections for Small & Large
8 & 12 East cross-sections for Small & Large

Bottom graphs:
Based on the data plotted above the minimum and maximum curves (thin line) were made for each model, as well as an average curve (thick line)

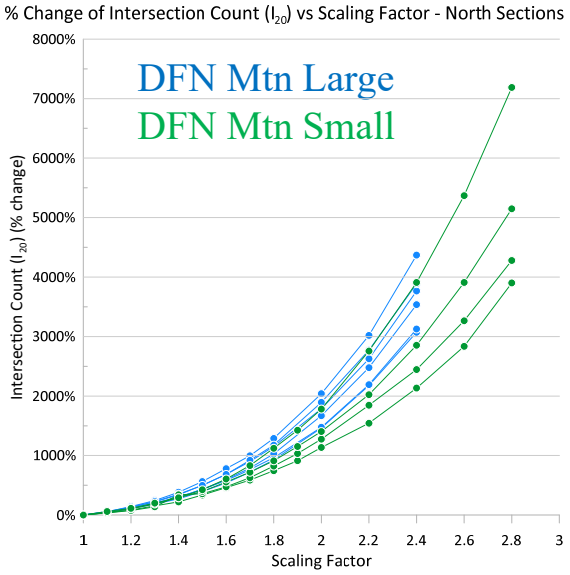

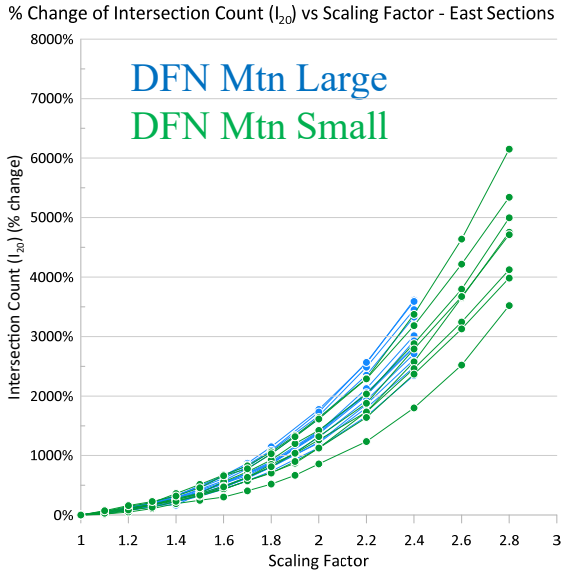

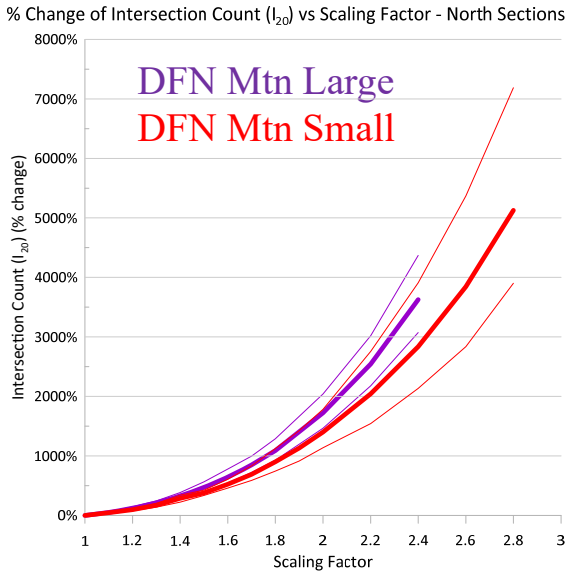

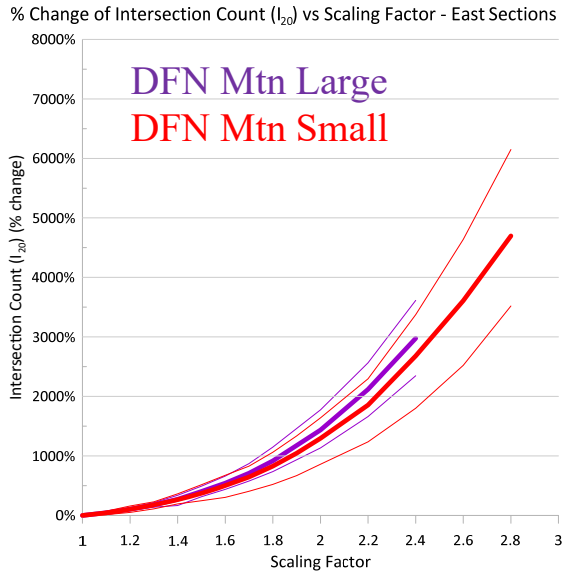

Intersection Count per unit area vs Scaling Factor

Comparison of DFN Mountain Large and Small (normalized as % change)

Top graphs:
Each curve represents a cross-section
4 & 6 North cross-sections for Small & Large
8 & 12 East cross-sections for Small & Large

Bottom graphs:
Based on the data plotted above the minimum and maximum curves (thin line) were made for each model, as well as an average curve (thick line)

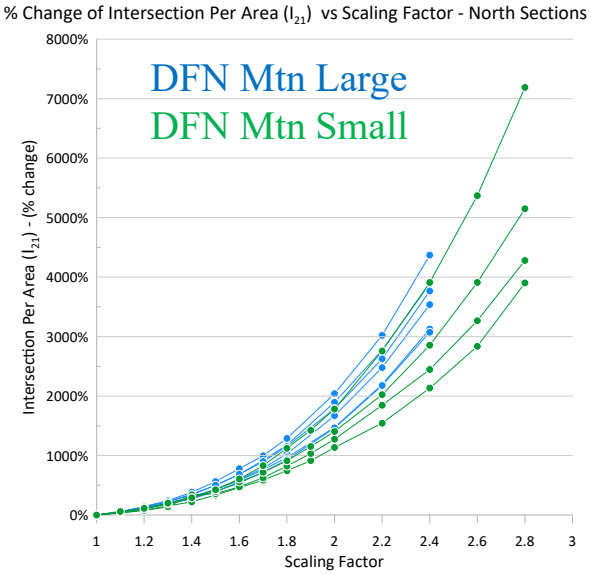

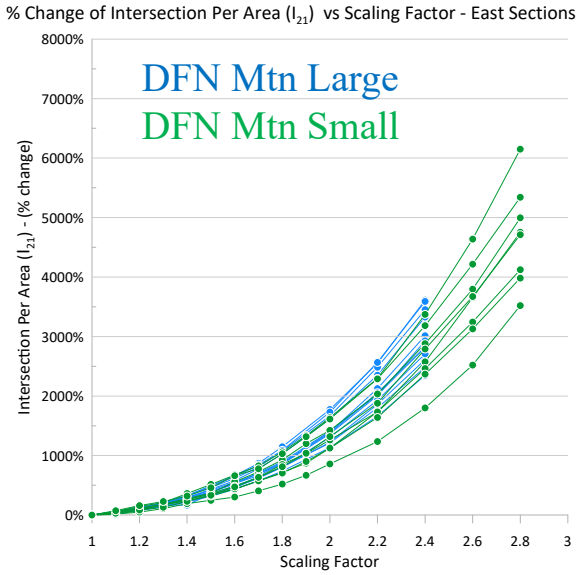

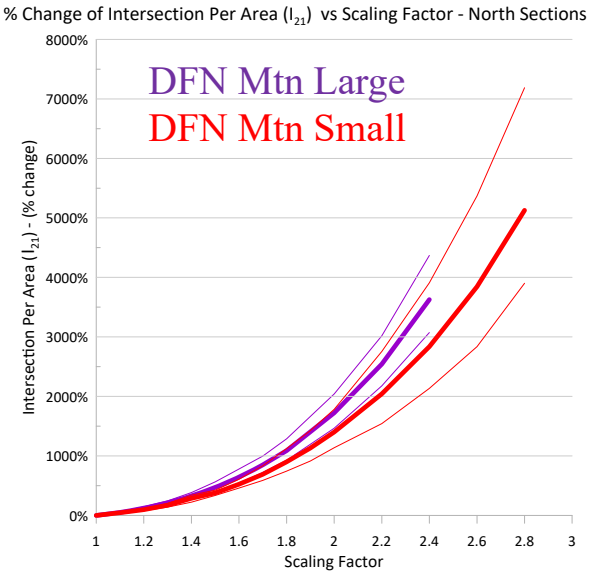

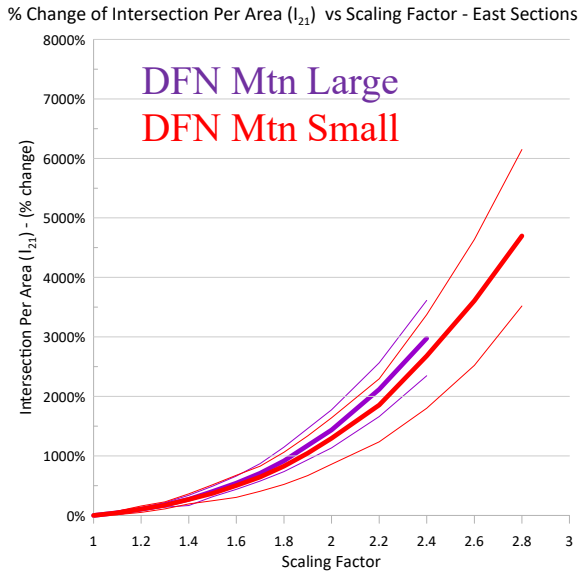

Network Connectivity vs Scaling Factor

Comparison of DFN Mountain Large and Small (normalized as % change)

Top graphs:
Each curve represents a cross-section
4 & 6 North cross-sections for Small & Large
8 & 12 East cross-sections for Small & Large

Bottom graphs:
Based on the data plotted above the minimum and maximum curves (thin line) were made for each model, as well as an average curve (thick line)

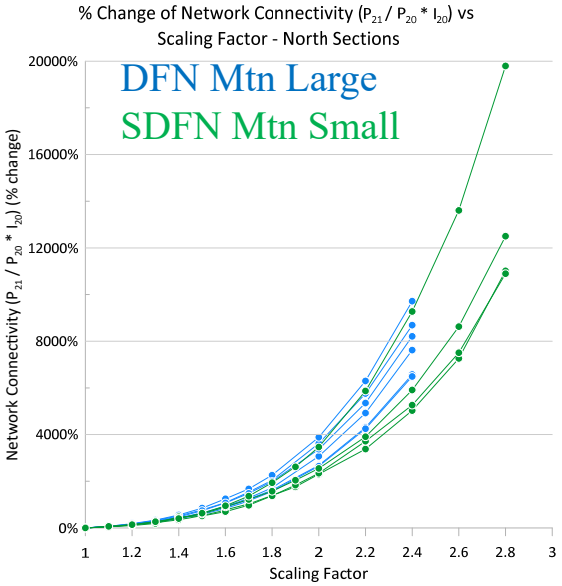

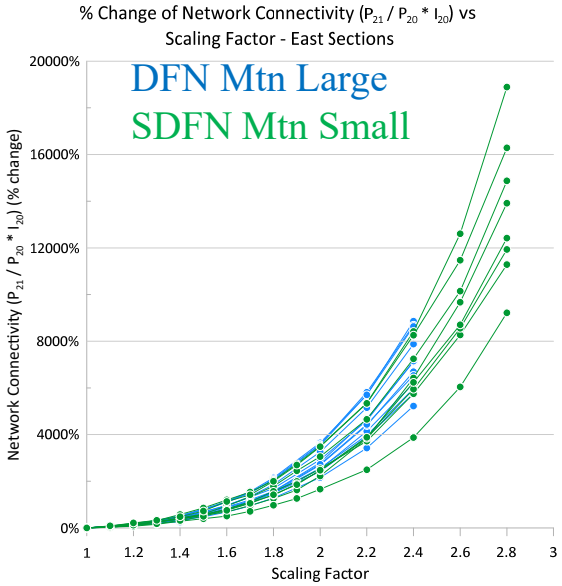

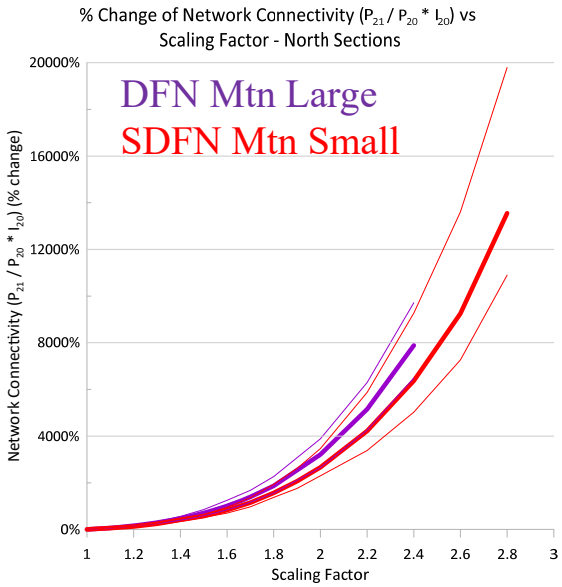

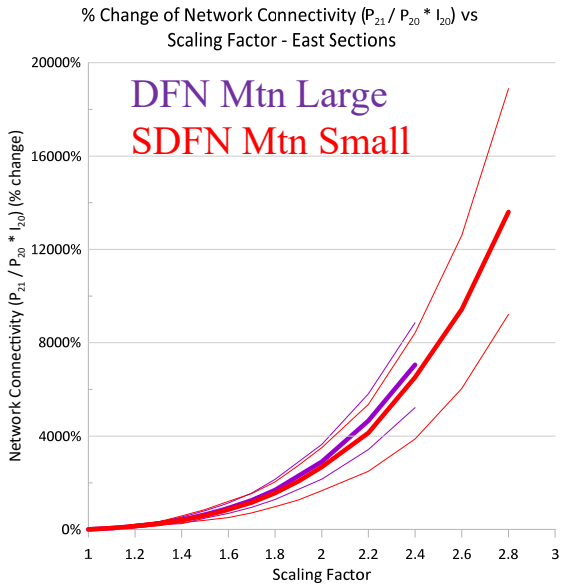

APPENDIX B: KINEMATIC ANALYSIS MODEL RUNS IN SIROMODEL

SIROMODEL Modeler
View
DFN Open Pit
Full Pit Model

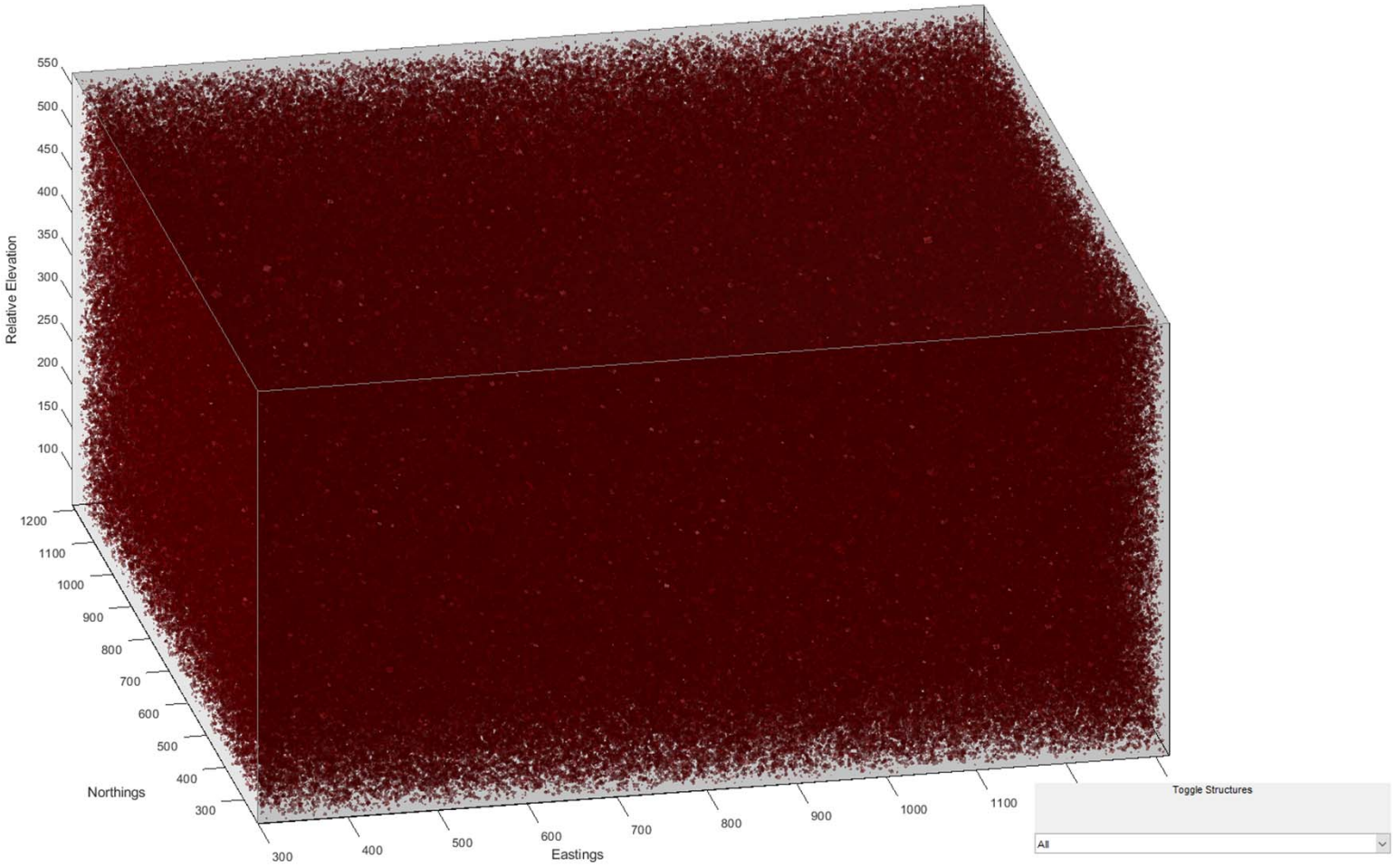

SIROMODEL
Structural Analysis
View

DFN Open Pit
Full Pit Model

*Did not generate
blocks

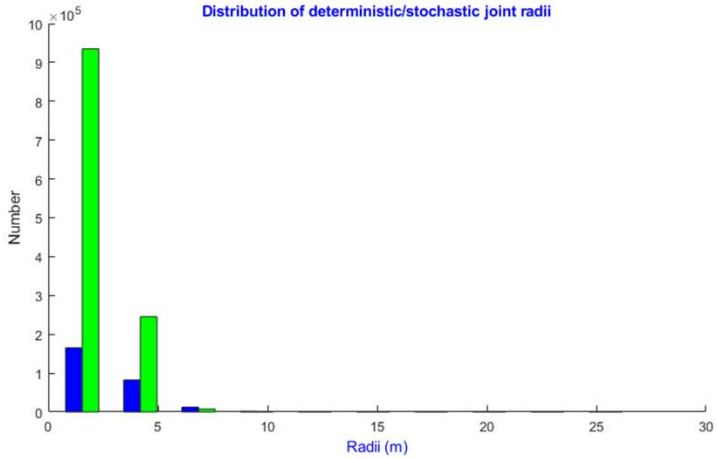

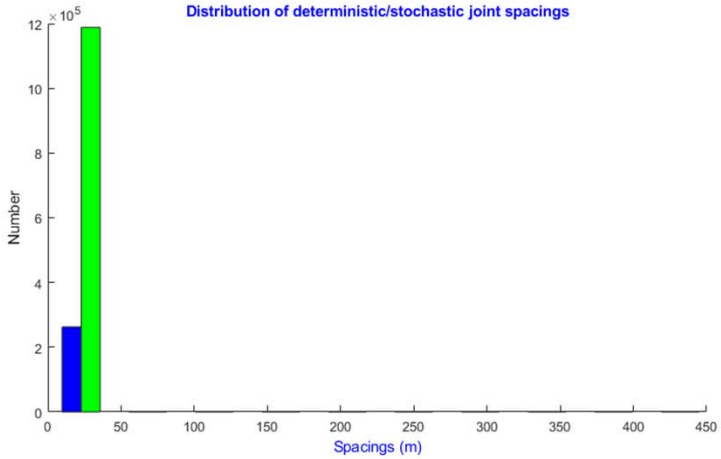

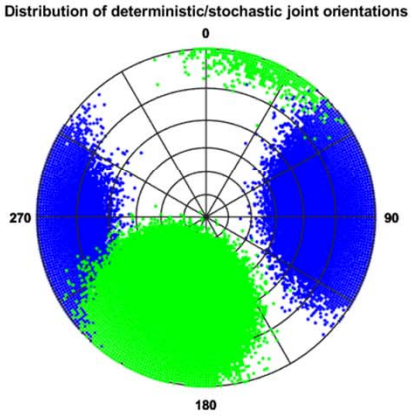

Stereonet Plot of Dip Vectors

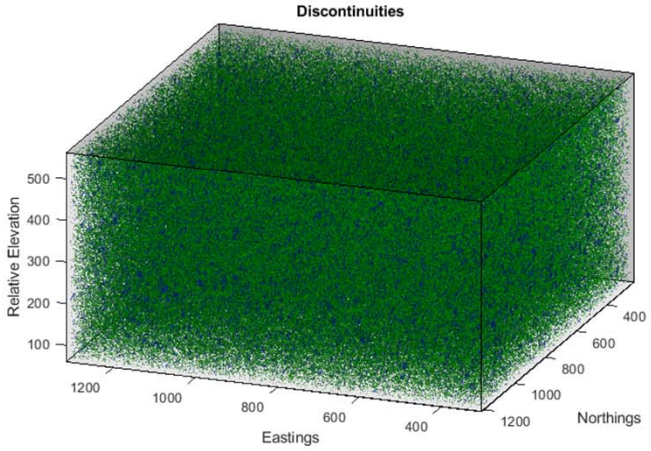

SIROMODEL
Modeler View

DFN Open Pit
Partial Pit Model

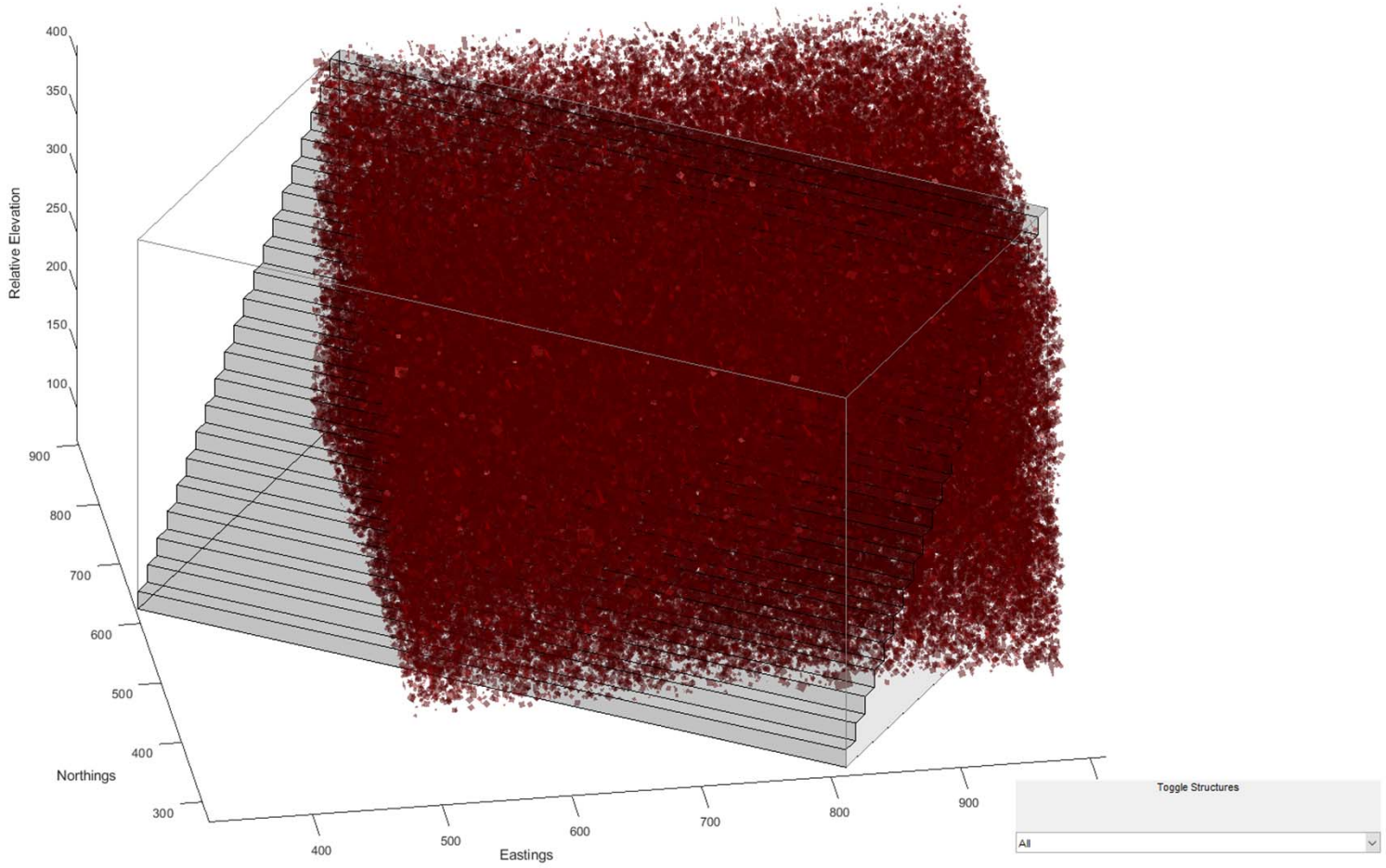

SIROMODEL
Structural Analysis
View

DFN Open Pit
Partial Pit Model

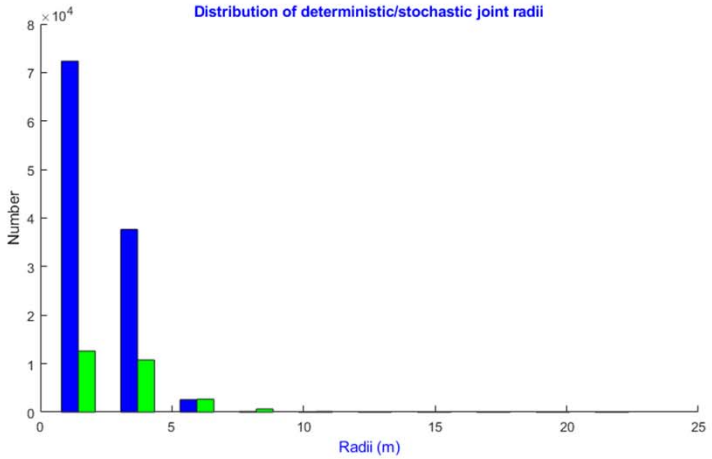

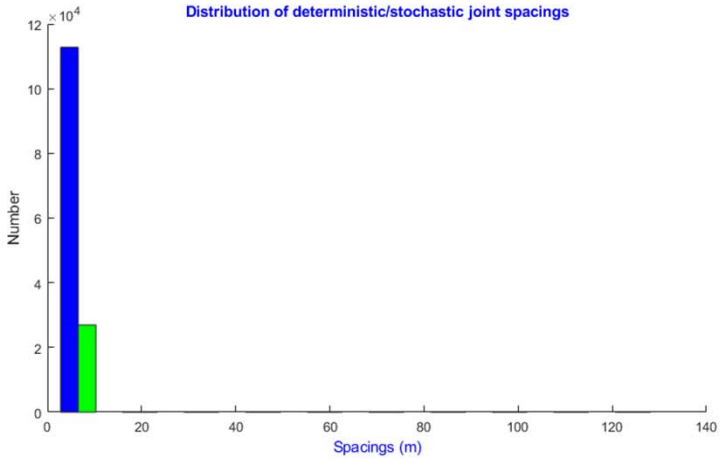

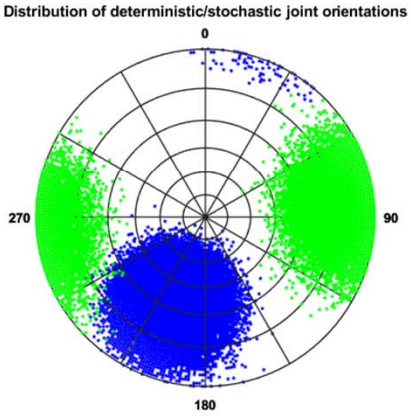

Stereonet Plot of Dip Vectors

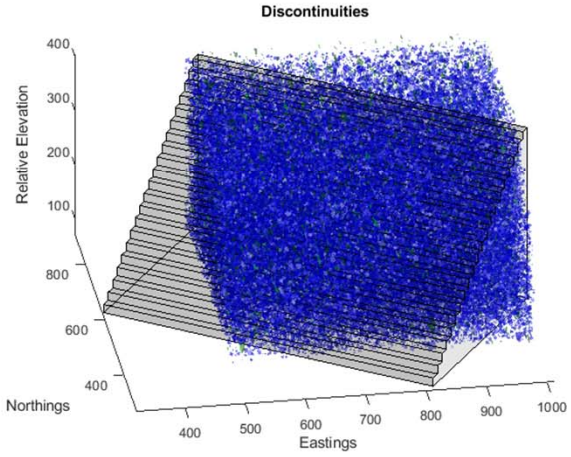

SIROMODEL
Block Visualiser

DFN Open Pit
Partial Pit Model

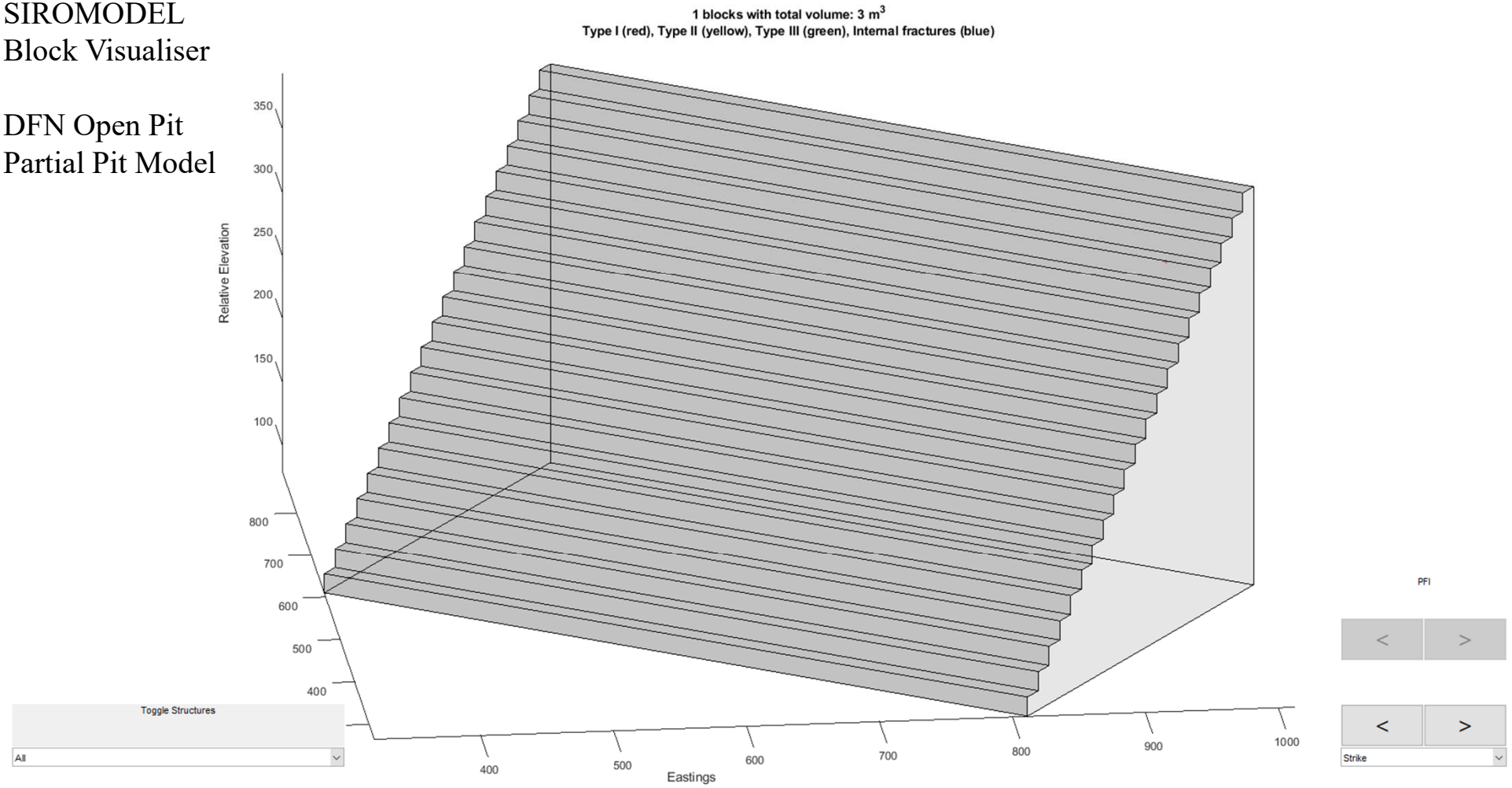

SIROMODEL
Structural Analysis
View

DFN Open Pit
Partial Pit Model
Scale Factor =3

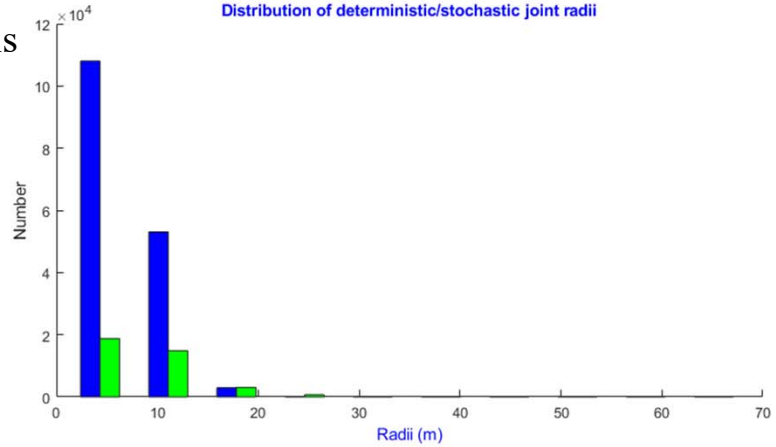

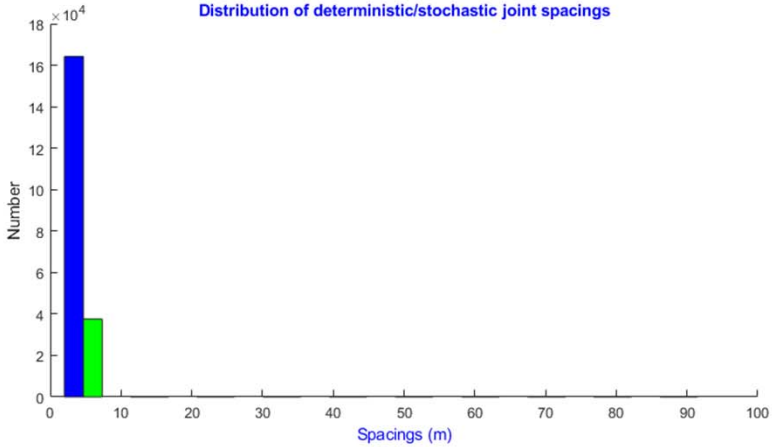

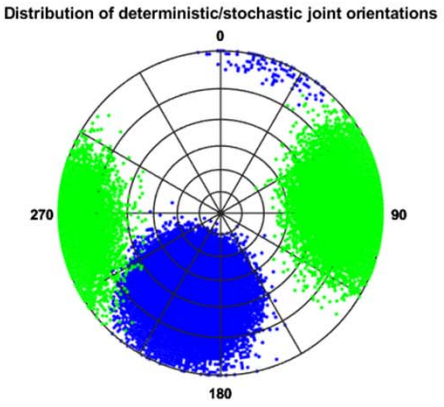

Stereonet Plot of Dip Vectors

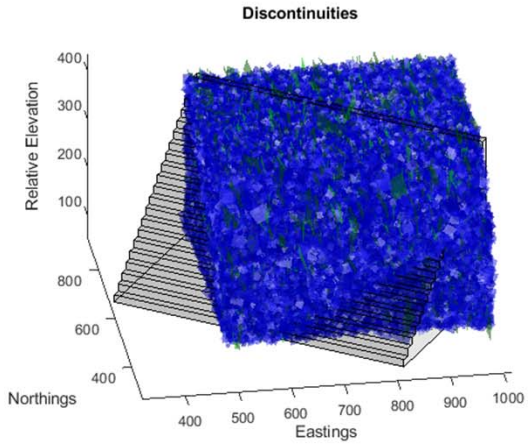

SIROMODEL
Block Visualiser

DFN Open Pit
Partial Pit Model
Scale Factor = 3

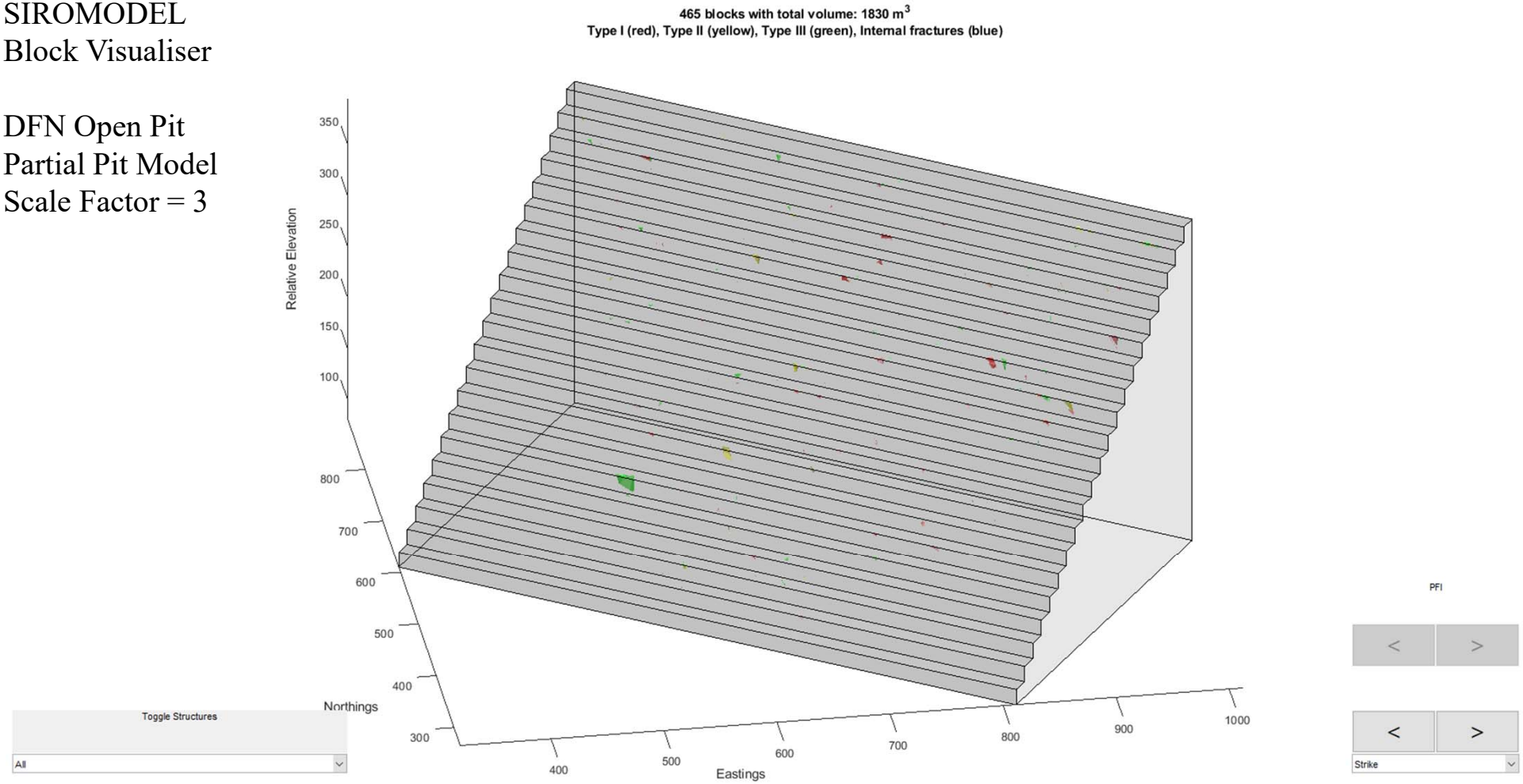

SIROMODEL
Modeler View

DFN Open Pit
10 Bench Pit Model

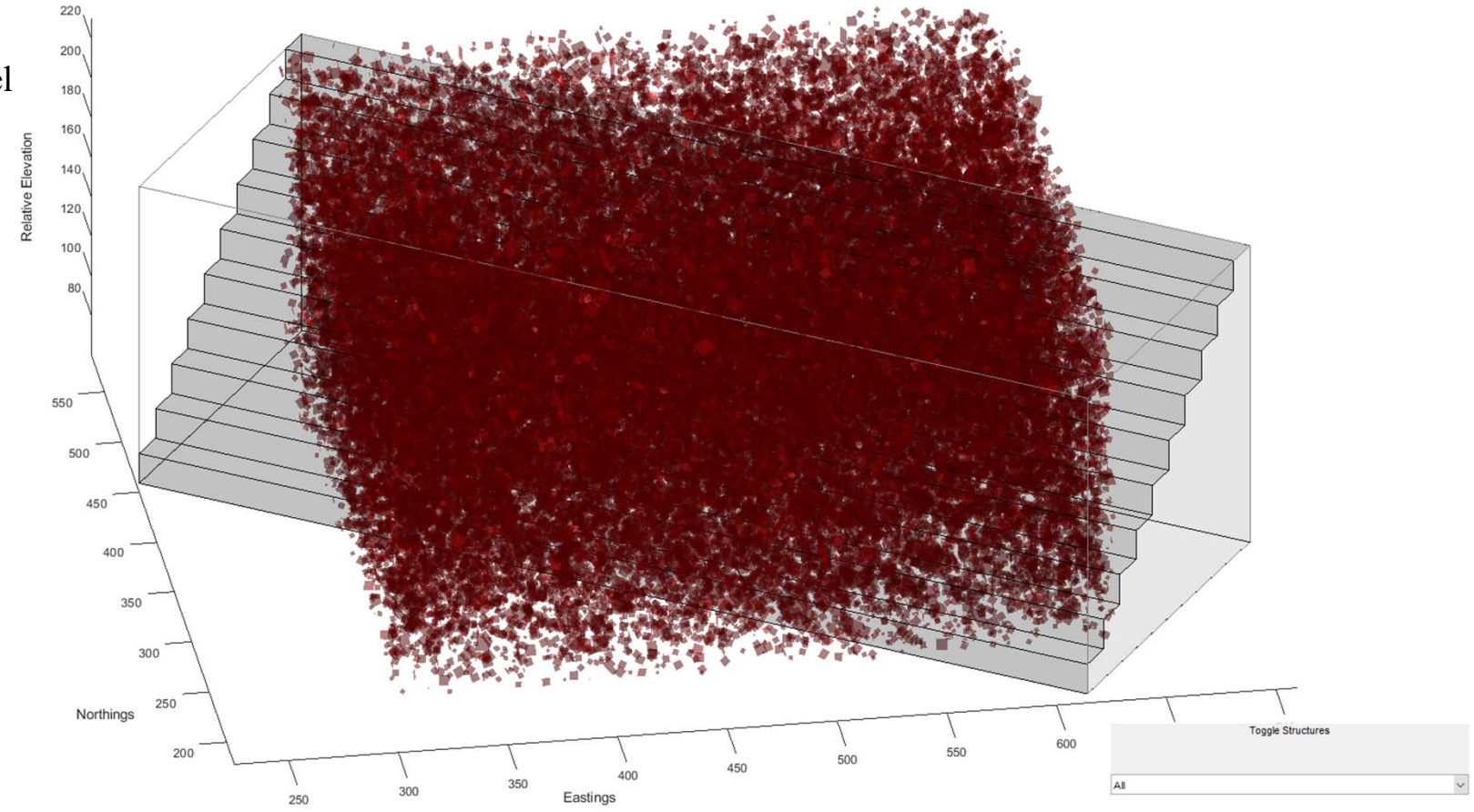

SIROMODEL
Structural Analysis
View

DFN Open Pit
10 Bench Pit
Model

Scale Factor =3

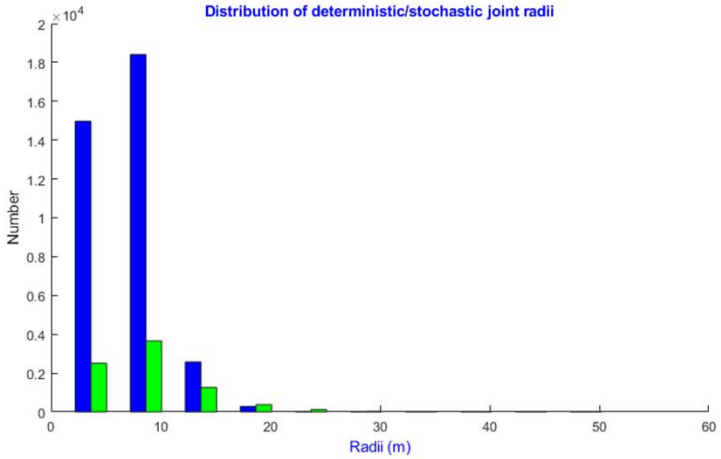

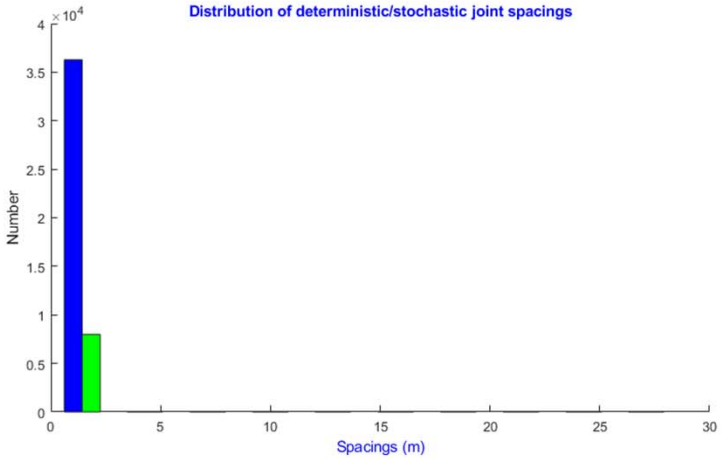

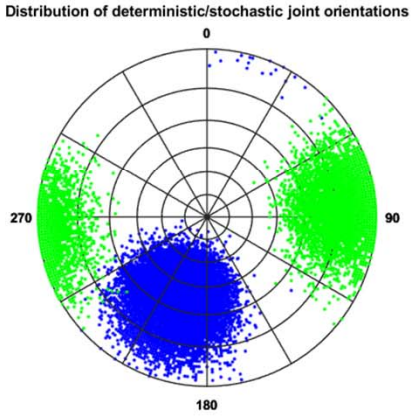

Stereonet Plot of Dip Vectors

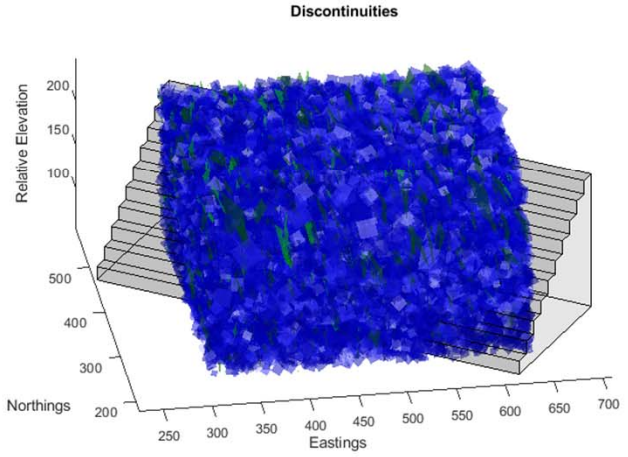

SIROMODEL
Block Visualiser

DFN Open Pit
10 Bench Pit
Model

Scale Factor =3

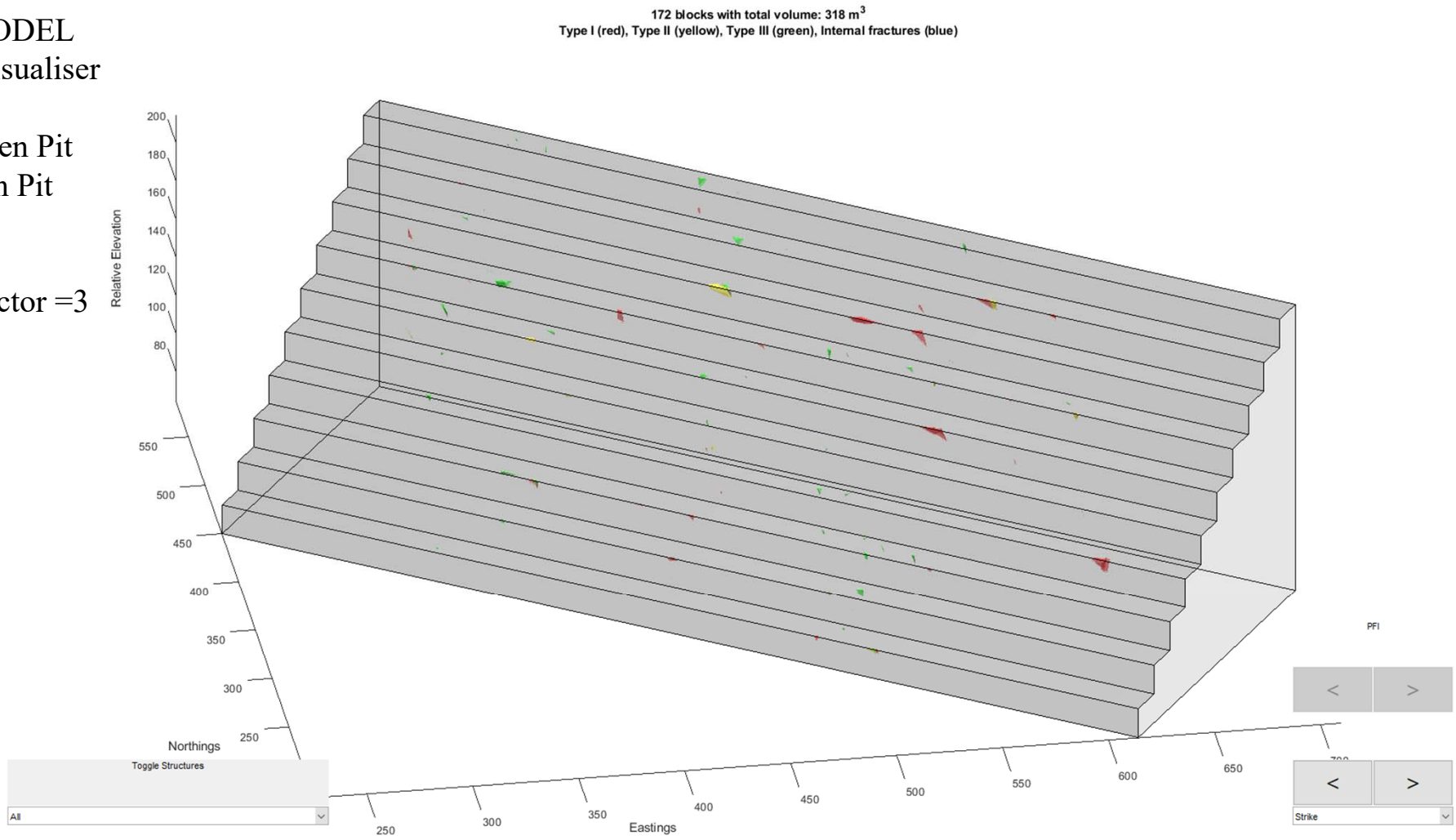

SIROMODEL
Modeler View

DFN Open Pit
90 x 90 x 90 metre model

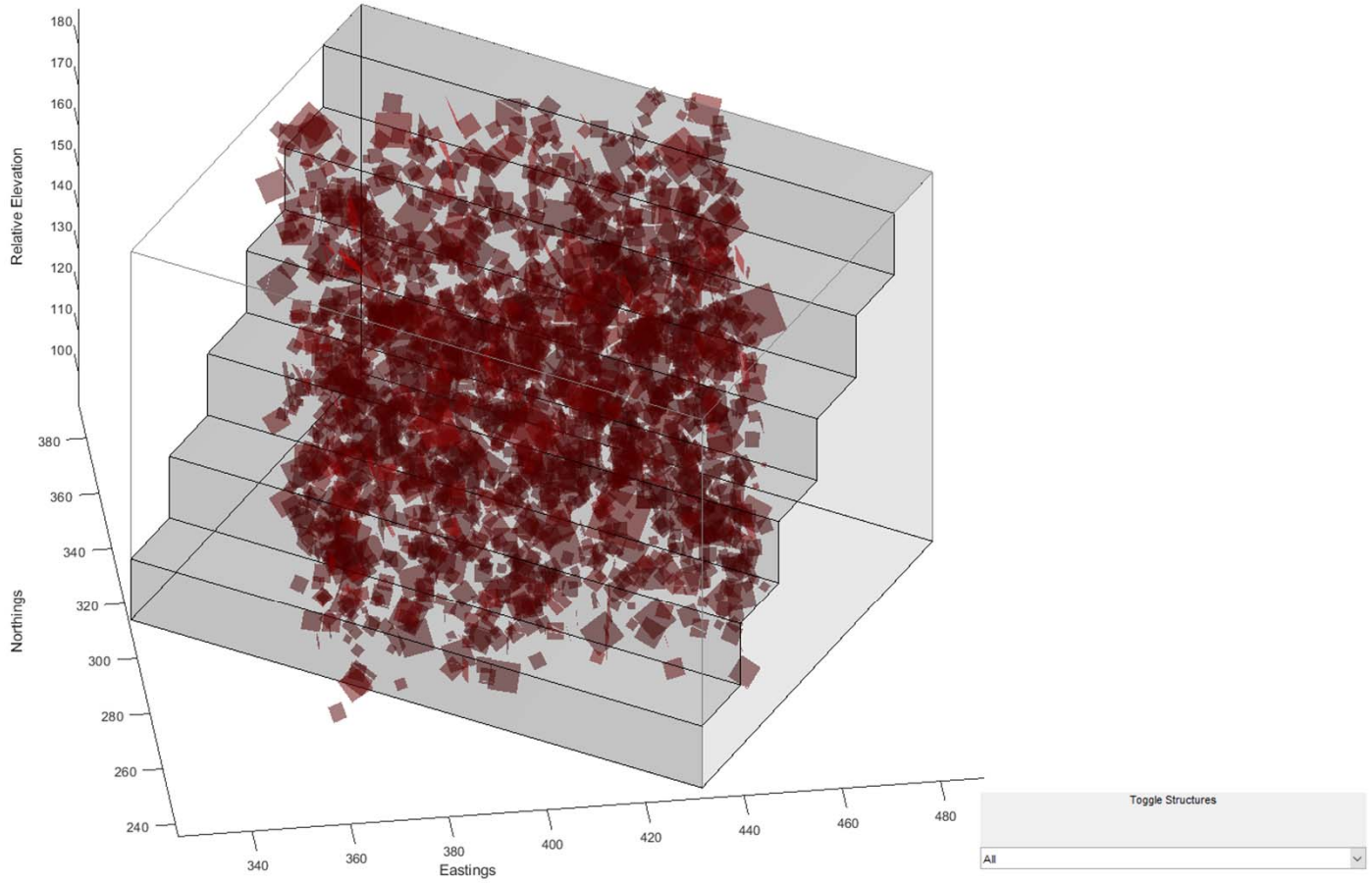

SIROMODEL
Structural Analysis
View

DFN Open Pit
90 x 90 x 90 metre
model

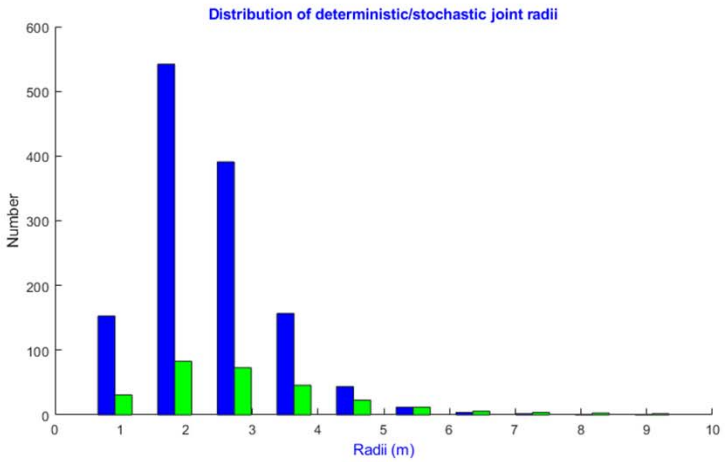

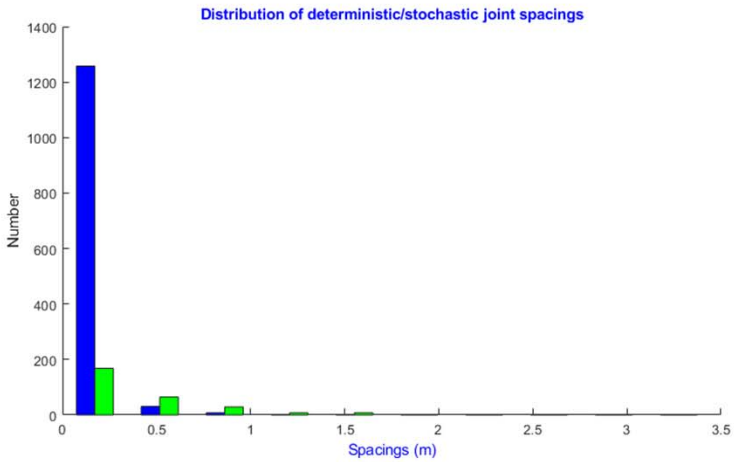

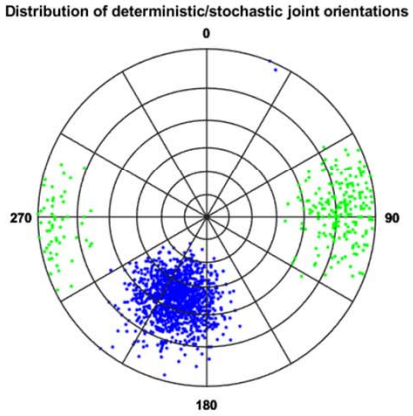

Stereonet Plot of Dip Vectors

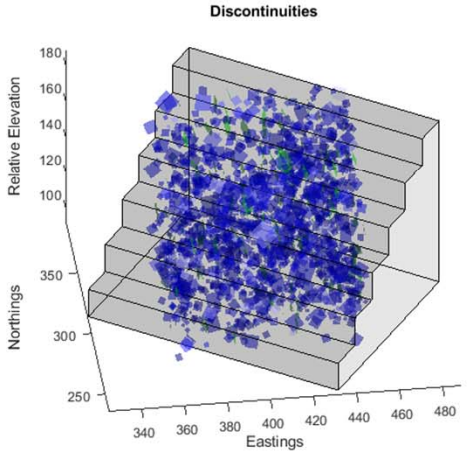

SIROMODEL
Block Visualiser

DFN Open Pit
90 x 90 x 90 metre model

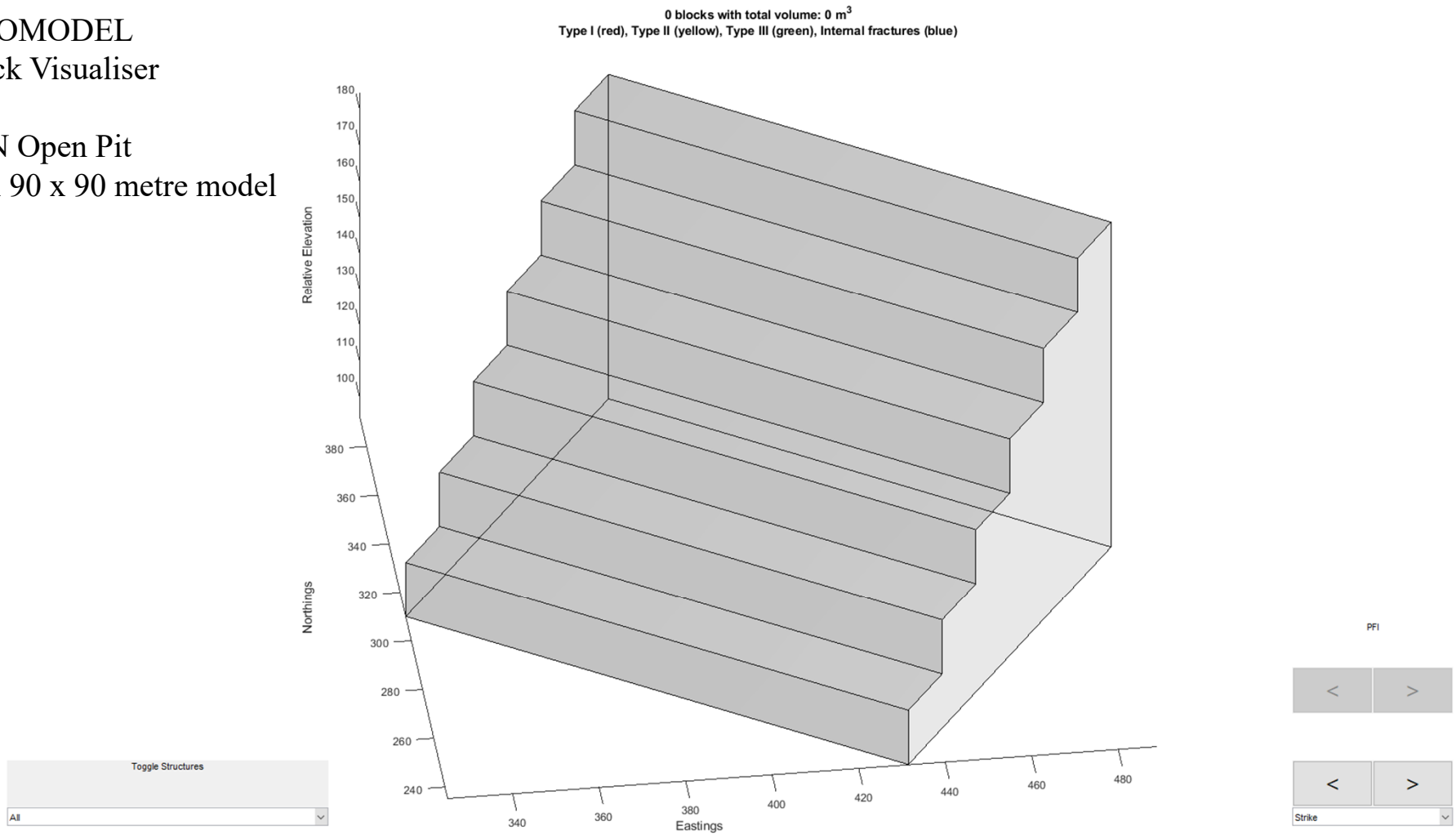

SIROMODEL
Structural Analysis
View

DFN Open Pit
90 x 90 x 90 metre
model

Scale Factor = 6

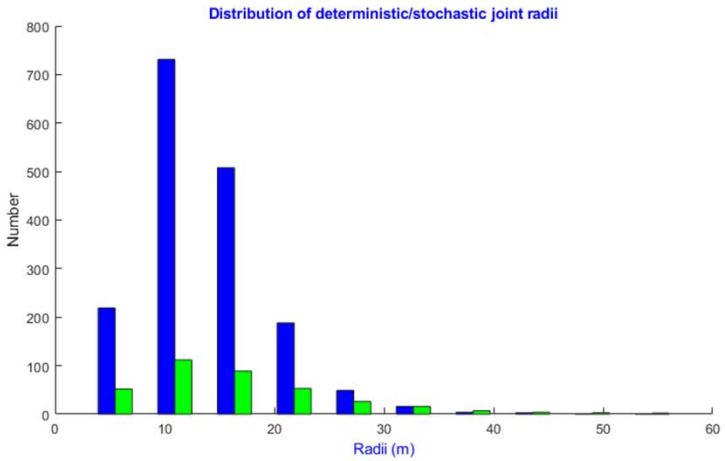

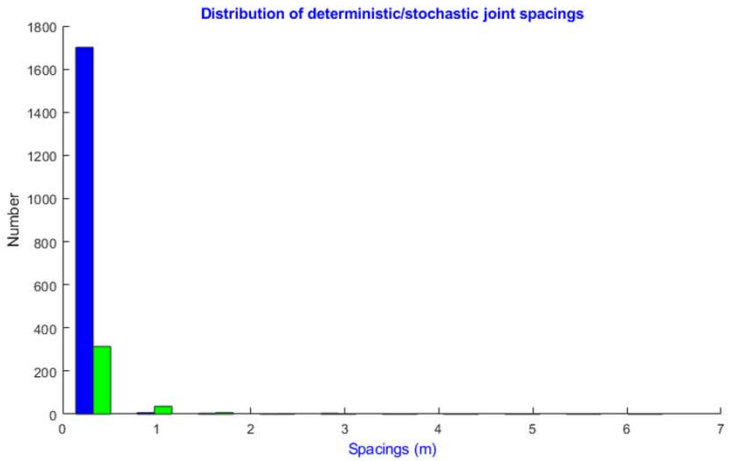

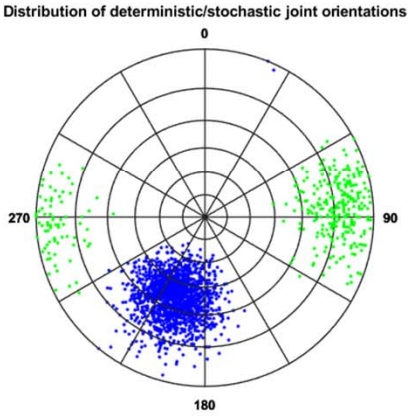

Stereonet Plot of Dip Vectors

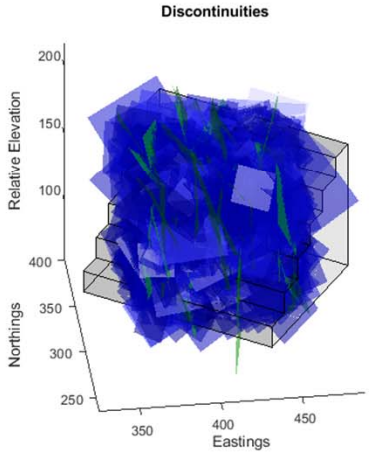

SIROMODEL
Block Visualiser

DFN Open Pit
90 x 90 x 90 metre model

Scale Factor = 6

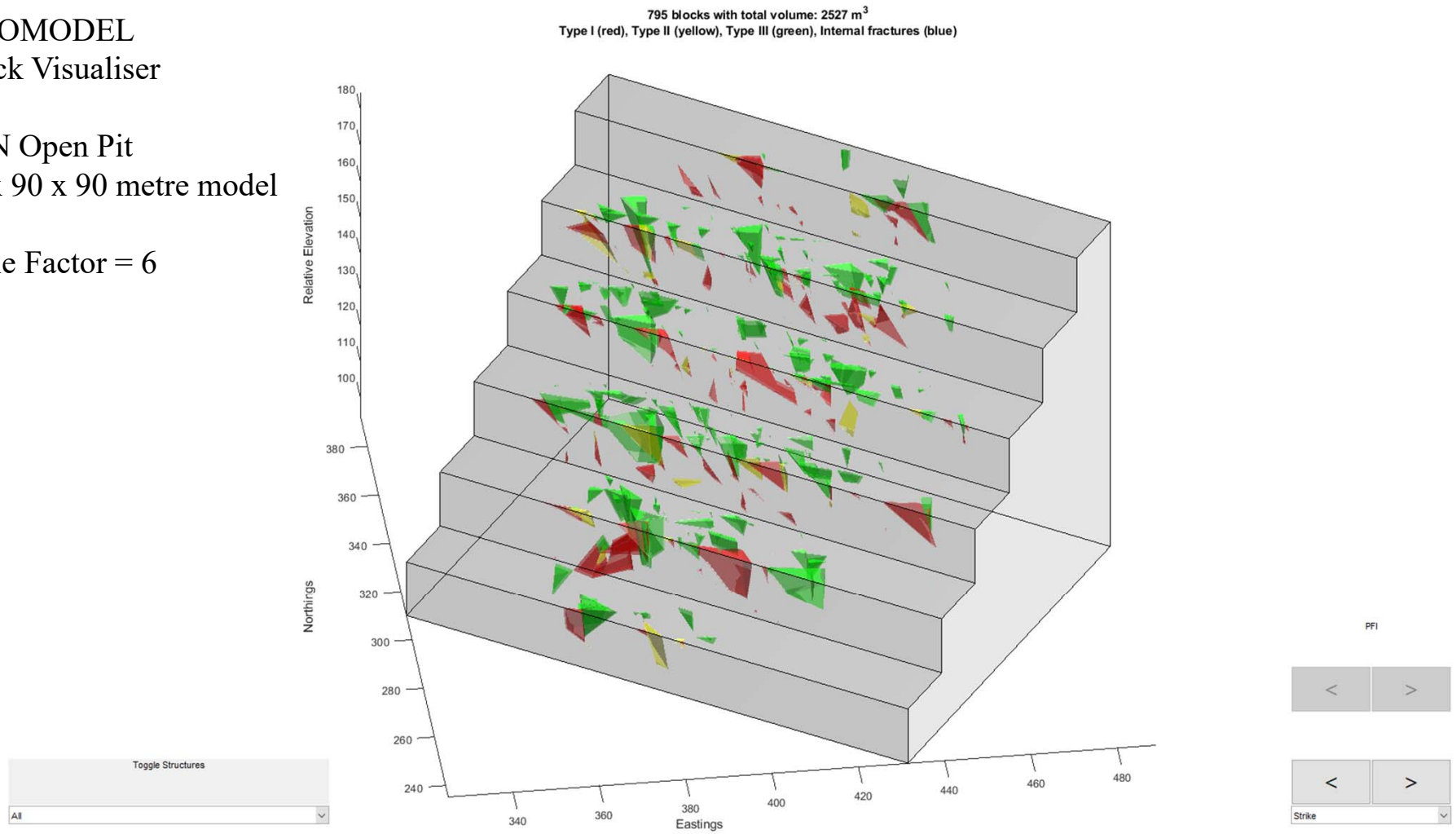

SIROMODEL
Modeler View

DFN Open Pit
4 bench model

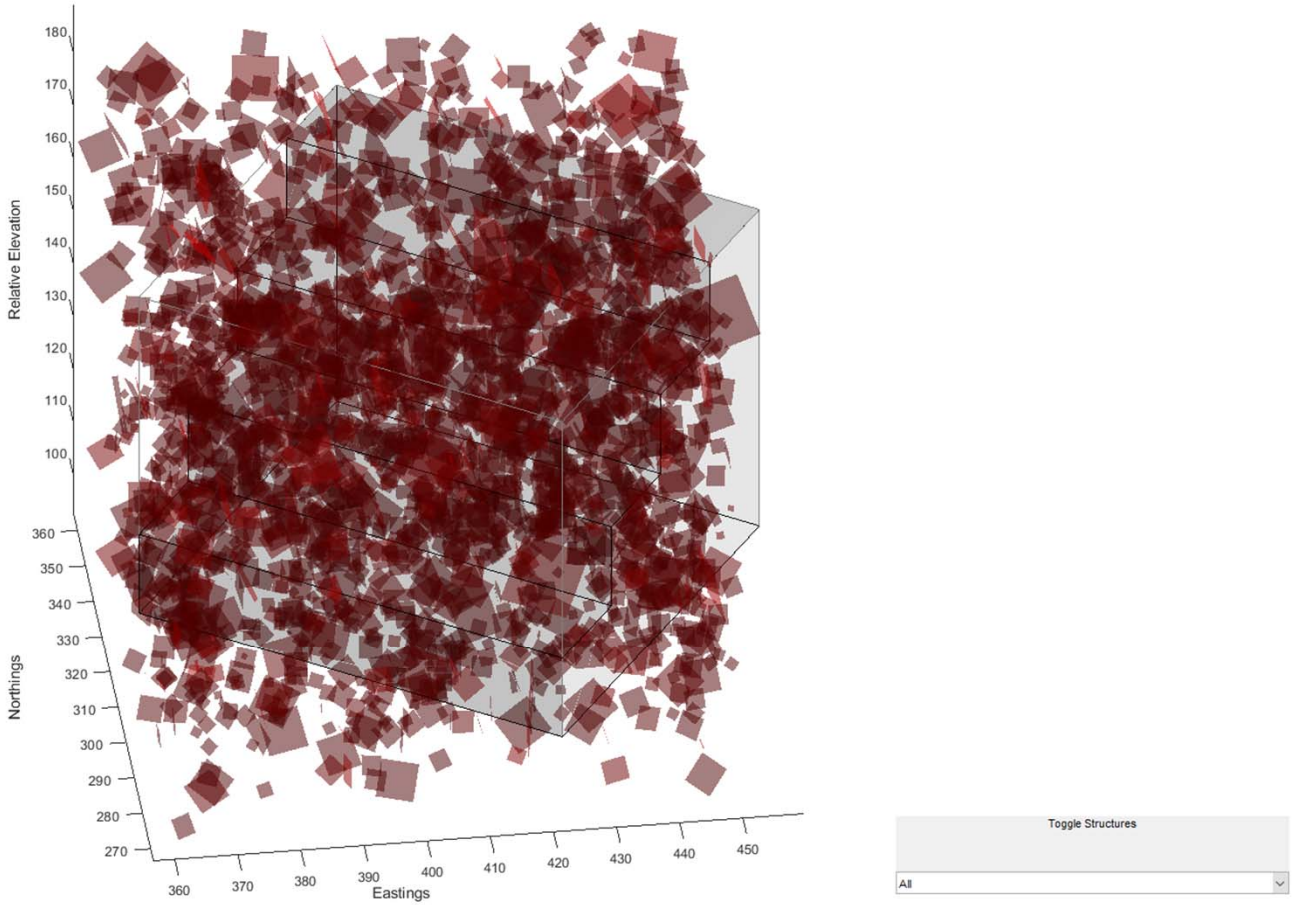

SIROMODEL
Structural Analysis
View

DFN Open Pit
4 bench model

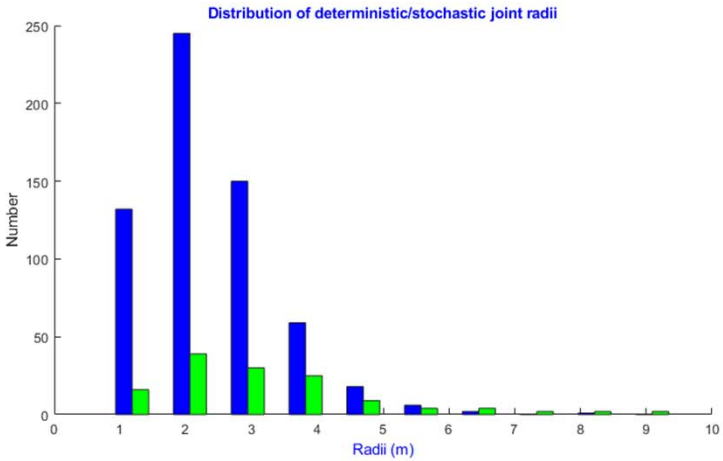

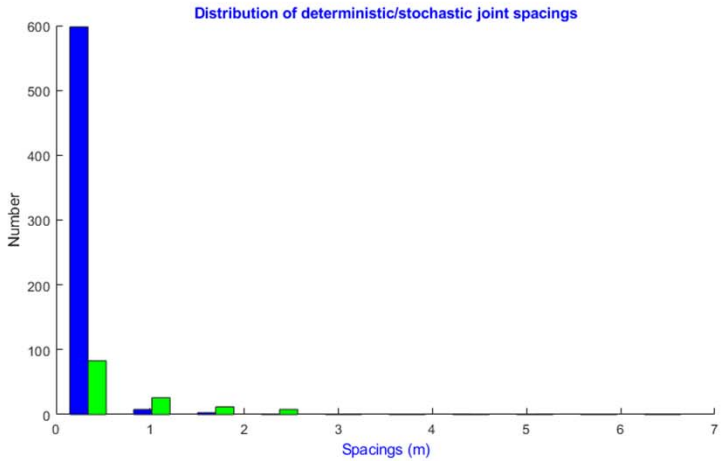

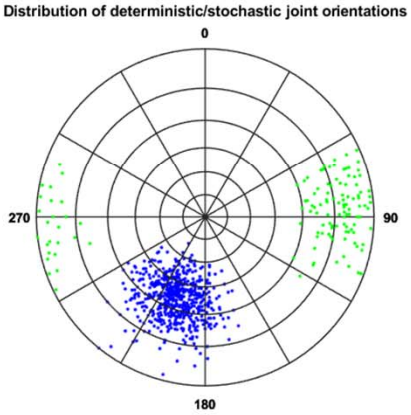

Stereonet Plot of Dip Vectors

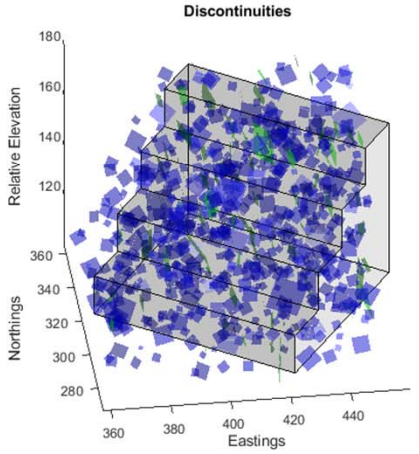

SIROMODEL
Block Visualiser

DFN Open Pit
4 bench model

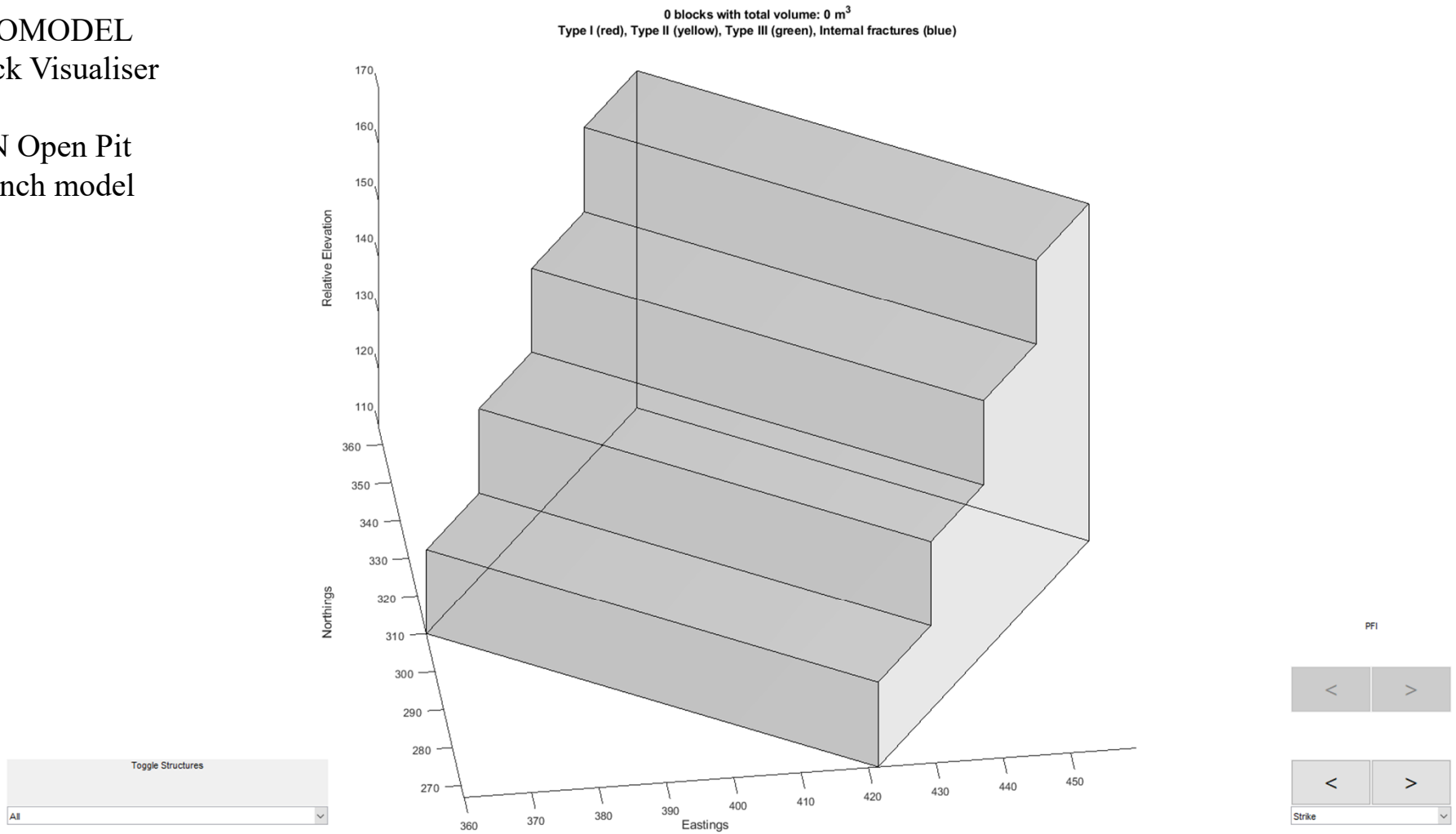

SIROMODEL
Structural Analysis
View

DFN Open Pit
4 bench model

Scale Factor = 5

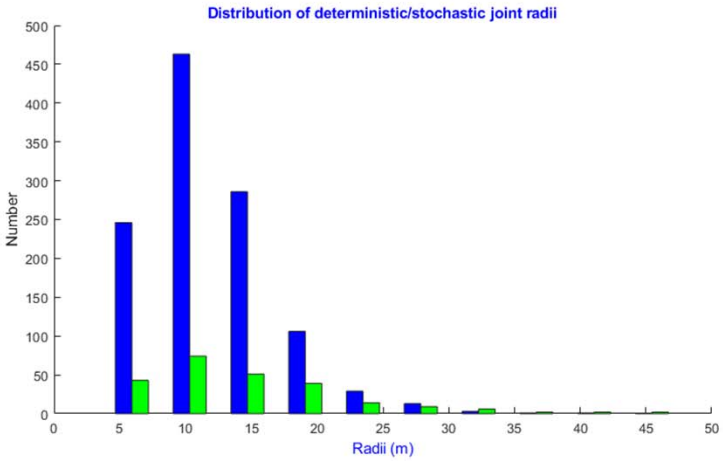

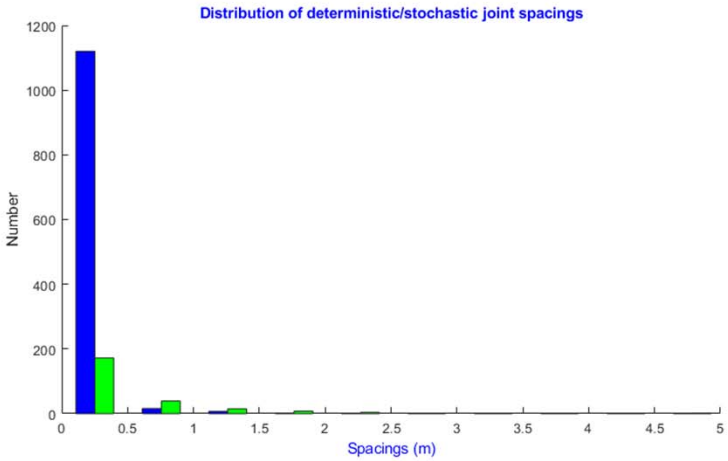

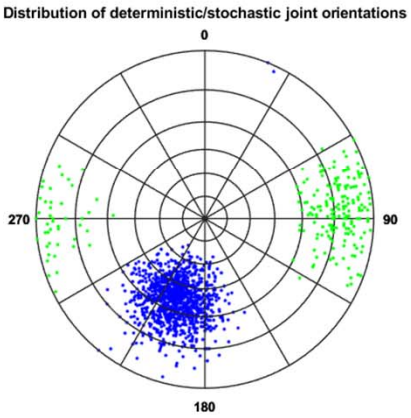

Stereonet Plot of Dip Vectors

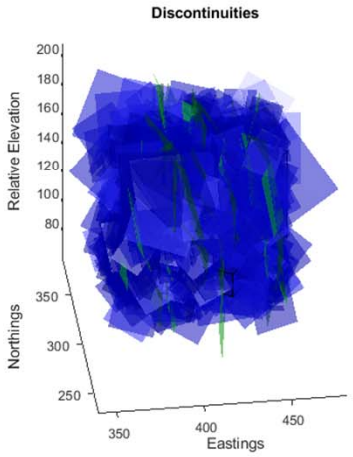

SIROMODEL
Block Visualiser

DFN Open Pit
4 bench model

Scale Factor = 5

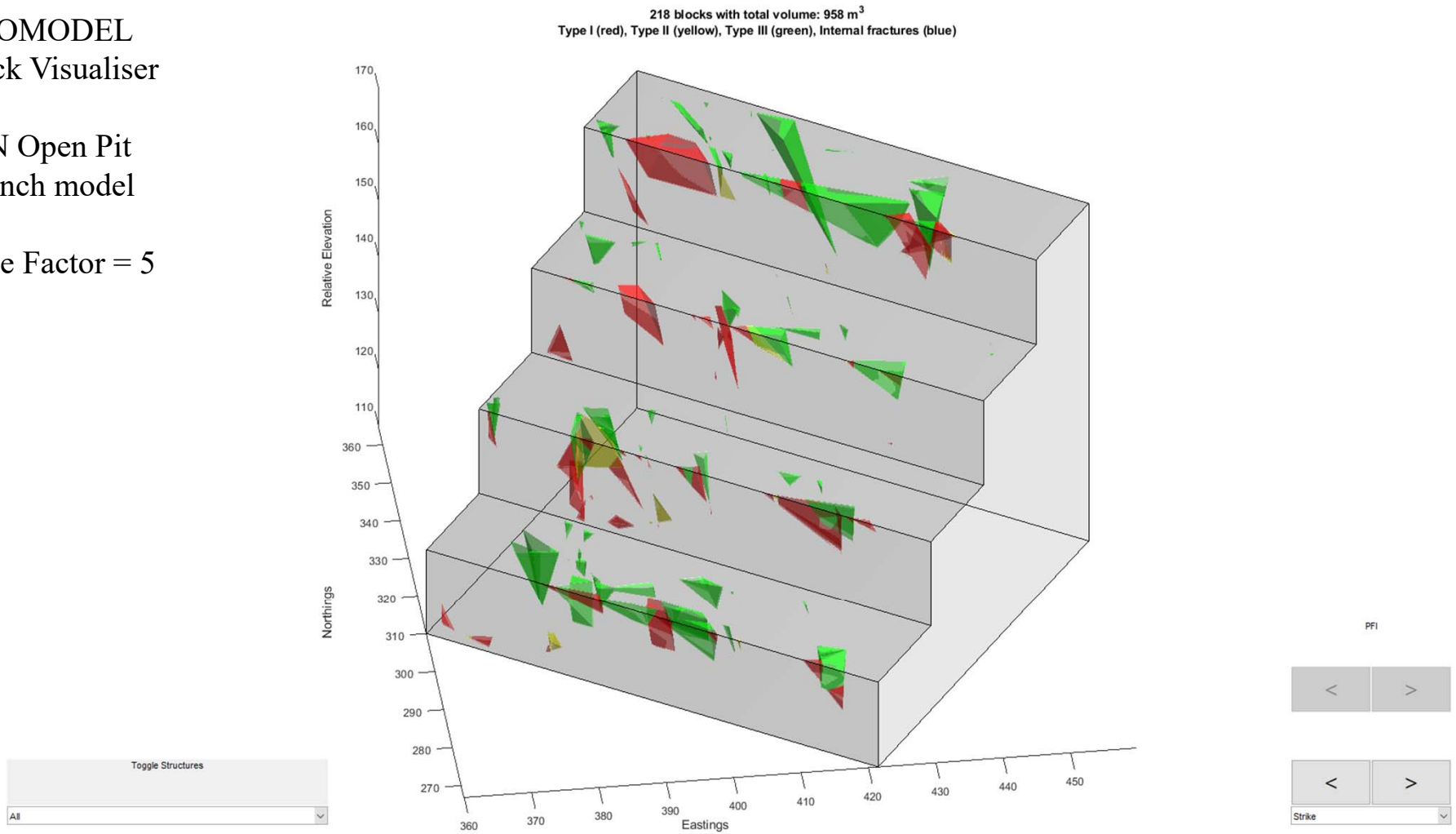

SIROMODEL
Block Visualiser

DFN Open Pit
4 bench model

Scale Factor = 5

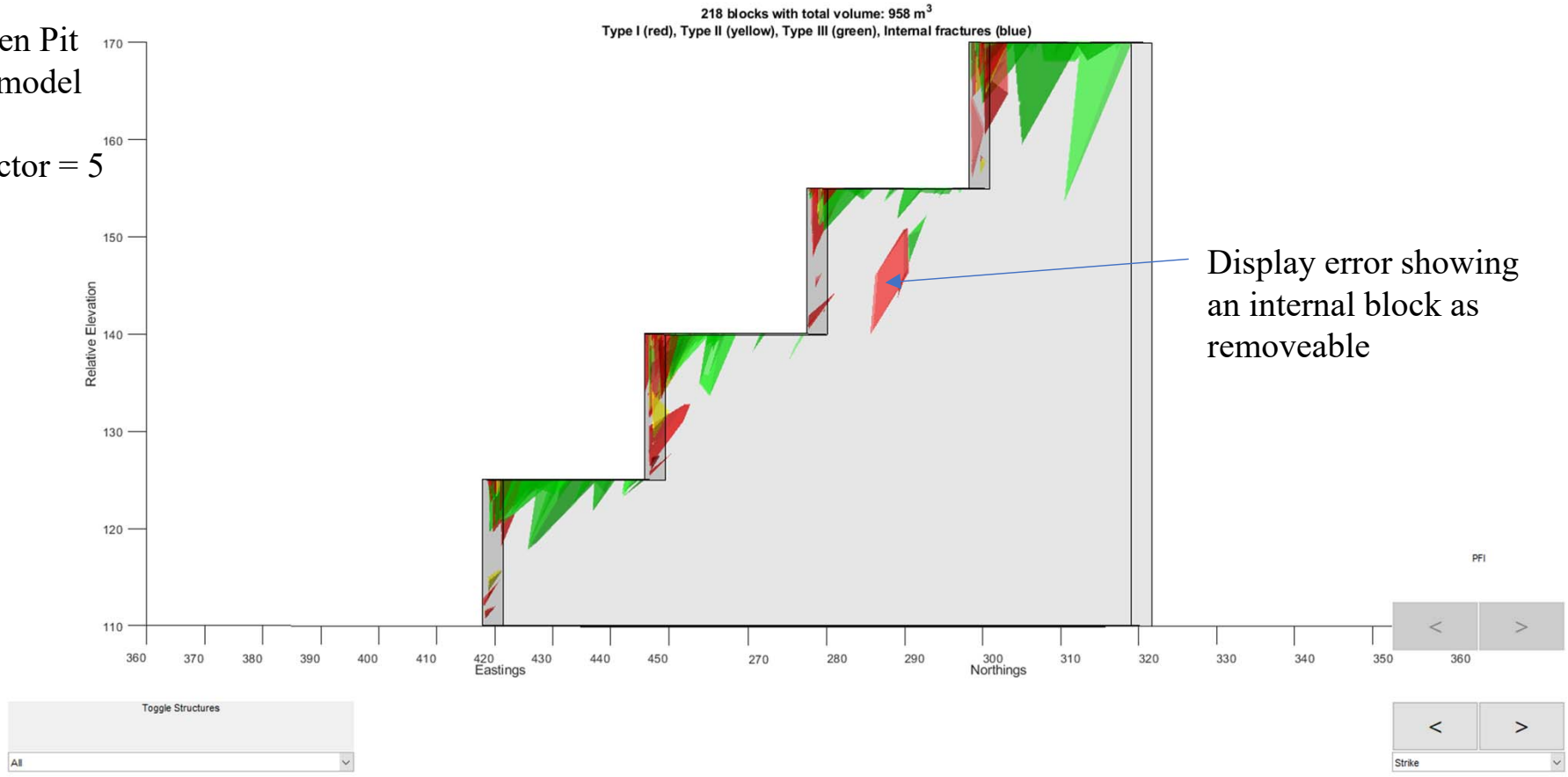

Display error showing an internal block as removeable

SIROMODEL
Block Visualiser

DFN Open Pit
Single bench model

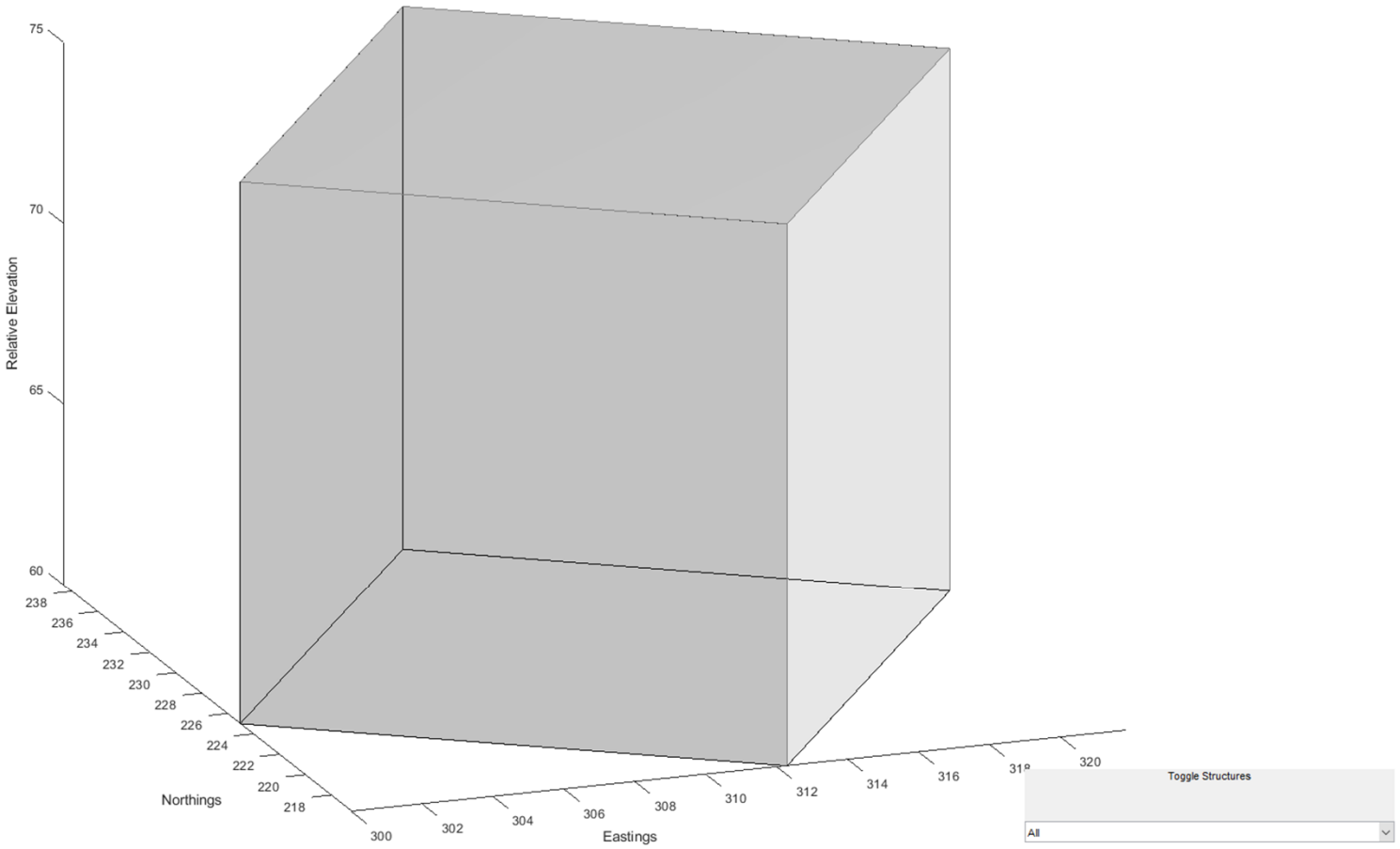

SIROMODEL
Structural Analysis
View

DFN Open Pit
Single Bench Model

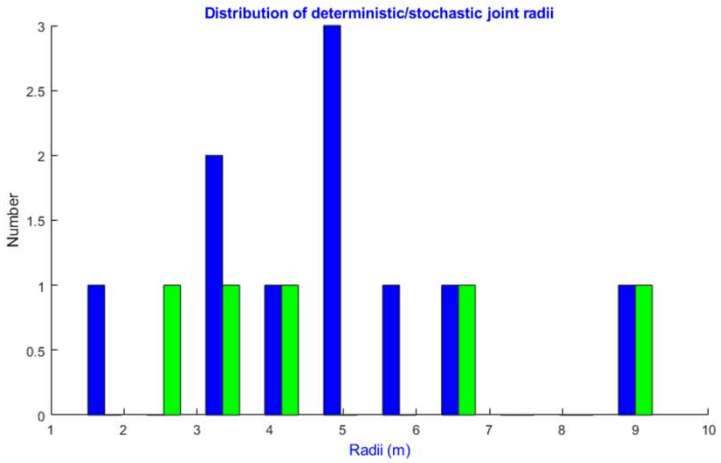

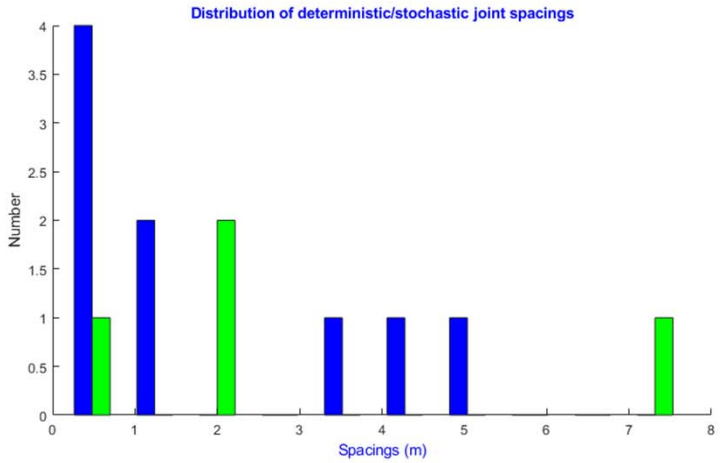

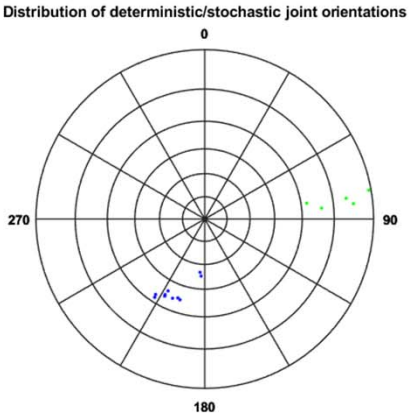

Stereonet Plot of Dip Vectors

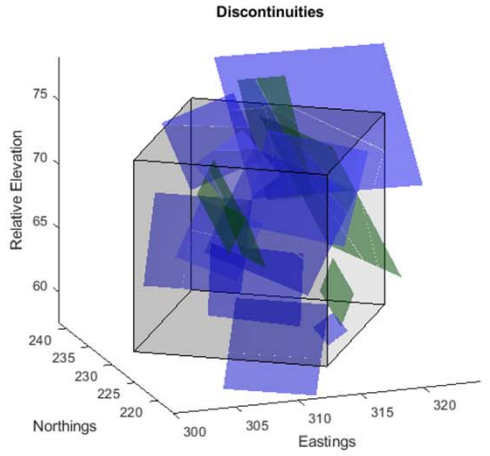

SIROMODEL
Block Visualiser

DFN Open Pit
Single Bench Model

Ran 1000 simulations, no blocks generated

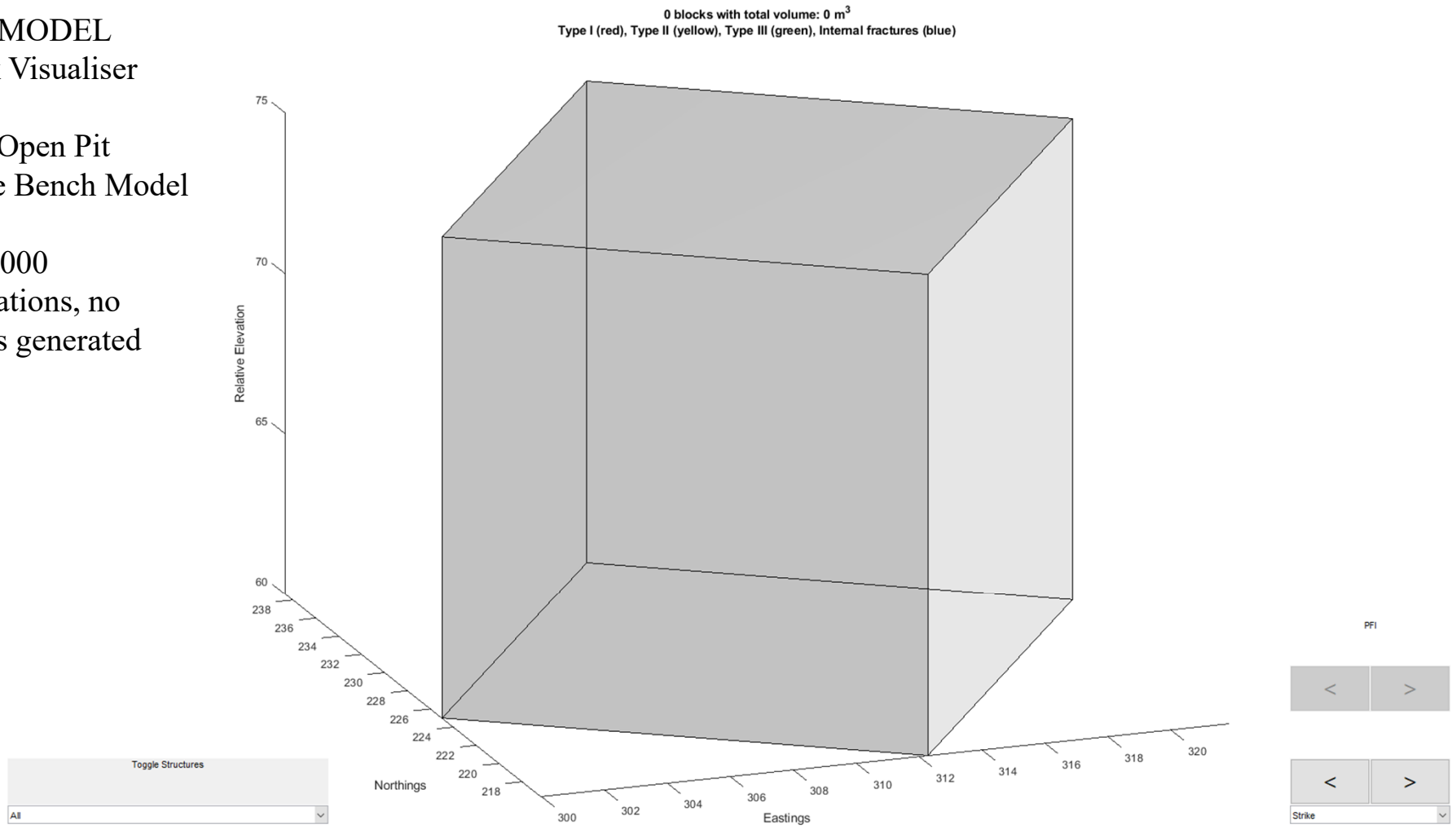

SIROMODEL
Block Visualiser

DFN Open Pit
Single Bench Model
150 m long bench

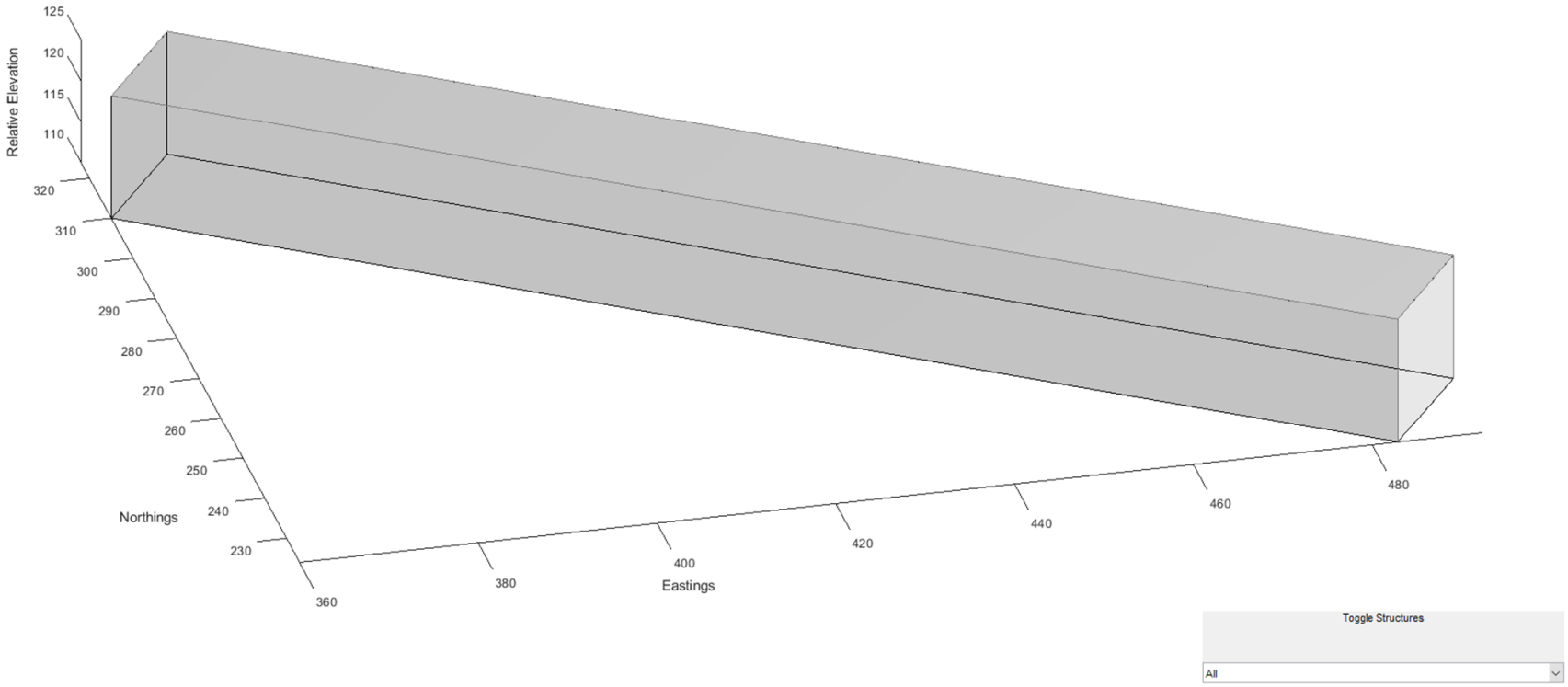

SIROMODEL
Structural Analysis
View

DFN Open Pit
Single Bench Model
150 m long bench

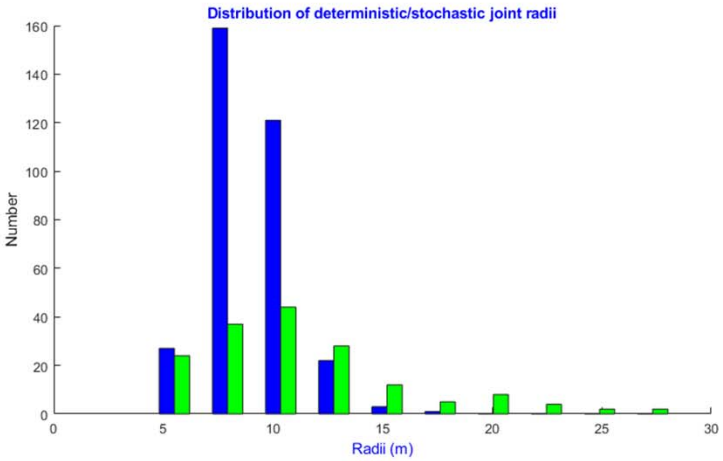

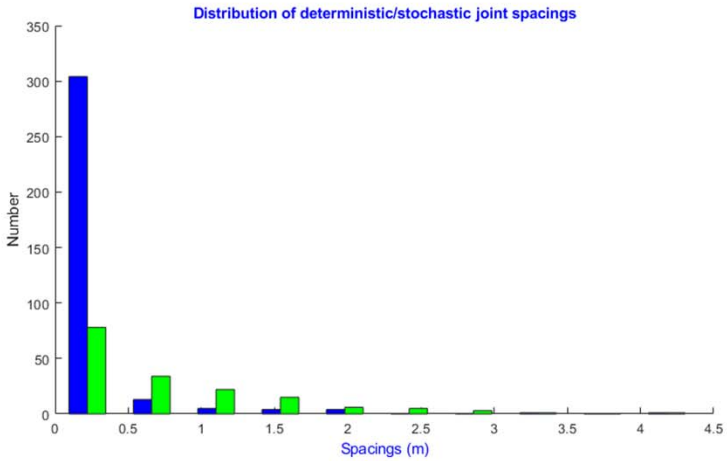

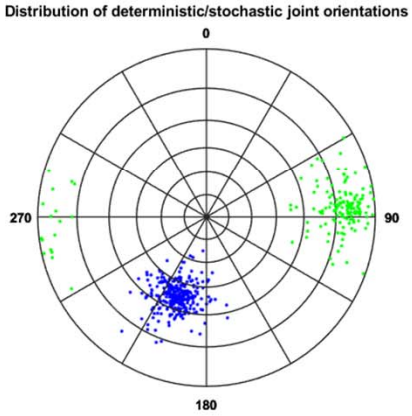

Stereonet Plot of Dip Vectors

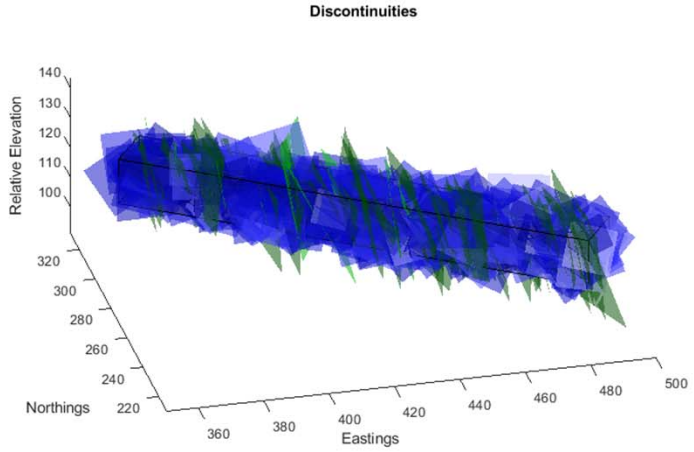

SIROMODEL
Block Visualiser

DFN Open Pit
Single Bench Model
150 m long bench

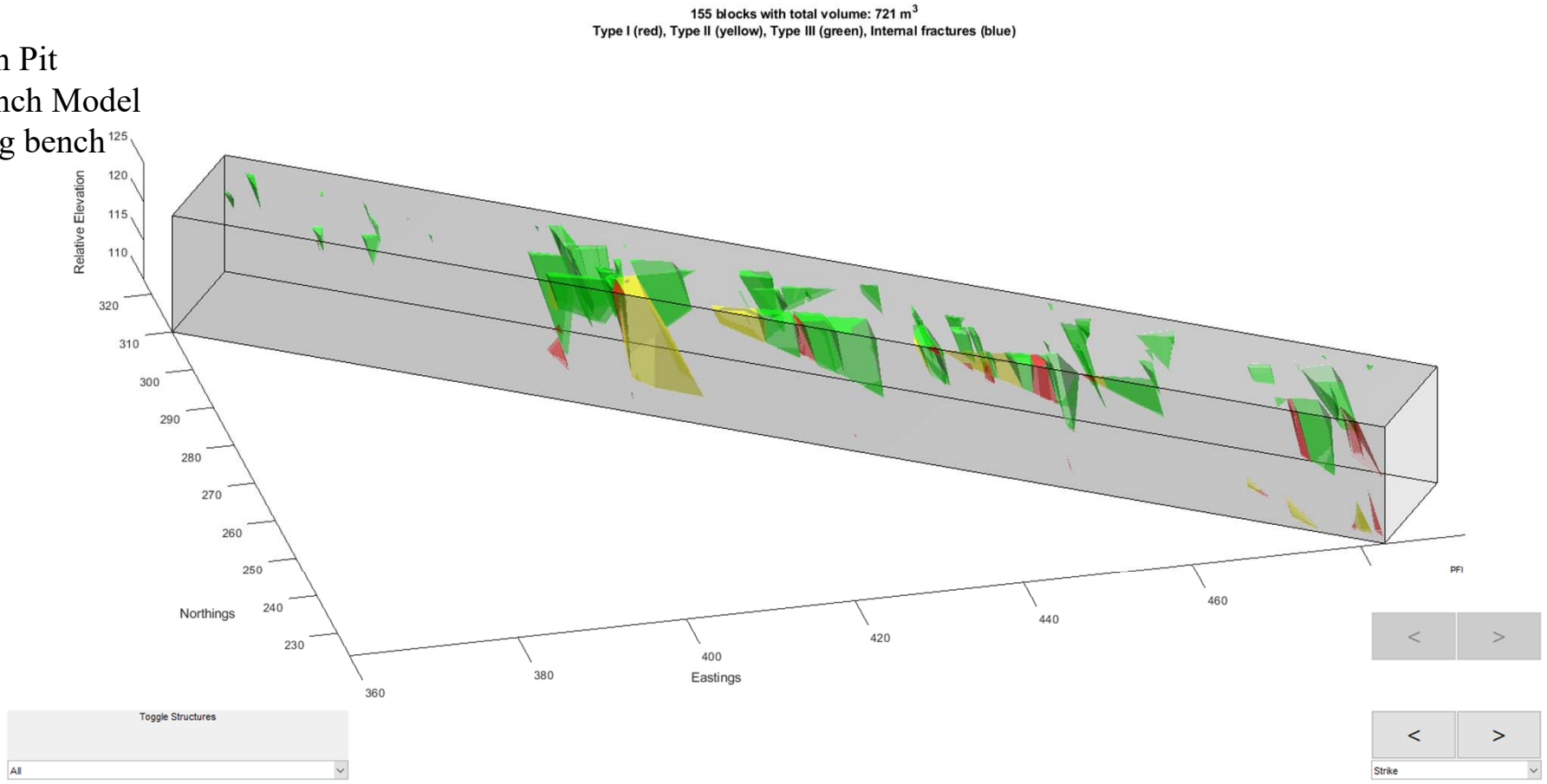

SIROMODEL
Back Break
Analysis

DFN Open Pit
Single Bench Model
150 m long bench

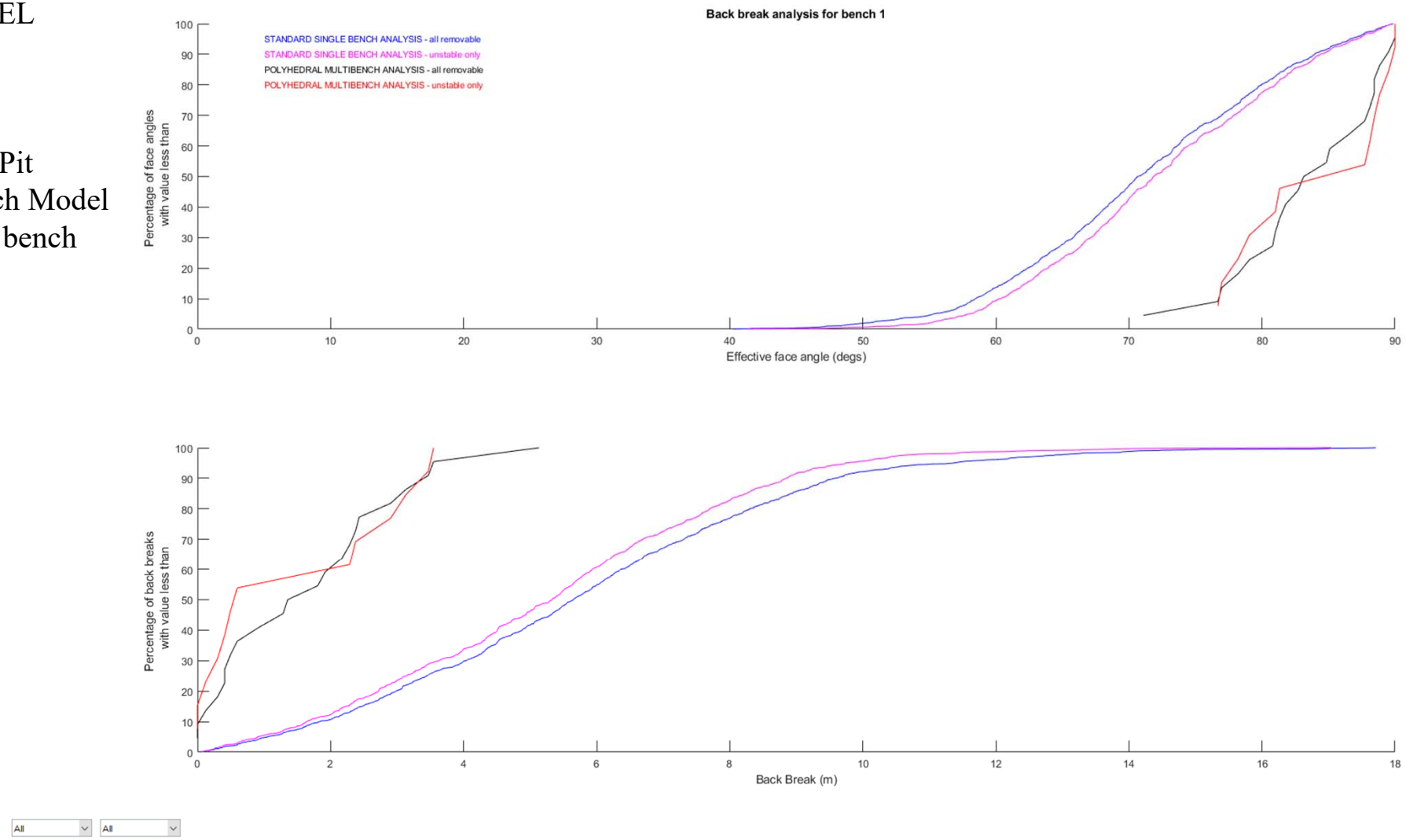

SIROMODEL
Block Visualiser

DFN Open Pit
Single Bench Model
450 m long bench

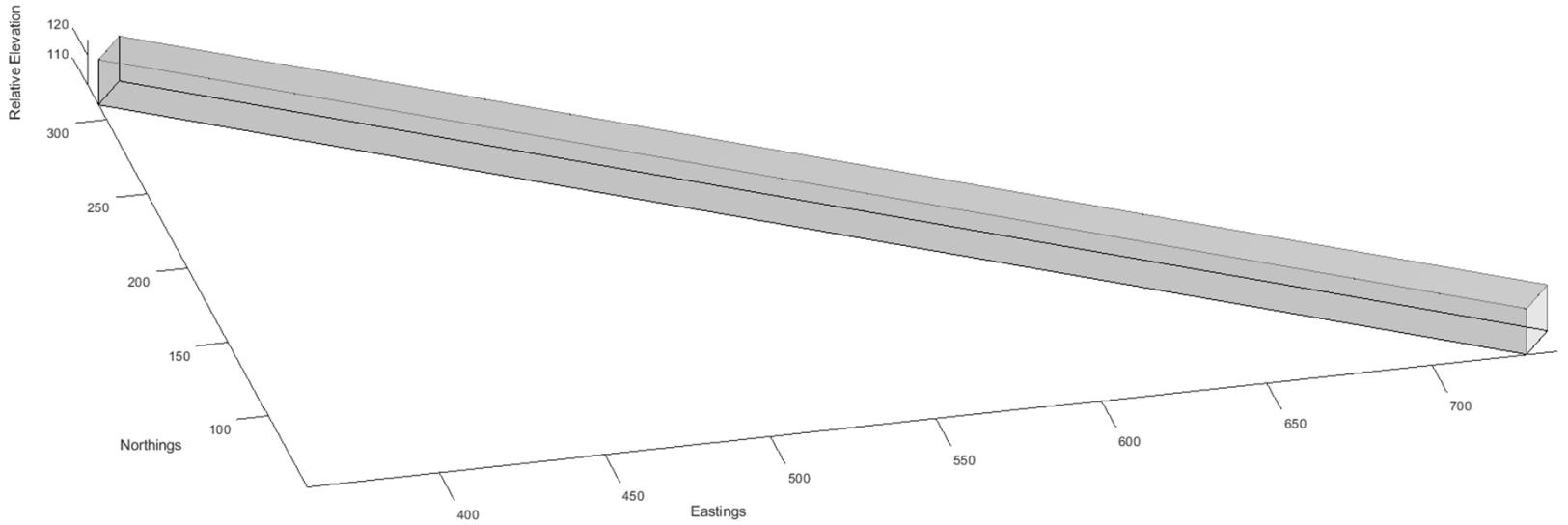

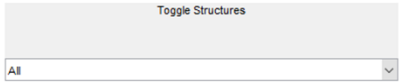

SIROMODEL
Structural Analysis
View

DFN Open Pit
Single Bench Model
450 m long bench

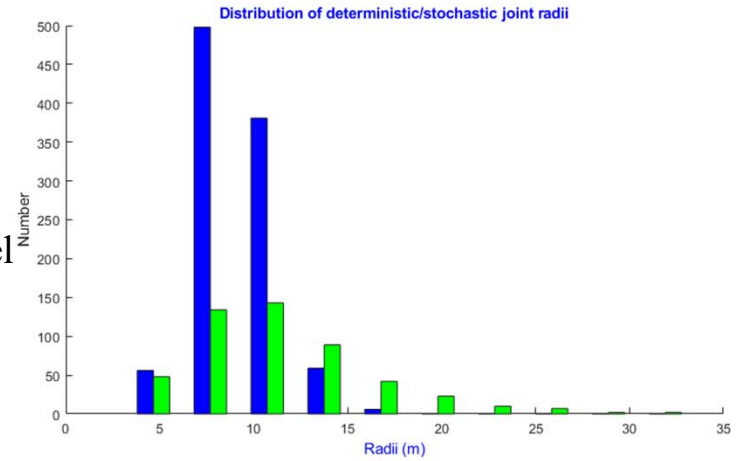

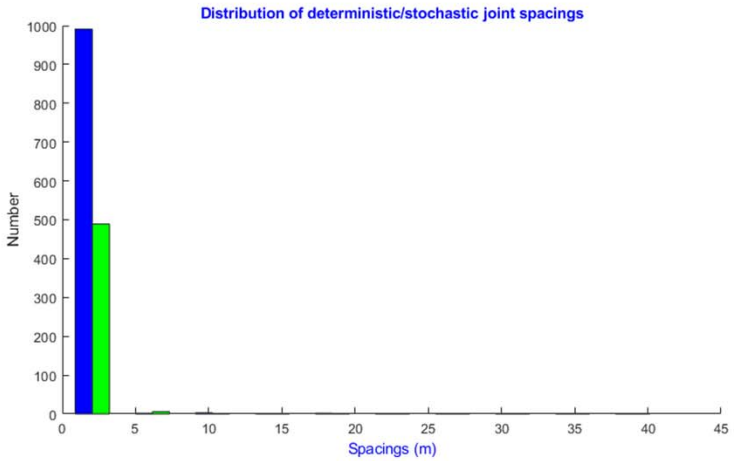

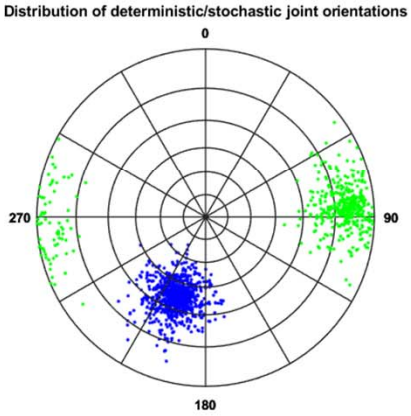

Stereonet Plot of Dip Vectors

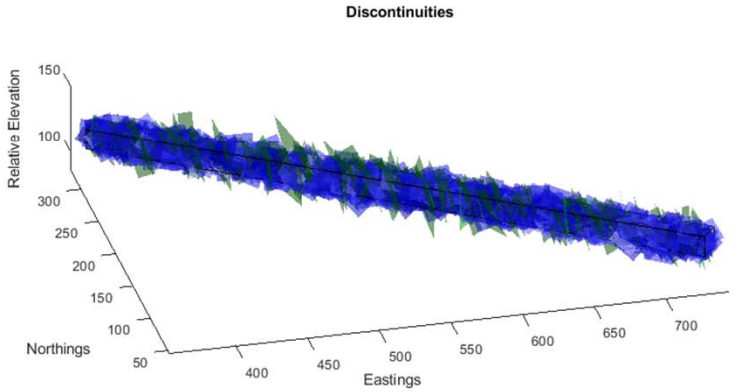

SIROMODEL
Block Visualiser

DFN Open Pit
Single Bench Model
450 m long bench

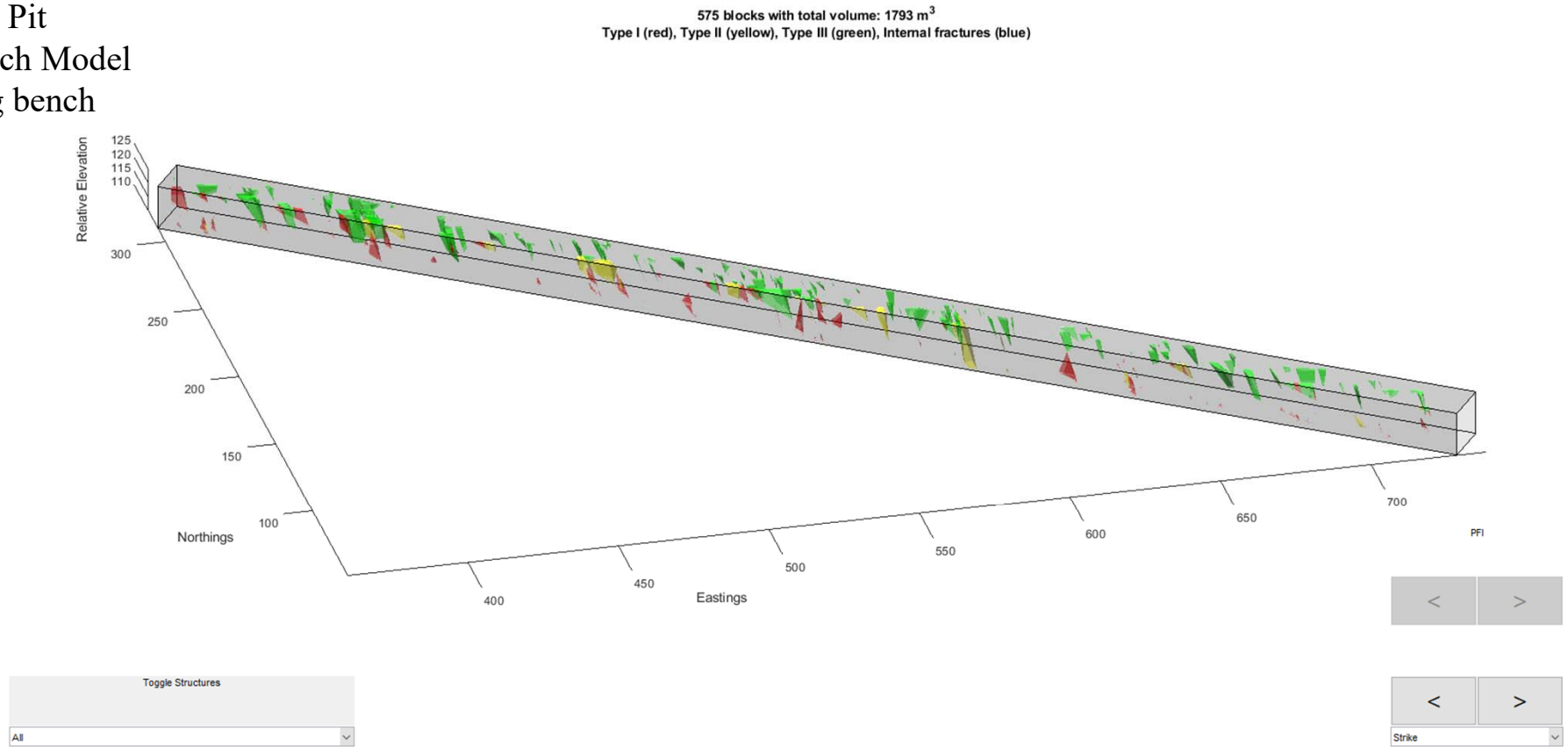

SIROMODEL
Back Break
Analysis

DFN Open Pit
Single Bench Model
450 m long bench

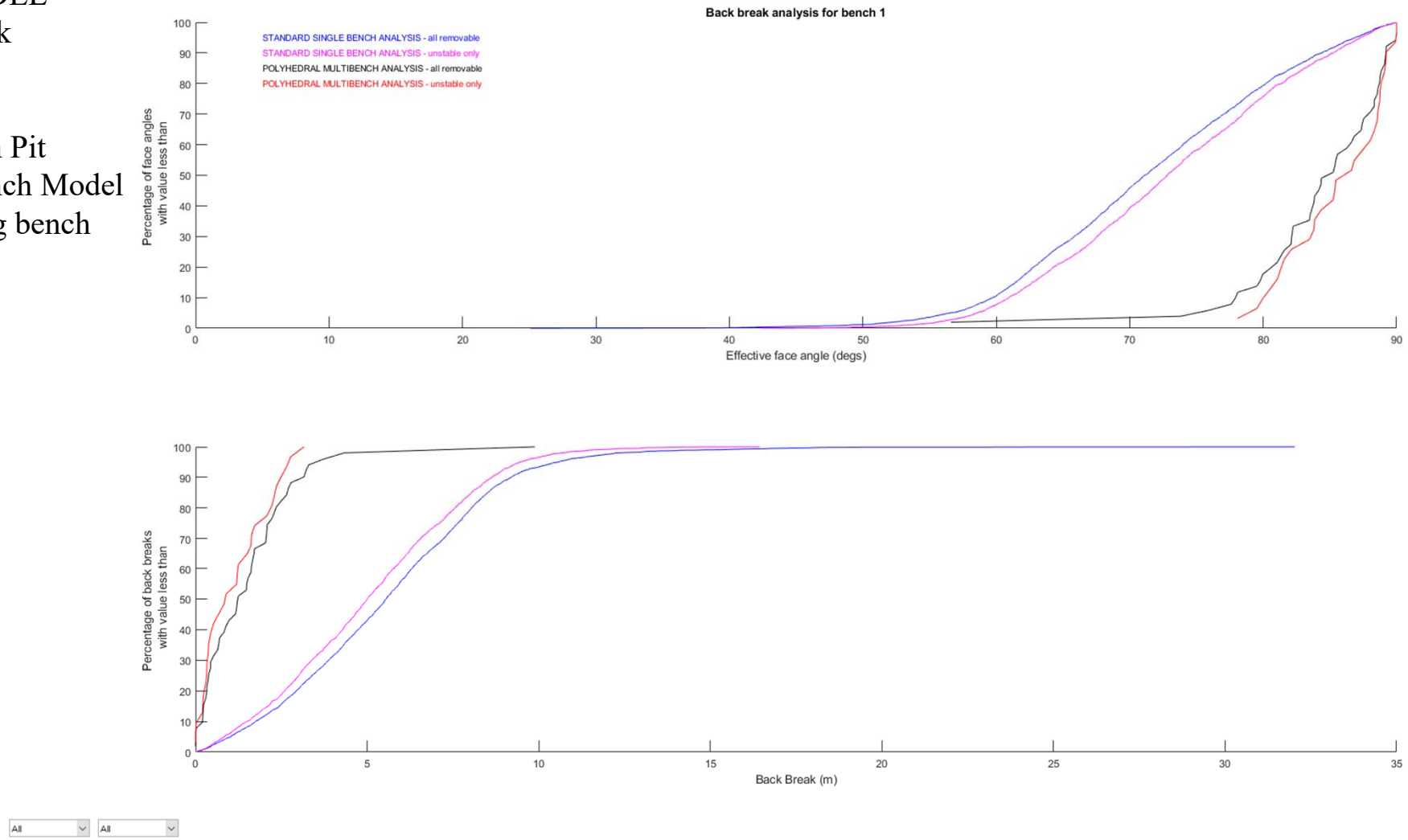

SIROMODEL
Block Visualiser

DFN Open Pit
Single Bench Model
1200 m long bench

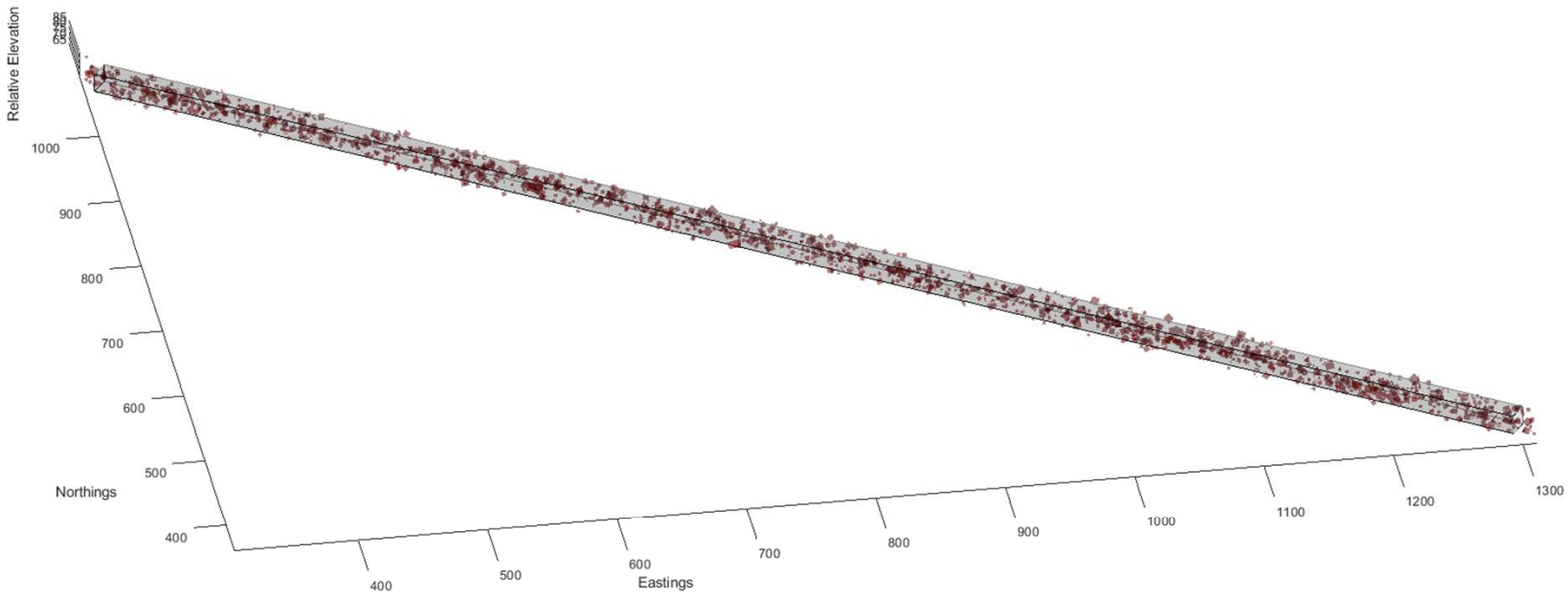

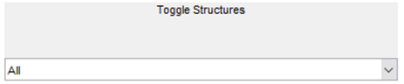

SIROMODEL
Structural Analysis
View

DFN Open Pit
Single Bench Model
1200 m long bench

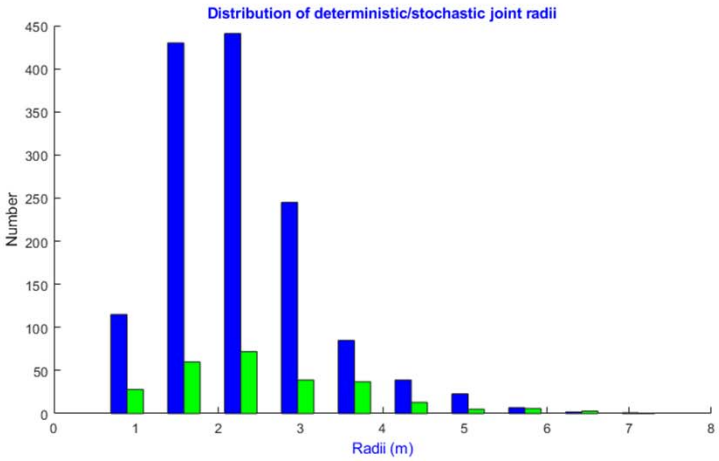

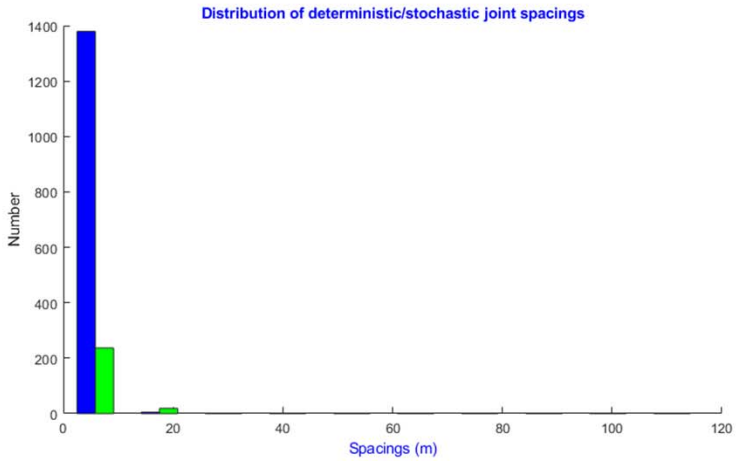

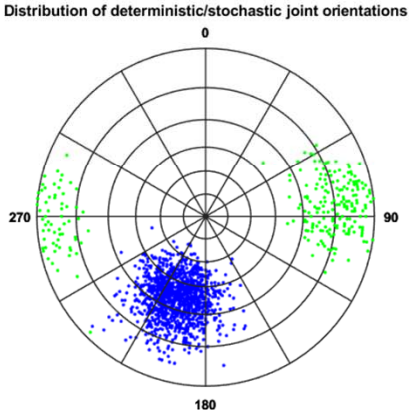

Stereonet Plot of Dip Vectors

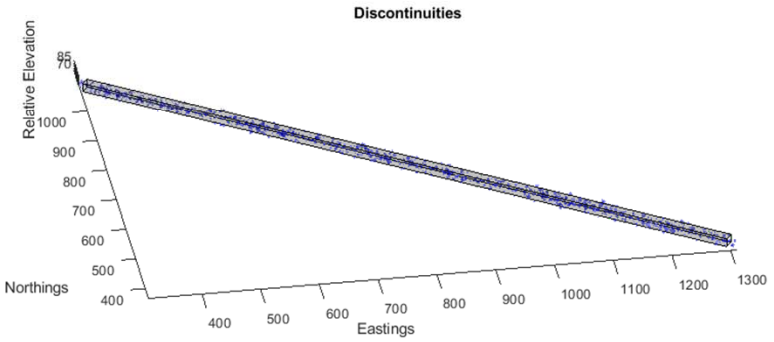

SIROMODEL
Block Visualiser

DFN Open Pit
1200 m long bench

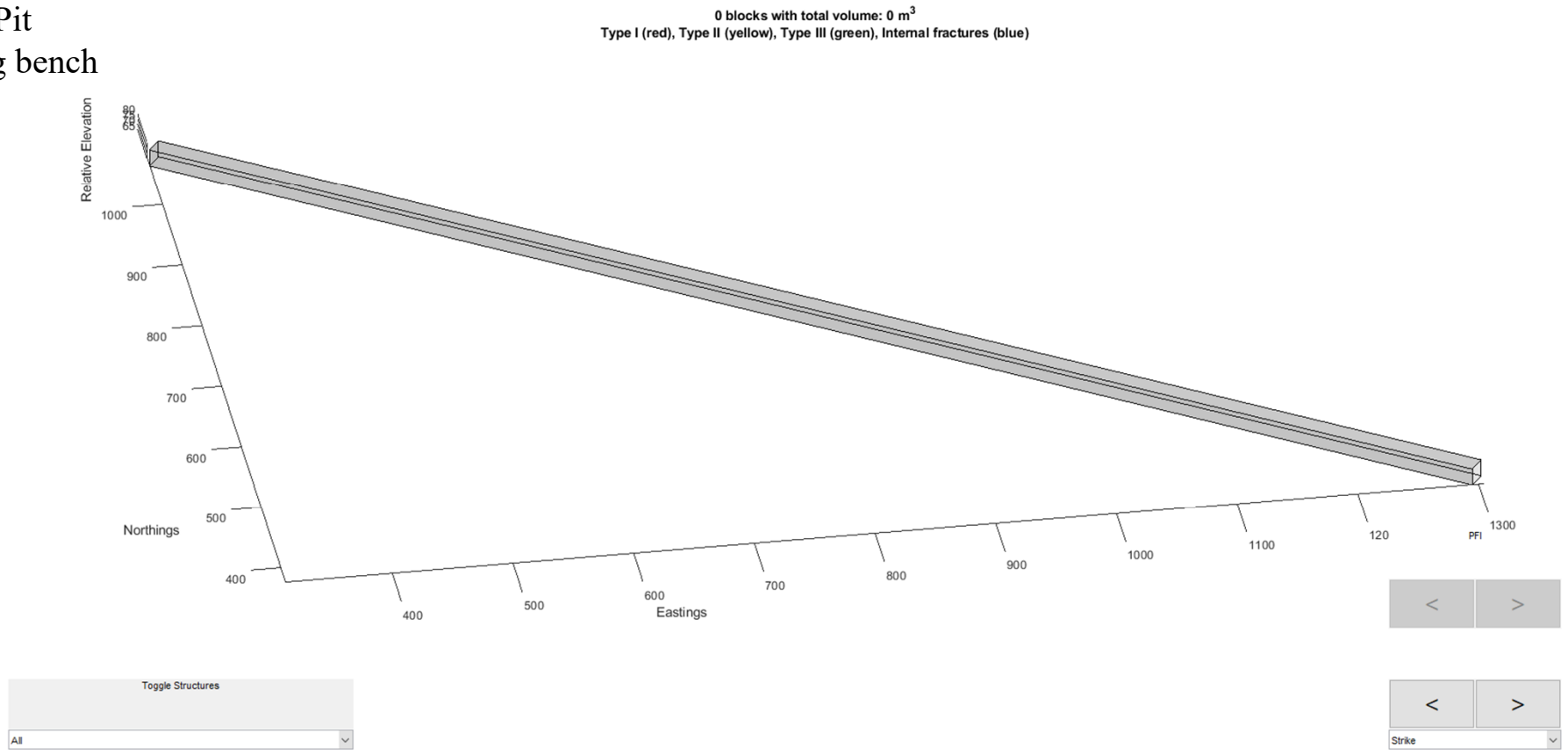

SIROMODEL
Structural Analysis
View

DFN Open Pit
Single Bench Model
1200 m long bench

Scale Factor =2

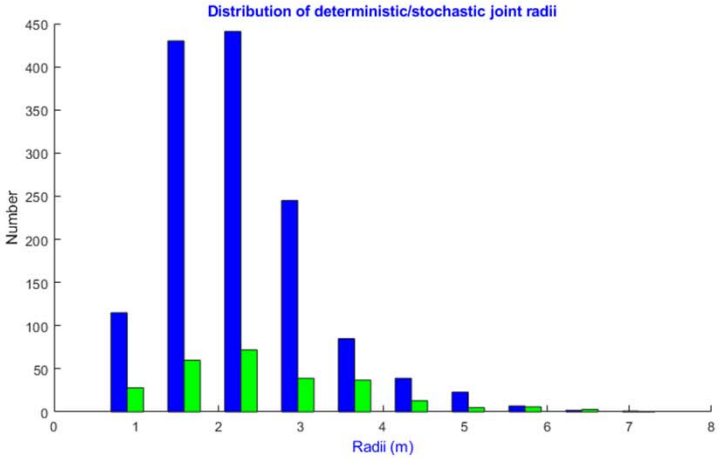

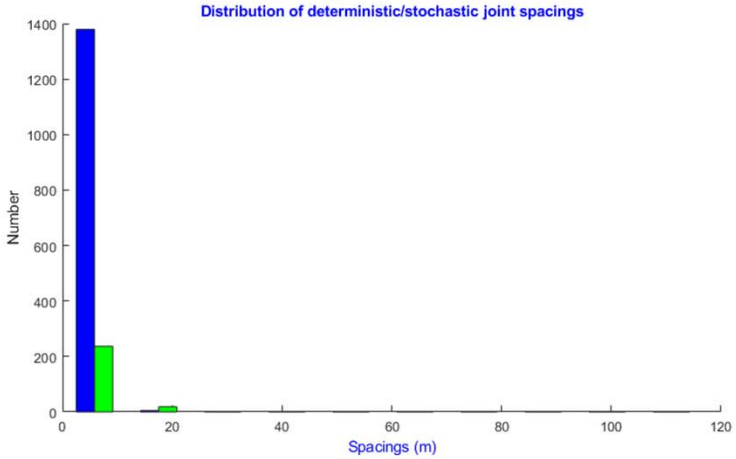

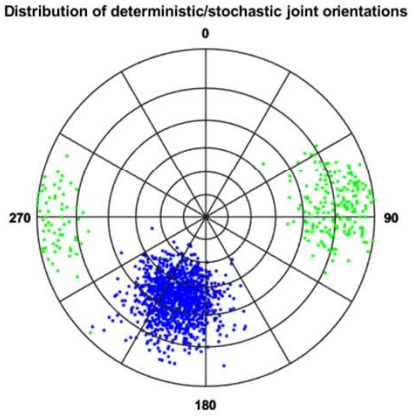

Stereonet Plot of Dip Vectors

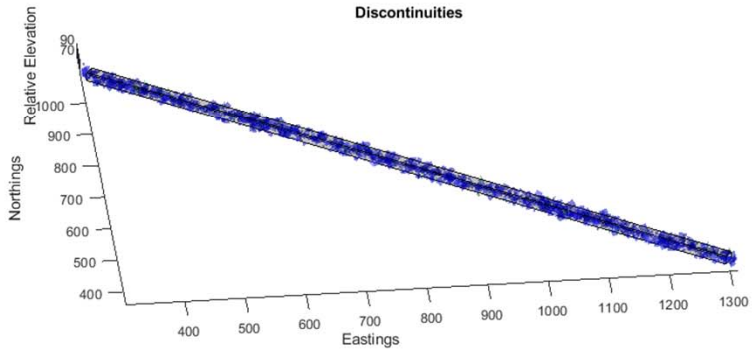

SIROMODEL
Block Visualiser

DFN Open Pit
1200 m long bench

Scale Factor = 2

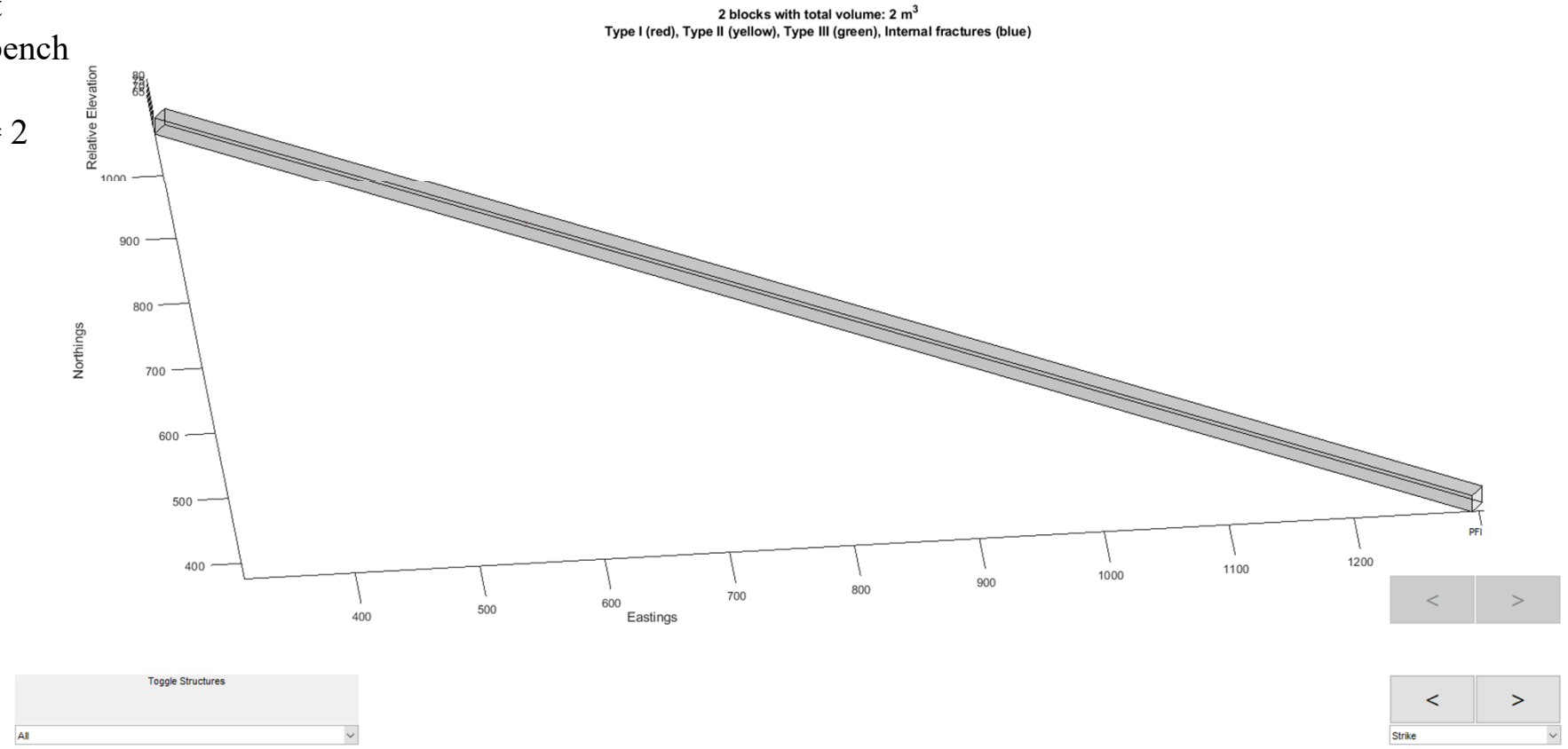

SIROMODEL
Structural Analysis
View

DFN Open Pit
Single Bench Model
1200 m long bench

Scale Factor = 3

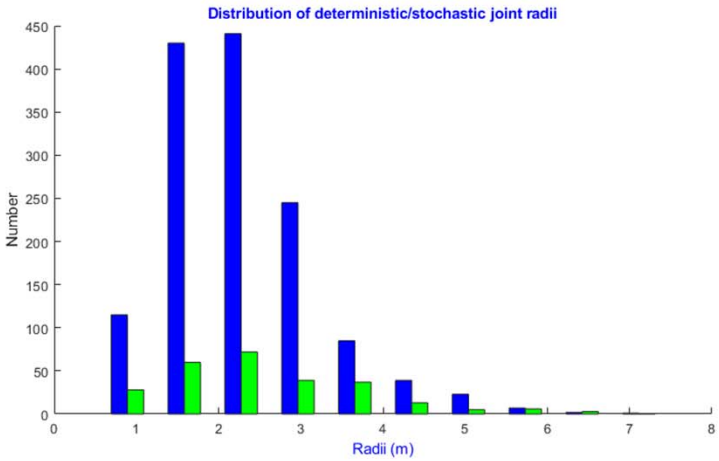

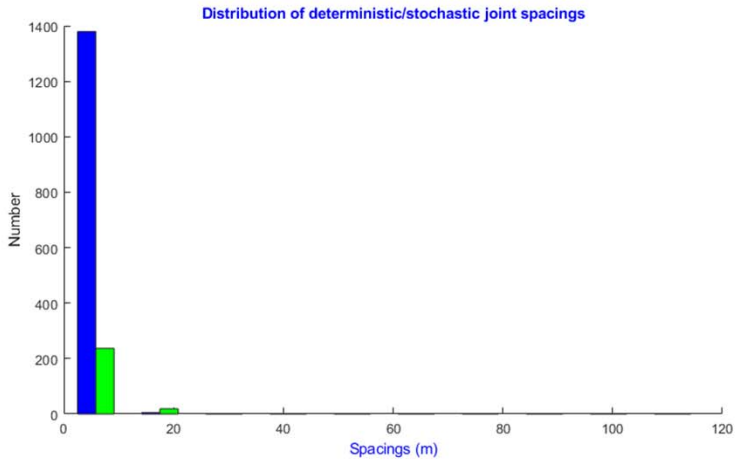

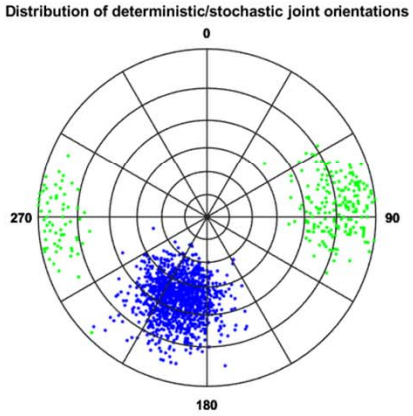

Stereonet Plot of Dip Vectors

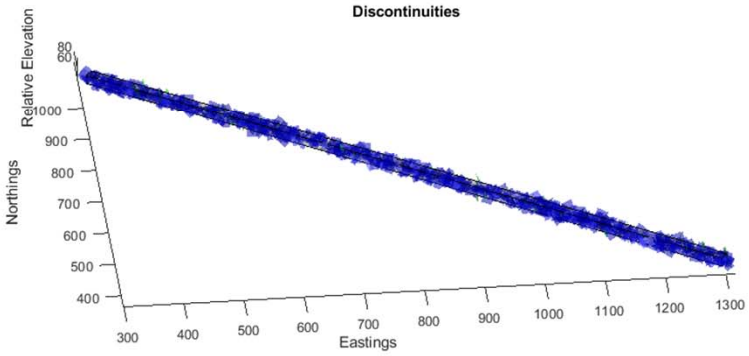

SIROMODEL
Block Visualiser

DFN Open Pit
1200 m long bench

Scale Factor = 3

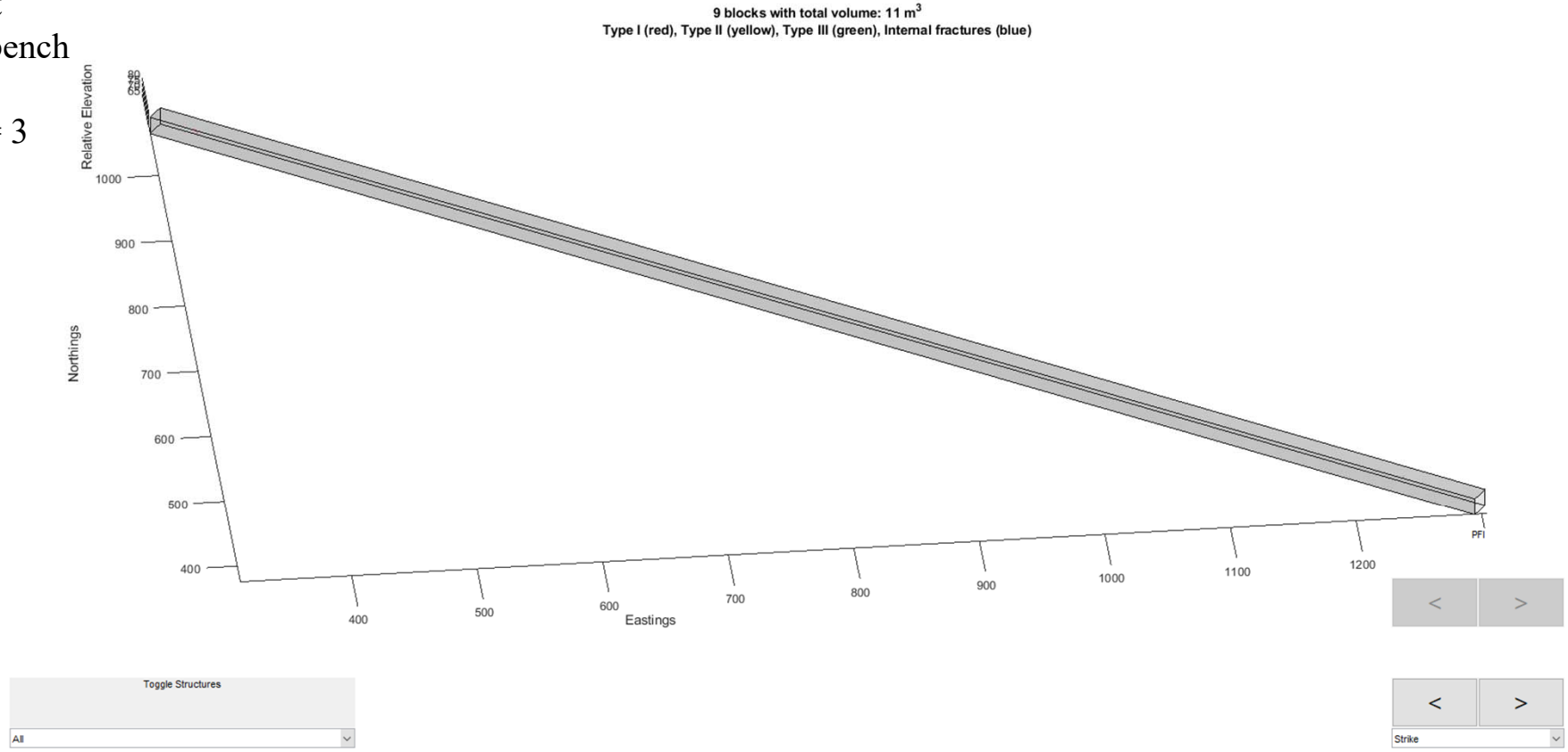

SIROMODEL
Structural Analysis
View

DFN Open Pit
Single Bench Model
1200 m long bench

Scale Factor = 4

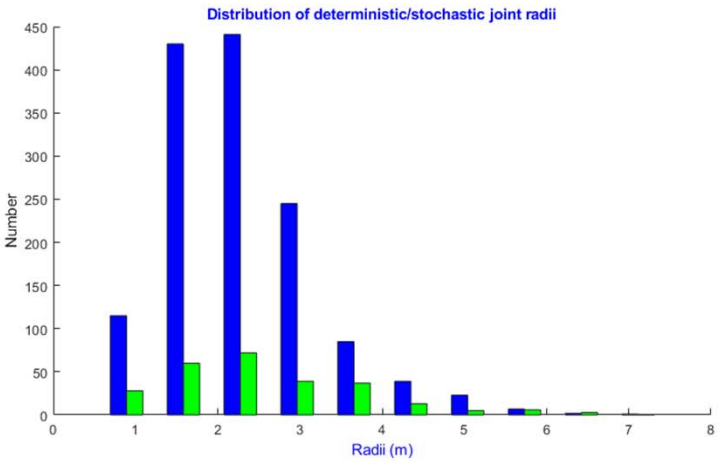

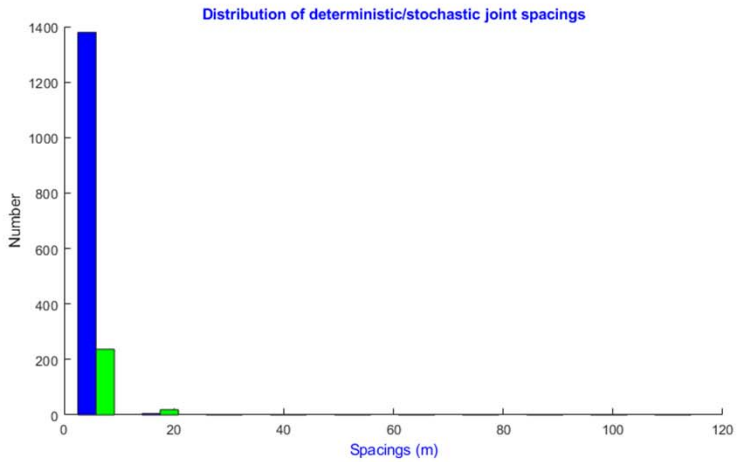

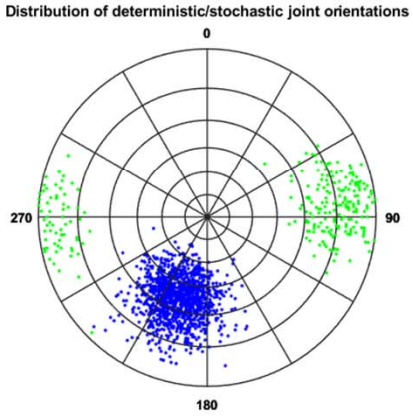

Stereonet Plot of Dip Vectors

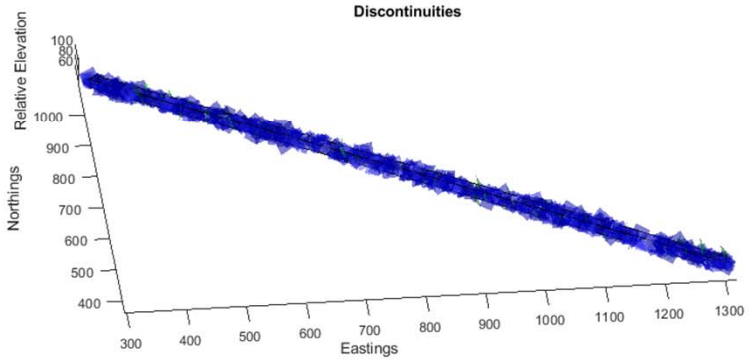

SIROMODEL
Block Visualiser

DFN Open Pit
1200 m long bench

Scale Factor = 4

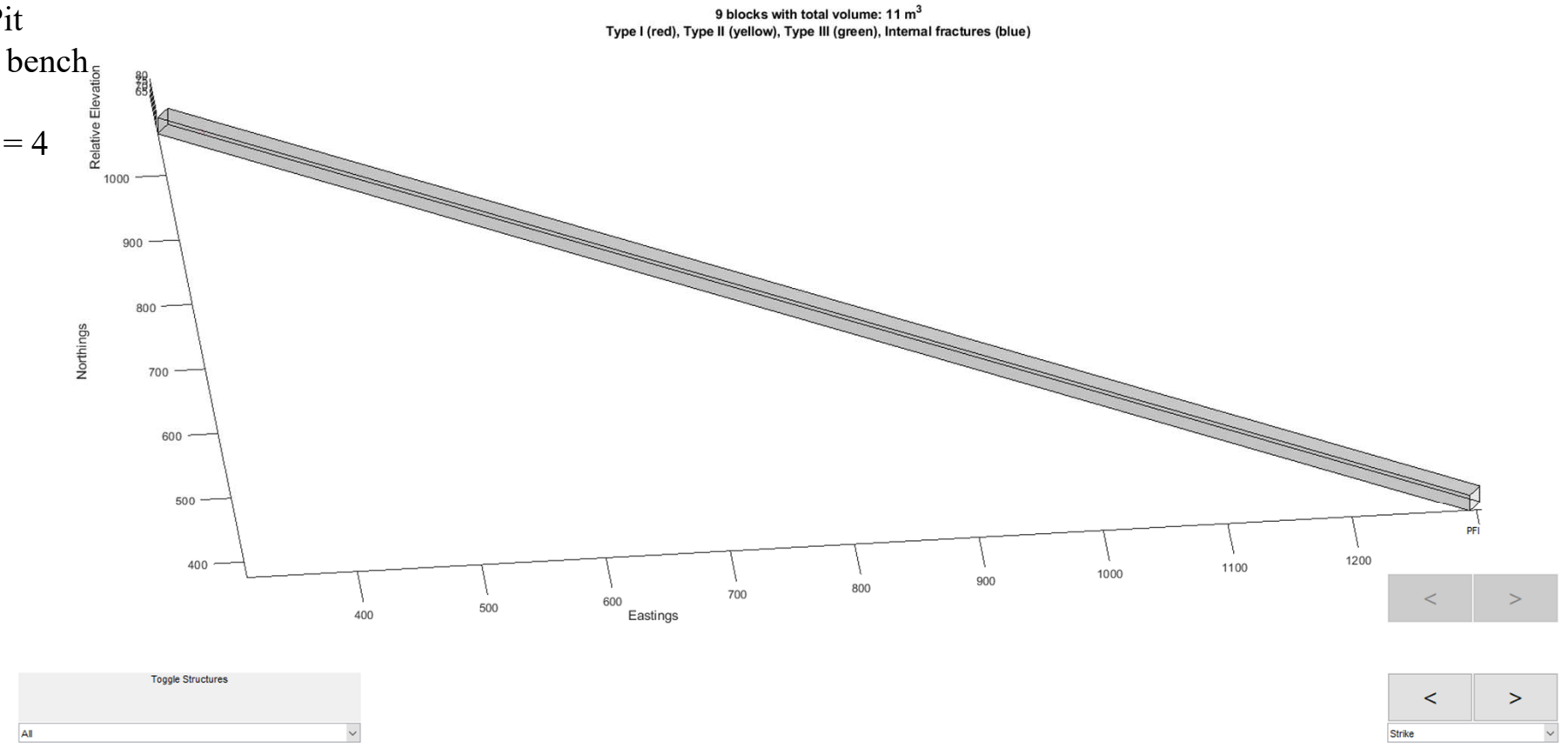

SIROMODEL
Structural Analysis
View

DFN Open Pit
Single Bench Model
1200 m long bench

Model 01
Increased structure
density

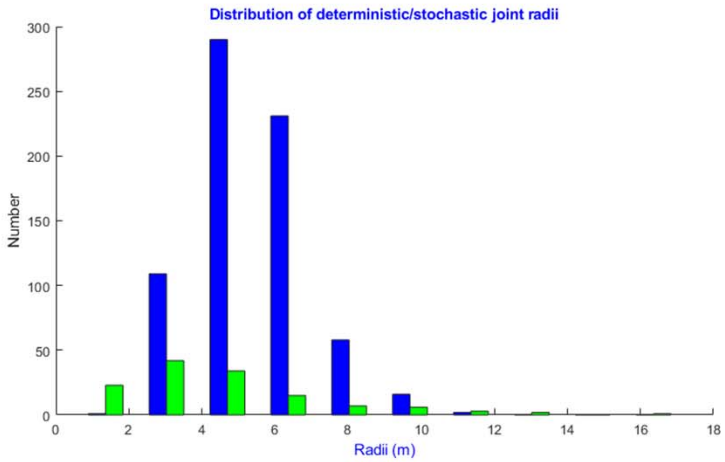

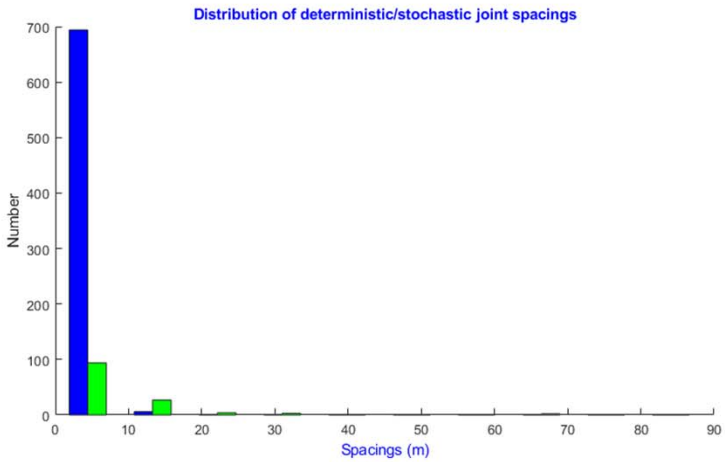

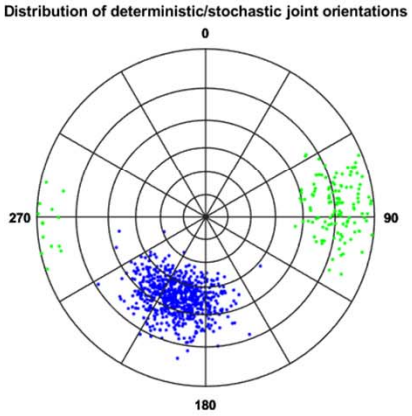

Stereonet Plot of Dip Vectors

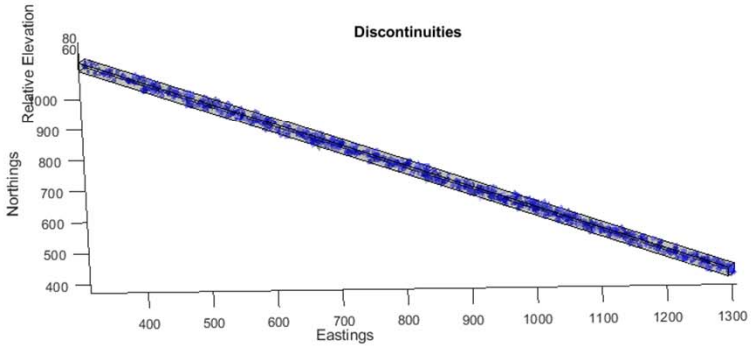

SIROMODEL
Block Visualiser

DFN Open Pit
1200 m long bench

Model 01
Increased structure density

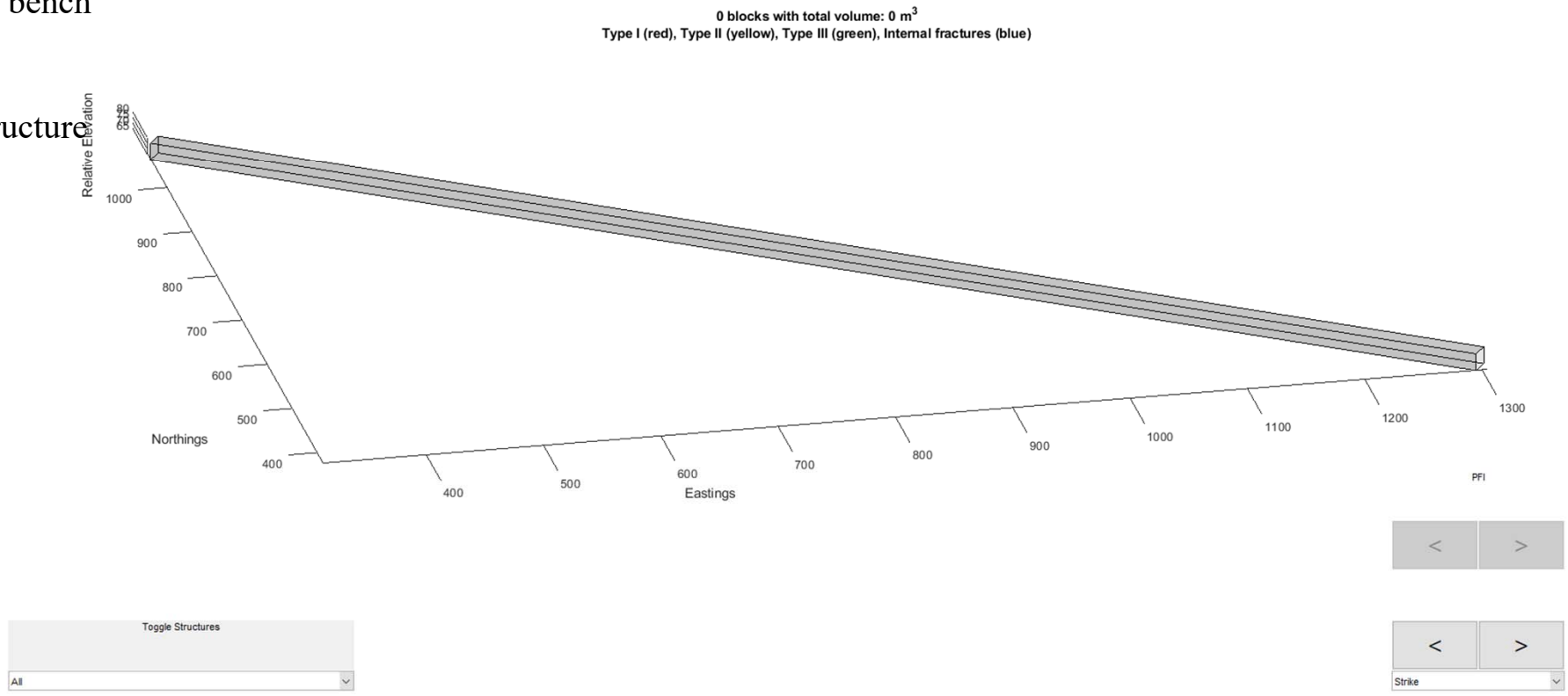

SIROMODEL
Structural Analysis
View

DFN Open Pit
Single Bench Model
1200 m long bench

Model 02
Increased structure
density

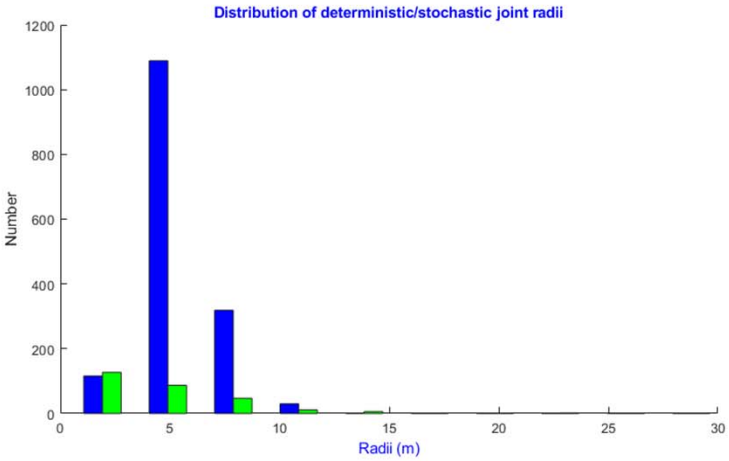

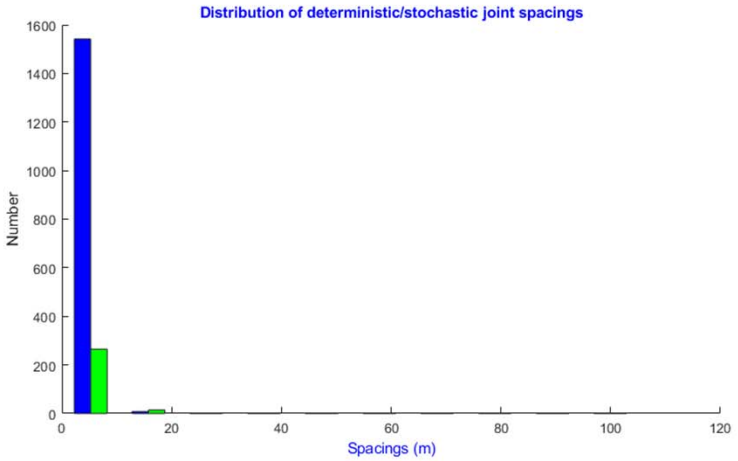

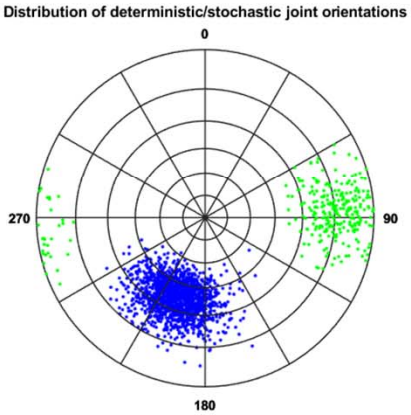

Stereonet Plot of Dip Vectors

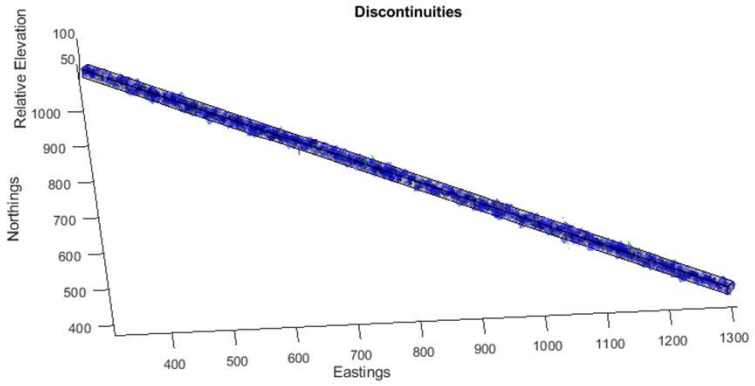

SIROMODEL
Block Visualiser

DFN Open Pit
1200 m long bench

Model 02
Increased structure density

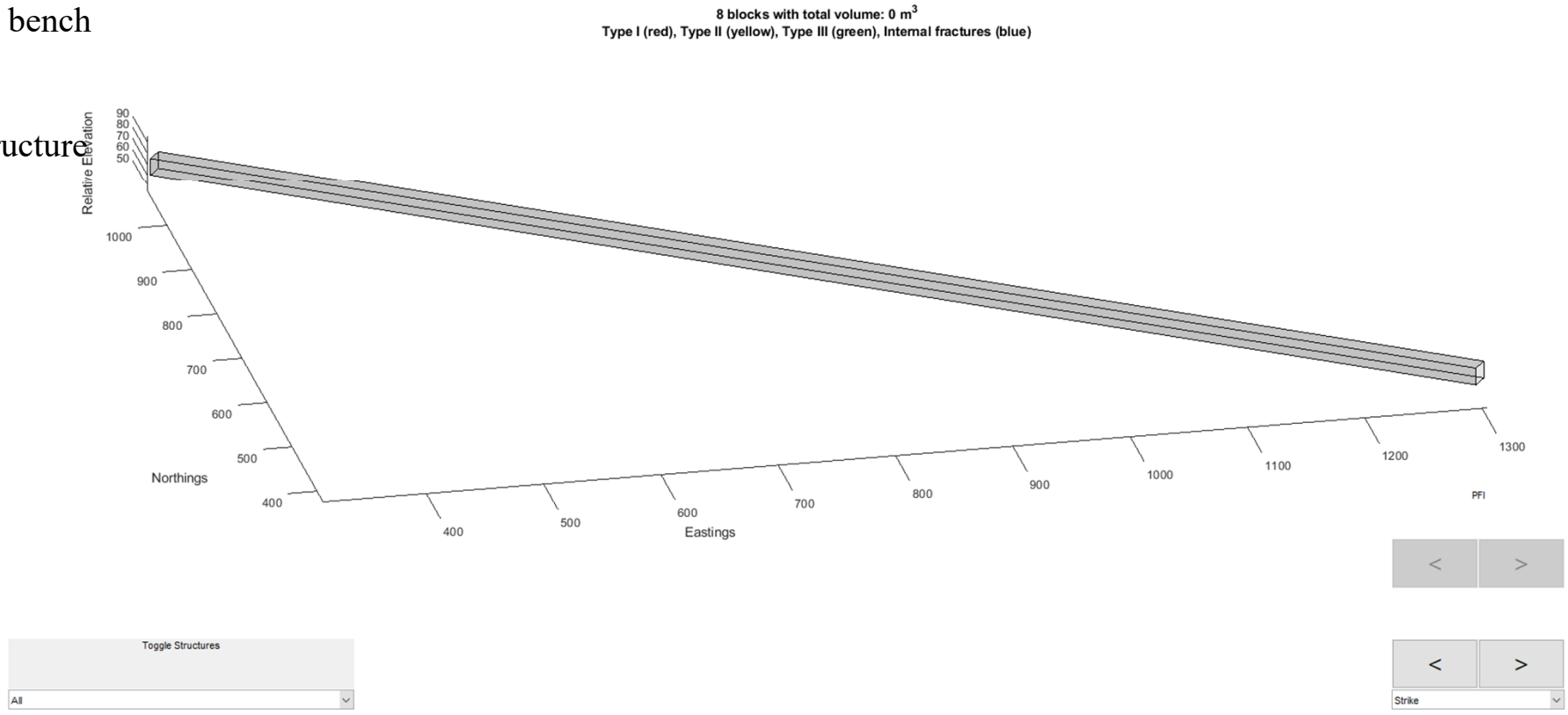

SIROMODEL
Structural Analysis
View

DFN Open Pit
Single Bench Model
1200 m long bench

Model 05
Increased structure
density and length

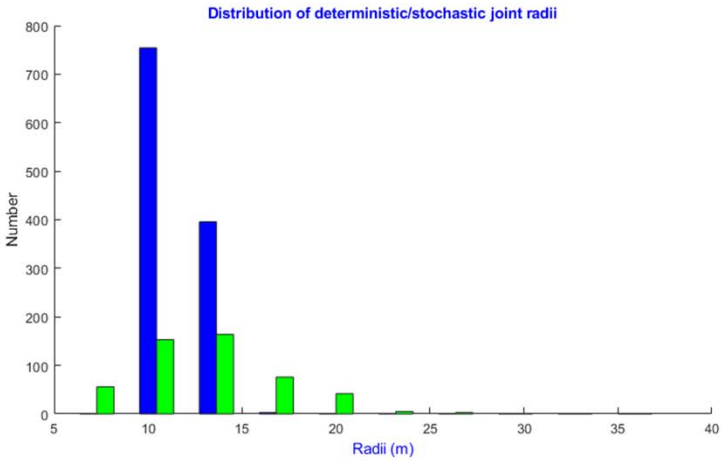

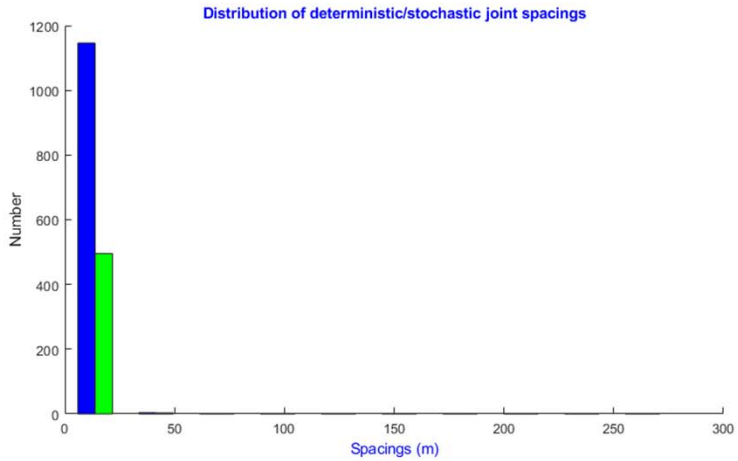

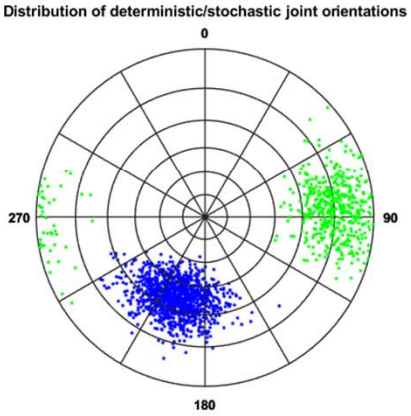

Stereonet Plot of Dip Vectors

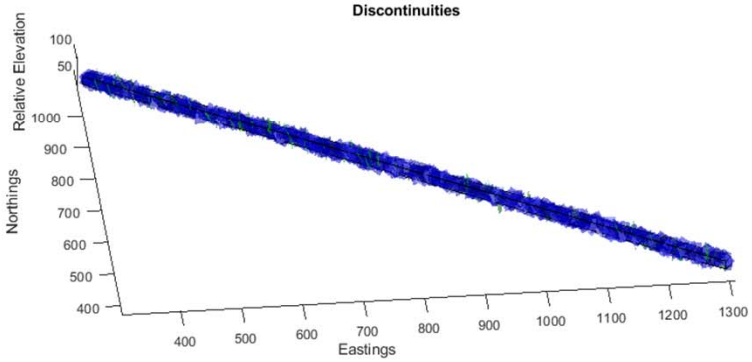

SIROMODEL
Block Visualiser

DFN Open Pit
1200 m long bench

Model 05
Increased structure
density and length

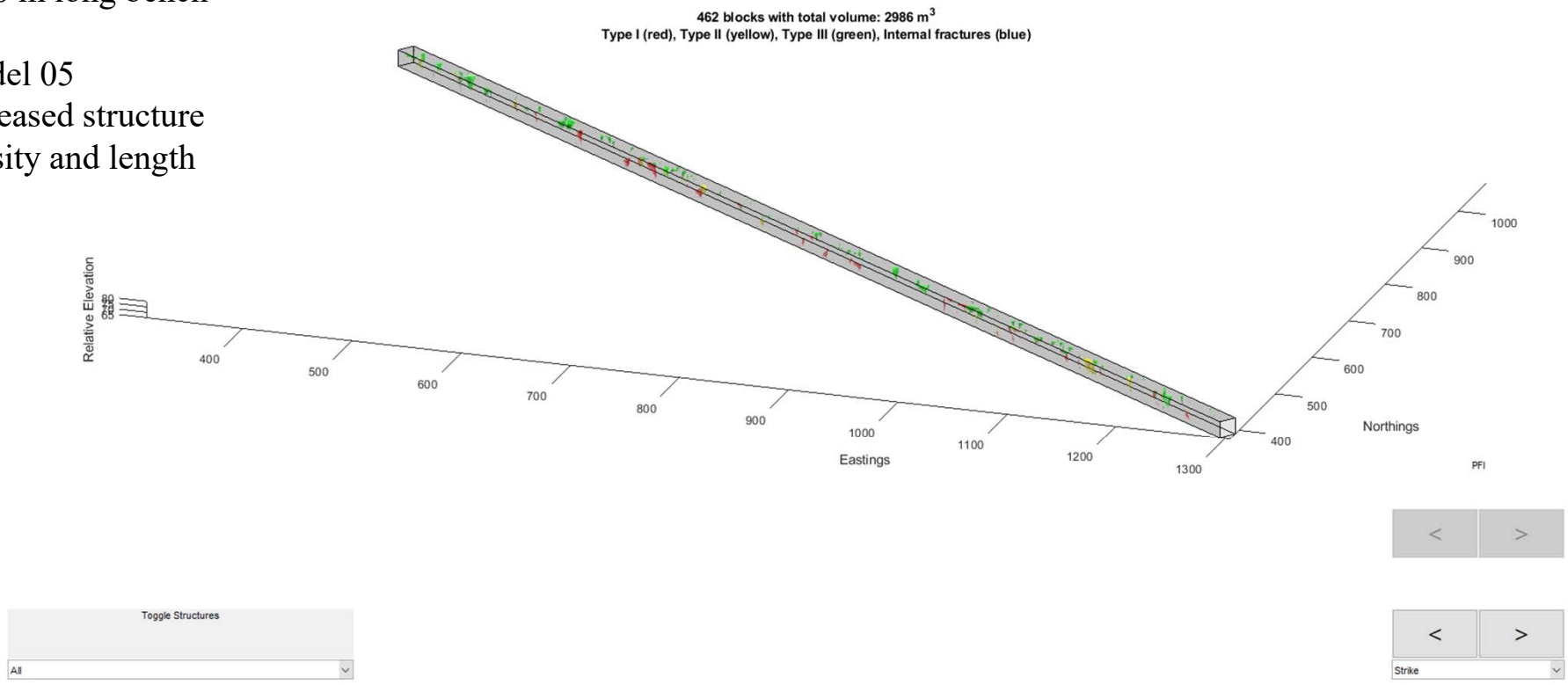

SIROMODEL
Back Break
Analysis

DFN Open Pit
Single Bench Model
1200 m long bench

Model 05
Increased structure
density and length

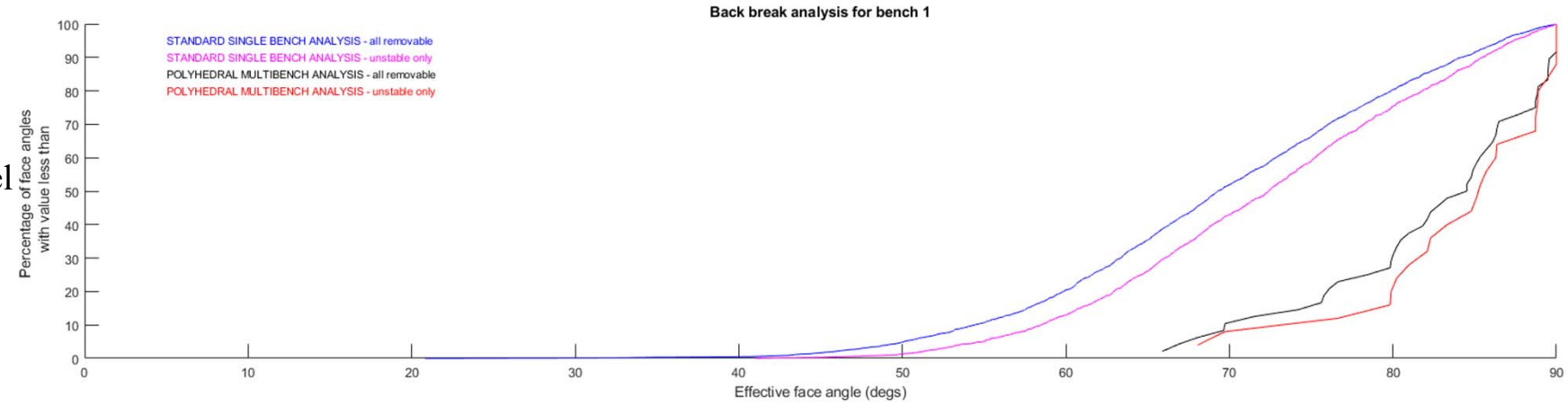

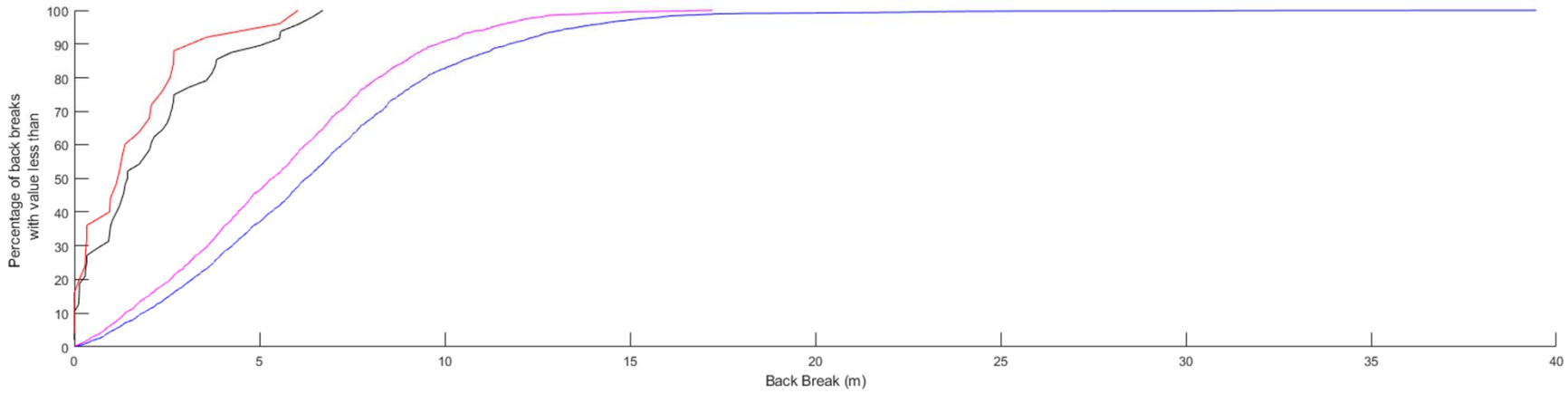

All All

SIROMODEL
Structural Analysis
View

DFN Open Pit
Single Bench Model
1200 m long bench

Model 06
Increased structure
density and length

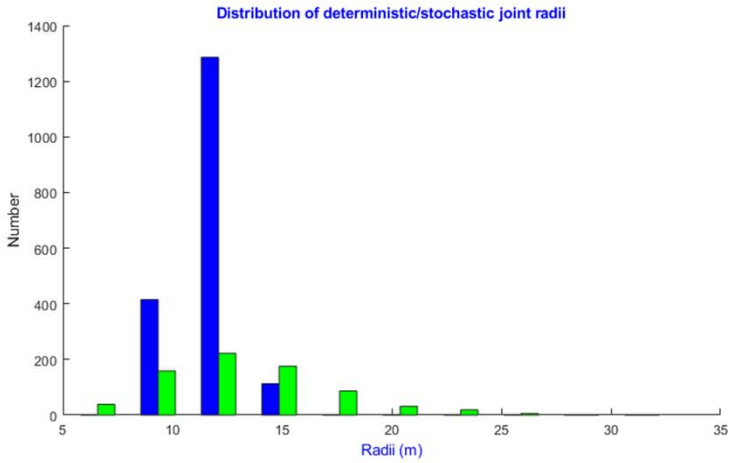

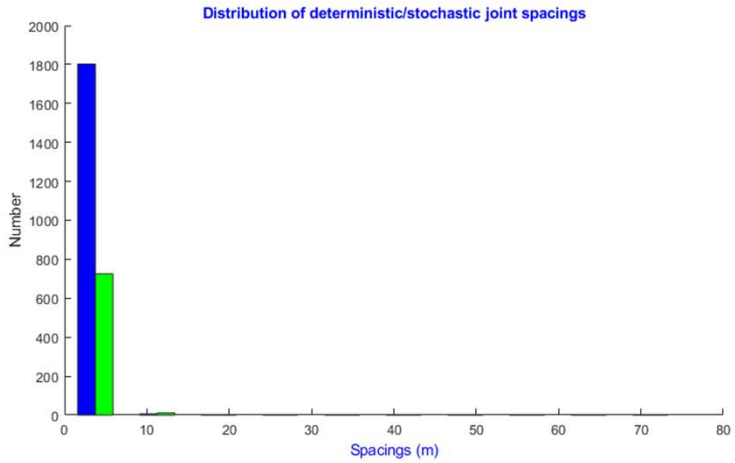

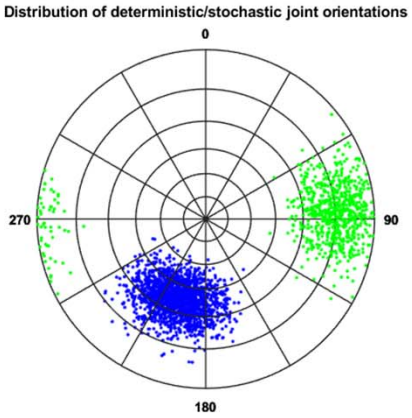

Stereonet Plot of Dip Vectors

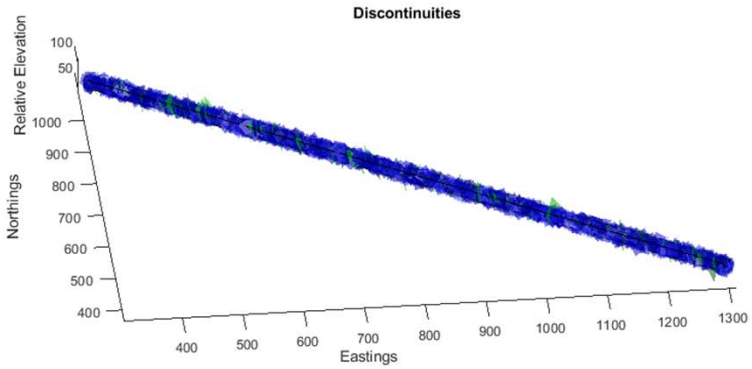

SIROMODEL
Block Visualiser

DFN Open Pit
1200 m long bench

Model 06
Increased structure density and length

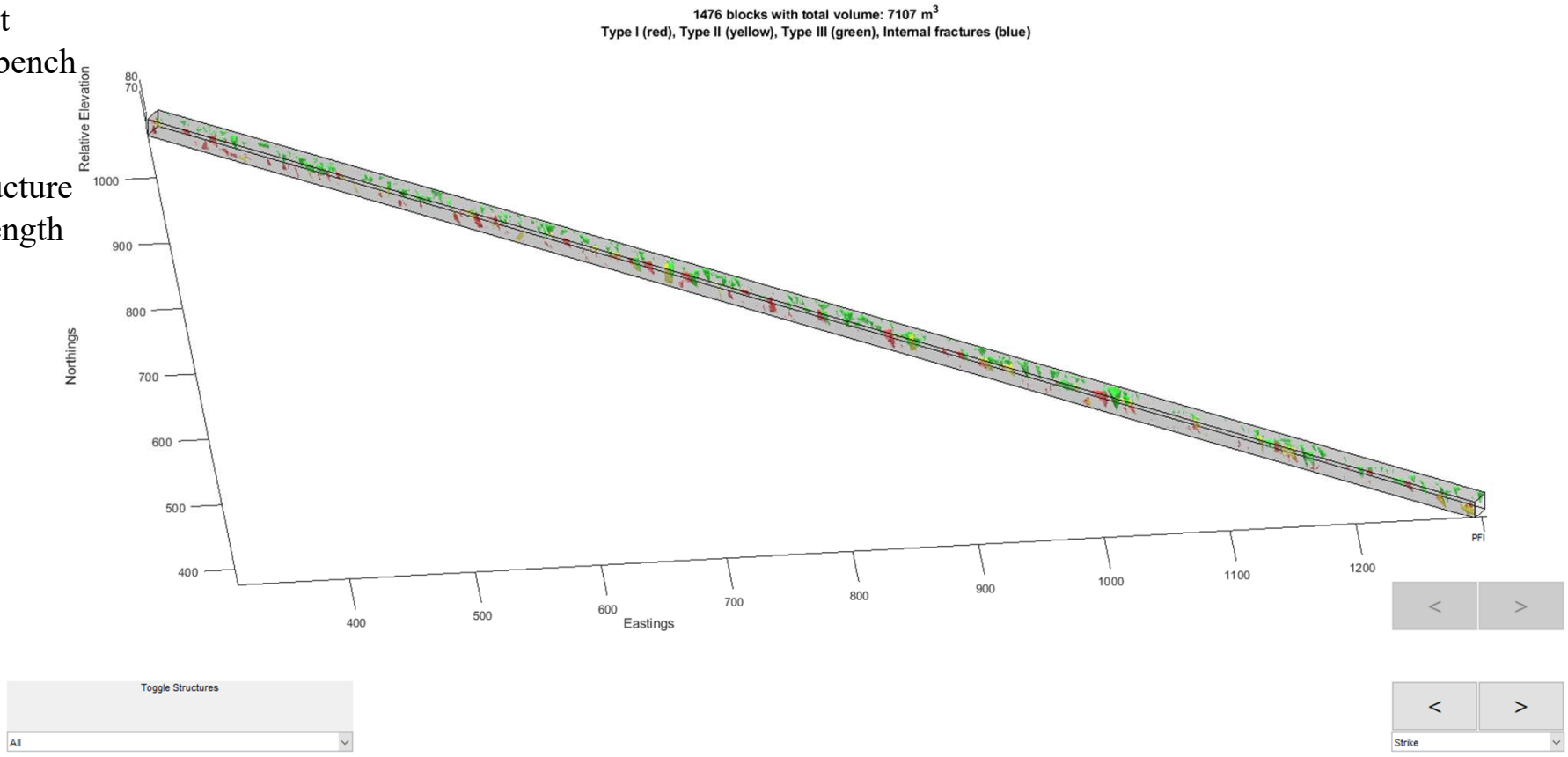

SIROMODEL
Back Break
Analysis

DFN Open Pit
Single Bench Model
1200 m long bench

Model 06
Increased structure
density and length

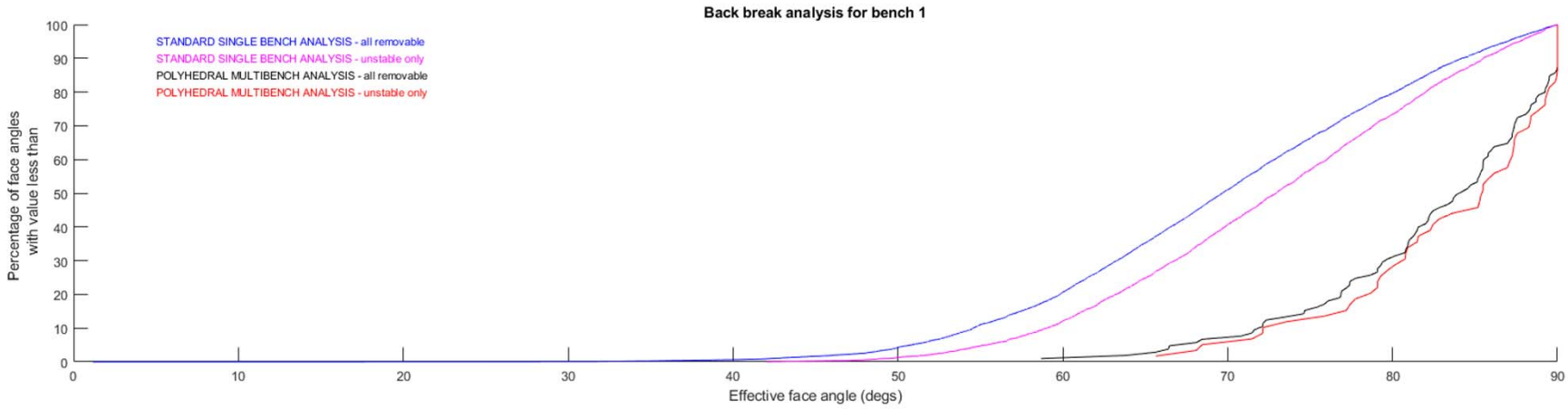

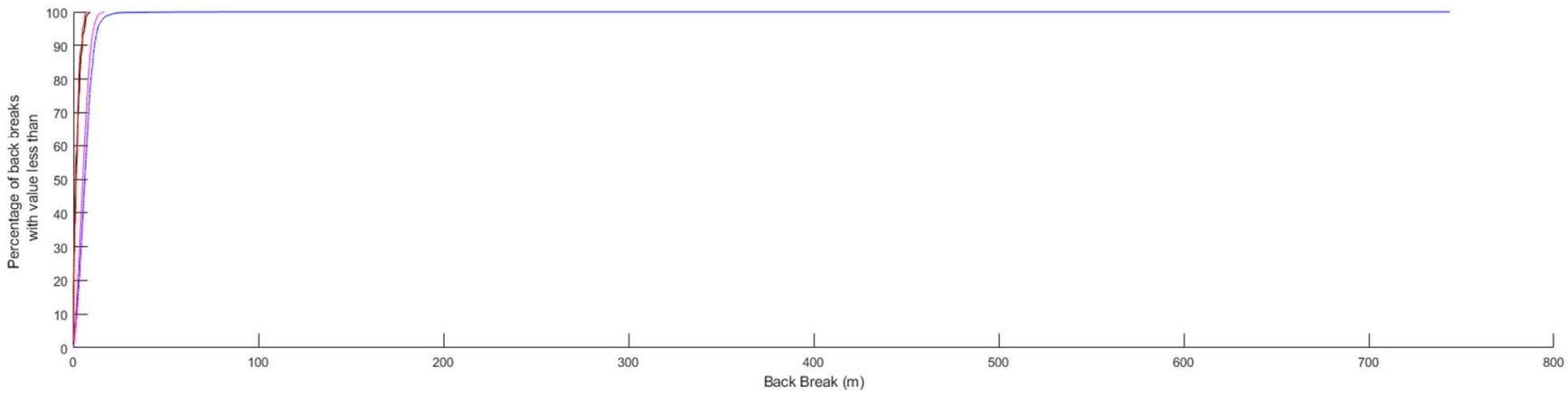

All All

SIROMODEL
Structural Analysis
View

DFN Open Pit
Single Bench Model
120 m long bench

Model 06
Increased structure
density and length

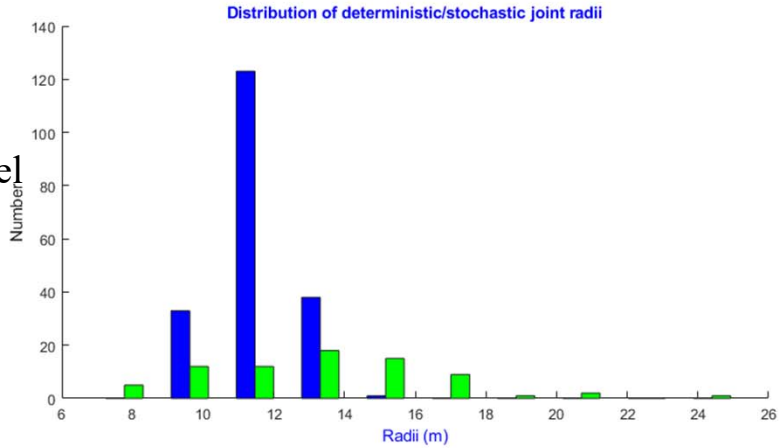

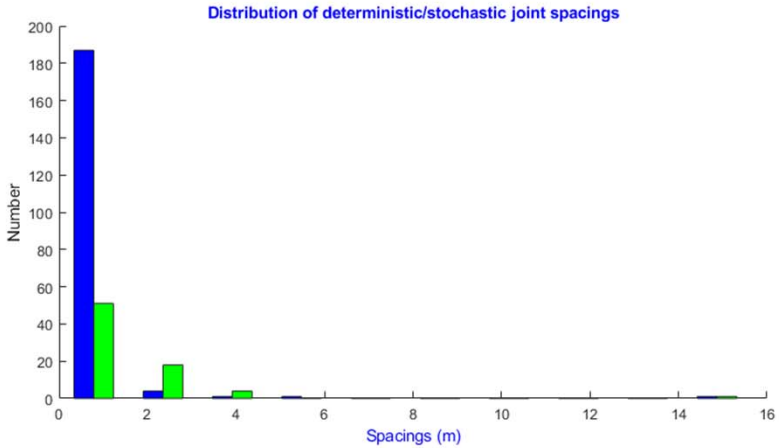

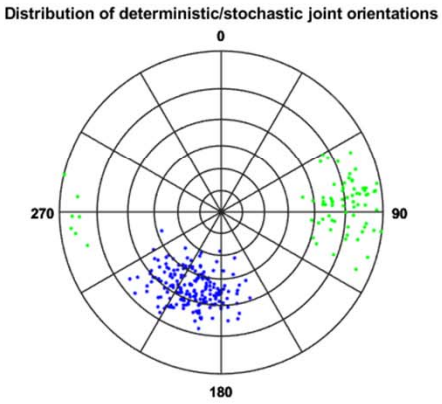

Stereonet Plot of Dip Vectors

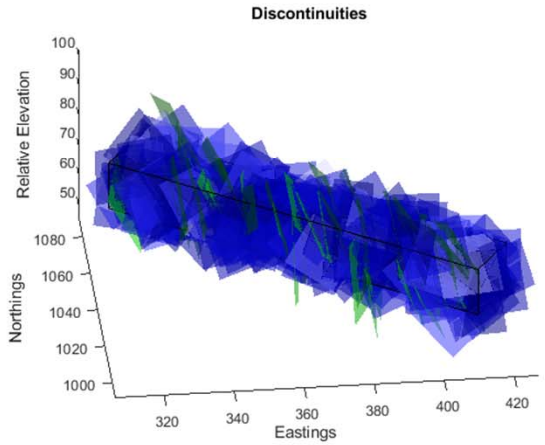

SIROMODEL
Block Visualiser

DFN Open Pit
120 m long bench

Model 06
Increased structure density and length

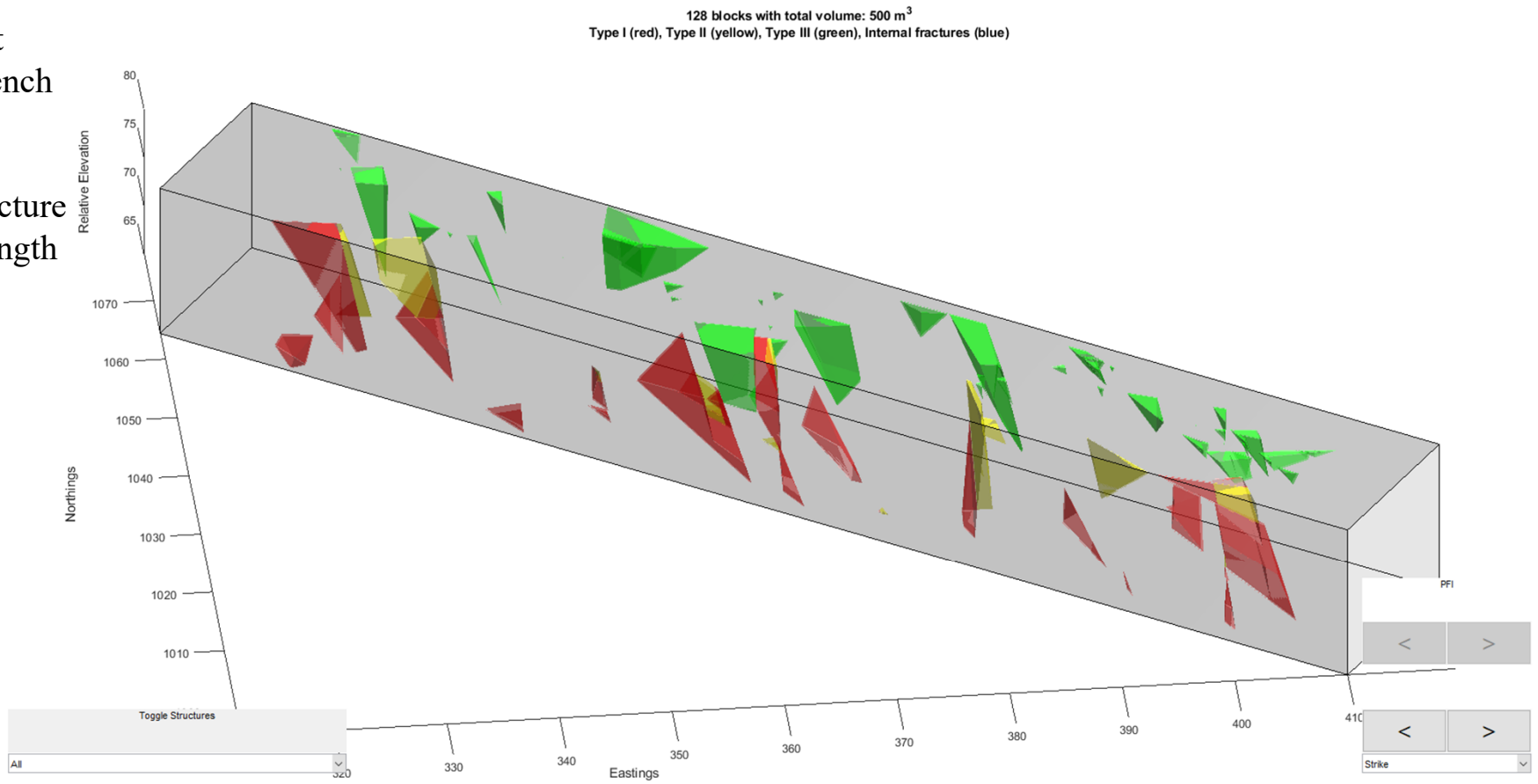

SIROMODEL
Back Break
Analysis

DFN Open Pit
Single Bench Model
120 m long bench

Model 06
Increased structure
density and length

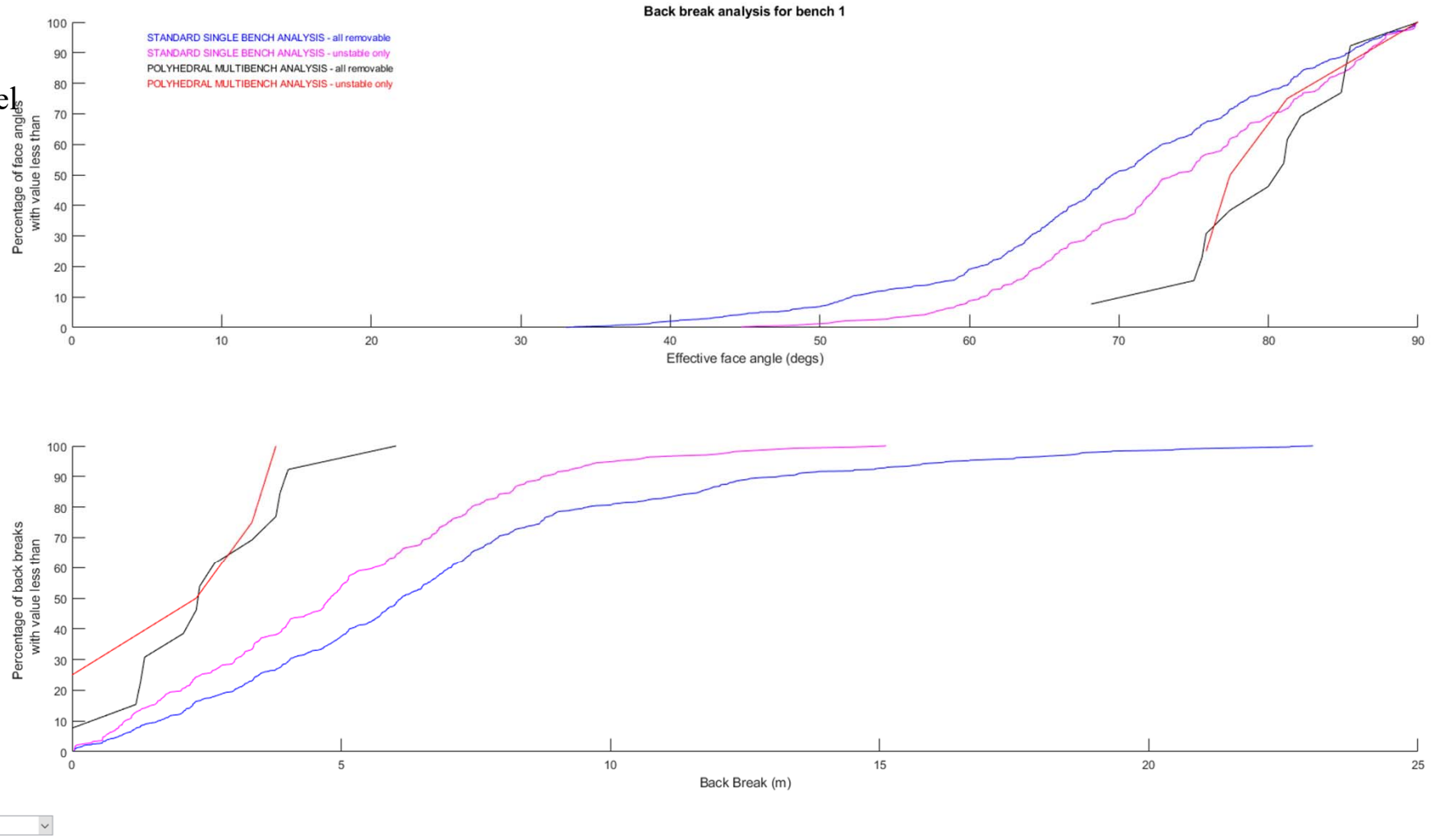

SIROMODEL
Structural Analysis
View

DFN Open Pit
Single Bench Model
120 m long bench

Model 07
Increased structure
density and length

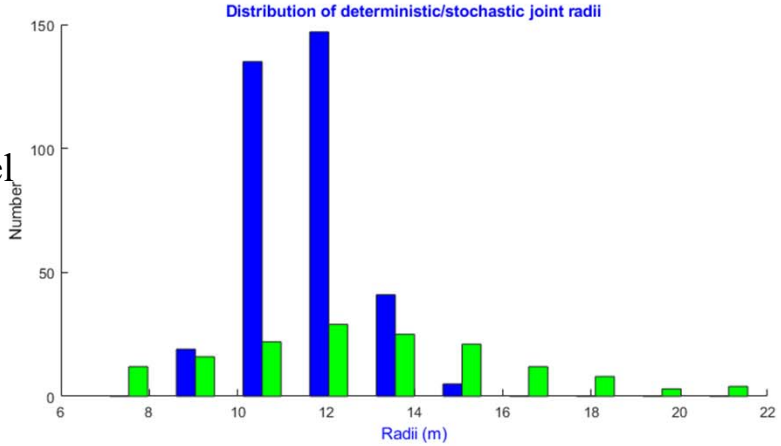

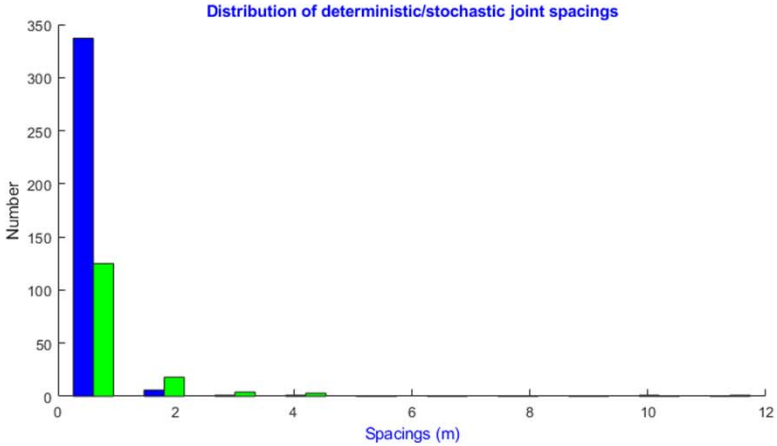

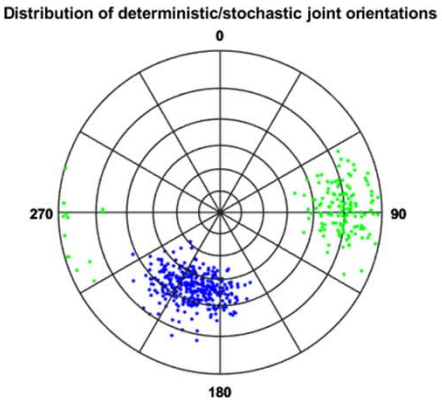

Stereonet Plot of Dip Vectors

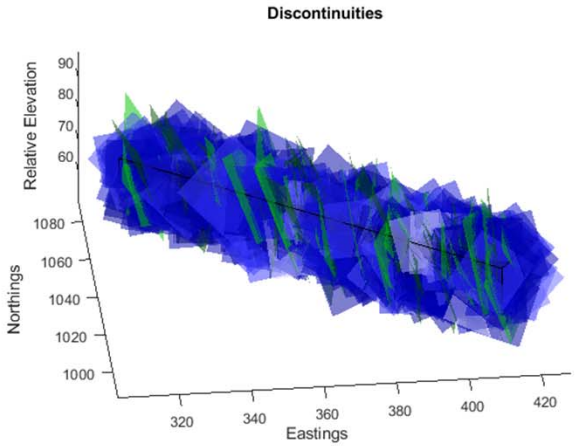

SIROMODEL
Block Visualiser

DFN Open Pit
120 m long bench

Model 07
Increased structure density and length

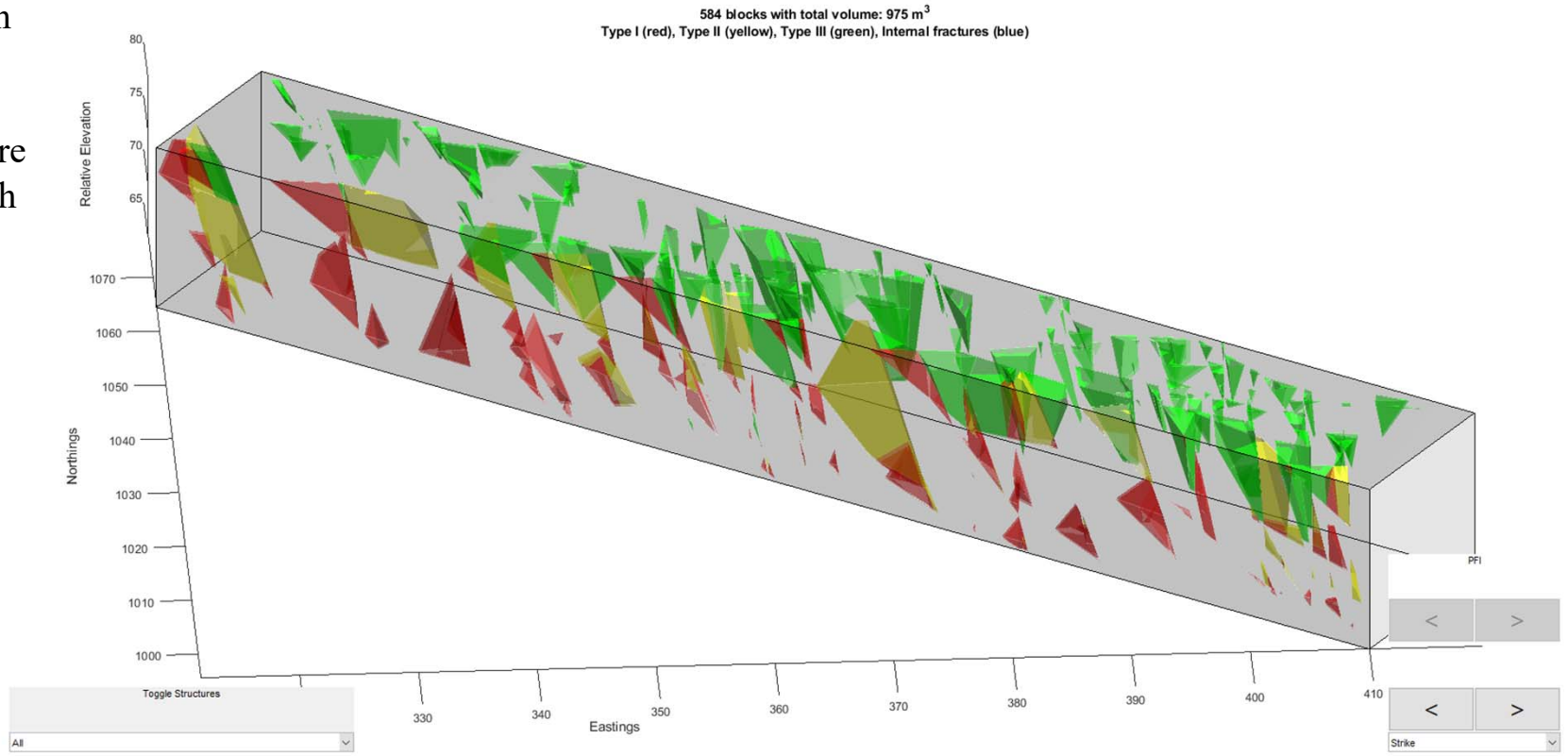

SIROMODEL
Back Break
Analysis

DFN Open Pit
Single Bench Model
120 m long bench

Model 07
Increased structure
density and length

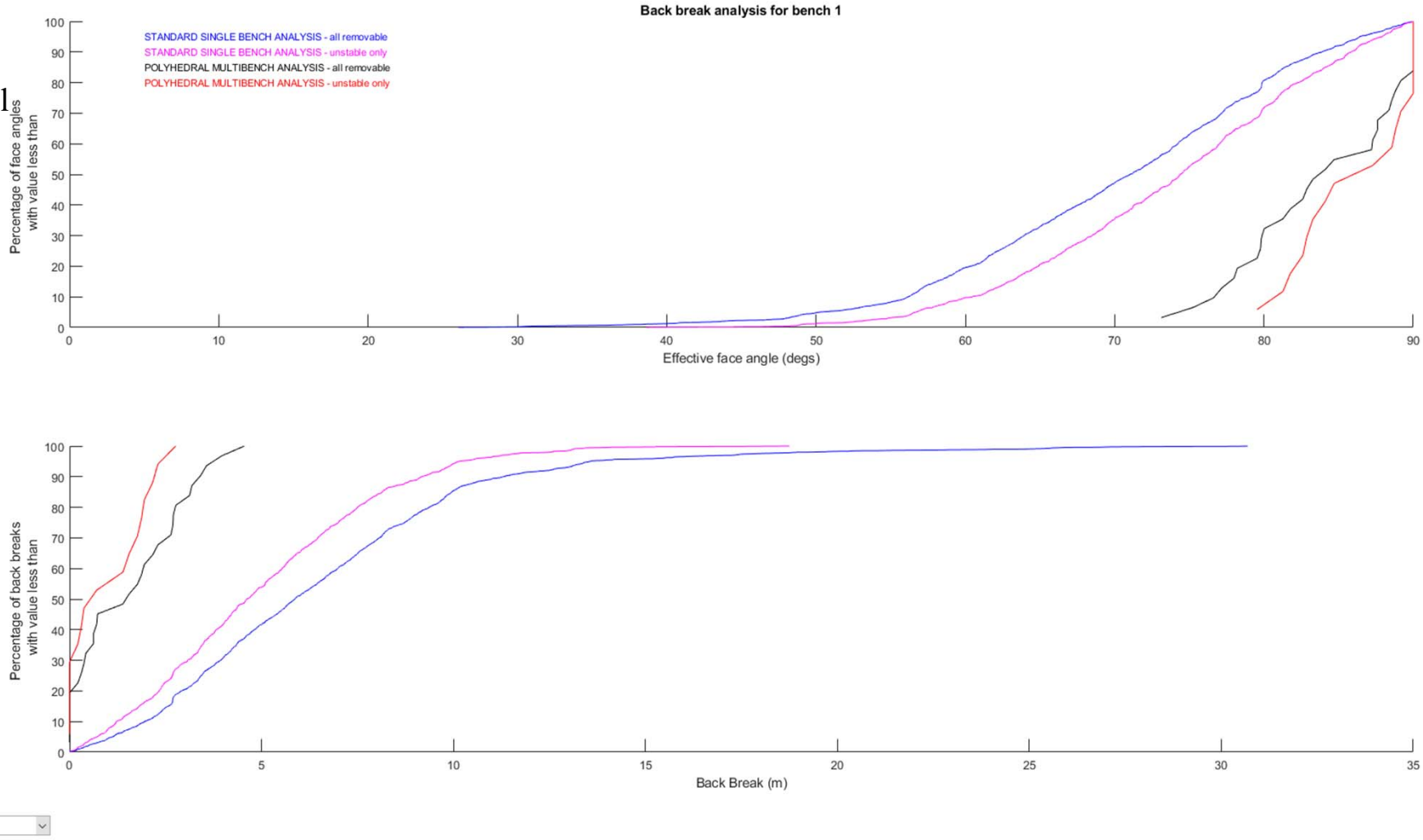

SIROMODEL
Structural Analysis
View

DFN Open Pit
Single Bench Model
450 m long bench

Model 08
Increased structure
density and length

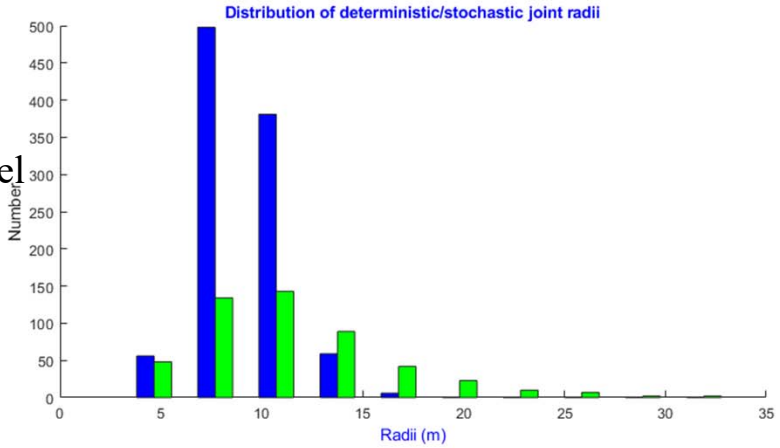

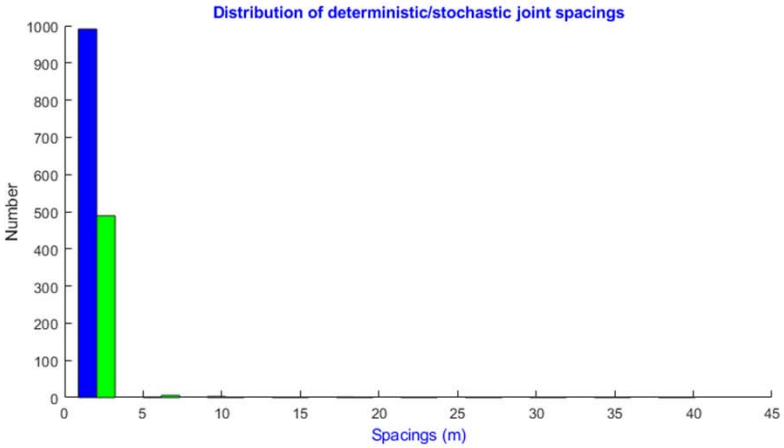

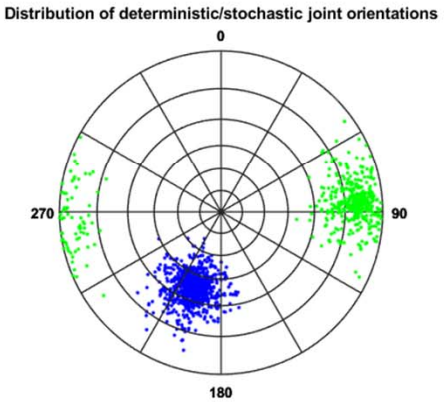

Stereonet Plot of Dip Vectors

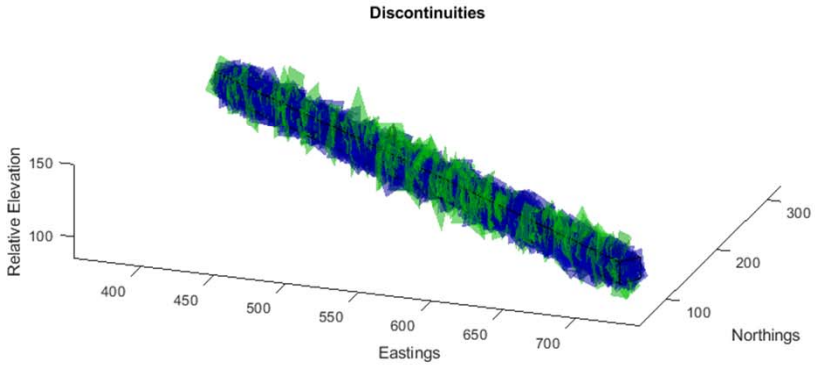

SIROMODEL
Block Visualiser

DFN Open Pit
450 m long bench

Model 08
Increased structure
density and length

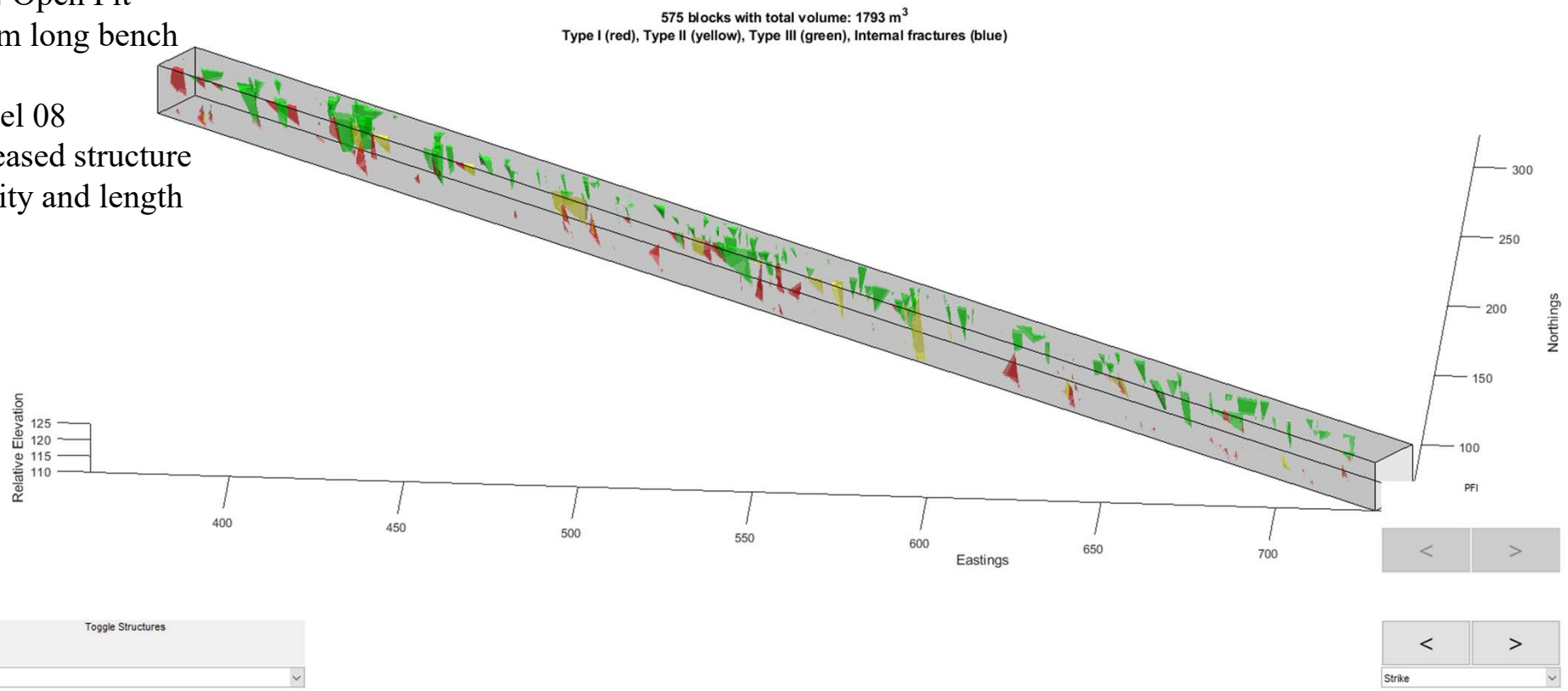

SIROMODEL
Back Break
Analysis

DFN Open Pit
Single Bench Model
450 m long bench

Model 08
Increased structure
density and length

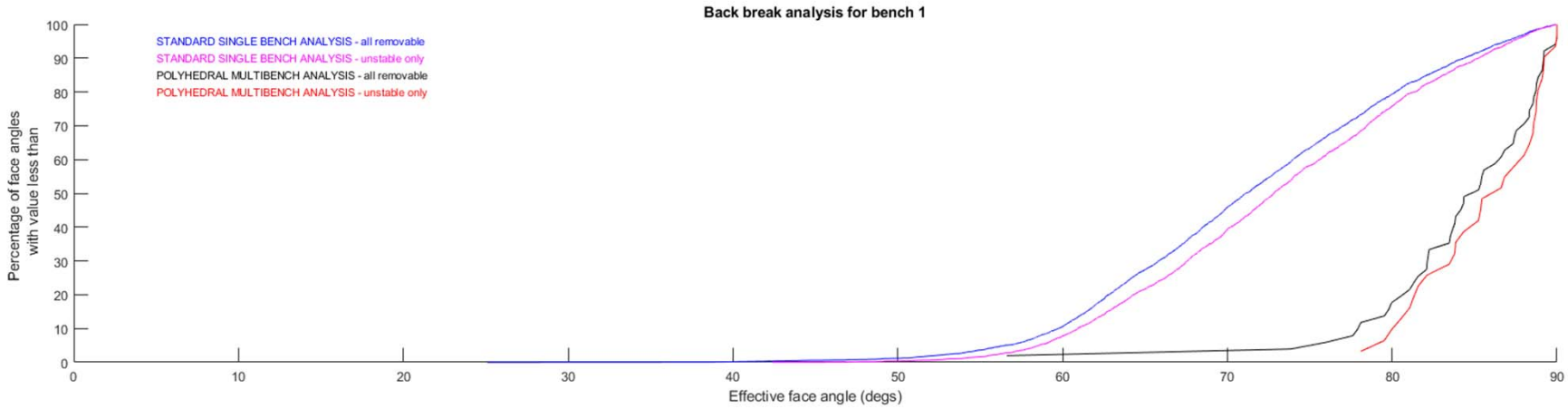

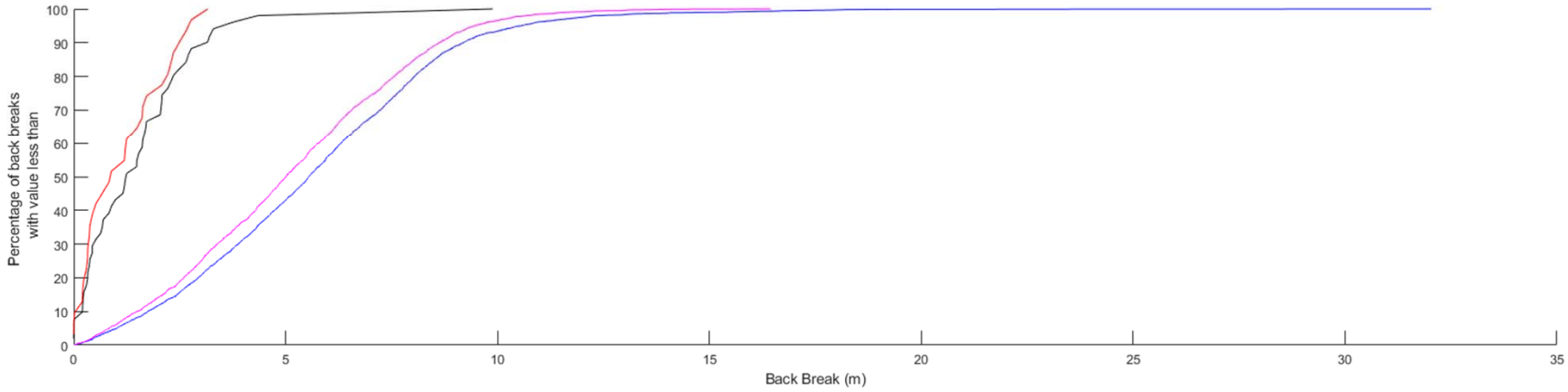

All All